Characterization of the human sperm centrosome and its role in (in)fertility

Farners Amargant i Riera

TESI DOCTORAL UPF 2018

Thesis Supervisor:

Dr. Rita Vassena

Dr. Isabelle Vernos

Clínica Eugin and Cell and Developmental Biology Programme, Centre for Genomic Regulation

A les meves àvies,
Dolors i Elvira

Acknowledgments

It seems like only yesterday when a 27th of January (in 2013!) I received an email from Isabelle, offering me the chance of carrying my PhD at Eugin and at the CRG. Almost 4 years and a half have passed, and I cannot think of a single day in which I don't feel happy of having accepted the position.

Many things have changed since I started. I learnt how to do science, from the most basic to its clinical application, and how to be a good scientist. However, what did not change at all during these years is the passion in which I am coming every day to the lab.

And those responsible for all these positive changes are Rita and Isabelle. You encouraged me to be a rigorous scientist, to be critic with my work and to aim higher. You also gave me the opportunity to attend many congresses, because as Rita says: "science has to be always transmitted". I am extremely proud of having two exceptional women as PhD supervisors and mentors. As I like to say, Rita and Isabelle are "super-women". Nevertheless, I cannot find a way to thank you enough your lessons and advises. I can only say THANKS; you made my PhD scientifically and personally so exciting.

I would also like to acknowledge Ursula, Joan, Elvan, Bernhard and Manel for being on my PhD thesis defense board, and for having some time to read and analyze our work. I am sure we will enjoy the defense. Thanks also to my thesis committee members; Bernhard, Montse, Sebastian and Pedro. It has been always a pleasure to keep you updated.

We spend a lot of time in the lab, and having labmates like the ones I have in the CRG and in Eugin, makes everything easier and funnier. At the CRG, thanks to the entire lab for the good moments, the lunches in our sunny terrace (how I will miss having lunch in front of the sea!) and the breakfasts after the labmeetings. Georgina and Alejandra, thanks for our coffee breaks. They were completely necessary to come back to the lab in a good mod. Alvaro, just because our corner is the best one! Krys, for the laughs and the

long talks together. Former lab members; Tommaso, I think I inherited your passion for doing science… and for attending to as many congresses per year as possible!

Eugin PCB lab, I was the first PhD student and now we are 6! I saw how the lab was getting bigger, and I am happy to see that now it is full of good people and scientists. Montse and Gustavo, thanks for tutoring me and having so much patience! I will never forget our never-endings labmeetings!!

Outside the lab we are a family, thanks for the Friday beers and dinners, for the party nights and all the times we celebrate "anything" together. Anna, thanks for being always there. Your expertise and knowledge are crucial in the lab, and you are always happy to help us. Agus, you deserve an especial acknowledgement. I admire your optimism, I admire your strength, I admire your will to live. This is just a period, I am sure that very soon you will come back to the lab. And remember, we need your help to have the Eugin PCB boys under control!

Members from Eugin clinic and CIRH. Aïda, Mercè, Meri and Désirée. You make many experiments possible and my live much more easily. You invest your time in helping me, just because you like doing science! Many thanks for everything. And I would also to acknowledge the entire embryo lab, for they patience in collecting samples.

Ale and Paula, you are not only labmates; you are friends, my family in Barcelona. I can't imagine this period without your help and support, neither with our lunches, dinners and… vermouths. Gaby, although you are far, I feel like you are always here for everything. I miss so much our travels, and I hope we can find soon a date for our next adventure! Maria Pau, thanks for taking care of me, to give me support during all these years. I am incredibly lucky to have you as a friend. Also to my flatmates, former and current. Gisela, Alba, Ari, Cris and Muguet… thanks for sharing so many good "after work" moments. And last but not least, to IBB former members. Kati, Olívia, Sílvia, Anabel and Tanco. You were my first mentors!

Albert, vas aparèixer quan menys m'ho esperava i t'has convertit en la millor coinciendència. Ens compenetrem i ens entenem. Ens donem suport i ens ajudem.

Compartim aficions i objectius. Riem i ens estimem. Espero continuar gaudint de la vida al teu costat.

Finalment als meus pares. Gràcies pel vostre suport incondicional, per estar sempre al meu costat, per sempre confiar amb mi. He après de vosaltres l'afany de superació i el valor de les petites coses, que em fan valorar encara més la vida. I perquè m'heu ensenyat a estimar.

Summary

The centrosome is an essential organelle for the development of a new organism in animals. Upon fertilization the spermatozoon enters into the oocyte providing the male chromosomes and its basal body, which will convert into the first centrosome of the new organism. Defects of the sperm basal body may be linked to sperm motility and morphology alterations as well as embryo early development failures, both leading to infertility.

In this thesis, I used a combination of tools and model systems to better understand the fertilization process, specifically the transition of the sperm basal body to a fully functional centrosome in the zygote and its importance in supporting early human embryo development. First, since studies on human fertilization have been hampered by ethical and technical issues alike, I developed a new approach based on the use of *Xenopus* egg extract and human spermatozoa to study the molecular events that the sperm triggers when it is placed in an oocyte cytoplasmic environment. Further to this, I used a combination of proteomics and IF analyses to define the sperm basal body composition. I determined that centrosomal proteins are biparentally inherited during human fertilization. Then, to functionally analyze the importance of inheriting the centrosome during fertilization, I set up a method in which sperm tails microsurgically separated from the DNA containing heads were injected into oocytes that were then parthenogenetically activated. The activated oocytes with a centrosome had an increased likelihood of completing pseudo-embryo compaction.

Finally, I attach two annexes: the first one summarizes the results I obtained on the distribution of tubulin post-translational modifications in sperm samples with different diagnoses. The second annex corresponds to a review that I wrote to summarize the current knowledge and to propose future perspectives on tubulin post-translational modifications, and their role in cytoskeletal function in gametes and embryos in model systems and in human reproduction.

Resum

El centrosoma és un orgànol essencial pel desenvolupament d'un nou organisme animal. En el procés de la fecundació, l'espermatozoide entra a l'oòcit proporcionant els cromosomes masculins i el seu cos basal, que es convertirà en el primer centrosoma del nou organisme. Defectes del cos basal dels espermatozoides poden estar relacionats amb alteracions de la motilitat i morfologia dels espermatozoides, així com també d'embrions que s'aturen durant el seu desenvolupament primari, provocant problemes d'infertilitat.

En aquesta tesi he combinat diferents mètodes i models animals per conprendre millor els esdeveniments que es donen lloc durant la fecundació, especificament la transició del cos basal de l'espermatozoide a un centrosoma functional en el zigot, i la seva importància durant el desenvolupament de l'embrió. Així doncs, en primer lloc, degut a que els estudis sobre la fecundació humana s'han vist obstaculitzats per qüestions ètiques i tècniques, he desenvolupat un nou sistema basat en l'ús d'extracte d'ous de *Xenopus* i espermatozoides humans per estudiar els esdeveniments moleculars que l'espermatozoide desencadena un cop es troba en el citoplasma de l'oòcit. A més, he combinat l'anàlisis per proteòmica i per immunofluorescència per definir la composició proteica del cos basal de l'espermatozoide. He pogut determinar que les proteïnes centrosomals són heredades durant la fecundació humana de manera biparental. Després, per analitzar funcionalment la importància d'heretar el centrosoma durant la fecundació, he establert un mètode en el qual les cues dels espermatozoides són microcirúrgicament separades dels caps i injectades en ooòcits que van ser activats partenogeneticament. Els oòcits activats que contenien el centrosoma tenien una major probabilitat de compactar.

Finalment, adjunto dos annexos, el primer resumeix els resultat que de moment he obtingut sobre la distribució de les modificacions postraduccionals de tubulina en mostres d'esperma amb diferents diagnòstics. El segon annex correspon a una revisió que vaig escriure on resumeixo el coneixement actual de les modificacions postraduccionals de tubulina i el seu paper en el citoesquelet de gàmetes i embrions en sistemes model i en reproducció humana, i proposo noves perspectives en la investigació d'aquests.

Preface

The work presented here is a collaborative project carried out in the basic research laboratory of Clínica Eugin and in the Cell and Developmental Biology Program at the Center for Genomic Regulation (CRG). This work has been supervised by Dr. Rita Vassena (Clínica Eugin) and Dr. Isabelle Vernos (CRG).

Fertilization is typically described as the fusion of the spermatozoon with the oocyte to form the zygote. This apparently easy step is one of the most complex but, at the same time, fascinating events that occurs in many species, including ours. First, because two highly specialized cells will produce a unique totipotent cell; second, because from this totipotent cell, a completely new organism will be formed. During the first days of embryo development many signaling cascades and cellular reorganizations take place to determine the embryo fate. Therefore, it is very important that all the processes occur in a correct and coordinated way to support the development of a healthy organism. However, the natural rate of success of this process is low, and any couples trying to conceive will experiment some difficulties. Infertility has been a focus of interest and concern throughout human history. It has been addressed in many different ways, from a religious point of view to the current scientific approach. Indeed, the desire of having a child is what ensures the persistence of our species.

The World Health Organization (WHO) recently defined the infertility as "a disease of the reproductive system defined by the failure of achieve a clinical pregnancy after one year or more of unprotected sexual intercourse". Most of these couples will need the help of Assisted Reproduction Technologies (ART) to conceive. The future of ART, in my opinion, goes through the implementation of personalized medicine to select the best treatment for each couple. Nevertheless, this can only be achieved if we first have a deep understanding of the basics of human fertilization and early development.

Abbreviations list

AID   Artificial Insemination with Donor Sperm
aMTOC   Acentriolar Microtubule Organizing Center
ART   Assisted Reproduction Technologies
ASRM   American Society for Reproductive Medicine
ATP   Adenosine Triphosphase
cAMP   Cyclic Adenosine Monophosphate
CatSper   Cation Channels of Sperm
CFP   Cyan Fluorescent Protein
CSF   Cytostatic Factor
DNA   Deoxyribonucleic Acid
DTT   Dithiothreitol
FSH   Follicle Stimulating Hormone
G1 phase   Gap 1 phase
G2 phase   Gap 2 phase
GC   Giant Centriole
GCPx   Gamma Tubulin Complex Protein x
GDP   Guanosine Diphosphate
GFP   Green Fluorescent Protein
GTP   Guanosine Triphosphate
γ-TuRC   Gamma Tubulin Ring Complex
γ-TuSC   Gamma Tubulin Small Complex
ICM   Inner Cell Mass
ICSI   Intracytoplasmic Sperm Injection
IF   Immunofluorescence
IUI   Intrauterine insemination
K-fibers   Kinetochore Fibers
LB   Loading Buffer
LH   Luteinizing Hormone
M phase   Mitotic phase
MAP   Microtubule Associated Proteins
MI oocyte   Meiosis I oocyte
MII oocyte   Meiosis II oocyte
mRNA   messenger RNA
MTOCs   Microtubule Organizing Centers
NEBD   Nuclear Envelope Breakdown
NES   Nuclear Export Signal
NLS   Nuclear Localization Signal
NPC   Nuclear Pore Complex
NTF   Nuclear Transport Factors
ODF   Outer Dense Fibers
PBS   Phosphate-Buffered Saline
PBS-T   Phosphate-Buffered Saline with Tween

PBS-TB	Phosphate-Buffered Saline with Tween and BSA
PCL	Proximal Centriole Like
PCM	Pericentriolar Material
PFA	Paraformaldehyde
PN	Pronuclear/ Pronucleus
PTMs	Post-translational modifications
PZD	Partical Zona Dissenction
RanGAP	Ran GTPase Activating Protein
RNA	Ran Guanine nucleotide Exchanging Factor
SDS-PAGE	Sodium Dodecyl Sulfate Polyacrylamide Gel Electrophoresis
STED	Stimulated Emission Depletion
TBS	Tris-Buffered Saline
TCA	Trichloroacetic Acid
TE	Trophectoderm
TP	Transition Nuclear Proteins
TZP	Transzonal Projections
WHO	World Health Organization
XEE	*Xenopus* Egg Extract
ZPG	Zona Pellucida Glycoproteins

Glossary

In this section, terminologies relevant for this thesis are outlined. Most of them are taken from the "International Glossary on Infertility and Fertility Care, 2017" (Zegers-Hochschild et al., 2017), and are accepted as consensus definitions.

Aneuploidy: an abnormal number of chromosomes in a cell. The majority of embryos with aneuploidies are not compatible with life.

Asthenozoospermia: reduced percentage of motile sperm in the ejaculate below the lower reference limit. When reporting results, the reference criteria should be specified.

Blastocyst: the stage of preimplantation embryo development that occurs around day 5-6 after insemination of ICSI. The blastocyst contains a fluid filled central cavity (blastocoele), and outer layer of cells (trophectoderm) and an inner group of cells (inner cell mass).

Blastomere: a cell in a cleavage stage embryo.

Centrosome: the main microtubule organizing center of the cell.

Centrosome reduction: a process during spermatogenesis in which most of the sperm centrosomal proteins are eliminated and centrioles modified.

Cleavage stage embryos: embryos beginning with the 2-cell stage and up to, but not including, the morula stage.

Compaction: the process during which tight junctions form between juxtaposed blastomeres resulting in a solid mass of cells with indistinguishable cell membranes.

Embryo: the biological organism resulting from the development of the zygote, until eight completed weeks after fertilization, equivalent to 10 weeks of gestational age.

Fertilization: a sequence of biological processes initiated by entry of a spermatozoon into a mature oocyte followed by formation of the pronuclei.

Genome Activation: during embryo early development, when they release from transcription silencing.

Germinal Vesicle: the nucleus in an oocyte at prophase I.

Hatching: the process by which an embryo at the blastocyst stage extrudes out of, and ultimately separates from, the zona pellucida.

Implantation: the attachment and subsequent penetration by a zona-free blastocyst into the endometrium, but when it relates to an ectopic pregnancy, into tissue outside the

uterine cavity. This process starts 5 to 7 days after fertilization of the oocyte usually resulting in the formation of a gestation sac.

In vitro **fertilization (IVF):** a sequence of laboratory procedures that enable extracorporeal fertilization of gametes. It includes conventional *in vitro* insemination and ICSI.

Inner cell mass: a group of cells attached to the polar trophectoderm consisting of embryonic stem cells, which have the potential to develop into cells and tissues in the human body, except the placenta or amniotic membranes.

Intracytoplasmic sperm injection (ICSI): a procedure in which a single spermatozoon is injected into the oocyte cytoplasm.

Mature oocyte: an oocyte at metaphase of meiosis II, exhibiting the first polar body and with the ability to become fertilized.

Microtubule Organizing Centers: structures within the cell that have the capacity to organize microtubules.

Morula: an embryo formed after completion of compaction, typically 4 days after insemination or ICSI.

Normozoospermia: ejaculated sperm with motility, morphology and concentration values above the reference limits.

Oligozoospermia: low concentration of spermatozoa in the ejaculate below the lower reference limit. When reporting results, the reference criteria should be specified

Oocyte: the female egg.

Ovulation: the natural process of expulsion of a mature egg from its ovarian follicle

Parthenote: the product of an oocyte that has undergone activation in the absence of the paternal genome, with (induced) or without (spontaneous) a purposeful intervention.

Parthenogenetic activation: the process by which an oocyte is activated to undergo development in the absence of fertilization.

Pre-implantation embryo: an embryo at a stage of development beginning with division of the zygote into 2 cells and ending just prior to implantation into a uterus.

Pronucleus: a round structure in the oocyte surrounded by a membrane containing chromatin. Normally, two pronuclei are seen after fertilization, each containing a haploid set of chromosomes, one set from the oocyte and one from the sperm, before zygote formation.

Spermatozoon: the mature male reproductive cell produced in the testis that has the capacity to fertilize an oocyte, A head carries genetic material, a midpiece produces energy for movement, and a long, thin tail propels the sperm.

Syngamy: the process during which the female and the nuclei fuse.

Teratozoospermia: a reduced percentage of morphologically normal sperm in the ejaculate below the lower reference limits. When reporting results, the reference criteria should be specified.

Zona pellucida: the glycoprotein coat surrounding the oocyte.

Zygote: a single cell resulting from fertilization of a mature oocyte by a spermatozoon and before completion of the first mitotic division.

Table of contents

List of figures

List of tables

I. A Short journey through the history of human (in)fertility:

A. In the ancient Egypt:

Fertility played a major part in the ancient Egyptian culture. Indeed, Khonsu was the god of fertility, and Nephtys the one for infertile women. Many amulets were carried by women in order to promote fertility, and statues of a woman carrying a baby were found in women tombs. It is thought that these statues were symbols of fertility for the next life (Morice et al., 1995) **(Figure 1A)**. Egyptians also wrote a complete medical gynecological text, the Kahun papyrus. In this text, the Egyptians detailed, among other concepts, methods to diagnose pregnancy and infertility. Two common early pregnancy diagnosis methods were the followings: 1) to mix the woman urine with grains of wheat. If the grains opened, it was a synonym that the woman was pregnant. 2) To introduce an onion bulb in the woman's vagina during the night. If the woman's breath had an onion smell the next day, she was pregnant (Haimov-Kochman et al., 2005). In ancient Egypt, the legal status of women was the same as men; they did not consider that all the cases of infertility were of female origin (Morice et al., 1995). Interestingly, Egyptians did not consider infertility as a divine punishment, in contrast with other cultures. Thus, the ancient Egypt society was interested in studying and understanding both fertility and infertility problems.

B. The Hebrews:

In the ancient Hebrew society, procreation was considered as a blessing in the Old Testament, and it was the main purpose of a marriage. Indeed, if a couple did not have children after 10 years of marriage, the husband could divorce. If not, polygamy was presented as a solution. In this society, women had very few rights. A barren woman was seen as inferior and had a reduced status, whereas male infertility was not even considered (Morice et al., 1995). In the Old Testament the use of "love plants" is mentioned as a natural remedy to cure infertility. One of these plants is the mandrake, whose root has the shape of a human body **(Figure 1B)**. Therefore, infertility in the ancient Hebrew society was seen as a divine punishment to the couple, and the knowledge about fertility and infertility was very limited.

C. The Greeks:

In ancient Greece, the goddess Aphrodite did not only represent beauty and love, but also fertility. It was in this time period that a big number of medical books were written. They are known as the "Hippocratic Corpus" and consist of a group of 60 medical books addressing different diseases (Flemming, 2013). Some of the books addressed specifically gynecological and obstetrical pathologies (Morice et al., 1995). In these books different infertility causes and treatments were described, some of them based on the Egyptians methods. Hippocrates of Cos was the most famous physician of that era. He described that infertility may be caused by various pathologies: the malposition of the cervix, the obstruction of the orifice of the uterus, an excessive menstrual flow, the softening of the inside of the cavity and uterine prolapse; and there were treatments to cure some of these pathologies, such as the insertion of a hollow tube to dilate the cervix (Morice et al., 1995). Despite the interest of the Greeks in infertility from a medical point of view, for some philosophers such as Aristotle, women were seen as a simple receptacle for the fertilizing spermatozoa. However, it was also accepted that infertility could be of either male or female origin (Flemming, 2013; Morice et al., 1995).

D. The Romans:

In contrast with the previous cultures, Romans thought that during procreation both partners contributed to the child formation by producing semen mixed in the woman womb (Rawson and Australian National University., 1986). It was common for women who wanted to get pregnant to visit Juno's temple, the goddess of childbirth and fertility. The priests of this temple hit the belly of the infertile women with a goatskin whip (Morice et al., 1995). Beside this, the gynecologist Sorano of Ephesus distanced his work from the religion. He hypothesized that the best moment for conception was just after menstruation, although we now know that this is not correct. Galien, another gynecologist, implemented the vaginal palpation during clinical examination and believed that the moon cycle had an effect on the feminine cycle. However, no big advances on the treatment of infertility were achieved during the Ancient Roman times.

E. The Arabs:

The Ancient Arab society (700 – 1200 AC) is known for their high knowledge in medicine and science, as they integrated concepts from the ancient Greeks, Romans, and Persians among others. However, they did not provide major advances in the area of (in)fertility. Rhazes and Avicenna were the two physicians that contributed more to infertility treatments. Rhazes suggested that obesity could be one of the causes of infertility in women. Avicenna proposed that infertility could originate from both the male and the female, and probably due to abnormalities in the "sperm" produced by both (Morice et al., 1995).

F. The Middle Ages:

The concept of fertility and human reproduction throughout the Middle Ages can be found in several literary works. For example, in the "Divine Comedy" work, Dante Alighieri raised the hypothesis that the sperm is formed from the blood: the food we eat would be first converted into blood in the heart and then into sperm when it arrives at the testicles. When the sperm derived from blood mixed with the female blood (menstruation), a clot would form, and will become the fetus (Locatelli et al., 2015). Again, during this period, women were considered as a passive participant in the process of procreation, whose main function was to carry the future newborn. Infertility was also believed to be a form of divine punishment, and the treatments were mainly based on rites or superstitions. Obesity, excess of humidity and heat were thought to be some of the causes of infertility and therefore diets to maintain the corporal temperature were used as an infertility treatment (Morice et al., 1995).

G. From the Renaissance to the early twentieth century:

The Renaissance was a period of strong scientific progress, especially in the actual Italy. Leonardo da Vinci (Italy, 1452 – France, 1519), between the years 1510 – 1512, drew in his private notebooks a human fetus in the uterus **(Figure 1C)**. Da Vinci is considered to be the very first person in history to determine the correct position of the fetus within the uterus (Leonardo et al., 1952). His interest in the anatomy of the reproductive system and the fetus was shared with other intellectuals of that time. André Vesale (Belgium, 1514 – Greece, 1564) drew the female pelvis, Bartolomeo Eustachio (Italy, between the 1500 and the 1514 – 1574) the uterus and its vessels, Gabriel Fallope (Italy,

1523 – 1574) described the Fallopian tubes, together with the clitoris, vagina and the placenta. In 1672, Regnier de Graaf (Netherlands, 1614 – 1673) described the ovary and the follicular function. In the 18th century, Antonie van Leeuwenhoek (Netherlands, 1632 – 1723) invented the microscope and discovered the spermatozoon **(Figure 1D)** describing spermatozoa of approximatley 30 species. In agreement with the preformationism theory, van Leeuwenhoek affirmed that each spermatozoon was carrying a small human, which was then transferred to the woman to grow. Nicolaas Hartsoecker (Netherlands, 1656 – 1725) shaped this idea in his famous spermatozoon draw in 1695 **(Figure 1E)** (Brinsden and Bourn Hall Clinic., 1999; Morice et al., 1995). However, there were only a few advances in the diagnosis and treatment of infertility. Bartolomeo Eustachio recommended that placing the husband fingers in the vagina after the sexual intercourse enhanced the probabilities of pregnancy. Johannes De Ketham (Germany, 1415 – Hungary, 1470) proposed the use of rabbit saliva as a method to cure infertility. Ambroise Paré (France, 1510 – 1590) used a vaginal dilator to treat infertile women. Several authors, such as François Blondel (1603 – 1703) published that obese women were less fertile compared with thin women. However, new medical concepts emerged in the 18th century. Ovarian sclerosis and tubal blockages, follicular absence or agenesis, abnormalities of the vagina, uterine aplasia and leukorrhoea were described and considered as possible causes of infertility. During the 19th and the beginning of the 20th century notable progresses in medicine were achieved including cervix dilatation, correction of the uterine malpositions and the use of thyroid extract. In 1868, J. Marion Sims (U.S. 1813 – 1883) published the book "The Microscope as an Aid in the Diagnosis and Treatment of Sterility" and emphasized the importance of analyzing the quality of the sperm sample under the microscope. In 1884, William Pancoast (U.S., 1839 – 1923) performed the first human AID (Artificial Insemination with Donor sperm). The biological and medical area of endocrinology started to be studied and, in 1928, Selman Aschheim (Germany, 1878 – France, 1965) and Bernhard Zondek (Germany, 1891 – U.S., 1966) managed to induce ovarian stimulation using gonadotropins. All these progresses throughout the 18th, 19th and early 20th centuries were crucial to establish the basis for infertility diagnosis and treatments including the IVF techniques that we are using nowadays (Morice et al., 1995).

H. The twentieth and twenty-first centuries:

The late twentieth and the twenty-first centuries are characterized by the acquisition of women's rights. In developing countries, infertility is no longer seen as only caused by women issues, marriage is not anymore the synonym of procreation and as a consequence of the access of women to university, education and the job market the decision of having children is delayed or takes a second role. All these factors, together with others such as anatomical, genetic and changes in the lifestyle, resulted in an increase of the infertility rate. In parallel, a revolution occurred concerning ART. In 1959, Min Chueh Chang (China, 1908 – U.S., 1991) performed successfully the first *in vitro* fertilization (IVF) in rabbits (Chang, 1959). A few years later, in 1973, Carl Wood (Australia, 1929 – 2011) and John Leeton (Australia) achieved the first human IVF pregnancy, although the pregnancy did not progress after a week. Three years later, Patrick Steptoe (UK, 1913 – 1988) and Robert Edwards (UK, 1925 – 2013) reported an IVF cycle with an ectopic pregnancy (abnormal attachment of the embryo in the uterus/Fallopian tubes). Finally, in 1976, the same scientist performed the first successful IVF cycle. Lesley Brown got pregnant and gave birth on the 26th of July to the first IVF child, Louise Brown (Steptoe and Edwards, 1978; Kamel, 2013). Due to the establishment of this new technology, Robert Edwards won the Nobel Prize in Physiology or Medicine in 2010 for the "Development of human in vitro fertilization (IVF), a medical advance that represents a paradigm shift in the treatment of many types of infertility". In 1992, Palermo established the ICSI method (Intracytoplasmic Sperm injection), based on the injection of an individual sperm cell into an oocyte (Palermo et al., 1992; Palermo et al., 1993).

To conclude, fertility and infertility problems are topics that have been reiterative throughout human history. They have been addressed in many different ways, but it was not until recently that we gained sufficient biomedical knowledge and new technologies to study them. However, there is still a long path to unravel human reproduction and infertility problems.
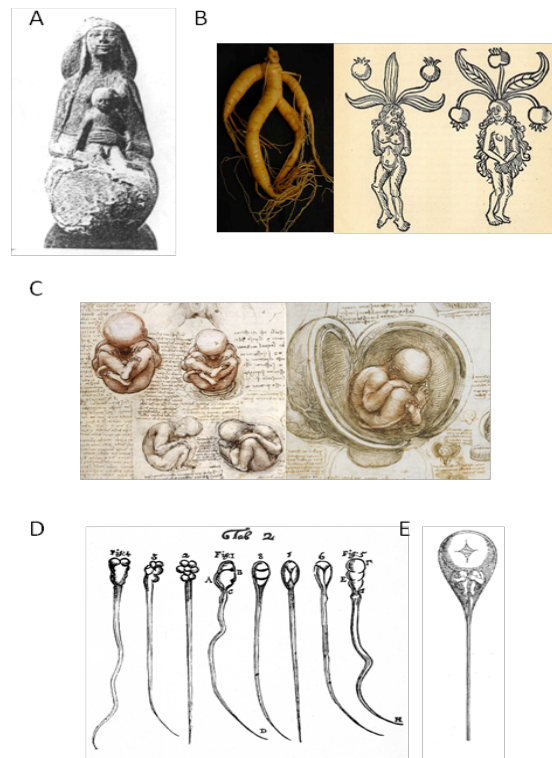
Figure 1: Historical Illustrations related to (in)fertility. A) Egyptian Woman Statue with a child. This type of statue was often found inside tombs. They were expected to provide fertility in the next life. Image obtained from Morice et al., 1995. **B)** Mandrake. The image on the left is the root of the mandrake plant. On the right, human figures associated with the mandrake root. Image source: Health Science Learning Center. University of Wisconsin. **C)** Human fetus drawn by Leonardo da Vinci. Image source: Royal Collection Trust. **D)** Antonie van Leeuwenhoek studied the morphology of spermatozoa from more than 30 species. These drawings are from his original studies. From 1 to 4, rabbit spermatozoa; from 5 to 8, dog spermatozoa. Image source: Smithsonian Museum. **E)** Nicolaas Hartsoecker shaped the preformationism theory in this illustration, in which a human fetus is drawn into a spermatozoon. Image source: Science communication blog: http://web.expasy.org

II. Microtubules and spindle assembly:

A. Microtubule dynamics:

Microtubules are intracellular cylindrical filaments involved in many functions. They are one of the elements of the cytoskeleton, together with the actin fibers and the intermediate filaments. Some of the cellular roles of the microtubules include cell division, cellular movement and intracellular organization.

Microtubules are hollow polymers composed of α- and β-tubulin dimers. α- and β-tubulin dimers are very similar in terms of structure and size (Nogales et al., 1998). The self-assembly of the α- and β-tubulin dimers results in polarized protofilaments that form the microtubule through lateral interactions. In mammals, most of the microtubules are composed of 13 protofilaments (**Figure 2**). However, this number can be variable in some species and *in vitro* microtubules can have between 12 to 17 protofilaments (Chretien and Wade, 1991). The protofilaments are organized in the so-called "B-lattice" structure, in which contacts occur with the same α or β monomer, with the exception of one protofilament, in which the interaction is α-β, known as "seam"; hence microtubule polymers are not completely symmetric (McIntosh et al., 2009). As mentioned before, microtubules are polarized structures. One end has an exposed α-tubulin (the minus-end) whereas the other has an exposed β-tubulin (the plus-end). This feature provides different dynamic characteristics to each end and a polarity that can be read by molecular motors.

Tubulins are intrinsically bound to GTP or GDP. α- and β-tubulin dimers have two GDP/GTP binding sites, one in the α-tubulin subunit (N or non-interchangeable site) and another in the β-tubulin subunit (E or exchangeable site). Free tubulin dimers have a GDP nucleoside in the E site, and a non-interchangeable GTP, at the N-site. When GDP is exchanged by GTP at the E site on β-tubulin, the dimer is competent for addition to the microtubule plus-end (Alushin et al., 2014). Once new heterodimers are incorporated to the growing microtubule end, GTP hydrolysis occurs at the E site so the lattice of the microtubule is formed by β-tubulin bound to GDP. This process induces a conformational change within the microtubule structure that confers instability to the growing microtubule while protecting it from depolymerization through the presence of the so-called GTP cap (Alushin et al., 2014; Nogales et al., 1999).

Microtubules are dynamic filaments; they can grow or shrink. This is probably the most interesting feature of the microtubules, which is still understudied because of its complexity. Already in 1986 Horio and colleagues observed that the microtubule minus and plus-ends have different kinetics of growing (occurring preferentially at the plus-end) and shrinking (Horio and Hotani, 1986).

Between the 60s and the 90s, a series of observations lead Mitchison and Kirschner to propose the concept of "Dynamic instability of microtubule growth". These observations were the followings:

1. When α/β-tubulin dimers are GTP bound, microtubule growth (or polymerization) is promoted.

2. When α/β-tubulin dimers are GDP bound (at the E site), microtubule shortening (or depolymerization) is promoted. This concept is known as catastrophe.

3. A GTP-cap is present at the microtubule plus-end.

4. In the same microtubule population, some microtubules can grow whereas others can shrink.

Taking all these data together, Mitchison and Kirschner proposed that microtubules have the dynamic capacity to polymerize and depolymerize constantly and that, depolymerization occurs when the GTP-cap is lost (Mitchison and Kirschner, 1984) **(Figure 2)**. Hence, a microtubule maintains its capacity to grow as long as it has a GTP-cap. A shrinking microtubule can grow again if a "rescue" occurs. Few year later, Verde and colleagues (Verde et al., 1992) postulated that the size of a microtubule population (L) can be described through a mathematical formula that considers four parameters: the velocity of growth (Vg), the velocity of shrinkage (Vs) and the frequencies of catastrophe (Fcat) and rescue (Fres).

$$L = (VgFres - VsFcat) / (Fcat+Fres)$$

Interestingly, several Microtubule Associated Proteins (MAPs) modulate these parameters and define microtubule dynamics. For instance, XMAP215 (*Xenopus laevis* Associated Protein 215) increases microtubule elongation and shortening velocity mainly at the plus-end; therefore, microtubules are more dynamic in the presence of XMAP215 protein *in vitro* (Gard and Kirschner, 1987; Vasquez et al., 1994).
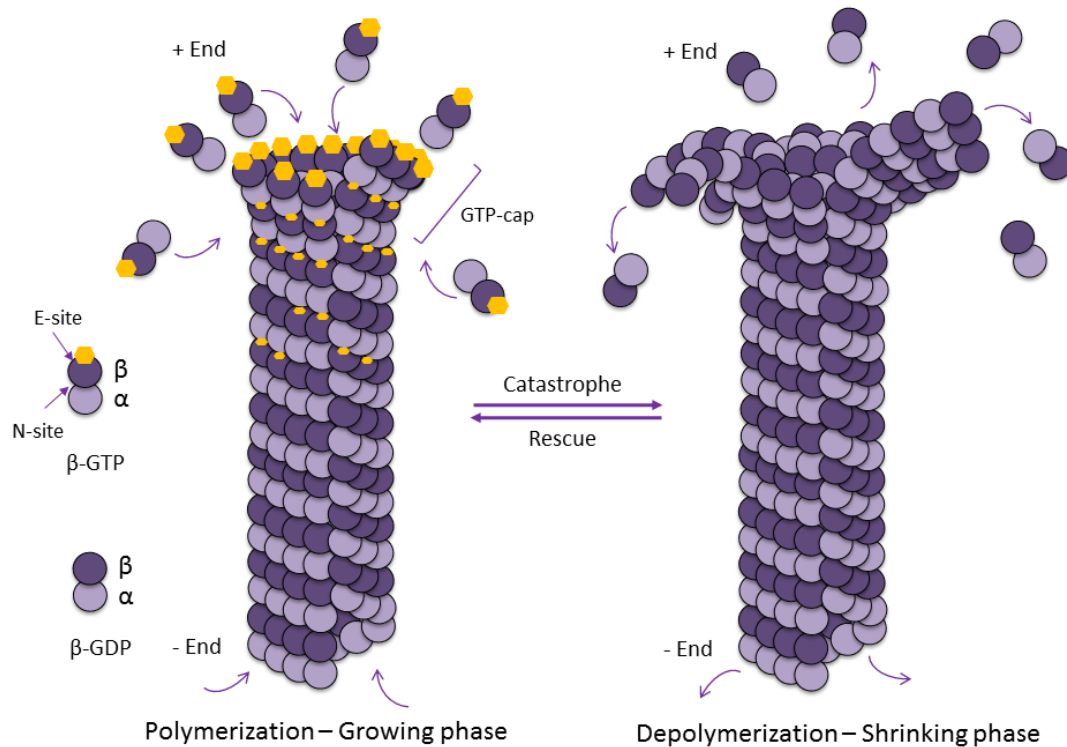
Figure 2: Microtubule dynamic instability. Microtubules are polarized hollow polymers composed of the head-to-tail association of α- and β-tubulin heterodimers forming a protofilament. In most mammals, microtubules are formed by the lateral interaction of 13 protofilaments. Because of microtubules are polymerized structures, the minus and plus-ends have different kinetics (the minus-end (α-tubulin) is less dynamic than the plus-end (β-tubulin)). There are two main types of interactions within the microtubule, the lateral and the longitudinal (interdimer interface). The lateral interactions are less strong compared with the longitudinal ones. Microtubules can grow and shrink stochastically. The switching between the two phases is mainly driven by the β-tubulin monomer capacity to hydrolyze the GTP. β-tubulin is GTP bound when it is incorporated to the microtubule forming a GTP-cap at the microtubule plus-end that prevents microtubule depolymerization. Upon the addition of sequential microtubule dimers, the GTP is hydrolyzed to GDP inducing a conformational change that destabilizes the microtubule lattice. When this GTP cap is lost, the microtubule becomes unstable and depolymerize. A depolymerizing microtubule can be rescued and grow again.

Many structural analyses have been performed to study how the GTP to GDP transition affects the microtubule structure to promote depolymerization. When GTP is hydrolyzed, α-tubulin compacts slightly and the longitudinal microtubule structure is in an unfavorable "intermediate" state reminiscent of the active microtubule depolymerization structure (Alushin et al., 2014; Mitchison, 2014; Ravelli et al., 2004). Next, the plus-end curls outward promoting the lateral destabilization of the protofilaments, whereas the longitudinal ones are maintained. Finally the microtubules are disassembled into α-β oligomers and dimers (Alushin et al., 2014; Mandelkow et al., 1991). As microtubules are polarized filaments, each microtubule end (plus and

minus) has different kinetics of polymerization/depolymerization. Plus-ends are more dynamic compared with minus-ends.

Beyond the mechanistic description of the "microtubule dynamic instability properties", why is this important for the cell? First, because it allows the rapid reorganization of the microtubule network (Burbank and Mitchison, 2006). Therefore, the cytoskeleton and the cell can adapt rapidly to external and internal signals. For example, microtubule dynamics is crucial for the rapid transitions between interphase and mitosis. Second, microtubules are involved in cellular migration (Etienne-Manneville, 2004). Although the main cellular components responsible for cell migration are the actin filaments through the formation of filopodia and lamellipodia, when the microtubule dynamics are perturbed, lamellipodia formation is inhibited, and therefore, cell motility is impaired (Liao et al., 1995). And third, microtubules give shape to the cell and their dynamics favors the rapid transition and adaptability to different cell shapes.

Microtubules can spontaneously polymerize *in vitro* by incubating only a few components: tubulin dimers, GTP and Mg^{2+} ions. However, polymerization only occurs above a critical tubulin concentration that is above physiological levels. In mammalian cells, the tubulin concentration is around 25μM. Therefore, additional mechanisms exist in the cell to promote microtubule nucleation under physiological conditions, and the most studied one involves the γ-tubulin complex.

B. Microtubule nucleation:

1. Microtubule nucleation complexes:

Because of the intrinsic high dynamicity of the microtubules, the cell has developed a machinery that promotes and defines microtubule nucleation in time and in space and constricts the number of protofilaments. This involves a γ-tubulin complex which is the main driver of microtubule nucleation acting as a seed. This "seed" is the γ-TuRC (γ-Tubulin Ring Complex). This complex is formed by the interaction of 6 different components: γ-tubulin, GCP2 (γ-tubulin complex protein 2), GCP3, GCP4, GCP5 and GCP6. A minimal subcomplex (also known as the core machinery of the γ-TuRC), the γ-TuSC (γ-Tubulin Small Complex) consists of 2 γ-tubulin units and CGP2 and CGP3 **(Figure 3A)**. Although both the γ-TuSC and the γ-TuRC can nucleate microtubules, the

γ-TuSC nucleates less microtubules than the γ-TuRC (Oegema et al., 1999), suggesting that the whole complex is not essential, but it is necessary to efficiently nucleate microtubules *in vivo*. Furthermore, some specific components of the γ-TuRC (GCP4, GCP5, GCP6) are important for the localization of the complex to different microtubule organizing centers (MTOCs) of the cell.

The γ-TuRC is composed of 13 γ-tubulin subunits forming an open ring structure of 25nm in diameter that caps the microtubule minus-end. It was characterized the same year in *Drosophila* (Moritz et al., 1995) and in *Xenopus laevis* oocytes (Zheng et al., 1995). In 2010, the γ-TuSC structure was resolved by cryo-electron microscopy (Kollman et al., 2010). Kollman and colleagues observed that the γ-TuSC can assemble 13 protofilament-like structures. All these data suggest that the γ-TuRC can act as a microtubule-nucleating template, where α- and β-tubulin dimers can be subsequently added, defining the number of protofilaments per microtubule **(Figure 3A)**.

More components of the γ-TuRC were identified that do not belong to the GCP protein family: Mozart 1 and 2 (Mitotic-spindle organizing protein associated with a ring of γ-tubulin) (Teixido-Travesa et al., 2010) (Cota et al., 2017) and NEDD1 (Neural precursor cell extressed developmentally down-regulated protein 1) (Luders et al., 2006). Their role within the γ-TuRC is to regulate its localization and activation (Cota et al., 2017; Kollman et al., 2011; Teixido-Travesa et al., 2010). For instance, Mozart 1 recognizes the fully assembled γ-TuRC and mediates γ-TuRC interaction with NEDD1 (Cota et al., 2017), which is the main γ-TuRC targeting factor. In mitosis, the phosphorylation of NEDD1 on different sites regulates the targeting of γ-TuRC to different MTOCs (Microtubule Organizing Centers) (centrosome, chromatin and pre-existing microtubules).

The γ-TuRC complex localizes to the different MTOCs, where it is the main microtubule nucleation complex. In the following section, I will discuss the main MTOCs identified so far.

2. Microtubule Organizing Centers of the Cell:
While the centrosome is recognized as the main MTOC of the cell, many other subcellular structures have the capacity to organize microtubules such as the Golgi

apparatus, the mitotic chromosomes, the mitochondria, the nuclear envelope and the cell cortex.

- **The centrosome:** the centrosome is the main MTOC of the cell **(Figure 3B)**. It is composed of two centrioles surrounded by pericentriolar material (PCM). Both components of the centrosome, the centrioles and the PCM are important for its microtubule nucleation activity. Centrioles are barrel shaped microtubule structures oriented perpendicularly to each other. The PCM is comprised by a mass of proteins important for different centrosomal activities, such as centrosome duplication and microtubule assembly. The process of centrosome maturation occurs as the cell prepares to enter mitosis. Centrioles acquire PCM components and their microtubule nucleation activity increases. Centrioles can also act as a template for cilia and flagella. In the following section I will explain and discuss further this exciting non-membranous structure.

- **The Golgi apparatus:** the Golgi apparatus is typically known for its role in protein biogenesis. Golgi receives proteins packaged into vesicles from the Endoplasmic Reticulum. The main function of the Golgi is to modify these proteins and sort them to be distributed to specific intracellular localizations or to the extracellular space. However, in 2001 Chabin-Brion and colleagues discovered that the Golgi apparatus is the second source of microtubule nucleation in interphase cells (Chabin-Brion et al., 2001) **(Figure 3C)**. To give a brief mechanistic explanation, AKAP450 (A-Kinase anchoring protein 450) protein accumulates at the cis-Golgi membrane though its interaction with the Golgi protein GM130 (Golgi Matrix protein 130kDa). This protein has a structure very similar to pericentrin. It recruits CDK5RAP2 (CDK5 regulatory subunit-associated protein 2 or centrosomin) and myomegalin, and this complex is able to recruit γ-TuRCs to the cis-Golgi side, stimulating microtubule nucleation (Wu et al., 2016). Recently it was also observed that the Golgi apparatus contributes to mitotic spindle assembly (Wei et al., 2015).

- **The mitotic chromosomes:** in mitosis, chromatin was found to trigger microtubule assembly (Karsenti et al., 1984a) and meiotic and mitotic spindle

assembly without the need of any other MTOC (Holubcova et al., 2015) **(Figure 3D).** It was then found that it is dependent on the formation of RanGTP in the proximity of the chromatin, hence often called the chromatin driven microtubule assembly pathway. When the cells enter into mitosis, the nuclear envelope breaks down (NEBD) and the nuclear and cytoplasmic material mix. Because RCC1, the Ran exchange factor, is associated with the chromatin, a RanGTP gradient forms centered on the chromatin. This results in the release of spindle assembly factors (SAF) in the vicinity of the chromatin promoting microtubule nucleation and spindle assembly. This pathway will be further commented in chapter II.D.

- **Mitochondria:** the role of the mitochondria as an MTOC has been only described in *Drosophila* spermatozoa (Chen et al., 2017) **(Figure 3E)**. γ-TuRC is recruited to the *Drosophila* spermatozoa mitochondria trough a testis specific centrosomin splice variant. This MTOC activity is important to support spermiogenesis, which is the last step of spermatogenesis, when the sperm tail is formed (Chen et al., 2017).

- **Nuclear Envelope:** in some specific cells such as plant cells (cells without centrosomes) or animal muscle cells (differentiated cells), the nuclear envelope can act as an MTOC. PCM and/or γ-TuRC proteins, such as Mozart, localize to the nuclear envelope and anchor the γ-TuRC **(Figure 3F)**. However, in most of the cells this is not the main microtubule nucleation pathway (Wu and Akhmanova, 2017).

- **Cell cortex:** there are some controversies on whether the cell cortex can also function as an MTOC or it only captures and anchores microtubules (Paz and Luders, 2018). In cells with apico-basal polarity, such as human epithelial cells, microtubules have a longitudinal organization with their minus-ends anchored to the apical side. This organization is important to maintain cell polarization (Wu and Akhmanova, 2017). γ-TuRC was found to be anchored to the apical cortex, however the exact mechanism is not known (Brodu et al., 2010) **(Figure 3G)**.
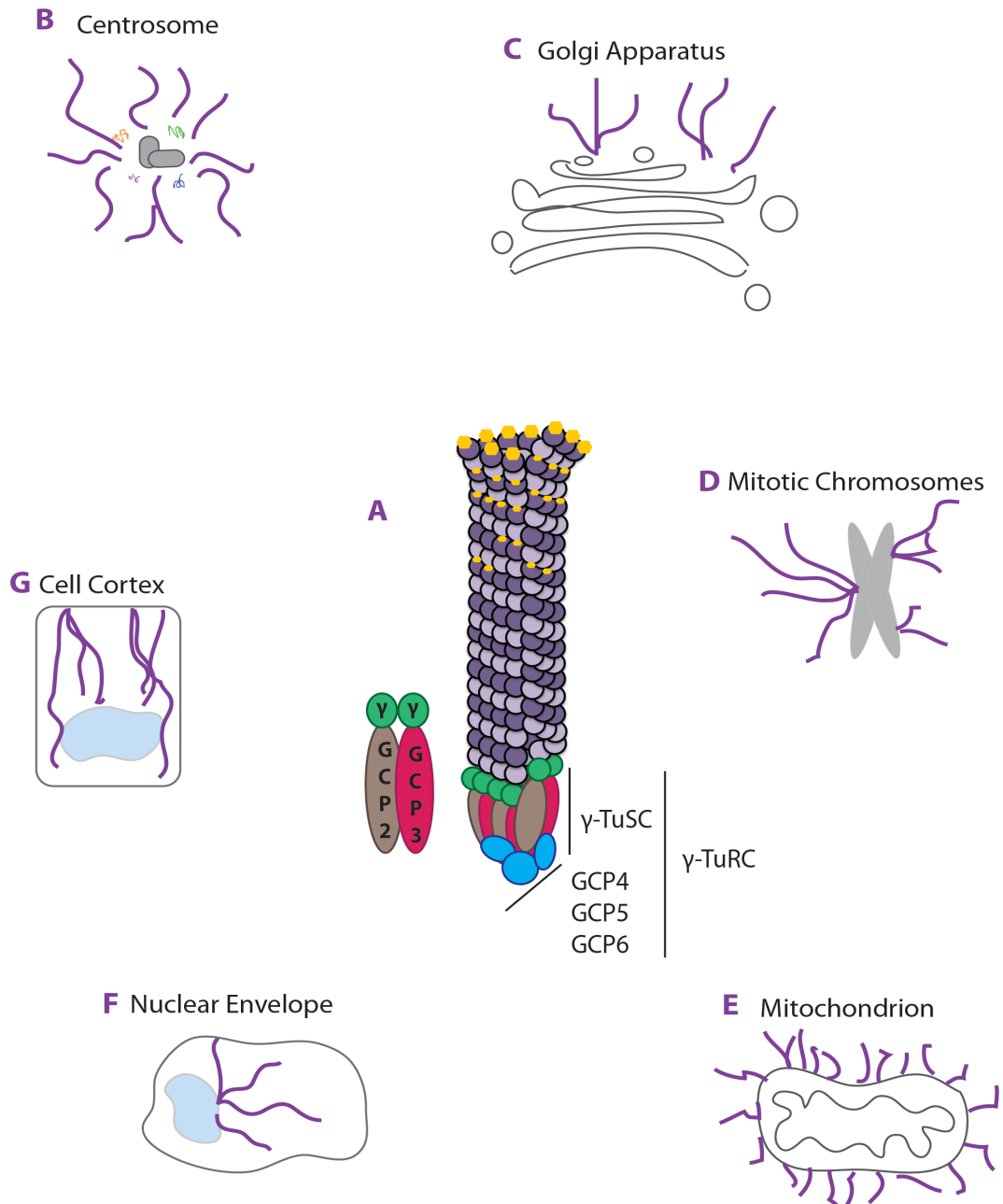
Figure 3: γ-tubulin complexes and MTOCs. A) The γ-TuRC complex is formed by a variety of proteins that organize a cylindrical structure. On the top of this structure**,** α- and β-tubulin dimers can be subsequently added establishing the characteristic 13-protofilament microtubule organization. These γ-TuRC complexes localize to the different cellular MTOCs, where they nucleate microtubules. In this representation, γ-tubulin, GCP2 and GCP3 are depicted in green, brown and red, respectively. GCP4 to 6 are in blue and α- and β-tubulin in purple. **B – G)** Main cellular MTOCs described so far. These MTOCs are the centrosome, the Golgi apparatus, the chromosomes, the mitochondria, the nuclear envelope and the cell cortex. The centrosome is the main MTOC in most of cells and organisms, whereas the Chromosomes can trigger the meiotic and mitotic spindle assembly without the contribution of the centrosome. Microtubules are represented as purple filaments.

C. The centrosome:

<u>1. Initial studies on the centrosome:</u>

In the late 19th century, two scientists, Edouard van Beneden and Theodor Boveri were independently studying the early mitotic divisions after fertilization in the nematode *Parascaris quorum*. In 1887, both scientists observed a structure at the spindle poles. Edouard van Beneden named it *corpuscule central* and Boveri *centrosome*. Boveri, who was at that time a postdoctoral researcher at the Zoological Institute in Munich, dedicated all his life to the study of this cellular organelle. He used to define the centrosome as "the true division organ of the cell; it mediates the nuclear and cellular division" (Scheer, 2014). But not only he discovered the centrosome as an organelle, but also published some observations that are still under study:

- The centrosome is maintained throughout the cell cycle.
- It duplicates and separates.
- It can form and organize the mitotic spindle.
- It defines the axis of cell division.
- Abnormal centrosome numbers cause abnormal mitotic spindles and cell divisions.
- At the center of the centrosome, there is a structure that he named *centriole*.
- Centrosomes are not essential, but they help to establish the bipolar spindle. He suggested that the centrosome is "the most elegant solution to a problem that can also be solved in other and probably multiple other ways".

One observation that Boveri did in 1888 is of special interest for this thesis. During that year, he was a visiting scientist in the Zoological Station in Naples. There, he started to study the process of fertilization in sea urchin. He observed that, after fertilization, a microtubule aster forms around the sperm midpiece (where the centrosome is located). This was the first hint that the centrosome can be inherited from the spermatozoon during fertilization.

Boveri, therefore, defined the main principles in the field of centrosome biology; but he also contributed to other scientific areas. For example, he contributed to the development of the chromosome theory of inheritance (Satzinger, 2008; Wunderlich,

2002). A special mention should also be made of his co-worker and wife, Marcella O'Grady Boveri. Originally from Boston, she was the first woman graduated in biology at the Massachusetts Institute of Technology (MIT), as well as one of the first women to be accepted in a German university (Satzinger, 2008). Although she is not recognized as a co-author of her husband discoveries, she contributed experimentally and intellectually to most of his investigations. Hence, in my opinion, taking into account the limited technologies they had at the time, I think that the Boveri couple (also known as "The Boveries") was scientifically exceptional.

<u>2. The centrosome structure and composition:</u>

The centrosome has typically two centrioles (the mother and the daughter) surrounded by an electro-dense material called the PCM. When no centrioles are present, an acentriolar MTOC (aMTOC) may form. The centrioles are cylindrical structures composed of 9 microtubule triplets. The diameter of the centrioles is around 250nm and their length varies from 150 to 500nm depending on the cell type (Winey and O'Toole, 2014) **(Figure 4)**. However, if we look closely at its structure, additional elements can be defined: the appendages, the intercentriolar linker and the cartwheel structure.

- **Centriolar microtubules:** each centriole is formed by microtubule doublets (A and B) at its distal part and microtubule triplets (A, B and C) at its proximal part **(Figure 4)**. Why this polarity? We really do not know. However, what we know is that the proximal part is enriched in PCM and it is where the cartwheel structure forms, and the distal part is where the appendages form. The centriolar microtubules are highly stable and do not depolymerize when exposed to Nocodazole or cold treatments, and they have a slow turnover (Kochanski and Borisy, 1990). The doublet/triplet structure also seems essential because when it is perturbed, centrioles fail to mature, and they finally disintegrate (Wang et al., 2017). The centriolar microtubules are enriched in tubulin post-translational modifications (tubulin PTMs) including: detyrosinated tubulin, acetylation, polyglutamylation and $\Delta 2$-tubulin. When cells are incubated with antibodies against polyglutamylated, detyrosinated or acetylated tubulin, centrioles are destabilized (Bobinnec et al., 1998a). This suggests a role for these tubulin modifications in long-term centriolar microtubule stability.

- **Pericentriolar Material:** the PCM is an electro-dense material composed of many different proteins. One important focus in centrosome research is the characterization and identification of PCM components. Many approaches have been used in order to identify new PCM components, such as proteomics and BioID methods (Andersen et al., 2003; Firat-Karalar et al., 2014a). So far, more than one hundred of proteins have been found to be components of the PCM (Andersen et al., 2003), but it is possible that there are many more. By the fact that many proteins localize to the centrosome could be explained because the centrosome acts as a hub to coordinate different signaling pathways. In many cases, the depletion /silencing of any of these components result in an increase of abnormal spindles and mitotic index (Lawo et al., 2009). One important challenge is to understand how all these proteins organize around the centrioles. Previous observations suggested that they form an electro-dense material randomly organized. However, in 2012, the structural organization of some of the PCM proteins was elucidated in human cells and in *Drosophila* embryos (Lawo et al., 2012; Mennella et al., 2012). The PCM is organized around the proximal part of the centrioles in a toroidal fashion during interphase **(Figure 5)**. Pericentrin is a key component in the organization of this matrix (Lawo et al., 2012). It is anchored to the centriole through its C-terminal part and extends through the PCM. Depletion of pericentrin highly affects the PCM toroidal structure and protein recruitment, suggesting that it acts as a protein scaffold (Lawo et al., 2012). This interphase PCM is known as "inner PCM layer". When cells enter into mitosis, the PCM expands and an "outer PCM layer" assembles involving different phosphorylation cascades (Conduit et al., 2010; Woodruff et al., 2014) that seems to be less organized. In mitosis, CdK5Rap2 (or Centrosomin) plays an important role. After PLK1 phosphorilation, CdK5Rap2 forms a scaffold that resembles the pericentrin longitudinal structure, and recruits many PCM proteins (Feng et al., 2017b). In the absence of this protein, the formation of mitotic centrosomes is highly affected (Conduit et al., 2014). Therefore, pericentrin and CdK5Rap2 seem to be the long time searched proteins that link the PCM with the centrioles. One of these PCM anchored components is the γ-TuRC. At this point, two different concepts arise and differences have to be pointed out: PCM referres to all the proteins that

surrounds the centrioles, whereas centrosomal proteins include centriolar and PCM proteins. In **table 1** I summarize some of the most important centrosomal proteins and the phenotypes observed upon their silencing/depletion.

Centrosomal proteins are on average, large and enriched in disordered and coiled-coil domains. This makes them difficult to study because they tend to precipitate or aggregate when overexpressed (Dos Santos et al., 2013). The fact that these proteins are enriched in disordered and coiled-coil regions may allow their interaction with many different proteins (Dos Santos et al., 2013; Garcia-Mayoral et al., 2011).

- **Appendages:** one of the two centrioles (the older one or mother centriole. See section II.C.3) acquires two different appendage structures: the distal and the subdistal appendages **(Figure 4)**. These structures are a marker of centriole maturation and age. They assemble on the distal centriolar microtubules. The main function of these appendages is to dock the centrosome to the cell membrane to form the basal body of cilia and flagella (Winey and O'Toole, 2014). Therefore, they are necessary for the conversion of the centrosome to a basal body **(Table 1)**.

- **Intercentriolar linker:** the intercentriolar linker provides a physical connection between the two centrioles **(Figure 4)** (Bornens et al., 1987). It is formed during S-phase and eliminated in G2/mitosis. The linker is mainly composed of C-Nap1, rootletin and Cep68 (Bahe et al., 2005; Graser et al., 2007).

- **Cartwheel structure:** this is the scaffold on which a new centriole forms during centrosome duplication. The cartwheel structure forms through a 9-fold symmetry oligomerization of the SAS-6 protein (Spindle assembly abnormal protein 6) through its N-terminus **(Figure 4).** The SAS-6 interacting partner, Cep135 (Centrosomal protein of 135 kDa), is essential for this ring structure to form *in vitro*. One ring acts as a seed for the sequential binding of ring pairs that stack vertically to form the cartwheel (Guichard and Gonczy, 2016; Guichard et al., 2017; Hilbert et al., 2016). Centriolar microtubules assemble then around this approximately 100nm high scaffold. Centrioles can also assemble *de novo*

and does not require SAS-6 protein self-oligomerization (Wang et al., 2015). These data were mainly obtained thanks to the development of a novel technique that uses cryo-electron tomography on purified centrioles and on purified centriolar proteins that reconstitute centriole assembly in a cell-free environment (Guichard et al., 2017). During mitosis, the cartwheel structure is lost (Arquint et al., 2014). However, the centrioles maintain its 9-fold typical structure.
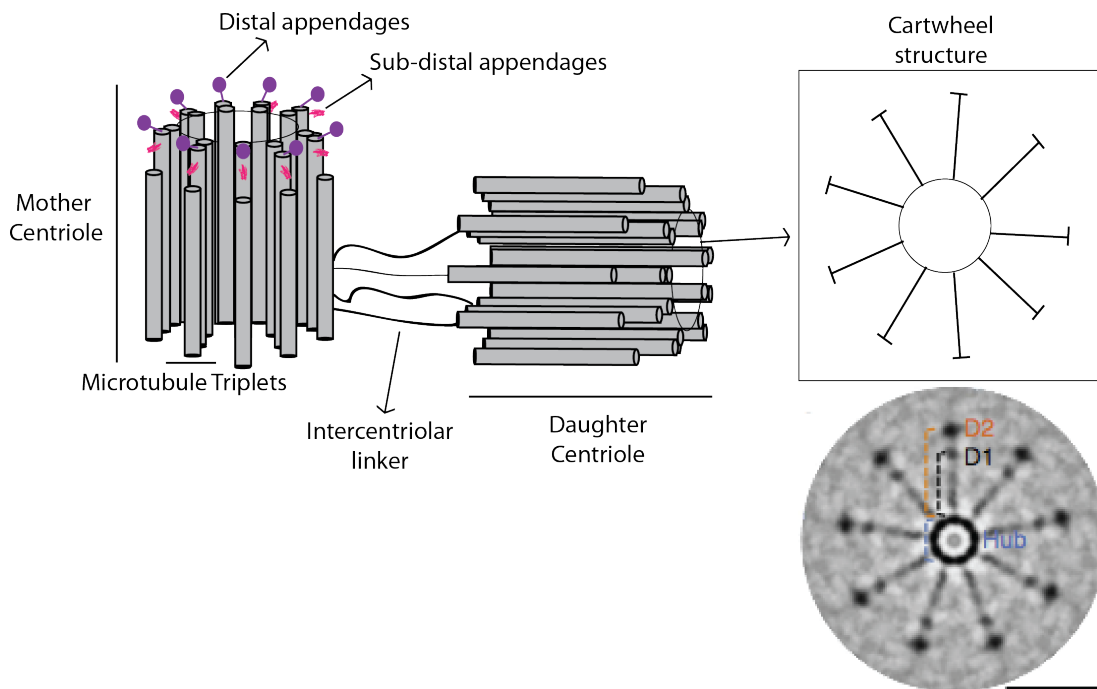
Figure 4: Centrosome structure. The centrosome is composed of two centrioles and the pericentriolar material (PCM). In this image I represented the centrioles and all the elements directly linked to them. Both centrioles, the mother and the daughter, are composed of 9 microtubule triplets. These microtubule triplets are A, B and C. A and B are full size tubules whereas C is proximately half in length. The mother centriole is decorated at its distal end with the distal and sub-distal appendages. These appendages are markers of centrosome age and they are needed to link the centrosome to the cell membrane to form the cilium in G0, therefore, they are essential for the centrosome to basal body conversion. The dynamic fibers that link both centrioles are known as intercentriolar linkers. Inside the centriolar lumen there is a 9-fold symmetry structure composed of oligomerized SAS-6, the cartwheel. This structure acts as a scaffold on which the microtubule triplets assemble to form the centriole *per se*. When cell enters into mitosis, the cartwheel and the linker are eliminated to allow the separation of the duplicated centrosomes. At the bottom of the figure: Native *Chlamydomonas* cartwheel structure Image taken by cryo-tomography. Guichard et al., 2016.

Table 1: Centrosomal proteins and the associated silencing phenotypes. Cep, centrosomal-associated protein; Spd, spindle defective; CPAP, centrosomal P4.1-associated protein; SasX, spindle assembly abnormal protein X homologue; Ana, anastral spindle; STIL, SCL/TAL1-interrupting locus protein; CDK5RAP2, CDK5 regulatory subunit associated protein 2; Cnn, centrosomin; CG-NAP, Centrosome and Golgi localized PKN-associated protein; AURKA, Aurora Kinase A; PPPX, Protein Phosphatase X; CP110, Centriolar coiled-coil protein of 110kDa; Bld10p, Basal Body protein 10; POC1, Protein of centriole 1; CCDCX, Coiled-coil domain containing X; SCLT1, Sodium channel and clathrin linker 1 and FBF1, Fast Binding Factor 1. Table adapted from (Bettencourt-Dias and Glover, 2009) and (Woodruff et al., 2014).

ACTIVITY	PROTEIN	PHENOTYPE
Scaffold	CDK5RAP2 (Cnn or Spd-5)	Reduced PCM, centriole-PCM attachment defects
	Cep152 (Asterless)	Centriole duplication defects, reduced PCM, no PLK-4 recruitment
	Cep192 (Spd-2)	Centriole duplication defects, reduced PCM, no PLK-4 recruitment. No SPD-5 polymerization *in vitro*
	Cep295 (Ana-1)	Centriole to centrosome conversion defects. PCM reduction
	CG-NAP	Centriole duplication defect
	CPAP (Sas-4)	Centriole duplication and assembly defects, reduced PCM
	γ-tubulin	Aberrant centriole duplication and structure. Impaired spindle assembly and MT nucleation
	Pericentrin	Reduced PCM
	STIL (Ana-2)	Centrosome duplication defects
Centriole biogenesis	Centrin	No duplication, aberrant centriole segregation, aberrant duplication geometry
	Centrobin	No duplication
	Cep135 (Bld10p)	No duplication, disorganized microtubules. Centriole assembly defects
	CP110	No duplication, no reduplication or amplification
	∂ and ε-Tubulin	Centriole stability disrupted, singlets, no duplication, aberrant PCM organization
	POC1	Smaller centrioles, no duplication.
	SAS-6/SAS-4	No duplication. If overexpression: overduplication
Kinases	AURKA	Centrosome separation defect, loss of effector recruitment
	PLK1	Reduced PCM, loss of phosphorylations of Cdk5RAP2, PCNT and SPD-5 (no SPD-5 polymerization *in vitro*)
	PLK4	It is a triggering factor. No duplication, no formation of basal bodies. If overexpression: overduplication
Phosphatases	PPP2ca	Centriole duplication defect, loss of MT stability via TPX2 and KLP-7, centrosome-nuclei detachment
	PPP2r1a	Centriole duplication defect
	PP4c	Aberrant pericentrin foci, loss of effectors and kinases
Appendages	Distal: CCDC41, CCDC123, Cep164, FBF1, SCLT1 Subdistal: Centrolin, Cep170, ε-tubulin, Ninein	Aberrant basal body docking. No cilia formation. Aberrant centriole microtubule triplets

3. The centrosome cycle:

The centrosome duplicates once per cell cycle during S-phase synchronously with DNA replication **(Figure 5)**. This cell cycle dependent mechanism ensures that the centrosome duplicates only once per cell cycle. Polo-like kinase 4 or PLK4 (member of a mitotic serine-threonine kinase family) is a key component for the centrosome duplication cycle. Its thigh regulation is crucial as PLK4 overexpression induces centrosome amplification. Heterozygous PLK4$^{+/-}$ adult mice develop tumors whereas the development of homozygous PLK4$^{-/-}$ mice arrests during gastrulation (Bettencourt-Dias et al., 2004; Habedanck et al., 2005; Bettencourt-Dias et al., 2005; Ko et al., 2005).

There are four main events during the centrosome cycle: centriole disengagement (G1 phase), procentriole formation (S phase), centriole maturation (G2 phase) and centriole separation and spindle pole localization (M phase).

Two main events license centriole duplication: the centriole disengagement and centriole to centrosome conversion (Nigg and Holland, 2018). Centriole disengagement requires the activity of separase and PLK1. This process consists on the separation of the newborn centriole attached to the mother centriole wall (Nigg and Holland, 2018; Tsou and Stearns, 2006). Centriole to centrosome conversion is the sequential loading of various centriolar and pericentriolar proteins such as Cep135, Cep295 and Cep152 (from the inner to the outer part of the daughter centriole respectively) around the newborn centriole during mitosis and G1 (Fu et al., 2016). The newborn centriole acquires thereby the competence for duplication in the following cell cycle. Interestingly, Cep295 is a key factor for this process. It physically interacts though its N-terminus with Cep135 and through its C-terminus with Cep152, acting as a linker (Fu et al., 2016). The absence of Cep295 abolishes PCM formation (Izquierdo et al., 2014).

At the beginning of S-phase, PLK4 foci form on each of the two centrioles (mother and daughter centrioles) (Sonnen et al., 2013) establishing the position where the two procentrioles will assemble. The phosphorylation of STIL by PLK4 leads to the recruitment of SAS6, and later CPAP. SAS-6 self-oligomerizes forming the cartwheel at the proximal end of the mother centriole. However, an alternative model based on centriole template has emerged. A transient recruitment of SAS-6 into the lumen of the mother centriole was observed in cultured cells. In the lumen, SAS-6 and CPAP oligomerize forming the typical cartwheel ring. Then, through the action of PLK4 and

STIL, this ring is released and, probably, loaded to the PLK4 foci at the surface of the mother centriole (Fong et al., 2014). These observations suggest that the centriole could acts as a template to ensure the 9-fold symmetry of the new procentriole and act as a regulator of the centriole structure. In any case, independently of the mechanism, it is now clearly established that SAS-6, STIL and CPAP are rapidly loaded to the procentriole formation site and they are involved in the early steps of centriole duplication.

The last centrosome maturation step occurs during G2 and M phase. It is defined by the expansion of the PCM and an increase of its microtubule nucleation activity (Piehl et al., 2004) to prepare the centrosomes for they role in bipolar spindle assembly. The PCM recruitment capacity is only acquired by the mother and daughter centrioles whereas procentrioles do not recruit PCM until the next cell cycle. This process is orchestrated by PLK1 dependent phosphorylation activity (Lane and Nigg, 1996; Wang et al., 2014; Woodruff et al., 2014).

Another event that is cell cycle regulated is the acquisition of appendages. Only the mother centriole has both distal and sub-distal appendages. Therefore, only one centriole per cell cycle has the capacity to dock to the cell membrane and act as a basal body. The daughter centriole acquire the appendages during G2 and/or M phase (Nigg and Holland, 2018).

Finally, when cells enter into mitosis, the mother and daughter centrioles (previously interconnected through the intercentriolar linker) separate forming two independent identities that move in opposite directions and get positioned at the spindle poles **(Figure 5)**.
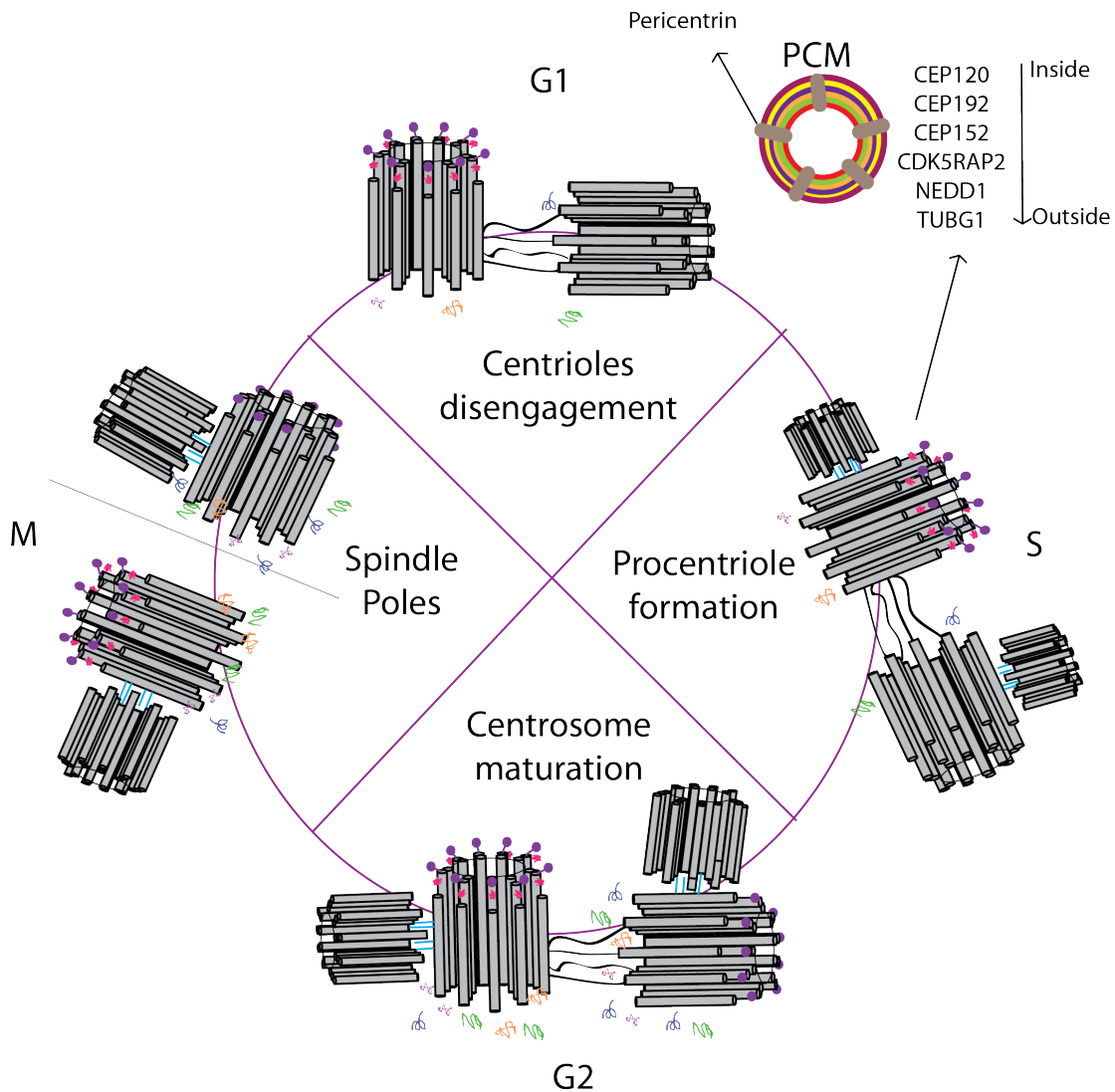
Figure 5: Centrosome cycle. The centrosome, in normal physiological conditions, duplicates only once per cell cycle. At each cell cycle phase, specific events occur that ensures correct centrosome duplication. In G1 the centrioles disengage. In the previous cell cycle, the centrioles and the procentrioles are linked with fibers (blue lines in the figure). At the M to G1 transition the linkers are eliminated by the action of separase. This separation licenses the centrosome to start its duplication cycle. During S phase different phosphorylation events, orchestrated by PLK4 mark the place and the timing of centrosome duplication. At the proximal end of the mother and daughter centrioles, a PLK4 foci licenses the accumulation of SAS-6. While the cartwheel is forming, microtubules build up around the cartwheel forming a procentriole at a right angle. PLK4 localization at the newborn centriole also exhibits an inhibitory effect to the mother centriole suppressing centriole overduplication (Kim et al., 2016). At the end of S-phase and G2-phase, procentrioles elongate and the PCM increases, a process known as centrosome maturation. The PCM is composed of many different proteins arranged in a toroidal way. Pericentrin acts as a scaffold protein. Its C-terminal part (PACT domain) is in contact with the centriole wall, and extends outward along the PCM. Other PCM proteins arrange around the centriole in a specific disposition: Cep120, Cep192, Cep152, CDK5RAP2, NEDD1 and TUBG1. During this phase, the daughter centriole starts to acquire the appendages, and in the next cell cycle the daughter centriole becomes a mother centriole. When cells enter into mitosis, the intercentriolar linker is disolved and each individual centrosome gets positionned at one spindle pole, to contribute to spindle assembly, bipolarization and positioning in the cell. To summarize, each cell cycle starts with one centrosome (one mother and one daughter centriole). During interphase, two centrosomes are formed. In the next cell cycle, the mother centriole continues being the mother centriole in one cell, and the daughter centriole takes the role of a mother centriole in the other cell.

Mother and daughter centrioles are different in terms of structure and in behavior. For example, when mitosis is completed, the mother centriole remains near to the cell center whereas the daughter centriole can move throughout the cytoplasm (Piel et al., 2000). When the centriole starts to duplicate, this behavior stops. This could be explained by the differences in microtubule nucleation. The mother centriole is already mature, with the appendages and many PCM material associated, whereas the daughter centriole still needs a cycle to acquire the same level of associated components.

4. Phase-separation as a new model for non-membranous structures – PCM as an example:

I would like to make a special mention to a new model based on phase-separation for the assembly of non-membranous organelles such as the centrosome. *In vitro*, the *Caenorhabditis elegans* PCM protein SPD-5 (CDK5RAP2 – human homologue) can polymerize into spherical condensates in a crowded environment. These condensates act as a scaffold for the recruitment of other proteins such as tubulin, TPX2 and XMAP215 (these last two proteins lower the critical tubulin concentration needed for spontaneous polymerization). Thereby, tubulin concentration increases and microtubule asters form. The assembly of this network is accelerated when two more PCM components are added: PLK-1 and SPD-2 (Cep192) (Woodruff et al., 2017; Woodruff et al., 2015). As the tubulin concentration in the cell is below the critical polymerization rate, this model suggests that the centrosome (or PCM) is a matrix that favors the accumulation of tubulin, in other words, it concentrates tubulin and favors microtubule nucleation without the requirement of γ-tubulin.

In the cell, not only the centrosome exhibits this biomolecular condensation property; other non-membranous organelles are assembled as liquid-like condensates and converted to harder condensates (gel-like state - amyloid-like fibers) such as the Balbiani body in oocytes (Boke et al., 2016; Woodruff et al., 2018).

The understanding of the mechanism of PCM assembly and organization has changed during these recent years. From the perception that the PCM is an amorphous mass of proteins, the use of high-resolution microscopy approaches has demonstrated that in fact these proteins are arranged and interact in specific patterns. However, the phase separation model suggests that a proteinaceous scaffold can concentrate MAPs without

a strict order. In fact, both models could be true, and could take place in the same cell. For instance it is possible that the first phases of centrosome formation are based on phase-separation condensates and latter, in aged centrosomes, the recruited proteins rearrange in a high-structured network.

5. A short description of the centrosome functions

In this section I will describe briefly some of the most important functions of centrosomes. Additional information can be found in the next chapters, where I define the role of the centrosome during development. As I explained before, the main function of the centrosome is to act as MTOC, therefore, microtubule nucleation and organization is the main role of the centrosome. However, it has many other functions in cell cycle regulation, intracellular components distribution, asymmetric cell division, polarity establishment and cilia and flagella formation, amongst others.

During interphase, the centrosome localizes next to the nucleus, in a privileged location to organize many cellular events. It is probably because of that fact that many proteins localize to the centrosome, such as cell cycle regulators. It also nucleates a big array of microtubules that not only provides cellular support but also polarity, important for the directional movement of intracellular components by molecular motors (Rusan and Rogers, 2009). Another important role of the centrioles is to act as a basal body of cilia and flagella. The cilium acts as a sensory organelle and performs essential functions in brain development, respiratory function, amongst other essential processes for the organism survival. The flagellum is particularly important for spermatozoa; the centrioles form the seed for the axomene formation and therefore spermatozoa motility.

In mitosis, the centrosomes contribute to spindle assembly, although it is dispensable. However, when mitotic cells are deprived of centrosomes, the genomic integrity is compromised, as well as cytokinesis with a subsequent cell cycle arrest (Bettencourt-Dias et al., 2005; Khodjakov and Rieder, 2001). The centrosomes also nucleate astral microtubules during cell division and play thereby an important role to position the spindle and establish the cell division plane. This is particularly relevant in asymmetric cell divisions. Finally, the differential distribution of proteins to one or the other centrosome can also specify the cell fate, as for example in the *Drosophila* male germ line (Yamashita et al., 2007).

With no doubt the centrosome plays a major role in most of animals and in humans. However, whether it is essential or not for organism survival is species-specific. For instance, flies without centrioles produce viable organisms (Basto et al., 2006), whereas PLK4$^{-/-}$ mice arrest after gastrulation (Hudson et al., 2001). Many human pathologies such as cancer and microcephaly are associated with abnormal centrosome number and/or function, (Bettencourt-Dias et al., 2011). Hence, it would be interesting to know whether centrosomes are essential for human early development.

D. The RanGTP pathway:

As I previously described, during meiosis and mitosis a centrosome independent microtubule assembly pathway plays a fundamental role in spindle assembly. This pathway relies on RanGTP. To understand this pathway, first we should take a glance at the nucleo-cytoplasmic transport.

1. The nucleo-cytoplasmic transport:

Cells consist of compartmentalized units separated, in most of the cases, by membranes. This is the case of the nucleus and the cytoplasm. They are independent units separated by two nuclear membranes, with an intranuclear lumen space between them (Strambio-De-Castillia et al., 2010). However, the cell needs to connect these two compartments and this happens through nuclear pore complexes (NPC). NPC are macromelecular structures of a molecular mass of approximately 50mDa and composed of more than 30 different proteins (Sorokin et al., 2007). The main function of the NPC is the exchange of proteins, RNA and other metabolites between the nucleus and the cytoplasm during interphase. But NPC components are also involved in other cellular roles such as DNA transcription and spindle assembly (D'Angelo, 2018). The nuclear-cytoplasmic exchange of small molecules through the NPC occurs freely, but the transport of larger proteins or macromolecules needs the help of other soluble factors known as karyopherin family proteins. Three main events occur during transport:

1. Members of the karyopherin family (such as Importin ß1 – or Nuclear transport factors (NTF)) recognize and bind proteins with nuclear localization

sequences (NLS) or nuclear export sequences (NES). These are sequences of aminoacids that tags a protein for being translocated into or outside the nucleus.

2. The NTF-cargo moves to the NPC and is translocated inside or outside the nucleus.

3. The complex is disassembled.

This is not a free energy process. This transport is regulated by the protein Ran, a Ras-like GTPase (Joseph, 2006). Ran can be bound to either GTP or GDP. Ran-GTP is mainly enriched in the nucleus and Ran-GDP in the cytoplasm. In the cytoplasm, Importins α and ß recognize NLS-proteins and mediate their transport inside the nucleus. In the nucleus, RanGTP binds to the importins promoting the release of the cargo. For exporting, proteins containing an NES bind preferentially to the RanGTP - exportin complex (such as CAS and CRM1). Once in the cytoplasm, GTP hydrolysis mediated by RanGAP1, releases NES-containing cargo and exportin. Ntf2 (Nuclear transport factor 2) helps RanGDP to enter back into the nucleus where the ran exchange factor RCC1 (Regulator of Chromosome Condensin 1 – asociated with the chromatin) exchange the GDP to GTP. This is a complex cycle process that ensures the directionality of transport **(Figure 6)**.
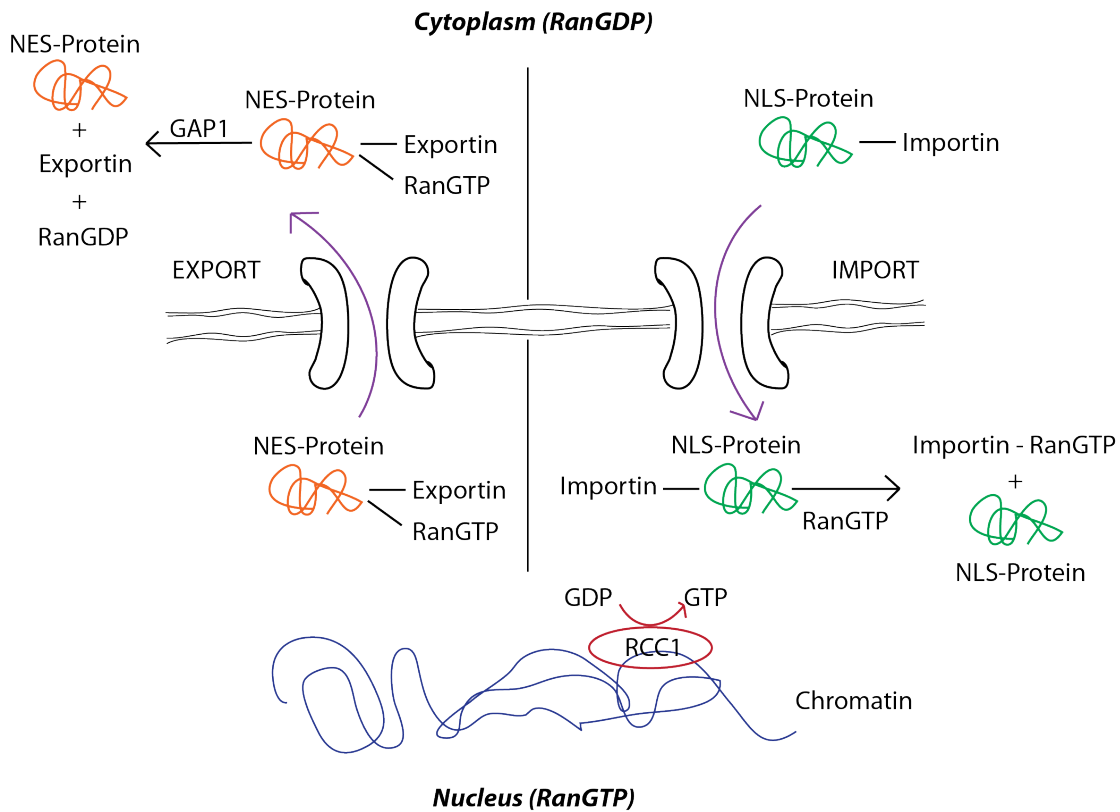
Figure 6: Nucleo-cytoplasmic transport mediated by the RanGTP pathway. In cells in interphase, the exchange of proteins from the cytoplasm to the nucleus and *vice versa* is achieved through an energy driven transport based on a RanGTP gradient. The cytoplasm is enriched in RanGDP whereas the nucleus is enriched in RanGTP. The hydrolysis of the GTP to GDP drives the export of proteins, while proteins with NLS are transported inside the nucleus.

2. The RanGTP dependent microtubule assembly pathway

What was the need for a detailed explanation of the nucleo-cytoplasmic transport mechanism? In fact, when cells enter into mitosis they use a similar strategy to assemble bipolar spindles.

Based on initial observations of Eric Karsenti after injection of phage DNA into *Xenopus* eggs (Karsenti et al., 1984b), Rebecca Heald in his lab, made a breakthrough discovery in 1996. DNA-coated beads incubated in *Xenopus* egg extracts triggered microtubule and spindle assembly (Heald et al., 1996) **(Figure 7A)**. In other words, her experimental approach showed that without the need of centrosomes and kinetochores, chromatin can trigger somehow microtubule nucleation, assembly and organization to form a bipolar spindle. In 1999 the underlying unknown mechanism started to be elucidated. Several groups demonstrated that a RanGTP gradient triggered around the chromosomes by its exchange factor RCC1, was required for chromosomal-mediated spindle assembly (Carazo-Salas et al., 2001; Carazo-Salas et al., 1999; Kalab et al., 1999; Wilde and Zheng, 1999; Ohba et al., 1999; Zhang et al., 1999). So, proteins

involved in the interphase nucleo-cytoplasmic transport were shown to be involved in spindle assembly. We know now that some nuclear proteins released from importins α and ß next to the chromatin by RanGTP **(Figure 7B)** trigger microtubule assembly and stabilization and organization (Garrido and Vernos, 2016). One important RanGTP regulated factor is TPX2 (Gruss et al., 2001). Some of these factors can have different roles in interphase. This is the case of MCRS1 (Microspherula protein 1) (Meunier and Vernos, 2011) and other chromatin regulated factors (moonlight proteins). This non-centrosomal microtubule assembly pathway was discovered and characterized in *Xenopus* egg extract, but later shown to also exist in somatic cells (Guarguaglini et al., 2000) (Gruss et al., 2002; Kalab et al., 2006; Khodjakov et al., 2000). In cells that do not have centrosomes, such as human oocytes, the RanGTP pathway alone can govern spindle assembly (Holubcova et al., 2015).
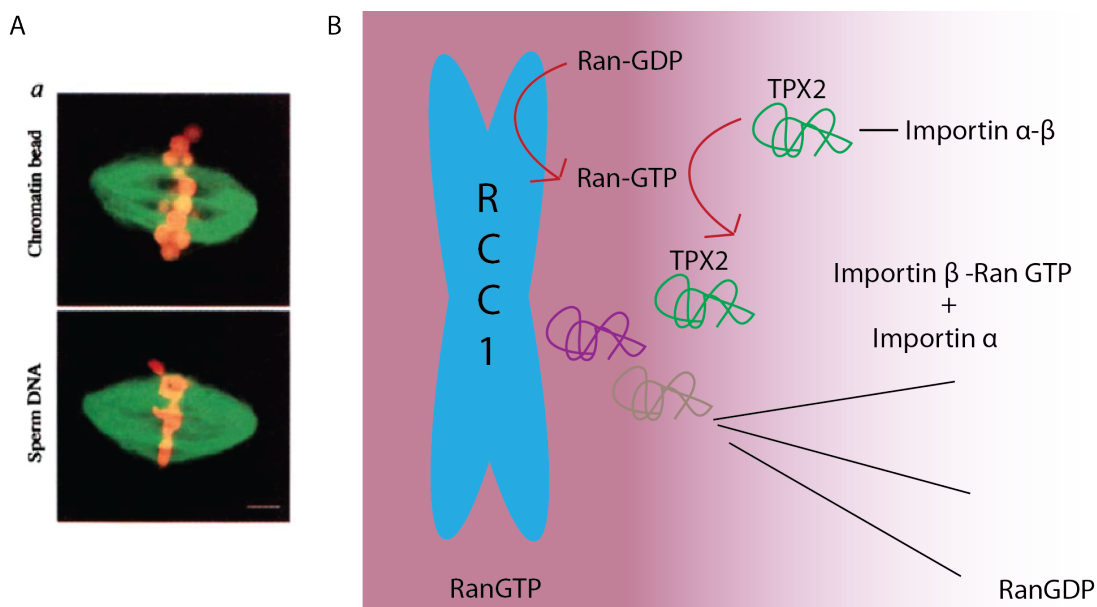
Figure 7: The RanGTP pathway in spindle assembly. A) Images taken from Heald et al., 1996. Spindles assembled in *Xenopus* egg extracts after addition of chromatin-coated beads or sperm DNA containing centrosomes. Note that both spindles are highly similar in terms of morphology. **B)** Schematic representation of the RanGTP pathway. The formation of a RanGDP – RanGTP gradient promotes the release of spindle assembly factors close to the mitotic chromosomes. These factors promote spindle assembly without the need of centrosomes.

E. Spindle assembly:

<u>1.The combined model of Search and Capture and Self-assembly:</u>

Although the RanGTP pathway alone can promote spindle assembly, very few cells take the risk of not having centrosomes; therefore, spindle assembly is mainly governed by the cooperation of the centrosome and the RanGTP pathway.

In 1986 the "Search and Capture" model for spindle assembly was proposed by Kirschner and Mitchison (Kirschner and Mitchison, 1986). According to the model, microtubules nucleated by the centrosome are highly dynamic and explore the space until they are captured and stabilized when they do contact a kinetochore. However, this model is not sufficient to explain spindle assembly. Indeed, the nucleation activity of the centrosome is not sufficient to support spindle assembly and the microinjection of a negative form of Importin-ß in somatic cells (RanGTP gradient perturbed), promotes the formation of a microtubule aster (Kalab et al., 2006). The current model for spindle assembly encompasses both centrosomal and non-centrosomal microtubule assembly pathways (Heald and Khodjakov, 2015).

In this model, when the cell enters into mitosis, the centrosomes act as the main MTOC. Their rapid microtubule nucleation provides an advantage to the cell, as they already establish spindle bipolarity cues. Indeed, cells with centrosomes display low multipolar spindles (Maiato and Logarinho, 2014). The activity of the RanGTP pathway, helped by the microtubule nucleation from preexisting microtubules, provides enough mass of microtubule to establish a functional spindle. Another important aspect is the timing. The RanGTP pathway accelerates this process but the centrosomes establish the kinetics of bipolar spindle assembly (Cavazza et al., 2016).

<u>2. Different classes of spindle microtubules:</u>

The bipolar spindle is a complex macromolecular machine constituted by three different classes of microtubules:

- **The astral microtubules:** they are only present in spindles with centrosomes. They are nucleated from the centrosome and extend towards the cell cortex. Their main role is to orient the spindle and define the cleavage plane.

- **The interpolar microtubules:** they form a robust mass of microtubules. They are generated from one pole and extend towards the other. They establish anti-parallel interactions that provide support for the forces required for chromosome movements (congressional and segregation). However, not all of them need to be connected.

- **The kinetochore microtubules/fibers (or k-fibers):** these are bundles of microtubules that connect the spindle poles with the kinetochores. These fibers provide forces that mediate chromosome movement. They are more stable than the other classes of microtubules.

3. Regulation of microtubule dynamics and organization

In interphase, microtubules are preferentially long and stable. However, when the cell enters into mitosis, microtubule dynamics increases exponentially. In mitosis, microtubules are rather shorts and unstable due to an increase on the frequency of catastrophe (Verde et al., 1992). These rapid changes in microtubule dynamics are regulated by the activity of different MAPs. For instance, the k-fibers of the bipolar spindle play with the microtubule dynamics to assemble functional spindles and to segregate the chromosomes in the two daughter cells. During anaphase, k-fiber + and – ends depolymerize. The NSL-complex is composed of 7 proteins, which main function in mitosis is to protect k-fibers – ends from depolymerization (Meunier et al., 2015). But many other proteins are involved in the microtubule dynamics regulation such as EB1, XMAP215 or the recently characterized FOR20 protein (Feng et al., 2017a).

But not only microtubule dynamics are important to assemble a bipolar spindle, also proteins that reorganize microtubules are needed. The proteins that perform this function are known as molecular motors. Two main motors exist in the cell: dyneins (Gibbons and Rowe, 1965; Vallee et al., 1988) and kinesins (Vale et al., 1985), and both share the principle that they move in an energy dependent manner along the microtubules (Reck-Peterson et al., 2018). They can either transport cargoes, which includes microtubules, or organize microtubules. Dyneins are MDa complexes with a - directed movement; on the other hand, kinesins are + end directed motors. One of the main functions of both proteins in mitosis is to mediate pole focusing. For instance,

when dynein is inhibited in XEE, spindle poles are open and the centrosomes are detached (Heald et al., 1997).

4. Spindle length:

The cell size changes during development and the mitotic spindle length needs to adapt. What mechanism dictates the spindle size? This has been characterized over the last decade and, interestingly, using again the powerful *Xenopus* egg extract system. It involves cytoplasmic components. Microtubule associated proteins such as TPX2, Eg5 and Katanin are major regulators of the spindle length (Helmke and Heald, 2014; Loughlin et al., 2011). Differences in their abundance and/or activity make *Xenopus tropicalis* spindles significantly shorter than *Xenopus laevis* ones. The cytoplasmic volume also drives spindle scaling. In a back-to-back paper in Science, both James Hazel and Matthew C. Good and colleagues used microfluidics to elucidate that the cytoplasmic volume rather than the cell shape is the major determinant of spindle scaling, by limiting the pool of cytoplasmic components (Good et al., 2013; Hazel et al., 2013). This mechanism is conserved across metazoans phyla, with the exception of the female meiotic spindle (Crowder et al., 2015).

F. Tubulin isotypes and post-translational modifications:

Microtubules are involved in diverse cellular roles and they interact specifically with different proteins, motors, MAPs and severing enzymes. To generate the specificity of intereactions, microtubules rely on a code based on the combination of different tubulin isotypes and a range of post-translational modifications occurring at the C-terminal tail domains of the α- and ß-tubulin. This generates diversity of microtubules and specific binding properties and/or activity of microtubule associated proteins.

Humans have 10 α-tubulin and 9 ß-tubulin gene isotypes. Moreover, there are 7 types of tubulin PTMs: tyrosination, detyrosination (generating Glu-tubulin), Δ-2 tubulin, monoglutamylation, polyglutamylation, monoglycylation and acetylation. When this code is perturbed the consequences go from cell cycle arrest to infertility or neuronal degeneration.

During my thesis I performed an extensive search in the literature to gather all the current information on the molecular characteristics of this code and its role during spermatogenesis, oogenesis and development, with a special focus on their clinical application (in ART). This information is reported in a review attached in **Annex II** and currently under review in the "Biology of Reproduction" journal entitled: Insights of the tubulin code in gametes and embryos: from basic research to potential clinical applications in humans.

III. The oocyte:

A. Oocyte structure:

The oocyte is the female gamete. In the human species, as in the vast majority of them, the oocyte is bigger in size than the male gamete, the spermatozoon. This is not by chance; behind this difference there is a whole series of reasons that we will find out throughout this section.

The human oocyte can be divided in two main parts: the oocyte *per se* that comprises the cytoplasm, the genetic material surrounded by the plasma membrane, called oolemma, and the zona pellucida. The second part comprises several somatic cellular layers, known in their complex as the Cumulus oophorus, which surround the oocyte **(Figure 8A)**.

In the oocyte we find the maternal genetic material, mitochondria, and other organelles, and a cytoplasm enriched in proteins and RNAs. The zona pellucida is an extracellular glycoprotein matrix that surrounds and protects the oocyte, but its main function is to provide species-specific fertilization (Claw and Swanson, 2012) and to avoid polyspermic fertilization. In humans, 4 different zona pellucida glycoproteins (ZPG 1-4) form a code that the spermatozoon recognizes and binds to (Pang et al., 2011). Upon fertilization, ZPG2 is cleaved, changing the three dimensional structure of the ZPG complex which will prevent fertilization by other spermatozoa (polyspermy).

The Cumulus oophorus is formed by cumulus cells (somatic cells) embedded in hyaluronic acid when it is expanded. We now know that the cumulus cells are necessary for a correct oocyte development because they directly communicate with the oocyte,

mediating the bidirectional transmission of regulatory factors and nutrients through gap junctions.

B. The development of a mature oocyte:

This is probably one of the most complex and long processes in the human body. The development of a mature oocyte starts before birth with oogenesis and ends with ovulation, which occurs once a month in women of reproductive age. Oocytes originate from primordial germ cells, which proliferate by mitosis to form the germ cell cyst. Following this proliferation phase, mitotic divisions stop, meiosis starts (chromosome recombination or "crossing over") and follicle formation is initiated (Gosden, 2013). In humans, meiosis starts between 12-16 weeks post-coitum (Zuccotti et al., 2011). However, meiosis arrests shortly after it starts, at prophase I. It is also during this fetal period that most oocytes in the ovary enter apoptosis, indeed less than 30% of the generated oocytes will continue their development.

At birth, oocytes are found in primordial follicles, consisting of a prophase I arrested oocyte surrounded by a single layer of flattered granulosa cells (epithelial cells that interact and provide to the oocyte growth factors and sex steroids – future cumulus cells) **(Figure 8B)**. Oocytes are retained in this developmental stage until puberty, when periodically a pool of primordial follicles is activated to initiate a growth phase (110-120 days), a process also known as folliculogenesis (Sanchez and Smitz, 2012; Coticchio et al., 2015). Many important changes occur during the growing phase. Granulosa cells change in morphology and start to divide, the oocyte increases in size, zona pellucida starts to form and RNAs and proteins accumulate to support oocyte growth, maturation and eventually, early embryo development. In the last stages of folliculogenesis, a fluid-filled cavity (the antrum) is formed in the follicle. It separates granulosa cells into mural granulosa cells and cumulus cells (Li and Albertini, 2013). It is also in this last follicular phase that the monthly surge of LH induces meiosis resumption and oocyte maturation. The Germinal Vesicle membrane breaks down and the first meiotic spindle is assembled (MI oocyte) and translocated close to the oocyte plasma membrane, where it will segregate half of the homologue chromosomes into the first polar body. The purpose of this highly asymmetric division is to eliminate as little cytoplasm as possible from the oocyte. A second meiotic spindle is assembled around the remaining chromosomes awaiting fertilization (MII oocyte – mature oocyte). However, for fertilization to occur, the MII oocyte needs to be released into the oviduct

from the follicle (a process known as ovulation). LH induces the secretion of proteolytic enzymes that will disrupt the follicular wall and mediate oocyte release in the oviduct. Once in the oviduct, the sperm fuses with the oocyte, and the second meiotic division is resumed (half of the sister chromatids are extruded by a second polar body) (Clift and Schuh, 2013) **(Figure 8B)**. This process continuously happens every month from puberty until menopause, which in most of the cases lasts around 30 years. This means that a pool of primordial follicles have the capacity to rest in this stage for more than 45 years. This concept is known as oocyte dormancy.
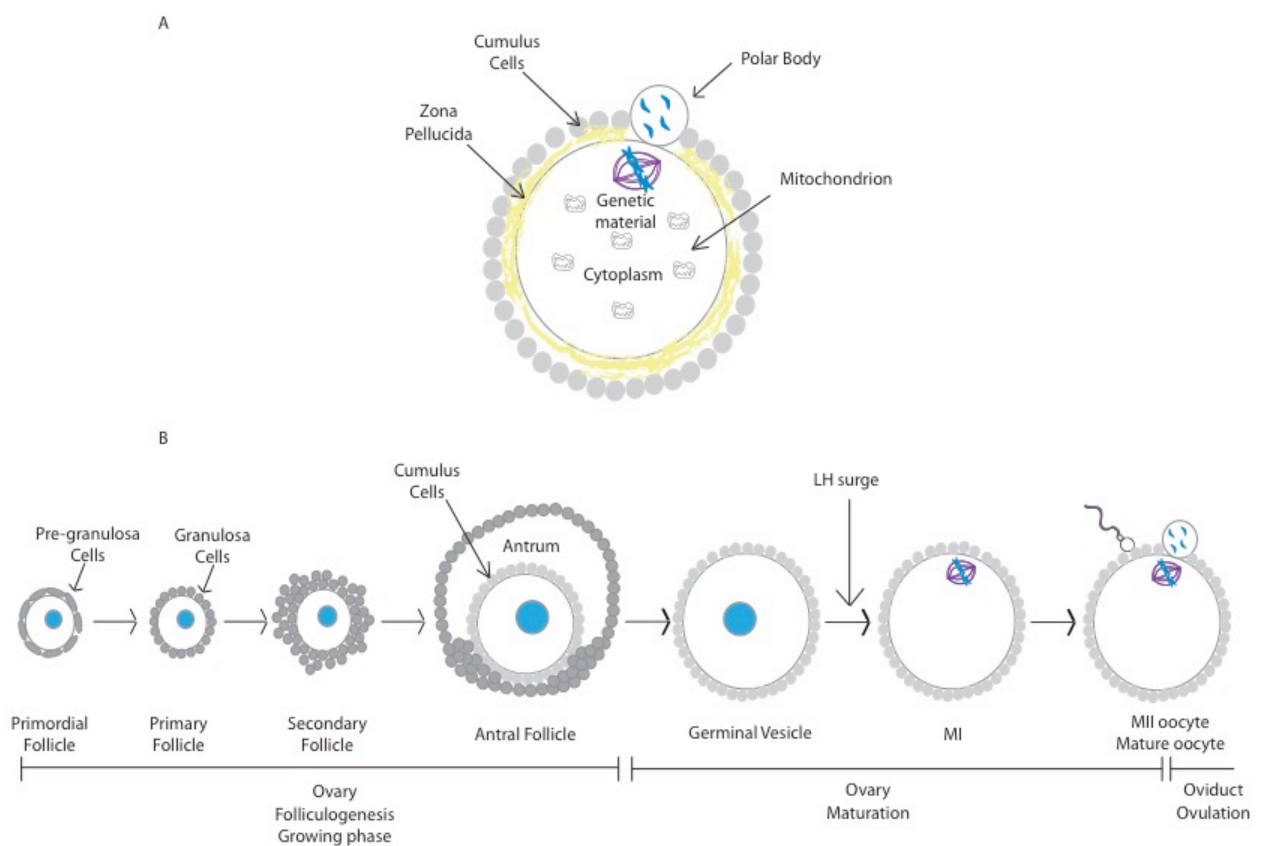
Figure 8: Oocyte structure and development. A) A mature oocyte or MII oocyte can be structurally divided in two main parts: the oocyte *per se*, formed by the cytoplasm, the genetic material and the zona pellucida; and the cumulus oophrous mainly composed by cumulus cells. **B)** Oocyte development is the process that comprises from oogenesis to MII oocyte formation. It is a complex process that involves many signaling cascades and cell-to-cell communication (granulose cells – oocyte). During the growing phase, the oocyte diameter increases more than 100 times (from less than 40 μm to approximately 120 μm). Oocytes are already arrested at meiosis prophase I when they are found as primordial follicles and will continue being arrested in this stage for most of their life cycle.

C. Microtubule dynamics during oogenesis:

Microtubule dynamics during the development of a mature oocyte are particularly fascinating because human oocytes show unique characteristics. Human oocytes eliminate or degenerate their own centrosome, but they are still able to assemble and move the spindle to segregate half of the genetic material in a highly asymmetrical division. In my opinion, this makes the oocyte maturation process very attractive to study. In this section, I will detail the described molecular mechanism behind this process.

1. Spindle assembly:

The morphology and functionality of the human oocyte spindle is associated with the oocyte quality and the ART success. The spindle is generally described as a barrel shape structure, with 47.7% of oocytes with both spindle poles flattened. Compared with the human oocyte size (approximately 120 μm in diameter) the spindle is very small, 11.8±2.6 μm in length and 8.9±1.7 μm in width, with a slightly shifted metaphase plate to the pole closer to the oocyte surface (Coticchio et al., 2013). There is relatively few information about how the human oocyte spindle is assembled. Until recently, it was generally accepted, but not demonstrated, that oocytes eliminate or degenerate their own centrosome and any other aMTOCs (acentriolar MTOCs)– no spindle pole markers could be found in human oocytes (pericentrin, γ-tubulin) (Combelles et al., 2002) – during oogenesis. Hence, spindle assembly completely relies on the RanGTP pathway (Holubcova et al., 2015). The fact that aMTOCs do not participate in the spindle assembly seems to be specific for humans. In other species, like in mice, aMTOCs largely contribute to the spindle assembly and bipolarization by a three-step aMTOC fragmentation and clustering mechanism (Gueth-Hallonet et al., 1993; Palacios et al., 1993; Carabatsos et al., 2000; Clift and Schuh, 2015; Schuh and Ellenberg, 2007).

Human oocytes are prone to be genetically unstable. There are several factors to take into account, which could explain this phenotype. First, human oocyte spindle assembly is extremely long; it takes 16 hours (mice oocyte requires only from 3 to 5h). The other factors have only been described in mice. One of these elements is the cytoplasm. Larger cytoplasm diminishes pole integrity (less focused) and spindle checkpoint stringency (as a consequence of diluting the spindle checkpoint factors) (Kyogoku and Kitajima, 2017). Besides, MTOC disruption (in pericentrin conditional mice knock-

down) also promotes spindle instability and aneuploidy by the incorrect microtubule to chromosome attachment, because the assembled spindles are only triggered by the RanGTP pathway (Baumann et al., 2017). Although these are observations obtained in mice oocytes, human oocytes also have a large cytoplasmic volume, and spindle assembly only relies on the RanGTP pathway. Therefore, it can be speculated that human oocyte genetic instability could also be due to these previously described factors. But the good news is that mice have generated a compensatory mechanism based on actin, which facilitates chromosome congression by supporting k-fiber formation (Mogessie and Schuh, 2017). It is possible that human oocytes have also this mechanism, although it is still unknown.

2. Mechanism of centrosome/centriole elimination:

The mechanism by which the human oocyte eliminates its own centrosome to ensure its asymmetric inheritance during fertilization, remains unknown. Different species eliminate the oocyte centrosome through different mechanisms; for instance, *Drosophila* first down regulates the PCM material (triggered by Polo activity) what promotes centriole loss (Pimenta-Marques et al., 2016). On the other hand, starfish eliminates 3 of the 4 centrioles by their incorporation into the extruded polar bodies. The remaining centriole (daughter centriole) is eliminated by first removing the PCM and then, the centriole (Borrego-Pinto et al., 2016). Although these mechanisms are different, the PCM plays a central role because when PCM is no longer present, centrioles become unstable and they are finally disassembled. It seems more likely that human oocytes follow a centrosome elimination mechanism similar to the *Drosophila* ones because, in humans, centrosomes are also eliminated before the meiotic divisions. When centrioles were prevented to be eliminated during oocyte development in *Drosophila* and starfish oocytes, multipolar spindles were assembled and, these fertilized oocytes arrested their development (Borrego-Pinto et al., 2016; Pimenta-Marques et al., 2016).

3. Spindle positioning:

To achieve a highly asymmetrical division, spindle positioning is critical. In most cells, the centrosome-nucleated microtubules (astral microtubules) move and orient the spindle by contacting with motor proteins and the plasma membrane. However, human oocytes do not have centrosomes or MTOCs. Thus, other mechanisms must govern the

asymmetric meiotic spindle positioning. In mice, spindle positioning has been described to be mediated by both internal and external cues. An example of external factors are the transzonal projections (TZPs). These are cumulus cells – oocyte interactions. Mice MI spindle tend to localize close to the region more enriched in TZPs (Barrett and Albertini, 2010), and when these interactions are lost, spindle in the oocyte is centrally assembled, which suggests that cumulus cells somehow could also mediate spindle positioning. An example of intrinsic factor, and probably the most important one, is actin. Indeed, mice oocytes fmn2$^{-/-}$ (formin 2 protein – actin binding protein involved in actin cytoskeleton assembly and reorganization) cannot position MI spindle close to the cortex (Leader et al., 2002). Actin filaments create a network in which spindle poles interact in a myosin light chain kinase-dependent manner relocating the spindle from the center to the cortex of the cell (Azoury et al., 2008; Holubcova et al., 2013; Schuh and Ellenberg, 2008). In human oocytes, an actin-dependent mechanism has not been described yet, but it seems plausible that a similar mechanism could also exist.

IV. The spermatozoon:

A. Sperm structure:

The spermatozoon is the male gamete. Like the oocyte, it is a highly specialized cell. During spermatogenesis, it goes through complex steps of cell remodeling to obtain its characteristic structure. The spermatozoon can be roughly divided in three different parts: the head, the midpiece and the tail, with a total length of approximately 50-60 μm in the human species (**Figure 9**).

1. The sperm head:

The sperm head is mainly formed by the acrosome and a highly packaged nucleus. The acrosome is a membrane-surrounded region derived from the Golgi apparatus with an acidic pH filled with proteins (Yao et al., 2002). When the spermatozoon contacts the oocyte's zona pellucida, the acrosome reacts (exocytotic process) and releases several lytic enzymes that promote the digestion of the zona pellucida and, therefore, the fusion of the male and female gametes (Liguori et al., 2005; Sutovsky, 2011; Okabe, 2013).

However, not only proteins needed for spermatozoon to pass through the zona pellucida are found; instead, the acrosome protein composition is complex due to its involvement in other processes such as the activation of the oocyte (kinases, phosphatases, phospholipases…) (Young et al., 2009).

The sperm nucleus contains chromatin packaged with protamines. Humans and mice have two different protamines, protamine 1 and protamine 2, which are small arginine and cysteine-enriched proteins (Human protamine 1 – 6.8 kDa and Human protamine 2 Isoform 1– 13 kDa; Isoform 2 – 17 kDa) (Hud et al., 1993). The fact that humans have 2 protamines does not probably mean that they have redundant activities, because in mice both proteins are necessary to sire offspring (Cho et al., 2001). The highly positive charge of the protamines promotes the packaging of chromatin by abolishing the electrostatic repulsion of the DNA (Johnson et al., 2011). Already in 1977, it was detected that in rat primary spermatocytes, histones were replaced by new "meiotic histones" that were tighter bound to the DNA (Mills and Means, 1977). These new "meiotic histones" were later defined as "protamines". In some animals, such as in fish and in birds, the transition from histone to chromatin-containing protamines occurs directly (Oliva and Dixon, 1991). However, in mammals this is a two-step process. First, histones are replaced by small and basic nuclear proteins called "transition nuclear proteins" (TPs) when chromatin starts to condense by a mechanism that involves phosphorylating and dephosphorylating events (Meetei et al., 2002). In mice, there are mainly two TPs, TP1 and TP2. Mice deficient in either TP1 or TP2 are apparently normal, with no reduction of sperm number and testis weight, but have an abnormal spermatogenesis and reduced fertility (Grimes et al., 1977; Zhao et al., 2001). Second, TPs are replaced by protamines to obtain the final highly compact sperm chromatin (Yu et al., 2000). The exchange of TPs by protamines is mediated by the Ca^{2+}/Calmodulin-dependent protein kinase. Mice deficient in Ca^{2+}/Calmodulin-dependent protein kinase are infertile, showing a reduced sperm count with also morphologically abnormal spermatozoa, all caused by an impaired exchange of TP by protamines (Wu et al., 2000). In humans, protamine-2 deficiency was correlated with male infertility (Balhorn et al., 1988). It is thought that the use of TP to exchange histones by protamines is to maintain the integrity of the genome while ensuring appropriate protamine replacement (Zhao et al., 2004). However, some specific chromatin regions could retain histones (15% of the sperm chromatin in humans). These histone regions are not randomly distributed; they seem to be bound to the nuclear matrix (Kramer and Krawetz, 1996)

and to contain genes involved in early embryogenesis (Braun, 2001; Johnson et al., 2011; Wykes and Krawetz, 2003)

But what is the reason behind this complex chromatin compaction? Different biophysical and developmental functions have been proposed: 1) it reduces the head size and remodels its shape creating a more hydrodynamic sperm head. 2) It protects the spermatozoa genetic material, specifically when the spermatozoon is moving through the female reproductive tract. 3) DNA-protamine packaging may also be necessary for transcriptional silencing and DNA imprinting changes (Braun, 2001; Carrell et al., 2007; Johnson et al., 2011). Sperm heads do not contain just DNA and protamines: signaling molecules, transcription factors, ribosomal and proteosomal proteins and RNAs are also found in mature spermatozoa. Most of these factors will be then delivered to the oocyte, where they can have a role in various developmental processes (de Mateo et al., 2011; Krawetz, 2005).

2. Sperm midpiece:

The midpiece is the region between the head and the tail. The centrosome, found as a basal body in the spermatozoon, and most of the mitochondria are located in this region. This region is important for the generation of the spermatozoon movement due to two aspects: 1) the basal body is the seed for the sperm axoneme formation/elongation and 2) the mitochondria provide the energy for the tail/flagellum movement. Sperm motility is a highly energy demanding process. Recently, with a sophisticated experimental approach, the amount of ATP consumed per axonemal beat was measured in demembranated sea urchin sperm axonemes. It was found that approximately 2.3×10^5 ATP molecules are consumed per beat (Chen et al., 2015). The presence of high amounts of mitochondria around the sperm basal body suggests that the required ATP can be derived from sugars and fatty acids metabolized in the mitochondria (Amaral et al., 2014b; Vadnais et al., 2014). Indeed, when the mitochondrial respiratory efficiency was analyzed in human spermatozoa, a positive correlation was found with sperm motility, indicating that samples with low motility could be due to a low energy production from mitochondria (Ferramosca et al., 2012).

Regarding the human sperm basal body, it is paternally inherited. It is a particular interesting organelle because it is not a conventional basal body. Instead, it is thought to be mostly naked of PCM and the distal centriole is considered as "degenerated". In the following section, I will go more into detail on this unconventional basal body. On the

other hand, mitochondria are only maternally inherited. Therefore, they are eliminated right after the sperm fuses with the oocyte with a mechanism that, in humans, is still not known, but in *C. elegans*, for instance, it is mediated through autophagy (Sato and Sato, 2011).

3. Sperm tail:

The sperm tail or flagellum is mainly formed by microtubules surrounded by outer dense fibers (ODF) and fibrous sheaths. Microtubules are organized in a 9+2 structure, a central pair of microtubules surrounded by a circular 9 doublets (A and B) of microtubules. A-doublets are formed by 13 microtubule protofilaments and B-doublets only by 10. The movement of the tails is mediated by the motor protein dynein that triggers the sliding of the microtubule doublets. Tubulin PTMs located at the microtubule doublets regulate the dynein transient interaction. An extensive explanation of the axoneme structure and how the flagella movement is generated can be found in the attached review I wrote: Insights of the tubulin code in gametes and embryos: from basic research to potential clinical applications in humans **(Annex II)**.
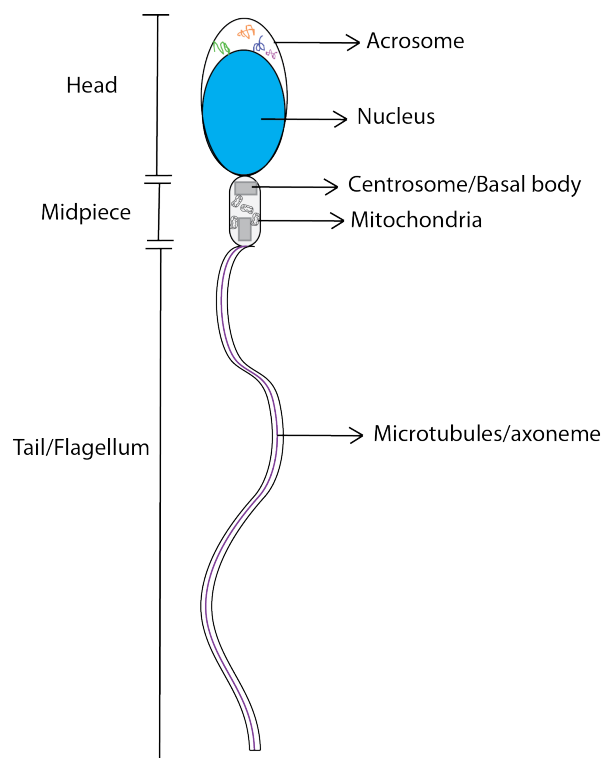
Figure 9: Human sperm structure. Human spermatozoon is in length approximately 50 μm, much smaller than the human oocyte. It can be divided in three main parts: the head that contains the acrosome and the nucleus; the midpiece, with a basal body and mitochondria, and the tail, composed by microtubule doublets. The nucleus is highly packaged thanks to the exchange of histones by protamines. The basal body and mitochondria are central components to generate the sperm cell movement, which is essential for natural conception.

B. Spermatogenesis:

Spermatogenesis consists in the formation of mature spermatozoa. Three main events occur during spermatogenesis: spermatogonia proliferation, meiosis of the spermatocytes and post-meiotic maturation of the spermatids to form mature spermatozoa **(Figure 10)**. To provide some numbers, this process in humans takes between 42 to 76 days, and approximately 1000 spermatozoa are produced every second (Amann and Howards, 1980). The progenitor of the mature spermatozoon is the spermatogonium. The spermatogonium is the undifferentiated male germ cell, and three different types can be found in humans: spermatogonia type A with a dark nucleus, spermatogonia type A with a pale nucleus and spermatogonia type B. The spermatogonia type A dark is considered the germ cell niche; they rarely divide. The spermatogonia type A pale are the proliferative spermatogonia, they actively divide by mitosis and will produce the type B spermatogonium, the one that will start the spermatozoon differentiation process. From each type B spermatognium, 4 mature spermatozoa will form (Neto et al., 2016) **(Figure 10)**. This process of differentiation starts during puberty and continues throughout the entire life of the man. Once a spermatogonium starts the differentiation process, a 4n content cell is formed, the primary spermatocyte. Following primary spermatocyte formation, 2 rounds of meiosis occur to form 4 round spermatids of 1n genetic material. The last spermatogenesis step is the post-meiotic maturation of the spermatids to form mature spermatozoa. During this process round spermatids suffer an important cellular reorganization because, from round cells, elongated spermatids will form. In mice, one of the first events that occur during this cellular reoganization is the formation of the acrosomal vesicle from the Golgi apparatus followed by the initiation of the axoneme assembly. On the other hand, the exchange of histones by protamines, the nuclear condensation, the elimination of the cytoplasmic lipid droplet and the positioning of the mitochondria around the sperm basal body are late processes. The cytoplasmic droplet contains many cellular components that will not be provided to the oocyte, such as centrosomal proteins (Gilbert et al., 2000).

Sperm production occurs in the seminiferous tubules, in a highly organized manner. From basal to luminal, spermatogonia, primary/secondary spermatocytes, round/elongated spermatids and mature spermatozoa are organized sequentially. Once

spermatozoa are formed, they are transferred to the epididymis where the maturation process will continue (acquisition of their fertilizing ability and motility) (Sullivan and Mieusset, 2016).
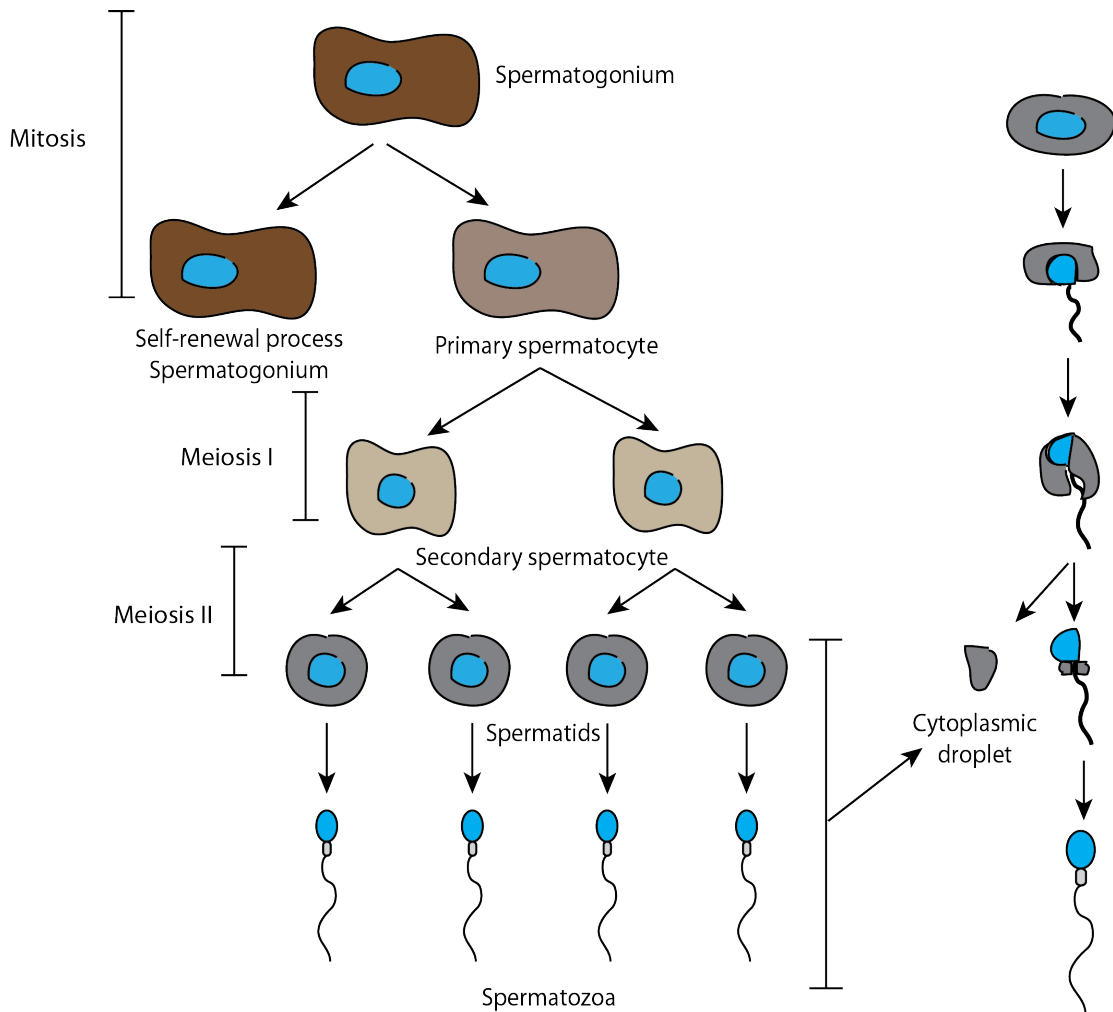
Figure 10: Human spermatogenesis. This diagram represents the process of spermatogenesis that occurs in the seminiferous tubules of the testis. This process involves cell differentiation and maturation, associated with a highly cell remodeling. The process starts with a spermatogonium that has the capacity of self-renewal or to start spermatozoa differentiation. Primary spermatocyte needs to go through 2 phases of meiosis to form 4 cells of 1n genetic material content. During the last step of spermatogenesis (from round spermatids to mature spermatozoa) cells eliminate most of their cytoplasmic material, the flagellum is formed and histones are exchanged by protamines. Once this differentiation phase is accomplished, spermatozoa are released to the epididymis where the maturation process finishes (spermatozoa motility acquisition).

C. Sperm basal body:

In the human sperm basal body the mother centriole, or distal centriole, acts as a seed for the axoneme assembly. The daughter centriole localizes in the region more proximal to the sperm head and it is known as the proximal centriole. As mentioned, the human sperm basal body is an "unconventional" centrosome. In this section, I will detail why we consider it as such.

1. Centrosome reduction:

In all the species studied so far, the sperm basal body undergoes a process of centrosome reduction, which is species-specific. Centrosome reduction is essential for post-fertilization events and comprises centrosome elimination, PCM reduction, and/or microtubule structural changes. This process, which occurs during spermatogenesis, has been mostly studied in rhesus monkeys, mice and *Drosophila*. As I mentioned, several species reduce their sperm basal body, but in different manners. For instance, while most species eliminate the PCM, some maintain both centrioles (*C.elegans*, sea urchin and *Xenopus*), few only degenerate the distal centriole (*Drosophila*, sea urchin and humans) and others eliminate both centrioles (mice) (Wolf et al., 1978; Avidor-Reiss et al., 2015; Manandhar et al., 1998). PCM seems to be reduced at the later stages of spermatogenesis. Indeed, mice and rhesus monkeys eliminate γ-tubulin and pericentrin within the cytoplasmic droplet. *Xenopus* eliminates γ-tubulin but not pericentrin. Mice also degenerate centrin by a mechanism still unknown, whereas rhesus monkey and *Xenopus* do not eliminate centrin (Manandhar and Schatten, 2000; Manandhar et al., 1999; Stearns and Kirschner, 1994). In spite of clear species–specific differences, it seems that the centrosome composition is consistently modified, reducing its capacity to nucleate microtubules. At this point, I would like to specifically describe the *Drosophila* sperm basal body because *Drosophila* has been extensively used to study the sperm basal body reduction and its transition to a functional centrosome in the fertilized oocyte. *Drosophila* spermatozoa have a particular basal body. It is composed by a Giant Centriole (GC – 2.6 μm in length) and a Proximal Centriole like (PCL) structure (Blachon et al., 2009). The PCL can be described as an early intermediate centriolar structure, since no microtubule triplets can be observed by electron microscopy but it contains centriolar proteins. *Drosophila* basal body also suffers a process of PCM reduction by diminishing proteins such as γ-tubulin, centrosomin, asterless, Ana1 and

Bld10 by a PLK4 (which is also reduced) mediated process (Blachon et al., 2014; Khire et al., 2015; Li et al., 1998). Human spermatozoa also undergo a complex process of centrosome remodeling, although this process is still not completely understood at the molecular level. Human ejaculated spermatozoa have an intact proximal centriole but an atypical or "degenerated" distal one, with a 50% less centriolar microtubules. Moreover, it has been proposed that it is "naked" of PCM **(Figure 11)** (Manandhar et al., 2000). Therefore, it seems that the centrosome reduction process is triggered to avoid having a functional centrosome in the spermatozoa, instead, a functional centrosome would only be formed during fertilization, where the sperm basal body can recruit from the oocyte the elements that eliminate during spermatogenesis.
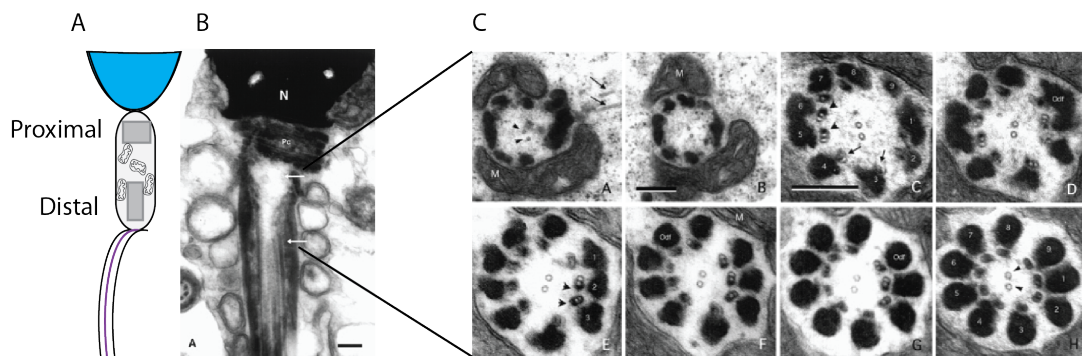
Figure 11: Atypical human sperm basal body. Image modified from Manandhar et al., 2000. The human sperm basal body is formed by a proximal and an atypical or "degenerated" distal centriole. These are electron microscopy images from the midpiece region. **A)** Representation of the B longitudinal section. **B)** We can appreciate that the proximal centriole (PC) maintains its structure. However, at the place where we expect to visualize the distal centriole, no microtubule structure can be seen. **C)** Transversal section of the distal centriole. Series of images in which we can appreciate that not all the microtubule triplets of the distal centriole appear in all the sections, instead they appear sequentially, and some of them are filled with electrodense material. Scale 0.25 μm

2. Centriole mode of inheritance:

Having the correct number of centrosomes per cell is a *sine qua non* condition for the development of a healthy individual. To ensure the correct number, mammals, with the exception of rodents, inherit the sperm centrosome during fertilization (oocytes do not have centrosomes). This sperm basal body will be the template of all the centrosomes of the new organism. However, the sperm basal body structure and composition are quite diverse among species. Therefore, several hypotheses have been proposed to explain the transition of the sperm basal body to a functional centrosome in the zygote (Avidor-Reiss et al., 2015):

- **"*De novo*" formation:** this hypothesis is based on the observational results from rodent spermatozoa. Rodents do not have sperm basal body and centrosomes in the fertilized oocyte are not detected until the embryo 64-cells stage. This hypothesis postulates that the centrosomes are formed *de novo* in the embryo (Courtois et al., 2012; Howe and FitzHarris, 2013)

- **The "restored hypothesis":** this hypothesis is only valid for species that only have one intact centriole, although, after fertilization, two well formed centrioles are detected. This hypothesis can be subdivided in two different models: A) the duplication hypothesis: this only applies in species with only one centriole. Shortly after fertilization, the centriole duplicates and a typical centrosome forms. Then, in parallel with DNA replication, the assembled functional centrosome duplicates again forming the two centrosomes. B) The regeneration hypothesis: this hypothesis is intended to explain the cases in which a typical and a degenerated centriole is found in the spermatozoa (human spermatozoa for instance). The degenerated centriole is rebuilt with centriolar microtubules to form a functional centrosome in the zygote. This "regenerated" centrosome duplicates in parallel with the DNA replication.

- **The "Paternal precursor hypothesis":** this hypothesis claims that a proximal degenerated centriole, or the PCL in *Drosophila*, is still active and does not need to regenerate to nucleate microtubules or to serve as a duplication template. This hypothesis is based on the *Drosophila* inheritance mechanism, in which a centrosome formed by a typical centriole and a PCL is sufficient to promote microtubule nucleation and centrosome duplication (Khire et al., 2016).

- **"Classical hypothesis":** two well-formed spermatozoa centrioles are inherited. This is the case of *Xenopus*. Therefore, right after the introduction of the centrioles into the oocyte, they just need to recruit PCM to actively nucleate microtubules.

Human spermatozoa have a typical proximal centriole and a "degenerated" distal one. It could be possible that the "restored" and the "paternal precursor"

hypotheses could be valid for humans. So far, none of them has been proven. However, in bipolar spindles of human zygotes only three centrioles were detected by electron microscopy (Sathananthan et al., 1996), suggesting that the "restored" hypothesis is not valid; nevertheless, we have to take into account that this study was performed more than 20 years ago, and maybe the 4th centriole could not be detected due to technical limitations.

V. Fertilization and zygote formation:

Once spermatozoa are ejaculated, they migrate from the vagina to the oviduct, where they fertilize the oocyte. During the movement of the spermatozoa to the oviduct two main events occur: 1) sperm capacitation and 2) the action of factors that induce sperm migration.

- **Sperm capacitation:** capacitation involves a series of biochemical and physiological changes in the sperm and its associated plasma membrane that renders spermatozoa capable of fertilizing (Visconti et al., 2011). In 1951, Chang and Austin were the first to observe that spermatozoa need to be incubated in the female reproductive tract to become fertilization-competent. Indeed, Chang performed very elegant experiments in rabbits demonstrating that a sperm ejaculate needs to be 6 h in the female reproductive tract to fertilize the oocytes. He proposed that "such a period of time in the female tract is required for the spermatozoa to acquire their fertilizing capacity" (Austin, 1951; Chang, 1951). Now, we know that the process they were referring to is capacitation (Austin, 1952). Capacitation comprises early events such as sperm motility hyperactivation, and late events, which include molecular changes that activate different signaling pathways (for example increased tyrosine phosphorylation) (Visconti, 2009). For sperm capacitation to occur, spermatozoa depend on the intracellular changes of cAMP, pH, calcium and the membrane potential (Gervasi and Visconti, 2016). Two main molecular events regulate the physiological changes associated with sperm capacitation: the inhibition of serine/threonine phosphatases and the activation of cAMP pathwyas by HCO_3^-

and Ca^{2+}. The early activation of these pathways will coordinate the intracellular changes of cAMP, pH, calcium and membrane potential. Several studies in animal models demonstrated that when any of these 4 factors are perturbed, mice are infertile (Esposito et al., 2004; Hess et al., 2005; Wang et al., 2007; Wang et al., 2003a) (Ren et al., 2001; Santi et al., 2010). One of the most important and sperm specific calcium channel is CatSper (Lishko et al., 2011). CatSper is found in many mammalian spermatozoa including humans. Indeed, in a recent publication, an IVF patient with a normal spermiogram but an idiopathic infertility was shown to have non-functional CatSper channels, leading to its infertility problem (Williams et al., 2015). All these data suggest that sperm capacitation is a critical process for the sperm to acquire its fertilization capacity.

- **The action of factors that induce sperm migration:** the second process is the interaction of female reproductive track-derived factors with the spermatozoa to guide the sperm movement inside the oviduct to reach the matured oocyte. This involves molecular factors such as hormones and female receptor-sperm ligand interactions, as well as the physical interaction of the sperm with the female tract walls, the direction of the fluid flow and the temperature gradient (Boryshpolets et al., 2015; Miki and Clapham, 2013). Most of this information is obtained from animal models, but the recent development of microfluidics could be a useful tool to reproduce female tract compartments and its physical properties (Suarez and Wu, 2017).

The multi-step process of fertilization also involves the specific sperm-oocyte zona pellucida recognition and the sperm-egg fusion. Having already introduced the concept of sperm-oocyte zona pellucida recognition in the oocyte section, I will only refer to the sperm-egg fusion mechanism. Two main proteins have been identified in mice to be involved in sperm-oocyte fusion, the oocyte localizing CD9 protein (Kaji et al., 2000; Le Naour et al., 2000; Miyado et al., 2000) and the sperm localizing IZUMO1 protein. *Izumo1*$^{-/-}$ mice spermatozoa are unable to fuse with the oocyte although they can penetrate the cumulus cells and be recognized by the zona pellucida proteins (Inoue et al., 2005). IZUMO1 is localized in the sperm plasma membrane and it is only exposed after sperm acrosome reaction (Satouh et al., 2012). Upon the fusion, several factors

released by the spermatozoon induce oocyte activation and meiotic resumption. One of these factors is PLCζ (Ferrer-Vaquer et al., 2016; Nomikos et al., 2013). PLCζ induce the release of calcium fom the endoplasmic reticulum causing the finalization of the meiosis II and the translation of maternal mRNAs among other actions.

In our species, as in most, once the second meiotic division is completed, the fertilized oocyte enters into interphase and the male and female pronuclei are formed. During this period, which lasts approximately 16 hours in human embryos, DNA replicates and the sperm-inherited centrosome should also duplicate (Sathananthan et al., 1991). Details of this process are very scarce in our species due to ethical and technical limitations in performing research at this developmental stage. Nevertheless, the sperm centrosome has been shown to nucleate a large array of microtubules in which the female pronucleus, in a microtubule motor-dependent way, will move towards the male pronucleus to apposition (Sathananthan, 1998). It is likely that both the centrosome and the RanGTP pathway cooperate in assembling the bipolar spindle in the human zygote, even though this has not been established firmly.

A. Microtubule dynamics during the transition from a meiotic to a mitotic cell division:

Microtubule dynamics are essential for the transition of a meiotic to a mitotic cell division machinery and from an asymmetric to a symmetric cell division. In this section, I provide information about both concepts, differentiating whether they occur during zygote interphase or mitosis.

1. Interphase:

During human zygote interphase the centrosome nucleates an array of microtubules that helps to the apposition of the male and female pronuclei. During apposition (also known as nuclear positioning) the nucleus also has to be centered in the middle of the cell, because the first cell division needs to be as symmetrical as possible to equally segregate the cytoplasmic material into the daughter cells. In my opinion, the molecular mechanisms behind nuclear positioning during fertilization are particularly interesting mainly due to the following two factors: 1) a symmetric cell division has to be correctly performed right after a highly asymmetrical one (polar body extrusion) 2) this process

occurs in a cell with a very big volume. Therefore, this process must be complex and carefully regulated. In humans, it could be possible that many different mechanisms cooperate for the nuclear positioning in the middle of the fertilized oocyte, rather than being only a microtubule dependent mechanism, as it occurs in smaller somatic cells (Reinsch and Gonczy, 1998). It would be interesting to check whether actin is contributing to this process. So far, what is known from model systems is that *C.elegans* uses the pulling force generated by the contact of the sperm aster with the cell cortex to center the centrosome and, therefore, the nucleus (Kimura and Onami, 2005). However, in species with bigger oocytes, the action of the centrosome alone is not sufficient to promote nuclear positioning, suggesting that an extra mechanism is involved in this process. The most plausible model for humans follows the observation that dynein (which was demonstrated to be the motor protein responsible for the female pronucleus movement towards the male one) can be anchored at different intracellular organelles generating the microtubule movement required for nuclear positioning, as it happens in many different animal models (Kimura and Kimura, 2011; Payne et al., 2003; Reinsch and Karsenti, 1997).

2. Mitosis:

In humans, the transition from a meiotic to mitotic spindle assembly has to occur in the zygote. Since the centrosome is provided by the spermatozoon, it probably plays an active role in spindle assembly, and therefore, the spindle is no longer only triggered by the RanGTP pathway. However, this is just speculative because no data exist for human zygotes. In contrast, in mice, this transition is gradual. Zygotes and early embryos still depend on multiple MTOCs to assemble the bipolar spindle, and it is not until the blastocyst stage that centrosomes are formed *de novo*, spindle poles are focused and the transition from meiotic to mitotic spindle assembly is completed (Calarco-Gillam et al., 1983; Courtois et al., 2012). Regarding the spindle positioning in the zygote, in humans, it probably follows a microtubule and motor-dependent mechanism similar to pronuclear positioning. However, in other species such as mice, actin is responsible for the spindle movement (Chaigne et al., 2016). Together with the previous cell cycle phase (interphase), it would be interesting to study further the contribution of actin to the nuclear and spindle positioning in the zygote, and its cooperation with a tubulin dependent mechanism.

B. Chromatin remodelling during the transition from a meiotic to a mitotic cell:

Not only microtubules play a major role during fertilization, also chromatin undergoes changes, as a new totipotent cell is formed from the combination of two highly differentiated ones. DNA replication initiation sites, timing and protein expression need to adapt to the new totipotent cell necessities. Because chromatin remodeling is not a topic I have studied during my PhD, I just summarize here some of the most important concepts related to this process.

The male and female DNA are organized differently. On one hand, the male DNA is tightly packed by protamines that are exchanged for histones after fertilization. On the other hand, the female DNA is organized in a meiotic metaphase plate. Both male and female genetic materials have to decondense and replicate to form the male and female pronuclei. The sperm and oocyte DNA are also highly methylated. This methylation starts to be erased after fertilization, reaching a minimum level at the blastocyst stage (Clift and Schuh, 2013). However, some specific genes, known as "imprinted genes", are kept methylated. This epigenetic mechanism regulates the expression of specific genes inherited from one parent whereas the other copy is silenced (Li and Sasaki, 2011).

VI. Embryo early development:

The human embryo is described as a "discrete entity that has arisen from the first mitotic division when fertilization of a human oocyte by a human sperm is completed and has not yet reached 8 weeks of development since the first mitotic division" (Findlay et al., 2007). After 8 weeks of embryo development, the product of the conception is named "fetus". Embryos can be classified as pre-implanted and post-implanted embryos. Implantation is the process in which the human embryo adheres to and invades the endometrium and uterine wall, and begins around day 6 – 7 after ovulation (Cakmak and Taylor, 2011). Implantation consists of three stages: embryo apposition, adhesion and penetration to the endometrium (Koot and Macklon, 2013).

This is a highly complex process because it involves embryo – endometrium specific cross-talk and because the women uterus is only receptive a short period of time each month, approximately 3 days; for these reasons human implantation often fails (Wang and Dey, 2006). Because most of my work has been focused on pre-implantation development, in this section, I only provide information about pre-implantation development or early embryo development.
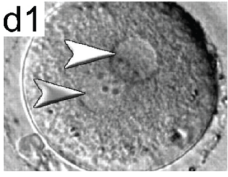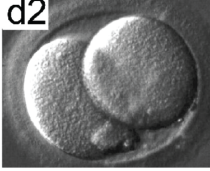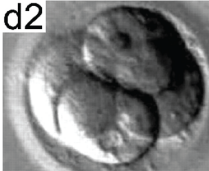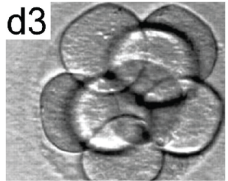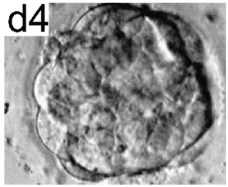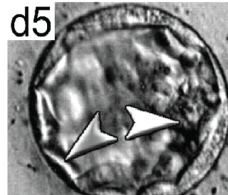
A. Stage of pre-implantation development:

Our understanding of human early embryo development primarly comes from *in vitro* embryos generated for IVF cycles. In IVF cycles, embryos can be cultured up to D+5 post-fertilization; in this section, I will detail the molecular and cellular features that an embryo is expected to have from D+0 to D+5 of development **(Figure 12 and 15)**.

- **D+0 or fertilization day:** it is established as the day of "fertilization". Oocyte activation and meiosis resumption are the main events occurring on D+0. Recently, the morphokinetic events that occur in human embryos at D+0 were described in an accurate time-lapse analysis (Coticchio et al., 2018). The second polar body extrusion occurs on average at 3.3h post-fertilization, the female pronucleus appears slightly before than the male one (6.2h vs 6.3h) and the zygote cleavage at 27.7h. It is also at D+0 that the cytoplasm undergoes major rearrangements and movements. Indeed, a radial cytoplasmic wave is observed from the position of the male PN (pronucleus) to the oocyte cortex. It is thought that this cytoplasmic wave could be the result of the sperm microtubule aster formation. Maybe this cytoplasmic wave could be used in the future as a new sperm centrosome functional biomarker.

- **D+1:** zygote cleavage occurs around 27h post-fertilization, therefore, at D+1 we expect to see a proportion of zygotes already divided and another committed in this first division. The two daughter cells have to be as symmetric as possible.

- **D+2:** cell division at D+2 occurs between 43 to 45h post-fertilization, therefore top quality embryos should have 4 symmetric blastomeres (or cells) at this time.

- **D+3:** embryos at D+3 post-fertilization are expected to have 8 symmetric blastomeres because cell division occurs between 67 to 69h post-fertilization. It is also at this specific day that embryos stop being transcriptional silent and the major wave of embryonic genome activation occurs (Niakan et al., 2012; Vassena et al., 2011).

- **D+4:** at day 4 the embryo compacts forming a "morula". This process is described as the tight union of the cells forming a cluster. In the morula, it is not possible to distinguish the boundaries between blastomeres. Compaction is an extremely important event because the fates of the cells begin to diverge.

- **D+5:** a blastocyst is formed. A blastocyst is a hollow structure with a fluid-filled cavity and an inner cell mass (ICM) surrounded by a layer of cells (trophectoderm – TE). A newly expanded blastocyst contains on average 58 cells, from which 38 are from the TE and 20 from the ICM (Hardy et al., 1989). The ICM just before implantation diverges into early epiblast and primitive endoderm, which will give rise to the fetus later. The trophectoderm will provide the embryonic contribution to the placenta.

DAY	STAGE	MORPHOLOGY
1	Pronuclear formation	
2	2 or 4 cells	
3	8 cells	
4	Morula	
5	Blastocyst	

Figure 12: Stages of pre-implantation development. Figure modified from: Niakan et al., 2012. Human embryos are classified according to the number of cells and the day of development. In this figure, I summarize the stage of development expected from day 1 to 5 post-fertilization (pre-implantation development). At each stage, different processes occur to finally form an expanded blastocyst at D+5. When the embryo compacts and forms a morula, the radial symmetry is lost. Blastocyst is formed by a fluid-filled cavity and two differentiated cell masses, the ICM and the TE. The total number of cells in the blastocyst is approximately 58.3±8.1 (ICM=20.4±4.0; TE=37.9±6.0) (Hardy et al., 1989).

B. Control of gene expression:

During fertilization and early development, gene expression switches from maternal to embryonic control (Clift and Schuh, 2013; Niakan et al., 2012; Vassena et al., 2011). Three main events occur to ensure a progressive transition:

- **Active genome transcription during oocyte growth:** during human oocyte growth the genome is actively transcribed and mRNAs are accumulated in the oocyte cytoplasm. These transcripts are kept "silenced" until fertilization. However, this transcription is dramatically stopped when human oocyte matures (from Germinal Vesicle to MII oocyte). The translation of these transcripts is carefully regulated.

- **Use and elimination of maternal mRNAs:** right after fertilization, and before the major wave of genome activation, the maternal-stored mRNA sustains early embryonic development. These maternal mRNAs are also gradually eliminated. Indeed, their elimination starts even before fertilization, at the onset of oocyte maturation and continues until the human embryo 4- to 8-cell stage. This degradation is performed in a selective manner; for instance, transcripts needed for meiotic progression are eliminated before than the ones needed for mitotic division (Zhang and Smith, 2015).

- **Activation of the embryonic genome:** this is the final step to end the transition of gene expression control. In mice, the major embryonic genome activation occurs at the 2-cell stage and in humans, after a small burst of preparatory transcription as early as the 2-cell stage, reaches its apex at the 8-cell stage (Vassena et al., 2011).

C. Polarity and cell division orientation:

During the first 5 days of embryo development, a series of mitotic divisions transforms a single large volume cell into multiple and polarized cells. The accuracy of the cell division orientation and the establishment of polarity are crucial because they will define the first developmental fates. The mechanisms governing cell polarity and asymmetrical cell divisions are still not know in our species, however, in animal models, such as *C.elegans*, *Drosophila* and mice, some of these mechanisms are conserved, therefore, it seems reasonable that these mechanisms could also be present in the human embryo (Ajduk and Zernicka-Goetz, 2016). Since new molecular and cellular information regarding these mechanisms is now arising from mice embryos, in this section, I decided to focus only on mice-described mechanisms.

In mice, the first cell divisions are completely symmetric and it is not until the 8-cell stage that asymmetric divisions and polarity acquisition occur. At the 8-cell stage, mouse embryos start to compact and a polarized apical domain is formed at the contact-free surface (Ajduk et al., 2014). This apical surface is enriched in Par proteins (Par-6) and F-actin, and downregulated in acto-myosin. At the 16-cell stage, these polarized cells can be either divided perpendicular or parallel to the embryo surface, generating two outer cells or one outer polarized cell and one inner apolar cell (Watanabe et al., 2014). The inner cells will be the precursors of the ICM, and the outer cells the ones of the TE (Morris et al., 2010). Cell internalization is mediated at least by 2 mechanisms: 1) when a parallel division occurs, the outer cell will push the inner one to become internalized. 2) If the division is perpendicular, two outer cells are formed. If the apical domain is equally distributed between them, no internalization occurs. However, when the apical domain is not equally distributed, cells have different contractility due to different cortical myosin distribution (apolar *versus* polar cell). When this differential cortical tension is high enough, the apolar cell is internalized (Maitre et al., 2016). The asymmetric inheritance of the apical domain is also associated with asymmetric distribution of transcripts and molecules that define the cell fate specification (Jedrusik et al., 2008; Skamagki et al., 2013). Therefore, asymmetric cell division of the polarized domains determines the cell fate specification.

To achieve this accurate asymmetrical division, it is necessary that the bipolar spindle is oriented properly. Korotkevich et al., demonstrated that apical domains trigger the recruitment of the spindle poles to orient the cellular division plane (Korotkevich et al., 2017). In mice, MTOCs cluster close to the apical domain. Although it is still not known in humans, it is plausible that the centrosome could be also recruited in this subapical region, and therefore, plays an important role in defining the cell fate specification.

VII. Centrosomes and infertility:

In most of the species, the centrosome is inherited during fertilization. We also know that centrosomes are essential for the development of an adult healthy organism, and an

abnormal centrosome number per cell is associated with many diseases. However, is the fact that they are inherited during fertilization indicating that they are essential for the early embryo development? Or is it just a mechanism to ensure the proper centrosome cycle and therefore number? Independently of the answer, abnormalities in this sperm-derived organelle that is involved in so many cellular processes could be the cause of some embryo arrests and, therefore, infertility cases.

It seems that the contribution and importance of the sperm-derived centrosome in early embryo development is species-specific. While some studies report that centrosome abnormalities or absence impairs embryo early development, others however, suggest that centrosomes are not essential. In *C.elegans* for instance, perturbing the function of centriolar duplication proteins such as Sas-4, Sas-5 and Spd-2 (Delattre et al., 2004; Kirkham et al., 2003; Pelletier et al., 2004) arrests embryonic development. On the other hand, *Drosophila* Sas-4 mutant can develop apparently normally until birth, although then they die (Basto et al., 2006). An important aspect in this last work is that these mutant flies do have centrosomes during the early stages of development because they are heterozygous, which do not provide an answer to whether centrosomes in *Drosophila* are important for early development. Nevertheless, it was completely unexpected that centrosomes were dispensable for later developmental stages. Authors suggest that asymmetric cell division, in which astral microtubules orientate the spindle, occurs normally because spindles occupy most of the cell, and spindle poles could make direct contact with the cell membrane. When analyzing studies in which the oocyte centrosome elimination was prevented (the centrosome is inherited by the both gametes), we found that in *Drosophila*, upon fertilization, early embryos arrested their development (Pimenta-Marques et al., 2016). In these embryos, abnormal mitotic divisions and scattered DNA were observed, with the subsequent embryo arrest. In the specific case of starfish embryos, multipolar spindles are also formed (Borrego-Pinto et al., 2016).

On the other hand, the spermatozoon basal body is found in a final stage of differentiation in the mature spermatozoa. In humans, as well as in *Drosophila*, centriolar microtubules are "degenerated" or even absent, and the PCM is severely reduced. In *Drosophila*, when the sperm PCM reduction was impaired, *Drosophila* embryos had reduced microtubule asters and significantly less embryos hatched (Khire

et al., 2015), suggesting that an incorrect centrosome reduction process hampers both zygote centrosome function and embryonic development. In mice, males depleted of centrin-1 are infertile due to sever sperm malformations, especially, in the tail (Avasthi et al., 2013). Few data correlating the sperm basal body reduction process with the spermatozoa fitness or reproductive outcomes exist, however, a short report claim that human semen samples with low concentration and motility had reduced levels of centrin, α- and γ-tubulin compared to normal samples (Hinduja et al., 2010), although, the results they presented are not convincing. But probably, the strongest experimental evidence of the importance of the centrosome during embryo early development was obtained in *Xenopus laevis*. When isolated human lymphoid cells centrosomes were injected into *Xenopus* eggs, they triggered parthenogenetic development (Tournier et al., 1989), whereas just pricking the oocyte, it does not.

Taking all this information into account, it seems that, in animal models where the centrosome is inherited during fertilization, the centrosome provides, at least, an advantage to the embryo to be successful in its development. Human reproduction is a highly inefficient process, especially during its early stages. Because sperm-inherited centrosomes are involved in early embryo development in animal models, we and others have hypothesized that centrosome abnormalities, either in structure, function or composition, could be the cause of some infertility cases. Therefore, many laboratories have been looking for a system to test the human sperm basal body functionality in an *ex vivo* system, and to integrate this system in the study of human fertilization related processes and sperm basal body to centrosome conversion. However, so far, the only set up methods consist in the injection of individual human spermatozoon into bovine or rabbit oocytes (Rawe et al., 2002; Terada et al., 2000; Ugajin et al., 2010) or in cell-free *Xenopus* egg extract (Simerly et al., 1999). In these studies, they observed that human spermatozoa with abnormal morphology and/or motility have centrosomal microtubule nucleation defects in bovine or rabbit oocytes. It is very likely, thus, that couples in which sperm basal body is defective will need the help of ART to have a child.

VIII. How does ART work?

1 in 9 couples trying to conceive will have some difficulties in achieving a pregnancy (Mascarenhas et al., 2012). Infertility was described in 1990 by the World Health Organization (WHO) as a "disease of the reproductive system defined by the failure to achieve a clinical pregnancy after 12 months or more of regular unprotected sexual intercourse". For many of these couples, a pregnancy will only be achieved with the help of ART.

According to the American Society of Reproductive medicine (ASRM), 1/3 of the infertility cases can be attributed to male factors alone, another 1/3 to female factors and the remaining 1/3 are a mix of male and female factors. However, another 20% of cases are idiopathic, it means that the causes are not known.

In this section I provide an explanation of gametes and embryo assessments, as well as a brief explanation of the main techniques that are performed in IVF clinics in order to bypass these infertility problems.

A. Sperm assessment:

One of the first procedures that an IVF laboratory performs in a new fertility cycle is the analysis of the semen sample. This analysis is known as "spermiogram" and reports many different semen characteristics such as pH, viscosity, spermatozoa motility and morphology. The objective of the spermiogram is not only to evaluate the sample but also to grade it to decide which is the best assisted reproduction treatment to perform. The WHO manual for semen analysis reported that the semen has two major quantifiable attributes: the total number of spermatozoa and the total fluid volume. However many other factors related to the nature of the spermatozoa and the composition of seminal fluids are also evaluated in a spermiogram because these parameters also provide valuable information regarding sperm quality.

Semen evaluation is a much more complex process than it seems because the results of the semen analysis can be quite variable due to the nature of the semen production. These uncontrollable factors include the variability among semen ejaculate fractions,

the activity of the accessory sex glands (more or less diluted sample), the abstinence period, and the size of the testis among other factors. Indeed, in a study in which the number of spermatozoa and sperm concentration was analyzed in 5 different individuals during one and a half year, these values were highly variable (Castilla et al., 2006; World Health Organization., 2010).

Here, I summarize some of the most common semen characteristics that are evaluated in a spermiogram, only the ones related to spermatozoa:

1. Motility:

This parameter evaluates the movement of the sperm and its trajectory. It is recommended to evaluate this parameter within 1 hour following ejaculation in order to reduce the negative effects of changes in temperature, pH among others. Sperm movement can be graded in 3 different categories (World Health Organization., 2010):

- **Progressive motility:** spermatozoa are moving linearly (**Figure 13A**) or in large circles (**Figure 13B**). However, in both cases they have an active movement.
- **Non-progressive motility:** this refers to all the movements in which the spermatozoon has a pattern of motility but it is not progressing (**Figure 13C**).
- **Immotility:** spermatozoa that do not move (**Figure 13D**).

When the sperm motility is analyzed, it is important to distinguish between total sperm motility, which includes progressive and non-progressive motility, or only progressive motility. In the 4rth edition of the WHO manual for the semen analysis published in 1999, the velocity of the spermatozoa movement was recommended to be analyzed and categorized as rapid (>25 μm/sec) or slow (<25 μm/sec). Nevertheless, the last edition did not recommended this value because the variability in its analysis did not provide useful information to grade spermatozoa samples.

The WHO also defines a lower reference limit for the evaluation of the different human semen characteristics (Cooper et al., 2010). The objective of establishing these reference values is to standardize the methodology and analyses for laboratories in which semen examinations are performed **(Table 2)**. Regarding motility, the WHO defines that the

lower reference limit for total motility (progressive and non-progressive) is 40%, and the lower reference limit for only progressive motility is 32%. When semen samples have values of spermatozoa motility lower than the reference limits, they are diagnosed as asthenozoospermic (low motility sample).
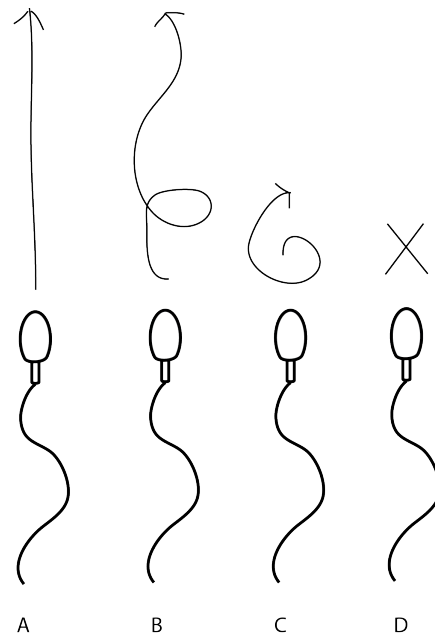
Figure 13: Sperm motility classification. Sperm motility is clinically classified in 4 different groups. A and B include progressive motility. C includes the cells that move around themselves, moving but in a non-progressive manner. Finally, D group includes the ones that do not move.

2. Morphology:

This parameter evaluates whether the morphology of the head, midpiece and tail is correct. The recovery of spermatozoa from the surface of the zona pellucida has helped to define morphologically normal spermatozoa (or at least the ones that arrive and bind to the zona pellucida) (Liu and Baker, 1992; Menkveld and Kruger, 1992). Since this parameter is very dependent on the biologist interpretation, the WHO recommends classifying the morphology as normal or abnormal, and more detailed information about abnormalities is restricted to each IVF clinic laboratory decision. For a spermatozoon to be considered normal, it has to present the following characteristics **(Figure 14 A)**:

-   **Head:** it has to be smooth, regularly contoured and oval in shape. The acrosome has to be well defined and contain only few vacuoles. The post-acrosome region should not contain vacuoles.

- **Midpiece:** has to be slender, regular and it has to be aligned with the major axis of the sperm head. Cytoplasmic droplets should not be present.

- **Tail:** it has to be thinner than the midpiece and uniform along its length. It has to measure approximately 45 μm.

But, when is a spermatozoon classified as morphologically abnormal? When spermatozoa heads are larger or smaller than expected, amorphous and/or vacuolated; the midpiece is asymmetrically inserted into the head, it is bent and/or abnormally thin or with an excess of residual cytoplasm; and the tail is short, or there are multiple tails in the same cell and/or it is coiled **(Figure 14B)**. Abnormal sperm sample can have any combination of these parameters. The reference limit for this spermatozoa parameter is 4% (Cooper et al., 2010). When a sample has less than 4% of spermatozoa with normal morphology, it is diagnosed as teratozoospermic **(Table 2)**.
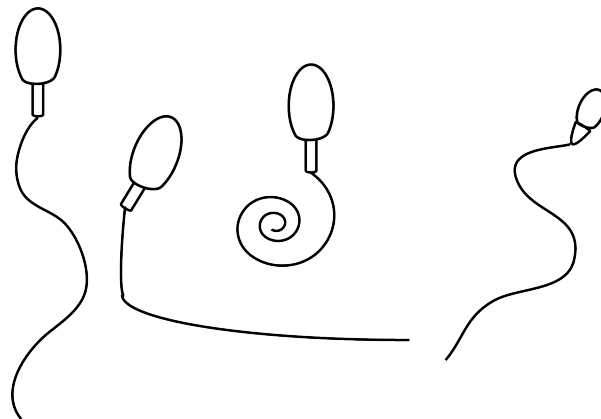
Figure 14: Sperm morphologies. This is a representation of the different sperm morphologies that can be observed in an heterogeneous sperm sample. The drawing on the left represents a morphologically normal spermatozoon. The following drawings represent cells with abnormal head to tail attachment, abnormal sperm tails and heads.

3. Sperm concentration and numbers:

It is a measure of the number of sperm cells per milliliter of ejaculate (sperm concentration). The total sperm number is a measure of the testicular sperm productivity. It is advisable to do the measurement of the sperm concentration and numbers in a Neubauer haemocytometer chamber of 100 μm in depth. In order to reduce the sampling errors, it is recommended to count at least 400 spermatozoa per sample.

The lower reference limits established for the spermatozoa concentration and number are 15×10^6 cells/ml and 39×10^6 per ejaculate, respectively (Cooper et al., 2010) **(Table 2)**. If any of these parameters is not equal or superior in a sperm sample analysis, the sample is diagnosed as oligozoospermic.

4. Sperm vitality:

The sperm vitality parameter measures the number of living cells and it is done by measuring the sperm membrane integrity. Like motility, it is recommended to evaluate this parameter within the first hour post-semen ejaculation. There are mainly two methods to analyze spermatozoa vitality. 1) Dye exclusion. This method is based on the principle that only death cells, or cells with a damaged cell membrane, will incorporate the dye. 2) Hypotonic swelling. In this scenario, only the living cells with intact membranes will swell in a hypotonic solution. The lower reference limit established for vitality is 58% (Cooper et al., 2010).

As mentioned, the threshold values are recommended and periodically updated by the WHO to classify sperm samples. In the following table, I summarize these values and the sample diagnosis when they do not reach the thresholds.

Table 2: WHO reference values for human semen characteristics. The following values are common parameters to classify sperm samples (Barratt et al., 2011; Cooper et al., 2010).

Parameter	Value	Diagnosis
Motility (% A+B+C)	40	Asthenozoospermia
Morphology (%)	4	Teratozoospermia
Concentration (mill/ml)	15	Oligozoospermia

When a sample has values above for each spermatozoa parameter, it is diagnosed as a "normal" sample, normozoospermic. However, semen samples can also have a combination of the previous abnormal diagnoses (asthenozoospermia, teratozoospermia and oligozoospermia), in this case, the samples are diagnosed with the combination of the different pathological diagnoses; for example, when samples have low motility and abnormal morphology, their diagnosis is asthenoteratozoospermia.

B. Oocyte assessment:

Oocyte selection is based, mainly, on their meiotic progression. Oocytes can be found at the Germinal Vesicle (GV) stage, MI or MII (or naturally matured oocyte). When women have enough MII oocytes, these are always the ones used for IVF/ICSI cycles. In the case that the patient does not have naturally MII oocytes, MI can be *in vitro* matured. MII oocytes are morphologically recognized by the extrusion of the 1st polar body.

Although oocyte assessment by meiotic progression is performed in all countries, the evaluation of other parameters are clinics-specific, therefore, it makes inter-clinic comparisons very difficult. In 2011, the Alpha Scientist in Reproductive Medicine and the ESHRE special interest group of Embryology met to define a common criteria and terminology for the grading of oocytes (Alpha Scientists in Reproductive and Embryology, 2011). The result of this meeting is a proposal document for assessing and grading oocytes not only by meiotic progression but also analyzing their anomalies. Anomalies should be discriminated in two groups depending on whether they occur in the cytoplasm or they are extracytoplasmic. Examples of intracytoplasmic anomalies are: refractile bodies, dense central granulation, vacuoles and aggregation of smooth-surfaced endoplasmic reticulum as a disc-like aggregate. On the other hand, extracytoplasmic anomalies are: first polar body morphology, perivitelline space size and granularity, discoloration, zona pellucida defects and shape anomalies.

Nevertheless, the consensus oocyte scoring analyzes the following oocyte parts: cumulus-oocyte complex, zona pellucida, perivitelline space, polar body, cytoplasm and vacuolization. A "good" cumulus-oocyte complex is defined as an expanded cumulus and a radiating zona. From the zona pellucida we should analyze its color and thickness only in particular cases because so far there are no solid evidences of zona pellucida color and thickness and IVF outcome. Regarding the perivitelline space, only the presence of inclusions should be noted as an anomaly. In the case of the polar body, it should be analyzed the presence of the 1st polar body as well as if it is exceptionally large. Oocytes with a large polar body should not be inseminated. The optimal oocyte cytoplasm is expected to be homogeneous. Cytoplasm with smooth-surfaced endoplasmic reticulum organized in disc-like aggregates is not recommended for

insemination. Finally, oocytes with large vacuoles (>14 μm in diameter) should be noted because if they persist after fertilization, they could influence the division plane (Alpha Scientists in Reproductive and Embryology, 2011; Magli et al., 2012).

C. Embryo assessment:

Grading an embryo includes an evaluation of the fertilization check, of the cleavage, the morula and the blastocyst stage. Each specific stage has a different evaluation criterion (Alpha Scientists in Reproductive and Embryology, 2011; Magli et al., 2012):

1. Fertilization check:

Two important elements to be analyzed at D+1 post-fertilization are the pronuclei and polar bodies. An optimal fertilized oocyte must have two juxtaposed pronuclei of a similar size, and two polar bodies also of a similar size and located each other in a close proximity. The fertilized oocytes with only one pronucleus or 3 or more pronuclei are directly discarded.

2. Cleavage-stage embryos:

This includes the analysis of embryos at D+2 and D+3 post-fertilization and involves the evaluation of 4 main parameters:

- **Cell number:** at D+2 an embryo must have 4-cells and at day D+3, 8-cells. Embryos that cleave slower or faster are considered to have a reduced implantation potential.
- **Fragmentation:** fragments are small cytoplasmic volumes surrounded by membranes that localize outside the cells. Fragments at D+2 have to be in size less than 45 μm in diameter and less than 40 μm at D+3. Three different degrees of fragmentation were defined: mild (<10%), moderate (10 – 25%) and severe (>25%).
- **Multinucleation:** it refers to the presence of more than one nucleus and/or micronuclei in a single cell or blastomere. When multinucleation is observed, the probability of this embryo to success is severely reduced because this parameter is associated with chromosome abnormalities.
- **Cell size:** cells at D+2 and D+3 must be symmetric.

Despite all these parameters, other features such as the presence of vacuoles and the cytoplasmic granularity should be also noted.

The characteristics that were established that define an optimal D+2 embryo were: 4 symmetric and mononucleated cells with less than 10% of fragmentation. The consensus for an optimal D+3 embryo was: 8 symmetric and mononucleated cells with less than 10% of fragmentation. These embryos will be graded as nº1, but two more grades were defined: grade 2 includes embryos with the correct number and size of the mononucleated cells, but with a moderate fragmentation. Grade 3 embryos, and the ones with a poorest rating, they have a severe fragmentation, abnormal cell size and number and are multinucleated. As much as possible, embryos graded as optimal (Grade 1) should be used.

3. Morula stage:

The assessment of an embryo at D+4 is basically the analysis of its compaction stage. 3 different grades were established for D+4 embryos. Grade 1 or good embryos includes embryos that are compacting or are already compacted and are in the 4th round of cell division. Grade 2 includes the embryos that, almost in their totality (as embryo volume), are compacting and they also have entered into the 4th round of cell division. Finally, grade 3 embryos (also rated as "poor") are the ones in which less than half of the embryo is compacted.

4. Blastocyst stage:

At D+5 post-fertilization an optimal embryo should be fully expanded with the two well-differentiated cell lineages: ICM and the TE **(Figure 15)**. The ICM must be easily detected, with many tightly adhered cells. The TE should be seen as a cohesive epithelium. Blastocysts were agreed to be graded by three main parameters, creating a complex formula: stage of development (1 to 4: early blastocyst, blastocyst, expanded blastocyst and hatched blastocyst); ICM (1 to 3: good, fair and poor) and TE (1 to 3: good, fair and poor). ICM and TE grade 2 and 3 share that they have few cells and are less tightly bound.
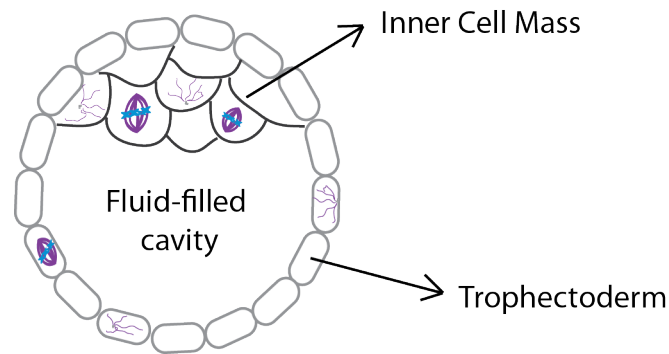
Figure 15: Expanded blastocyst. When a blastocyst at D+5 is expanded we can differentiate 3 different parts: The trophectoderm (TE), which will give rise to the placenta; the inner cell mass (ICM), which will give rise to the fetus and finally a fluid-filled cavity.

D. Intrauterine insemination (IUI):

The intrauterine insemination consists on the introduction of spermatozoa previously selected in the female's uterus with a cannula. Compared with other ART, IUI is relatively simple. It can be performed during a natural or an hormonal stimulated cycle and with the partners' semen or with a donor's (Kim et al., 2014). The IUI was first introduced in 1962 and according to the ESHRE, nowadays, more than 200,000 cycles are carried out every year in Europe (European et al., 2016; Matorras et al., 2018). However, its main inconvenient is that the number of multiple pregnancies is higher compared to other ART. Among others, IUI is specially recommended in cases in which the ovulation cycle is altered and the quality of the semen sample is not severely affected.

E. *In vitro* fertilization (IVF):

This technique consists in obtaining the male and female gametes and performing the fertilization process outside the body of the woman. Therefore, using this technology, the fertilization occurs *in vitro* rather than *in vivo*. Unlike IUI, in IVF both male and female gametes can be from patients or from donors.

How are the gametes obtained? Sperm ejaculates, like in the IUI technique, are first diagnosed (section: sperm assessment) and then processed. The processing consists in obtaining a fraction enriched in motile spermatozoa and with normal morphology. There are different techniques to do that, like the swim-up (Materials and Methods section) or discontinuous gradient. The process to obtain the oocyte is much more complex. First

the woman must undergo a hormonal stimulation in order to obtain a sufficient number of COCs (cumulus – oocyte complex) for the IVF cycle (Hamdine et al., 2014). Before ovulation, the oocytes are retrieved by ultrasound-guided transvaginal puncture and then they are immediately identified and evaluated in the IVF laboratory (Van Voorhis, 2007).

Once male and female gametes are obtained, two different techniques can be performed: the classic IVF or ICSI (Intracytoplasmic Sperm Injection).

1. Classic IVF:

Oocytes and processed spermatozoa are incubated in the same plate over-night. The ratio of spermatozoa per oocyte was proposed to be adjusted depending on the sperm diagnosis (Fiorentino et al., 1994). The following day, oocytes are analyzed for pronuclei formation to check whether they have been successfully fertilized.

2. ICSI:

This technique is based on the injection of an individual spermatozoon into an oocyte. This technique was introduced in humans in 1992 by Palermo (Palermo et al., 1992) to improve fertilization in couples that either have a severe male factor and/or with fertilization failures in previous classic IVF cycles (Benadiva et al., 1999; Practice Committees of the American Society for Reproductive and Society for Assisted Reproductive, 2012). It is interesting to say that this technique was already developed in 1966 for non-mammalian gametes (Hiramoto, 1962).

In both cases, fertilized oocytes are maintained in culture and evaluated according to the previously described "embryo assessment". Embryos at D+2, D+3 or D+5 are the normally preferred for their transfer into the woman uterus. The number of embryos transferred depends on their quality, the women's age and the number of cycles that the couple has performed, however, the tendency is, in the cases of favorable prognosis, to transfer only one embryo, because it is the safest condition for the women and the newborn (Klitzman, 2016).

IV. The *Xenopus* egg extract system as a tool to study microtubule dynamics during fertilization:

The *Xenopus* egg extract system (XEE) is a tool used to study microtubule nucleation, spindle assembly and microtubule dynamics. Some of the advantages of this system are the following:

- Each frog lays thousands of eggs. The cytoplasmic material of these eggs (XEE) can be isolated and approximately 1 ml of cytoplasm is obtained per frog.
- XEE is arrested at MII phase. The transition from meiosis to interphase and then to mitosis can be externally triggered.
- XEE do not contain chromosomes and centrosomes
- It is an open system; the effect of removing or adding different components or proteins on microtubule dynamics can be studied.
- It is enriched in protein, mRNA and other components. 12 cell cycles can be performed without the need for transcription.

All these advantages make the XEE system a suitable tool to study microtubule and spindle dynamics. Moreover, the addition of sperm and calcium to the MII arrested XEE mimics fertilization. Therefore, this system can be also used to study the molecular details of the fertilization process.
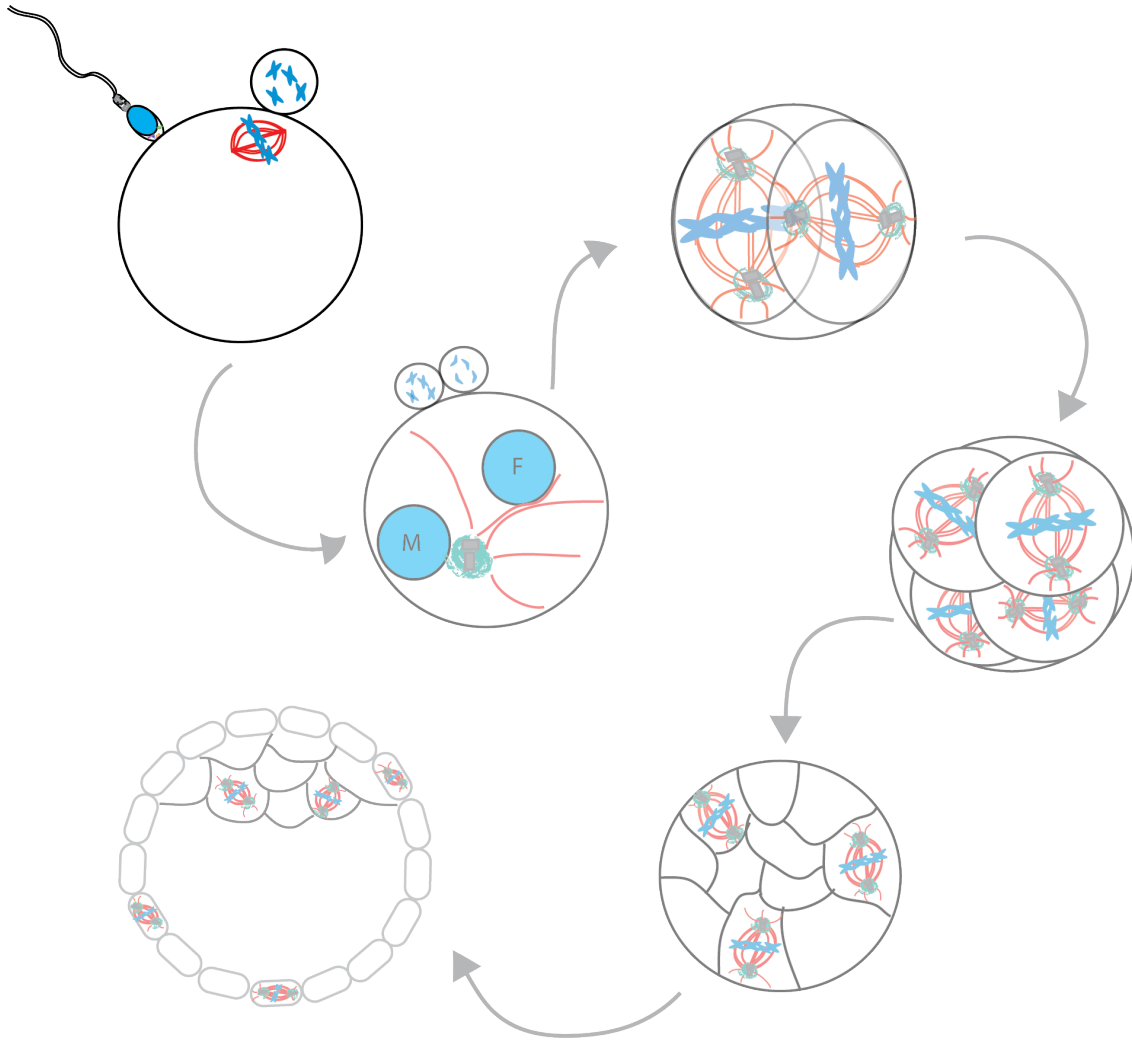
The main objective of this thesis is to understand and provide novel methodologies to study the fertilization process, specifically the sperm basal body to centrosome transition and its importance in supporting early embryo development, with a special emphasis in understanding the molecular causes of pre-implantation arrests.

Specifically, the objectives are:

1. To set up a method to study the molecular mechanisms that the spermatozoon triggers upon oocyte fusion and to functionally evaluate pathological sperm samples in an *ex vivo* oocyte cytoplasm.

2. To analyze the inheritance mechanism of the human sperm basal body and how it is converted into a functional centrosome in the zygote, with the objective of improving our basic knowledge on centrosome biology during fertilization.

3. To evaluate whether the inheritance of the centrosome during human fertilization provides an advantage during the embryo pre-implantation development.
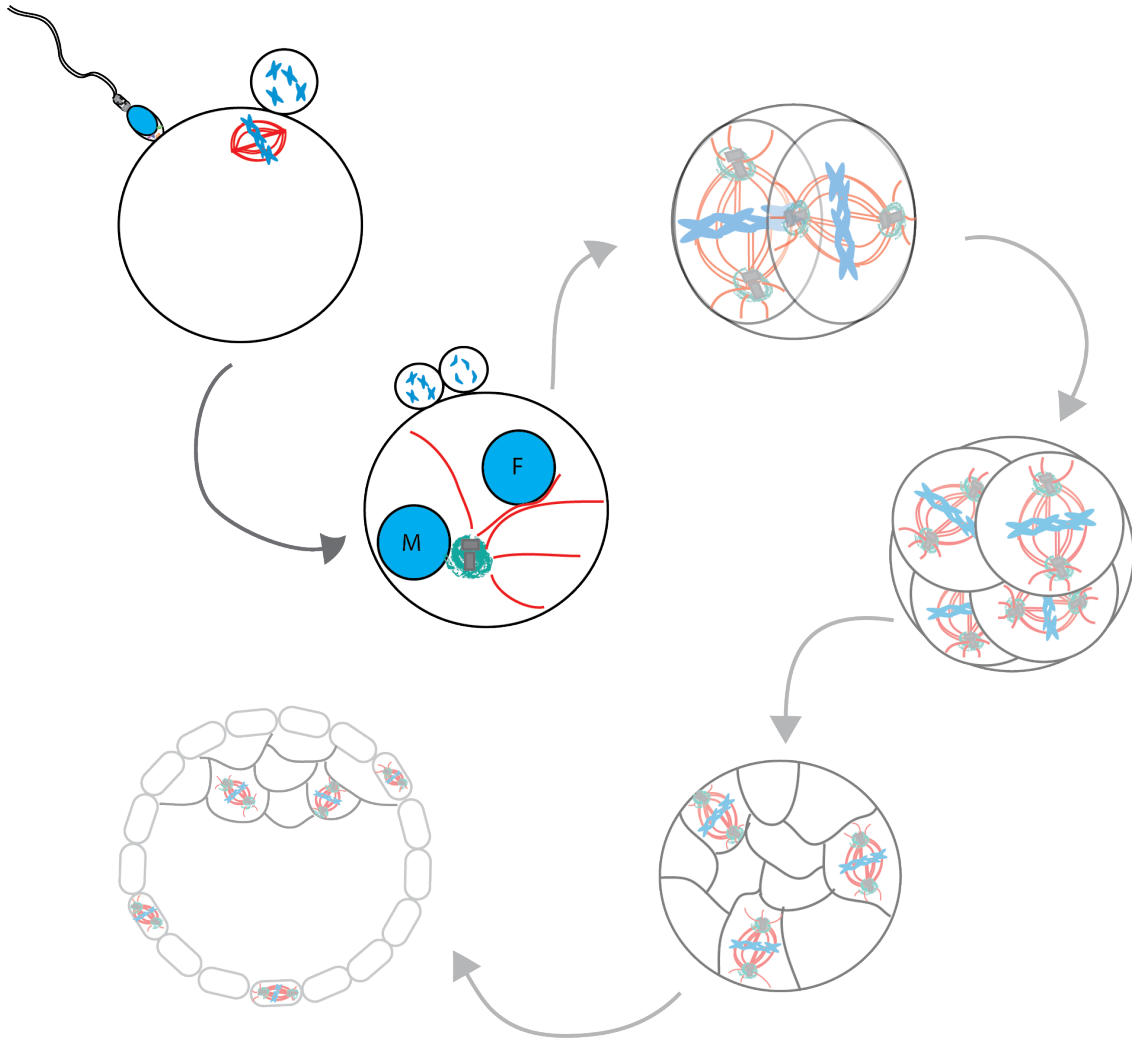
I. Results overview:

I decided to present the results section in three chapters. The first chapter contains a method to study the molecular mechanisms that the spermatozoon triggers upon fertilization. This method can also evaluate the functionality of human semen samples in terms of microtubule nucleation and spindle assembly. The idea of translating this basic method to reproductive clinics is attractive, because we demonstrated that it could be used as a new diagnostic and prognostic test.

The second and third chapters contain a descriptive and functional characterization of the human sperm basal body and its transition into a functional centrosome upon fertilization. Furthermore, the third chapter includes functional assays in human oocytes, to study whether the centrosome inheritance during fertilization is needed to support human embryo early development.

With these three studies, I wanted to obtain a global view of the microtubule organizing centers and microtubule dynamics of the mature spermatozoon, during fertilization and in the early embryo development.

II. Chapter 1: Functional analysis of human pathological semen samples in an oocyte cytoplasmic *ex vivo* system.

Information about human fertilization is very scarce, mainly due to ethical and technical limitations. Moreover, because human samples are limited, and the natural biology of the gametes, many techniques cannot be applied.

In order to bypass these limitations, we decided to set up a methodology based on the use of *Xenopus* egg extract and human spermatozoa. This system not only allows us to study the behavior of the human spermatozoon once it is placed in an oocyte environment in a molecular perspective, but also to use it as a diagnostic method to analyze human semen samples functionality in terms of microtubule nucleation and organization.

This chapter is written in a "manuscript" format, and submitted to "Science Translational Medicine".

Title: FUNCTIONAL ANALYSIS OF HUMAN PATHOLOGICAL SEMEN SAMPLES IN AN OOCYTE CYTOPLASMIC EX VIVO SYSTEM

Authors: Amargant F[1,2], García D[3], Barragán M[2], Vassena R[2*], Vernos I.[1,4,5*]

Affiliations:

[1] Cell and Developmental Biology Programme, Centre for Genomic Regulation (CRG), Barcelona Institute of Science and Technology, Doctor Aiguader 88, 08003 Barcelona, Spain.

[2] Clínica EUGIN, Travessera de les Corts 322, Barcelona, 08029, Spain.

[3] Fundació EUGIN, Travessera de les Corts 314, Barcelona, 08029, Spain.

[4] Institució Catalana de Recerca I Estudis Avançats (ICREA), Passeig de Lluis Companys 23, 08010 Barcelona, Spain.

[5] Universitat Pompeu Fabra (UPF), Barcelona, Spain.

*To whom correspondence should be addressed:

rvassena@eugin.es, isabelle.vernos@crg.es

One Sentence Summary: *ex vivo* system to functionally study human fertilization events.

Abstract:

Human fertilization and embryo early development involve a wide range of critical processes that determine the successful development of a new organism. Although Assisted Reproduction Technologies (ART) solved the infertility problems associated to severe male factors, the live birth rate is still low. A high proportion of ART failures occur at very early stages before implantation. Understanding the causes for these early failures has been difficult due to technical and ethical limitations. Diagnostic procedures on human spermatozoa in particular have been limited to morphology and swimming behaviors while other specific functional requirements during early development have not been addressed due to the lack of suitable assays. Here, we have established and validated a quantitative system based on the use of *Xenopus* egg extracts and human spermatozoa. This system provides novel possibilities for the functional characterization of human spermatozoa. Using clinical data we show that indeed this approach offers a set of complementary data for the diagnosis of spermatozoa from patients.

Introduction:

Infertility is a global disease affecting 1 in 9 couples in developing countries. The introduction of ART such as *in vitro* fertilization (IVF) (Steptoe and Edwards, 1978) and especially intracytoplasmic sperm injection (ICSI) (Palermo et al., 1993), have helped to address infertility due to severe male factor; nevertheless, the live birth rate per cycle of IVF/ICSI is still less than 30%. One of the most important bottlenecks in IVF/ICSI cycles occurs during the first five days of development, i.e. up to blastocyst formation. Approximately 25% of the oocytes injected with a sperm arrest their development at day 1 due to fertilization errors, while 25-30% of the remaining embryos are lost in culture during the first days of *in vitro* development. Although some factors affecting embryo development, such as complex aneuploidies and severe sperm DNA fragmentation, have been identified, the systematic characterization of possible causes of embryo loss, at the molecular level, has been hampered by ethical and technical issues alike. The development of functional assays that recapitulates the process of human fertilization and early embryo development should improve our understanding of developmental arrest, allowing for better selection methods for gametes, and ultimately improving the success rate of IVF/ICSI.

After ovulation, the human oocyte is arrested at the metaphase of meiosis II (MII). When the sperm fuses with the oocyte, the oocyte is activated, meiosis resumes, and half of the sister chromatids are extruded into a second polar body. The fertilized oocyte enters interphase before starting mitosis. In interphase, the male and female chromatin decondenses, replicates, and forms the male and the female pronuclei. Protamines are exchanged from the male chromatin for histones (Johnson et al., 2011). In addition, the basal body from the sperm recruits pericentriolar material (PCM) stored in the oocyte cytoplasm. The centrosome in the fertilized oocyte generates an array of microtubules that mediates the male and female pronuclei movement and apposition, and prior to the first division of the zygote, the centrosome duplicates (Clift and Schuh, 2013).

The centrosome is the main microtubule organizing center of the cell. It is formed by two centrioles, oriented perpendicularly to each other, surrounded by PCM (Bettencourt-Dias and Glover, 2007). In interphase, most microtubules are nucleated at the centrosome; it is therefore a main player in the intracellular organization as well as in cilia/flagella assembly, among other functions. In mitosis, two main pathways of microtubule assembly, the centrosomal and the chromatin-dependent pathway, cooperate to support spindle assembly (Cavazza et al., 2016). The mitotic spindle is defined by the presence of the duplicated centrosomes that define the two spindle poles and spindle orientation thereby also defining the axis of cell division.

Spindle assembly and microtubule dynamics have been widely studied using the *Xenopus* egg extract system (XEE) (Karsenti and Vernos, 2001). *Xenopus* eggs are naturally arrested in MII and do not contain centrosomes, resembling human oocytes. The cytoplasm of *Xenopus* eggs can be isolated and manipulated in the test tube to follow interphase and mitotic events associated with the chromatin and the microtubules. These events are physiologically relevant as they occur *in vivo* upon fertilization and culminate with the assembly of the first mitotic spindle (Hannak and Heald, 2006).

In the present study, we developed an *ex vivo* heterologous system based on the incubation of human spermatozoa in XEE in order to obtain functional information on the activity of the human sperm once placed in an oocyte cytoplasm environment. We

further characterized the performance of semen samples from patients in this *ex vivo* heterologous assay. We show that this system provides functional data that may improve clinical diagnosis as well as our basic knowledge of the mechanisms that the spermatozoon triggers upon fertilization.

Results:

Human spermatozoa assemble functional chromatin in *Xenopus* egg extracts

Xenopus eggs are laid arrested in the second metaphase of meiosis ready for fertilization. Undiluted cytoplasmic extracts prepared from these eggs (XEE) have been widely used to study the cell cycle and spindle assembly **(Figure 16A)**. We decided to test whether this system could be suitable to perform functional studies on human spermatozoa and provide tools to address male infertility. One of the first and limiting events that occur after fertilization is the reorganization of chromatin. In interphase the spermatozoa chromatin deconsenses and forms the male pronucleus; in mitosis, the chromatin condenses into chromosomes that align at the metaphase plate. We first addressed whether XEE could provide a system to study the chromatin-associated events that occur in the fertilized oocyte. We monitored chromatin decondensation and condensation of human normozoospermic samples incubated in XEE, using the *Xenopus* spermatozoa as control. The XEE were sent into interphase by calcium addition. Samples were collected at different time points during the 90min of interphase and then during the 60min after cycling the extract back into mitosis. DNA decondensation during interphase and condensation during mitosis was quantified by measuring the area occupied by the chromatin. Human sperm chromatin decondensed gradually during interphase reaching a maximum area at the end of the 90min interphase period, following a similar trend of the *Xenopus* sperm chromatin (**Figure 16B and C**). As previously reported, the DNA of human sperm samples not pretreated with DTT did not decondense when incubated in interphase XEE (Lohka and Maller, 1988; Ohsumi et al., 1988) **(data not shown)**. This suggests that the reduction of the disulfide bounds of protamines is necessary for their exchange by histones. The human sperm chromatin decondensation occurred in 3 phases: during the first 10 minutes the chromatin went through a rapid initial decondensation phase expanding to an area of 63 ± 10.5 μm^2 although a local constriction was still visible, probably reflection a steric hindrance **(Figure 16B and C)** (Gordon et al., 1985). Subsequently the chromatin

85

condensed slightly over a period of approximately 30 minutes. After 40 minutes, the chromatin occupied an area of 50 ± 10.5 μm^2. Towards the end of interphase (90 min), the chromatin had expanded into a round pronucleus with a maximum area of 126 ± 42.2 μm^2. Although the overall pattern of decondensation of the human sperm chromatin was similar to that of *Xenopus*, the area occupied by the human chromatin was systematically smaller at the same time points. Indeed it was 2.3 times smaller than the *Xenopus* sperm chromatin after 3 min in interphase XEE, and 2.7 times smaller at the end of interphase when the *Xenopus* sperm induced pronucleus occupied an area of 343 ± 49.8 μm^2. Upon entry into mitosis by addition of CSF-EE, both human and *Xenopus* chromatin condensed rapidly and aligned forming the metaphase plate (**Figure 16B and C**).

Having established the profile of chromatin decondensation/condensation for human normozoospermic samples during interphase and mitosis we then looked at sperm samples with altered spermiogram. The chromatin decondensation profiles of asthenozoospermic samples was very similar to the normozoospermic ones during the first 2 phases, occupying areas of 62 ± 4.1 μm^2 in phase 1 and 52 ± 2.7 μm^2 in phase 2. More variability was observed in the last step of decondensation although the difference with the normozoospermic samples was not significant (area of 86 ± 6.6 μm^2; ns $p=0.4359$). Chromatin from asthenozoospermic samples condensed upon entry into mitosis and formed the metaphase plate as efficiently as the chromatin from normozoospermic samples (**Figure 16B and C**).

Overall we conclude that the XEE system is suitable to study human sperm chromatin decondensation in the interphase oocyte cytoplasm and its condensation into chromosomes during the first zygotic mitosis.

The human spermatozoa DNA replicates in *Xenopus* egg extracts

After fertilization and during the first interphase, the sperm chromatin replicates in preparation for the first mitosis of the zygote. We monitored human spermatozoa DNA replication upon incubation in interphase XEE containing biotin-dUTPs. Immunofluorescence analysis at different time points of incubation showed that $16\pm3.6\%$ of the spermatozoa had incorporated biotin-dUTP in their chromatin after 30 min in interphase and $51\pm9.0\%$ after 90 min (**Figure 16D and E**). In mitosis we

detected that 89±3% of the human chromatin groups had incorporated biotin-dUTPs suggesting that sperm chromatin replicated correctly. These percentages are similar to the control *Xenopus* spermatozoa. As expected, the global replication process appeared to be coordinated with the DNA decondensation phases. Asthenozoospermic samples showed a similar pattern of DNA replication as normozoospermic ones.

Altogether these data suggest that the main chromatin-associated events (DNA decondensation and replication) which the sperm chromatin undergoes in the oocyte cytoplasm can be visualized in XEE. Moreover, this provides a novel system to evaluate patient samples. Here we assessed DNA decondensation and replication kinetics in human sperm samples showing abnormal motility and found that they did not present any chromatin decondensation or replication defects.

The human sperm basal body converts into a centrosome that nucleates microtubules in *Xenopus* egg extracts

Fertilization in humans and other organisms involves the fusion of a female gamete devoid of any centrosome and a male gamete with a basal body between the head and the flagellum. Upon fertilization, the basal body converts into the first centrosome of the new organism. The basal body of the human spermatozoa is an atypical centrosome with a 'degenerated' distal centriole and with little or no associated Pericentriolar Material (PCM). It has been proposed that upon fertilization, the human basal body recruits PCM components required for the formation of the first functional centrosome of the new organism from the oocyte cytoplasm.

Indeed, human spermatozoa incubated in pure tubulin *in vitro* did not nucleate microtubules. We then addressed directly the recruitment of PCM by the human sperm basal body centrioles using the XEE system. Human spermatozoa were stripped from PCM proteins and applied onto a coverslip. After incubation with XEE, the samples were washed and incubated with pure tubulin. Immunofluorescence analysis showed that the sperm centrioles did nucleate microtubules **(Figure 17A)**. This suggested that the human sperm centrioles had recruited PCM components from the egg cytoplasm.

Human spermatozoa trigger bipolar spindle assembly in *Xenopus* egg extracts

The correct formation of a bipolar spindle is not only an essential mechanism for the segregation of the genetic material in two daughter cells, but also for the development and survival of a healthy individual. We decided to test whether human spermatozoa can trigger spindle assembly in XEE. Human normozoospermic spermatozoa were pre-treated to loosen their membrane and incubated in XEE (**Supplementary Table 1**). The extract was sent into interphase by addition of Calcium and cycled back into mitosis by addition of CSF-EE, as previously described for cycled spindle assembly assays with *Xenopus* sperm nuclei (**Figure 16A**). After 60min in mitosis the samples were centrifuged onto coverslips, fixed and processed for fluorescence microscopy analysis. As a control, *Xenopus* sperm nuclei also pre-treated to loosen their membrane were processed in parallel. Microtubule structures associated with the sperm chromosomes were classified into three categories: Bipolar Spindles (BP) having two focused spindle poles and the chromosomes well aligned at the metaphase plate, Abnormal Structures (AB) consisting of disorganized microtubule arrays, and No Structure (NS) when chromosomes had no associated microtubules. Human spermatozoa triggered bipolar spindle assembly in XEE as efficiently as the control *Xenopus* sperm nuclei; the proportion of bipolar spindles was 65±3.2% for the human spermatozoa and 61±10.5% for the *Xenopus* sperm nuclei (p=0.5378; ns). The proportion of disorganized structures was also very similar for human spermatozoa (21±4%) and *Xenopus* sperm nuclei (24±1.7% ; p=0.2622 ; ns). Finally, 14±7% (human) and 15±9.5% (Xenopus) (p=0.8945; ns) of the nuclei had no associated microtubules (**Figure 17B and C**).

The morphology of the bipolar spindles formed around the human sperm chromosomes was also very similar to the control ones formed around *Xenopus* sperm nuclei. However, their length measured from pole to pole was 15.5% shorter (40 spindles per condition, p≤0.0001) (**Supplementary figure 1**).

We then tested whether sperm samples with different spermiograms can also form bipolar spindles, and whether they do it with different proportions. Asthenozoospermic (n=4) and teratozoospermic (n=6) samples, as well as normozoospermic ones (n=14) were tested for cycled spindle assembly in XEE as described above. We found that all samples triggered bipolar spindle assembly albeit with different efficiencies: 60±7.6% of bipolar spindles for normozoopermic samples, 56±4.6% for asthenozoopermic ones and 57±9.8% for teratozoospermic (**Figure 18A**). Moreover, asthenozoospermic

samples formed a higher proportion of abnormal spindles compared with normozoospermic ones (p=0.0066).

We then investigated whether centrioles were present at the poles of the spindles assembled by human spermatozoa by immunofluorescence microscopy (Cavazza et al., 2016) **(Figure 18B and C)**. We could detect centrioles at the spindle poles with a similar frequency for both human and *Xenopus* samples. These data suggested that the human sperm centrioles had duplicated during interphase and correctly localized at the spindle poles. We obtained similar results for asthenozoospermic samples **(Figure 18B and C)**.

Altogether our data show that human spermatozoa efficiently trigger the formation of bipolar spindles with centrosomes at their poles when incubated in XEE. They suggest that patient sperm samples with different diagnosis have different spindle assembly efficiencies not associated with centrosome defects.

Predictive value of the spindle assembly test in *Xenopus* egg extracts in the context of clinical data

To determine whether the spindle assembly assay in XEE has any predictive value for IVF/ICSI for patients with different spermiogram results, cycled spindle assembly assays were performed for 26 individual samples. The assays were performed independently four times with different XEE. The ratio of bipolar spindles in each experiment was then quantified as described above and normalized to the results obtained from parallel experiments with control *Xenopus* sperm nuclei incubated in the same XEE. The averages from the four experiments showed a moderate positive correlation between the ratio of bipolar spindle and three clinical parameters: spermatozoa motility B (R=0.506) and C (R=0.408), spermatozoa concentration (R=0.495), and the percentage of normal spermatozoa morphology (R=0.420) **(Figure 19A, B, C and D respectively)**. Interestingly, we obtained a negative correlation between the ratio of BP and the motility parameter D **(data not shown)**. This suggests that the assay is sensitive enough to obtain data for samples with bad prognosis.

Altogether, these results indicate that scoring spindle assembly efficiency of human sperm samples in XEE provides a novel and reliable test for assessing the human

spermatozoa functionality into the oocyte. Moreover, specific functional information can be obtained for difficult cases concerning chromatin physiological condensation/decondensation and replication as well as basal body conversion to a centrosome.

Discussion:

Although many oocytes fail to fertilize and a number of zygotes arrest their development during the first cell divisions after IVF/ICSI, the molecular causes of these failures remain difficult to investigate. Advances in this area are hampered by the lack of experimental systems that could provide functional information on the human gametes during and after fertilization. The present study describes an *ex vivo* heterologous system based on the use of XEE to obtain functional information on human spermatozoa, by testing their capacity for driving microtubule nucleation and spindle assembly providing essential information for their role in fertilization and early development. Although a previous study had used XEE to study human spermatozoa (Simerly et al., 1999), here we have expanded the array of functional analysis and taken them to a quantitative level to define different chromatin and microtubule-associated events that must occur for a successful fertilization and early development.

Some of the sperm factors reported to be related with poor embryo development are severe DNA damage (Simon et al., 2014), epigenetic abnormalities (Gannon et al., 2014), severe aneuploidies (Templado et al., 2013) and centrosome dysfunction (Rawe et al., 2002), among others. One of the earliest and critical events that occur in the zygote is the formation of a functional bipolar spindle to segregate correctly the genetic material into two daughter cells (Van Blerkom et al., 2004). According to Simerly et al (1995), about 25% of the fertilization failures observed in ART cycles are associated with defects in microtubule nucleation and organization (Simerly et al., 1995). Therefore, a system that could score the probability of assembly a functional spindle would inform about the chances of a successful IVF/ICSI cycle. We validated our functional system by scoring 26 patient samples for bipolar spindle assembly in XEE, and found that samples with a higher percentage of motile spermatozoa, higher concentration and a normal morphology trigger bipolar spindle assembly more efficiently. These results suggest that our quantitative system can be used to

functionally diagnose sperm samples with IVF/ICSI cycles of already bad prognosis to propose the most convenient ART approach. They also provide some molecular evidences to the open question of whether the sperm selection criteria currently in use are effective clinically. Indeed our results provide a validation of the current sperm selection criteria showing that normozoospermic samples with optimal parameters have higher probabilities to support fertilization and early development (Arikan et al., 2012; Li et al., 2014).

We did not detect major differences for chromatin-associated events (decondensation-condensation, replication) for normozoospermic and asthenozoospermic sperm samples. We found a negative correlation between type D motility and bipolar spindle formation efficiency. This correlation is in agreement with the poor fertility prognosis of immotile spermatozoa but goes beyond the difficulties in fertilization proper (Ortega et al., 2011).

To our knowledge this is the first assay that provides a correlation between semen diagnosis parameters and molecular data related to cell division in the oocyte. With this validation, we posit that our system will be useful to study several sperm dependent processes as well as the causes of male idiopathic infertility. For instance, it could be used to study spermatozoa that fail to activate the oocyte resulting in absent pronuclei, which represents the 15% and the 40% of cases in IVF and ICSI cycles respectively; or the ones with abnormal pronuclei formation (approximately 20% of the failed fertilizations) (Rawe et al., 2000). In ART, the timing of pronuclear formation and cell division is an important indicator of fertilization and embryo quality. Our assay is amenable to check whether longer S-phases correlate with abnormal chromatin decondensation-condensation patterns and/or protamine exchange by histones, and whether these alterations affect later molecular events as bipolar spindle assembly. This would indicate whether the timing of pronuclei formation is a limiting factor for embryo development.

Several studies remarked the importance of the centrosome for pronuclei migration, syngamy and embryo cleavage (Hewitson et al., 1997; Navara et al., 1995; Rawe et al., 2002). Indeed, individual cases of severe asthenoteratozoospermia with abnormal head – to – tail attachment exhibit no microtubule nucleation from the centrosome once they are injected into a bovine oocyte (Rawe et al., 2002). Another study showed that the

average rate of sperm aster formation was lower for spermatozoa from infertile patients injected in bovine oocytes than those produced by spermatozoa from fertile patients (Yoshimoto-Kakoi et al., 2008). Our system could be very useful to analyze whether some idiopathic infertility cases are due to abnormal centrosome function as well as to obtain quantitative data for the basal body to centrosome transition and its microtubule nucleation activity *in vitro* for specific sperm samples.

Overall, we have developed and validated a quantitative heterologous system using human spermatozoa and XEE that mimics the events triggered by the human spermatozoa during fertilization. The system was validated using clinical data. It provides a quantitative approach to address molecular mechanisms that are very difficult to study in human oocytes due to ethical restrictions. Moreover, it reduces the bias originated by the heterogeneous human oocyte sample population, which in clinical studies cannot be ignored. It will be particularly interesting to use this system for cases of unexpected fertilization and early embryo development failures. The system could provide some molecular evidences to address these infertility cases.

Materials and Methods:

Ethics

Permission to conduct this study was obtained from the local Ethical Committee for Clinical Research. All procedures performed were in accordance with the ethical standards of the institutional research committees and with the 1964 Helsinki declaration, as revised in 2013. Written informed consent to participate was obtained from all participants prior to their inclusions in the study.

Sperm preparation

Human sperm samples were washed with HSPP buffer (250mM sucrose, 15mM Hepes pH 7.4, 0,5mM spermidine, 0,2mM spermine and protease inhibitors) and centrifuged at 850xg for 10 minutes at room temperature. After some initial optimization **(Supplementary Table 1)** sperm samples were treated with HSPP buffer containing 1mM of DTT during 10 minutes at room temperature. Next, the same volume of HSPP buffer containing 1mM of DTT and 0,5% Triton X-100 was added to the solution and kept under movement for 30 minutes at room temperature. The reaction was stopped

adding HSPP-BSA 3% in excess and chilled on ice for 10 minutes followed by centrifugation at 850xg for 10 minutes at 4ºC. The pellet was washed with HSPP – BSA 0,3% and then diluted with HSPP – 0,3% BSA – 30% glycerol and adjusted to $2x10^7$ cells/ml before freezing. *Xenopus* spermatozoa were treated as previously described (Murray, 1991).

Egg extract and spindle assembly

Preparations of fresh CF-arrested *Xenopus* egg extract (CSF extract) and cycled spindle assembly reaction were performed as previously described (Desai et al., 1999). Briefly, *Xenopus laevis* frogs were stimulated with 100 and 1,000 I.U PMSG and hCG respectively to lay eggs arrested at MII. The eggs were centrifuged at 10,000xg at 4ºC and then the cytoplasmic layer was isolated. To analyze spindle assembly in cycled XEE, 3,000 sperm nuclei (human or *Xenopus*) together with 0,4mM of calcium and ≈0,2 mg/ml of Rohodamine-labelled tubulin (to visualize microtubules) were added to the CSF-extract and placed at 20ºC to release the XEE into interphase (90 minutes). Then the interphasic XEE were cycled back to mitosis by adding the same volume of CSF-EE (60 minutes; total time of 150 minues) **(Figure 16A)**. Bipolar spindles assembled were pelleted by centrifuging the XEE at 4,000xg for 20 minutes at room temperature through a spindle cushion buffer (40% glycerol, 1x BrB80 (80mM K-pipes, pH 6.8, 1mM $MgCl_2$, 1mM Na_3EGTA)). The samples were fixed with methanol and the DNA was stained with Hoechst (1μg/ml, 33342 Invitrogen) for 30 minutes.

Decondensation and replication assays

To analyze the decondensation dynamics of the spermatozoon nucleus, 2 μl of cycling XEE was stained with Hoechst (1μg/ml, 33342 Invitrogen). The area of individual sperm nucleus was analyzed for each time point using Fiji (ImageJ software, NIH, USA). For the replication assay, 40 μM of biotin-dUTPs (R0081, ThermoFisher) were added to the cycling XEE. 10 μl of the mix was taken every 30 minutes and fixed for 1 hour at room temperature in 200 μl of XB (10 mM Hepes, 100 mM KCl, 0.1 mM $CaCl_2$, 1 mM $MgCl_2$, 50 mM sucrose) containing 4% formaldehyde. The samples were centrifuged at 2,500 g through a 0.7 M sucrose cushion in XB onto coverslips and post-fixed for 4 minutes in methanol at -20ºC. Finally, a Streptavidin-Alexa Fluor 488 conjugate antibody (S11223, ThermoFisher) and Hoechst (1μg/ml, 33342 Invitrogen)

were used to detect replicated and total amount of DNA, respectively. 20 spermatozoa per condition and time point were analyzed for each experiment.

Tubulin and centrosome detection

Rhodamine-labeled tubulin was added to the XEE to visualize the nucleation of microtubules. Centrioles of the bipolar spindles were detected by adding Nocodazole (0,5uM, 20minutes at 20ºC, M1404 Sigma) to the XEE before spinning them down (Cavazza et al., 2016). Monoclonal mouse anti-centrin antibody (20H5, Millipore, 1:2,000) was used to immunodetect the centrosomes.

Centrosome complementation assay

To assess the capacity of the human centrioles to recruit pericentriolar material and to nucleate microtubules, we used a previously published protocol with minor modifications (Moritz et al., 1998). Briefly, 100,000 human spermatozoa were incubated with 4M KI in 1xBRB80 and applied to a poly-lysine coated glass coverslip during 10 minutes at 30ºC. The adhered sample was washed by pipetting three times with 60 μl of Hepes block buffer (100 mM KCl, 10 mg/ml BSA, 1 mM β-mercaptoethanol) before incubation with 60 μl of XEE for 10 minutes at 30ºC and then washed briefly three times with 60 μl of TDB wash buffer (1x BRB80, 10% Glycerol, 1 mM GTP and 10 mg/ml BSA). 25 μl of unlabeled brain cow tubulin at 2 mg/ml in TDB (1x BRB80, 10% Glycerol, 1 mM GTP) was added to the sample for 10 minutes. Next, the samples were fixed for 3 minutes in 1% glutaraldehyde and post-fixed for 3 minutes in methanol at -20ºC. The coverslips were quenched with 0.1% sodium borohydride in TBS (Tris buffer saline) for 7 minutes. Microtubule and centrosomes were visualized by immunostaining with a rabbit monoclonal anti-beta-tubulin antibody (ab6046 Abcam, 1:200) and a mouse polyclonal anti-centrin antibody (20H5 Millipore, 1:2,000). Samples were visualized with an inverted DMI-600 Leica wide-field fluorescent microscope using a 63x objective.

Statistical analysis

For each sperm sample analyzed in XEE, 100 and 200 sperm nuclei were counted for *Xenopus* and human samples respectively in individual XEE (a total of 4 independent XEE incubations with a total number of 400 and 800 *Xenopus* and human sperm nuclei analyzed, respectively). The microtubule structures associated with the spermatozoa

DNA were classified as: bipolar spindles, abnormal structures or no structures. The analysis of spindle structures was done applying the t-test in Prism 6 (GraphPad Software, La Jolla, CA). To analyze spindle assembly by sperm patient samples, the percentage of bipolar spindles was normalized by the percentage of *Xenopus* sperm bipolar spindles in the same XEE. Semen diagnoses and fertilization rate were described for each sperm patient sample and associated IVF/ICSI cycle. Pearson's R coefficient was calculated to evaluate the lineal association between the previous parameters and bipolar spindle assembly. All statistical analyses were performed using the Statistical Package for the Social Sciences (SPSS, version 22). A Pearson's R coefficient between 0.3 and 0.7 was considered as a moderate correlation.

For spindle length measurements, the length of 40 spindles per sample was analyzed using a straight line from ImageJ software and the nonparametrical Mann-Whitney test applied with the Prism 6 program.

Supplementary Materials:

Fig. S1. Human-*Xenopus* bipolar spindles are smaller than *Xenopus-Xenopus* bipolar spindles.

Table S1. Conditions tested to optimize the human sperm membrane destabilization.

References:

Arikan, II, B. Demir, G. Bozdag, I. Esinler, L.K. Sokmensuer, and S. Gunalp. 2012. ICSI cycle outcomes in oligozoospermia. *Clin Exp Obstet Gynecol*. 39:280-282.

Bettencourt-Dias, M., and D.M. Glover. 2007. Centrosome biogenesis and function: centrosomics brings new understanding. *Nat Rev Mol Cell Biol*. 8:451-463.

Borges, E., Jr., A.S. Setti, D.P. Braga, R.C. Figueira, and A. Iaconelli, Jr. 2016. Total motile sperm count has a superior predictive value over the WHO 2010 cut-off values for the outcomes of intracytoplasmic sperm injection cycles. *Andrology*. 4:880-886.

Cavazza, T., I. Peset, and I. Vernos. 2016. From meiosis to mitosis - the sperm centrosome defines the kinetics of spindle assembly after fertilization in Xenopus. *J Cell Sci*. 129:2538-2547.

Clift, D., and M. Schuh. 2013. Restarting life: fertilization and the transition from meiosis to mitosis. *Nat Rev Mol Cell Biol*. 14:549-562.

Desai, A., A. Murray, T.J. Mitchison, and C.E. Walczak. 1999. The use of Xenopus egg extracts to study mitotic spindle assembly and function in vitro. *Methods Cell Biol*. 61:385-412.

Gannon, J.R., B.R. Emery, T.G. Jenkins, and D.T. Carrell. 2014. The sperm epigenome: implications for the embryo. *Adv Exp Med Biol*. 791:53-66.

Gordon, K., D.B. Brown, and F.H. Ruddle. 1985. In vitro activation of human sperm induced by amphibian egg extract. *Exp Cell Res*. 157:409-418.

Hannak, E., and R. Heald. 2006. Investigating mitotic spindle assembly and function in vitro using Xenopus laevis egg extracts. *Nat Protoc*. 1:2305-2314.

Hewitson, L., C. Simerly, and G. Schatten. 1997. Inheritance defects of the sperm centrosome in humans and its possible role in male infertility. *Int J Androl*. 20 Suppl 3:35-43.

Johnson, G.D., C. Lalancette, A.K. Linnemann, F. Leduc, G. Boissonneault, and S.A. Krawetz. 2011. The sperm nucleus: chromatin, RNA, and the nuclear matrix. *Reproduction*. 141:21-36.

Karsenti, E., and I. Vernos. 2001. The mitotic spindle: a self-made machine. *Science*. 294:543-547.

Li, B., Y. Ma, J. Huang, X. Xiao, L. Li, C. Liu, Y. Shi, D. Wang, and X. Wang. 2014. Probing the effect of human normal sperm morphology rate on cycle outcomes and assisted reproductive methods selection. *PLoS One*. 9:e113392.

Lohka, M.J., and J.L. Maller. 1988. Induction of metaphase chromosome condensation in human sperm by Xenopus egg extracts. *Exp Cell Res*. 179:303-309.

Moritz, M., Y. Zheng, B.M. Alberts, and K. Oegema. 1998. Recruitment of the gamma-tubulin ring complex to Drosophila salt-stripped centrosome scaffolds. *J Cell Biol*. 142:775-786.

Murray, A.W. 1991. Cell cycle extracts. *Methods Cell Biol*. 36:581-605.

Navara, C.S., C. Simerly, S. Zoran, and G. Schatten. 1995. The sperm centrosome during fertilization in mammals: implications for fertility and reproduction. *Reprod Fertil Dev*. 7:747-754.

Ohsumi, K., C. Katagiri, and R. Yanagimachi. 1988. Human sperm nuclei can transform into condensed chromosomes in Xenopus egg extracts. *Gamete Res*. 20:1-9.

Ortega, C., G. Verheyen, D. Raick, M. Camus, P. Devroey, and H. Tournaye. 2011. Absolute asthenozoospermia and ICSI: what are the options? *Hum Reprod Update*. 17:684-692.

Palermo, G., H. Joris, M.P. Derde, M. Camus, P. Devroey, and A. Van Steirteghem. 1993. Sperm characteristics and outcome of human assisted fertilization by subzonal insemination and intracytoplasmic sperm injection. *Fertil Steril*. 59:826-835.

Rawe, V.Y., S.B. Olmedo, F.N. Nodar, G.D. Doncel, A.A. Acosta, and A.D. Vitullo. 2000. Cytoskeletal organization defects and abortive activation in human oocytes after IVF and ICSI failure. *Mol Hum Reprod*. 6:510-516.

Rawe, V.Y., Y. Terada, S. Nakamura, C.F. Chillik, S.B. Olmedo, and H.E. Chemes. 2002. A pathology of the sperm centriole responsible for defective sperm aster formation, syngamy and cleavage. *Hum Reprod*. 17:2344-2349.

Simerly, C., G.J. Wu, S. Zoran, T. Ord, R. Rawlins, J. Jones, C. Navara, M. Gerrity, J. Rinehart, Z. Binor, R. Asch, and G. Schatten. 1995. The paternal inheritance of the centrosome, the cell's microtubule-organizing center, in humans, and the implications for infertility. *Nat Med*. 1:47-52.

Simerly, C., S.S. Zoran, C. Payne, T. Dominko, P. Sutovsky, C.S. Navara, J.L. Salisbury, and G. Schatten. 1999. Biparental inheritance of gamma-tubulin during human fertilization: molecular reconstitution of functional zygotic centrosomes in inseminated human oocytes and in cell-free extracts nucleated by human sperm. *Mol Biol Cell*. 10:2955-2969.

Simon, L., K. Murphy, M.B. Shamsi, L. Liu, B. Emery, K.I. Aston, J. Hotaling, and D.T. Carrell. 2014. Paternal influence of sperm DNA integrity on early embryonic development. *Hum Reprod*. 29:2402-2412.

Steptoe, P.C., and R.G. Edwards. 1978. Birth after the reimplantation of a human embryo. *Lancet*. 2:366.

Templado, C., L. Uroz, and A. Estop. 2013. New insights on the origin and relevance of aneuploidy in human spermatozoa. *Mol Hum Reprod*. 19:634-643.

Van Blerkom, J., P. Davis, and S. Alexander. 2004. Occurrence of maternal and paternal spindles in unfertilized human oocytes: possible relationship to nucleation defects after silent fertilization. *Reprod Biomed Online*. 8:454-459.

Yoshimoto-Kakoi, T., Y. Terada, M. Tachibana, T. Murakami, N. Yaegashi, and K. Okamura. 2008. Assessing centrosomal function of infertile males using heterologous ICSI. *Syst Biol Reprod Med*. 54:135-142.

Figures:

Figure 16: Human spermatozoa nuclei reorganize and replicate their DNA in XEE.
(A) Schematic representation of the experimental design. 3,000 human (or *Xenopus*) sperm nuclei and calcium were incubated in the XEE to mimic fertilization. These incorporations induce the resumption of the cell cycle, first by 90 minutes of interphase followed by 60 minutes of mitosis. **(B and C)** Time course of sperm nucleus decondensation. *Xenopus* and human spermatozoa (normozoospermic and asthenozoospermic) incubated in XEE were retrieved at different time points along the

150 minutes of the experiment, to measure the nuclei area. The graph shows the area evolution in μm^2 of the three different spermatozoa samples. The images on the right are representative pictures of the nuclei decondensation per time point. Scale 10 μm. **(D and E)** Time course of sperm DNA replication. *Xenopus* and human (normozoospermic and asthenozoospermic) spermatozoa, calcium and biotin-labeled dUTPs were incubated in the XEE and retrieved every 30 minutes. The graph shows the percentage of incorporated dUTPs per sample. The images are representative pictures of the dUTPs incorporation. In green fluorescence is the dUTPs incorportaed in the DNA (blue). In red are the microtubules. Scale 10 μm.

A

B

C
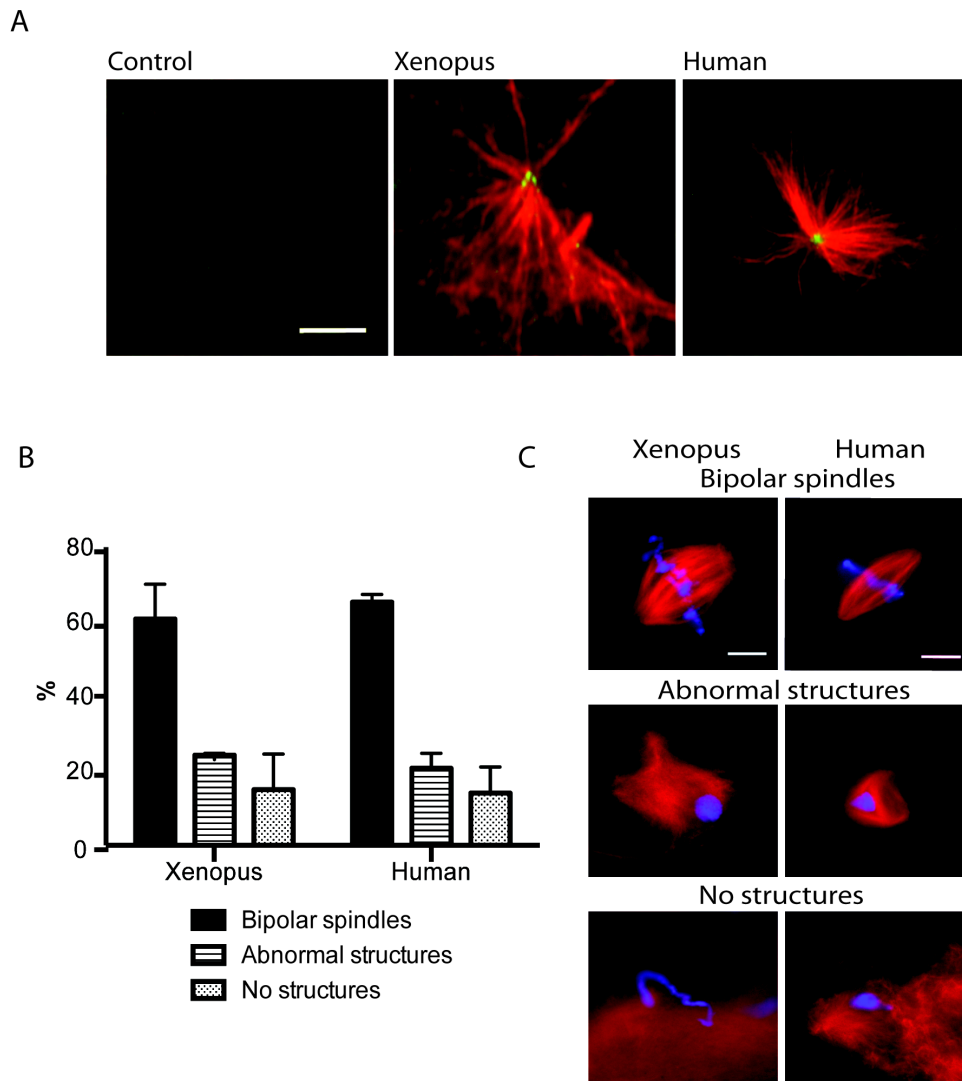
Figure 17: The human sperm basal body is converted into a fully functional centrosome in the oocyte cytoplasm. (A) Human sperm basal body actively nucleates microtubules in XEE. Immunofluorescence images of KI treated sperm samples incubated with XEE and pure tubulin. Microtubule asters are in red and centrioles in green. Scale 5μm. **(B and C)** Capacity of the *Xenopus* and human spermatozoa to assemble microtubule mitotic structures. The microtubules are in red and the DNA in blue. The structures associated with the DNA were classified as bipolar spindles, abnormal structures and no structures as shown in the images on the right. Scale 10 μm. The graph on the left shows the analysis of 100 and 200 sperm nuclei for *Xenopus* and human samples respectively.
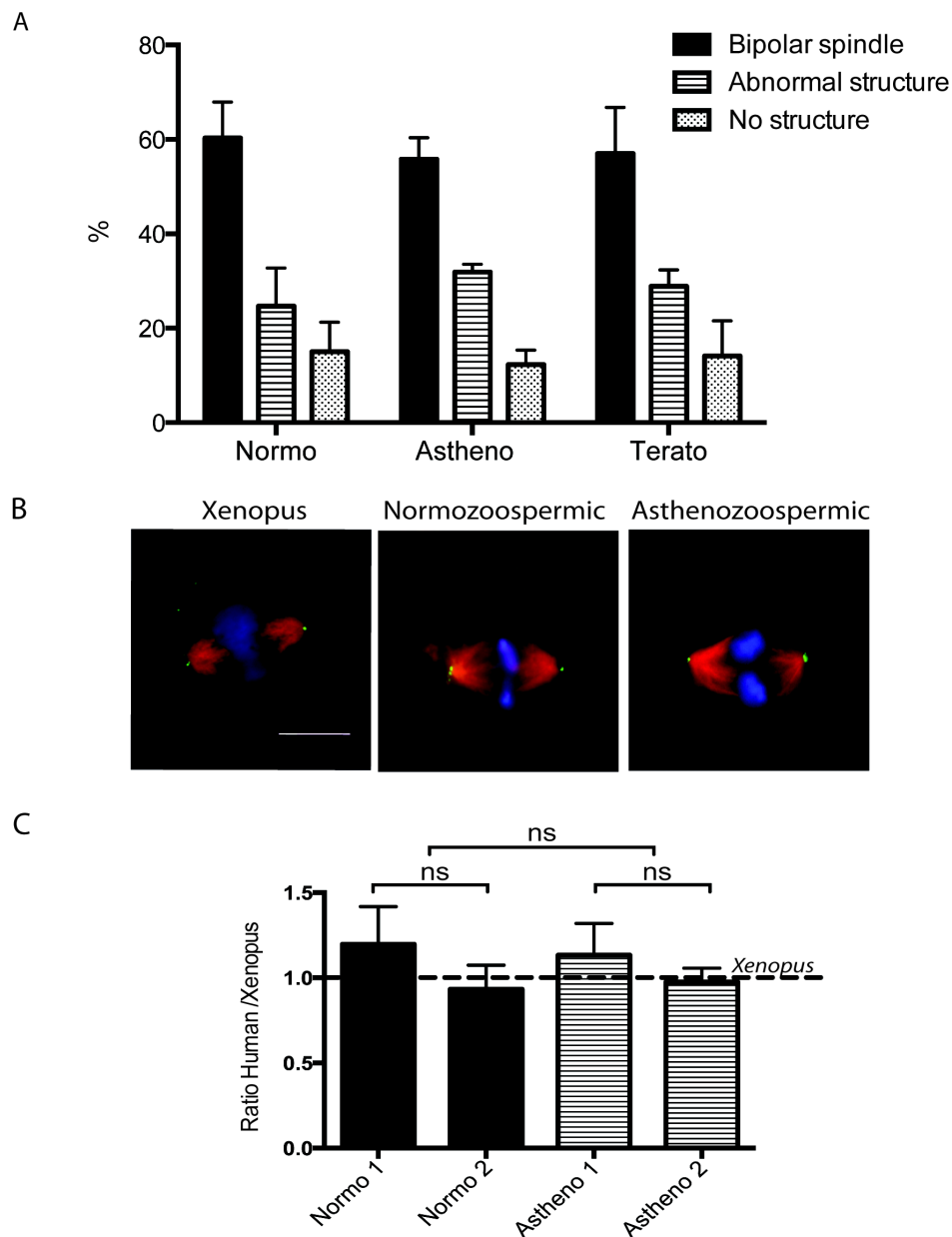
Figure 18: Human spermatozoa are able to assemble bipolar spindles in XEE independently of the sperm diagnosis. (A) Capacity to assemble microtubule mitotic structures of human spermatozoa samples with different diagnosis. The graph shows the percentage of bipolar spindles, abnormal structures and no structures per sample. **(B and C)** Human basal body duplicates in XEE. Bipolar spindles assembled in XEE were treated with Nocodazole and processed for immunofluorescence. The number of bipolar spindles with centrosomes at both poles were analyzed in 2 normozoospermic and 2 asthenozoospermic samples and normalized by the number of bipolar spindles with centrosomes at both poles in *Xenopus* spermatozoa. The images show in blue the DNA, in red the microtubules and in green the centrosome. Scale 10μm.
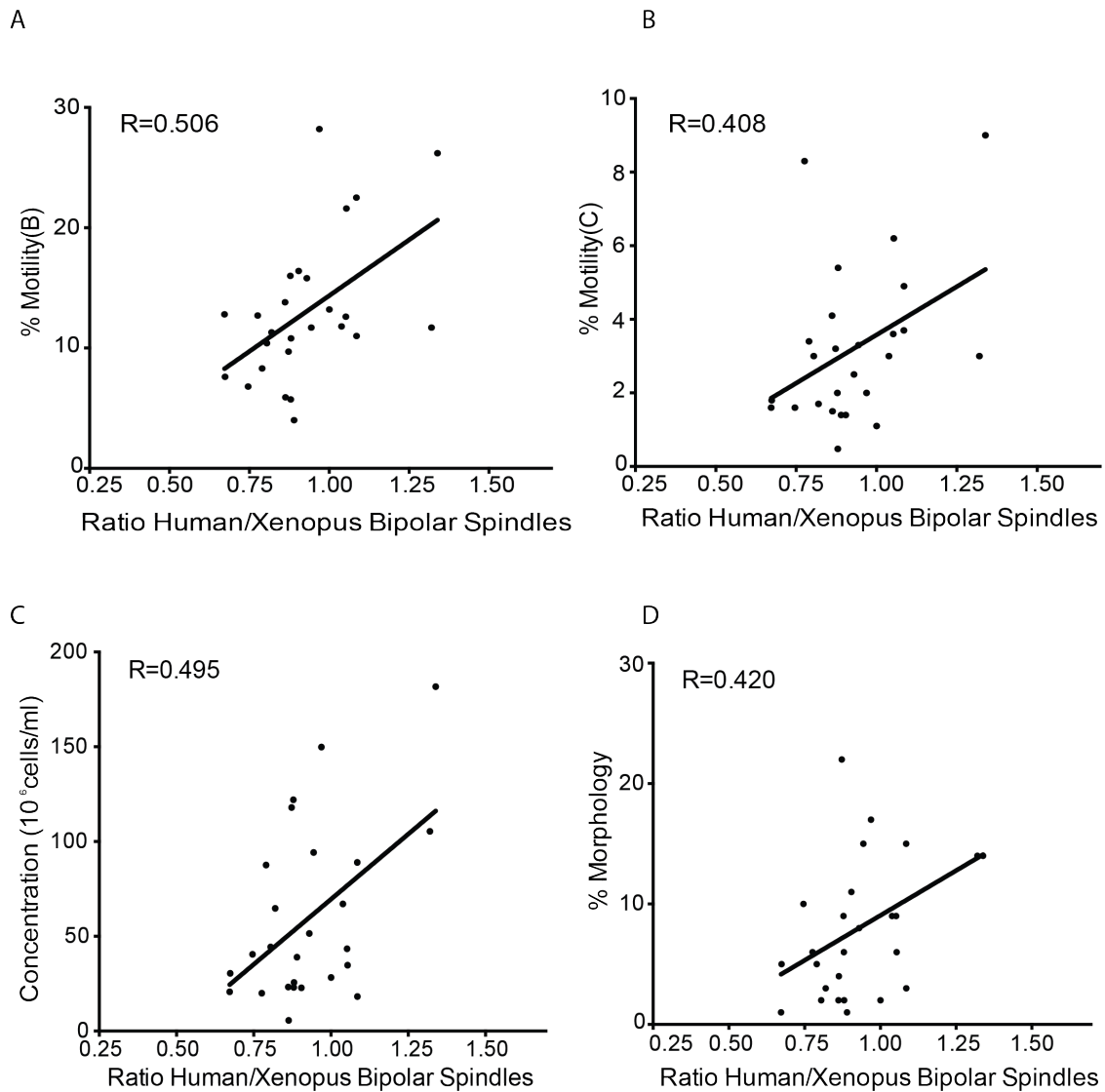
Figure 19: Human sperm samples have different capacities to trigger functional bipolar spindles. (A – D) The percentage of bipolar spindles per XEE was normalized by the percentage of bipolar spindles triggered by *Xenopus* spermatozoa in the same XEE. The average of bipolar spindles of each sample in the four XEE was correlated with each sperm sample characteristics and clinical outcomes for their respective IVF/ICSI cycle. A positive moderate correlation was found for the following parameters: motility B (R=0.506), motility C (R=0.408), morphology (R=0.420) and concentration (R=0.495).

Supplementary Materials:
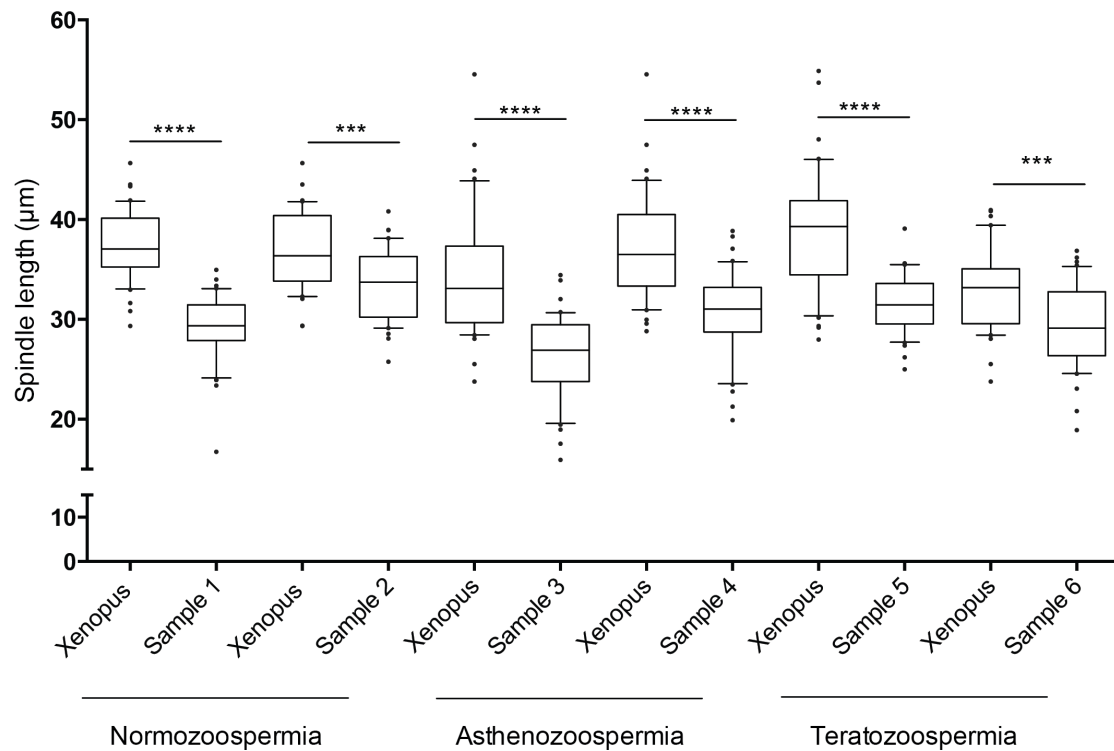
Supplementary Figure 1: Human-*Xenopus* bipolar spindles are smaller than *Xenopus-Xenopus* bipolar spindles. The spindle length in μm of 20 bipolar spindles per sample was analyzed by measuring the distance from the two spindle poles. 2 normozoospermic, 2 asthenozoospermic and 2 teratozoospermic patients' samples were analyzed in 2 independent XEE per sample. p≤0.001 (***), p≤0.0001 (****).

CONDITION	BIPOLAR SPINDLES (%)	ABNORMAL STRUCTURES (%)	NO STRUCTURES (%)
Xenopus	60.8	24.2	15.0
Human not treated	2.3	0.9	96.8
Lysolecithin 1,5%	9.0	2.2	88.8
Lysolecithin 1,5% + 1mM DTT	57.3	22.0	20.7
Triton 0,05%	13.3	1.6	85.1
Triton 0,25%	2.2	5.0	92.7
Triton 0,25% + 1mM DTT	65.3	20.7	14.0
NP40 0,05%	5.4	3.6	91.0
NP40 0,25%	12.4	3.7	83.9
NP40 0,25% + 1mM DTT	65.7	18.7	15.7
1mM DTT	50.7	20.0	29.3

Supplementary Table 1: Conditions tested to optimize the human sperm membrane destabilization. Different permeabilization agents combined with or without DTT were used to treat the human spermatozoa before incubation in XEE. Their efficiency was analyzed by their capacity to assemble mitotic microtubules structures.

III. Chapter 2: PCM characterization of the human sperm basal body.

Several authors have postulated that the centrosome is biparentally inherited during mammalian fertilization (centrioles provided by the spermatozoon and PCM by the oocyte). This statement is based on different observations: 1) many animals inherit the centrosome asymmetrically (centriole *versus* PCM). 2) The elimination of the centrosome from the oocyte prevents its parthenogenetic development in *Xenopus*.

Humans are not an exception. Electron microscopy studies showed that the sperm basal body consists of two centrioles, one of them partially degenerated with incomplete microtubule triplets. On the other hand, the human oocyte does not have a centrosome, but it likely contains centrosomal proteins and/or mRNAs encoding them. Therefore, the working model so far is that the sperm basal body, which has lost most of the centrosome associated proteins and the capacity to nucleate microtubules, reconstitutes a functional centrosome after fertilization by recruiting centrosomal proteins from the oocyte cytoplasm.

There are evidences supporting this idea. *Drosophila* spermatozoa also follow a centrosome reduction process (involving centrosomal protein degradation). When this process is not correct, early embryo development is compromised. Other species such as *Xenopus* or mice eliminate completely centrosome proteins like γ-tubulin and centrin respectively. On the other hand, defects in centrosome elimination from *Drosophila* and starfish oocytes, result in fertilization and early development problems.

It is highly likely that an asymmetric inheritance of the centrosome also occurs during human fertilization. However, although it is broadly accepted that human sperm centrosome proteins are degraded during spermatogenesis and therefore, the mature spermatozoon only carries a pair of centrioles, there are no direct experimental evidence to support this idea. We, therefore, decided to investigate this issue by determining whether centrosomal proteins are associated with the human sperm basal body and may participate in the transition to a functional centrosome in the fertilized oocyte.

A. The sperm degenerated centriole (distal centriole) has the capacity to recruit PCM:

In order to test the hypothesis that 1) the mature spermatozoon lacks most of its PCM and 2) the sperm basal body is only converted into a functional centrosome once it recruits PCM from the fertilized oocyte; we decided to perform immunofluorescence (IF) for 2 centrosomal proteins: centrin and Cep63 **(Figure 20A and B)**. Centrin is a structural protein that localizes inside the centrioles and it is actually often used as a maker for centrioles by IF (Middendorp et al., 2000; Paoletti et al., 1996; Salisbury et al., 2002; White et al., 2000). It may therefore also be a good marker for general centriole structure and, in particular, to get some hints about the "degenerated" distal centriole. In principle, we expected that the degenerated centriole contained very low amounts of centrin compared to the other centriole. Using Stimulated Emission Depletion (*STED*) on fixed human spermatozoa we found that both the proximal and distal centrioles were positive for centrin **(Figure 20A).** Moreover, centrin localization and distribution was very similar for both centrioles. A similar staining was observed for the centrosomal duplication protein Cep63: it is recruited to both centrioles **(Figure 20B)**. We were surprised by these findings because they suggest that the hypothesis that the mature spermatozoon lacks PCM was not carefully evaluated and that, although the distal centriole has an incomplete microtubule structure, it retains some centrosomal components which in turn may play a role after fertilization in its replication and microtubule nucleation function.
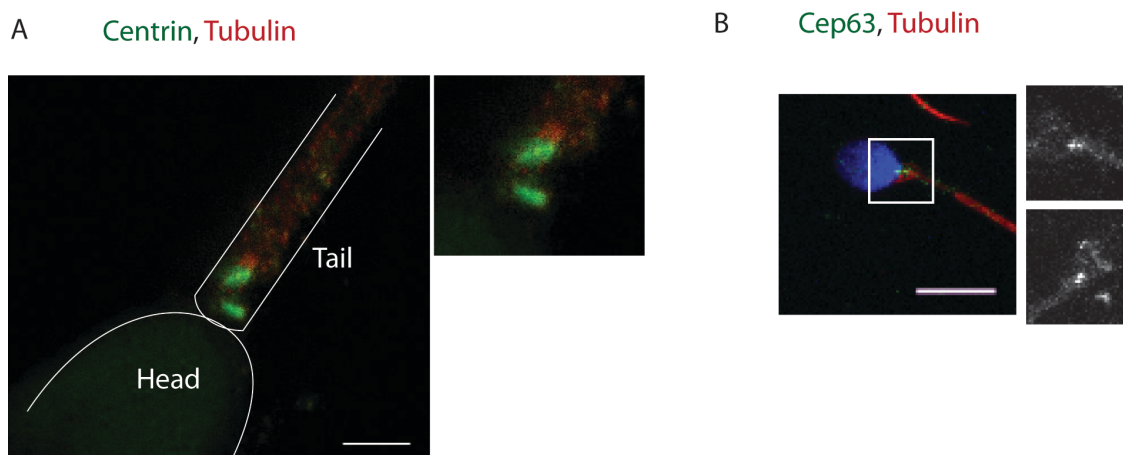
Figure 20:Mature human spermatozoon still has PCM. A) High resolution image of the sperm centrioles. Centrioles are shown in green and tubulin in red. Proximal and distal centrioles are completely perpendicular. Scale 1 μm. **B)** Representative images of Cep63 IFs. Proteins (centrin and Cep63) are shown in green and tubulin in red. Scale 5 μm.

B. Sperm tails fraction enrichment:

Because our IF analysis suggests that the sperm basal body could contain more PCM than expected, we decided to use a high-throughput technology to identify these proteins. We decided to apply proteomics only on normozoospermic samples with more than 50% of A+B motility because, although 50% of motility does not ensure that the centrosomes are not altered, at least it suggests that the spermatogenesis was not severely impaired.

Since centrosomal proteins are usually in low abundance and often difficult to detect by mass-spectrometry based proteomic approaches (Bauer et al., 2016), we aimed at enriching the samples in basal bodies components by fractioning the head and tails.

Searching the literature we found that sonication has been successfully used for subcellular fractionation of mammalian sperm samples and sperm tail proteomics analysis (Amaral et al., 2013; Firat-Karalar et al., 2014b). We therefore tested several conditions to optimize the separation of sperm heads from tails. We tested 9 different conditions (data not shown) changing the output values as well as the number of bursts, while maintaining a constant time for each burst. The most efficient separation of head and tails was obtained with 70% output, 5 x 15 seconds bursts at 30 seconds intervals as tested by IF against DNA and tubulin (55% of the heads did not even contain a small fraction of tail). Then, sonicated samples were centrifuged twice through a 30% sucrose cushion (200xg, 10 min at 4˚C) and a fraction enriched in sperm tails free of heads (in the pellet) was recovered at the top of the gradient **(Figure 21A and B)**. We analyzed by bright-field microscopy the purity of fraction 2 and found that the presence of heads was less than 0.01% **(Figure 21B)**. To further validate the purity of the tail sample, we assessed by Western Blot (WB) analysis the presence of protamines, which are specifically associated with the packaged chromatin in the sperm head **(Figure 21C)**. A very low amount of protamines could be detected in the sperm tail fraction 1 but not anymore after the second purification step (fraction 2), whereas tubulin was detected in both fractions. These results demonstrate that we had obtained a sample enriched in tails and with very few heads as contaminants. Furthermore, when this process was repeated with other sperm samples, the percentage of sperm heads present in the tail fraction was less than 0.01% in all cases, indicating that our protocol is highly efficient and reproducible.

To finally determine whether centrosomes are present in the sperm tail fraction 2, we performed IF analysis against DNA, centrin and tubulin **(Figure 21D)**. The head fraction contained isolated heads sometimes associated with pieces of flagella (labeled with the anti-tubulin antibody) and centrosomes. The tail fraction 2 did contain sperm tail fragments and some of them had an associated centrosome.

These data suggest that the protocol was appropriate to obtain a fraction enriched in sperm tails that sometimes are associated with a centrosome. This fraction is amenable for proteomic analysis.
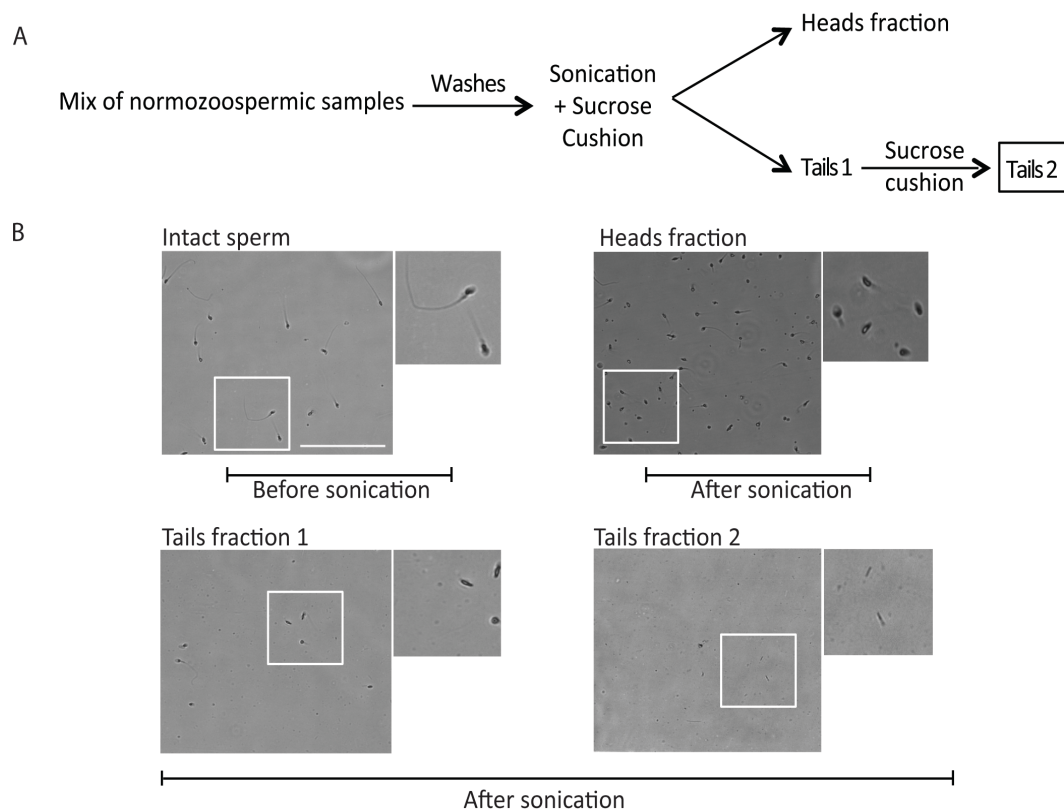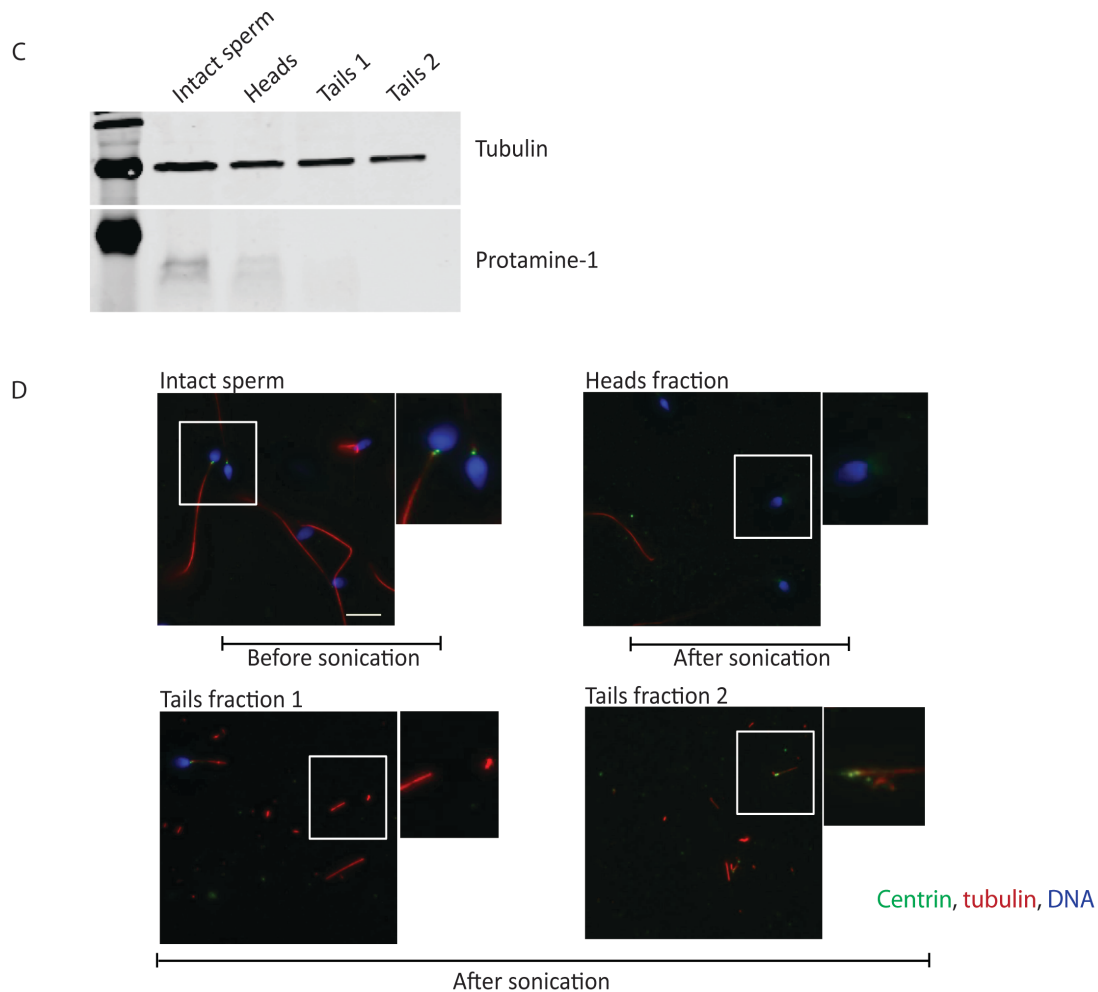
Figure 21: Isolation of human sperm tails. A) Protocol followed to isolate human sperm tails. Briefly, a mixture of normozoospermic samples was sonicated prior to two sucrose gradient purifications. **B)** Intact human sperm, heads and tails fractions visualized by phase-contrast microscopy. Note that tails fraction 2 is enriched in tails and very few heads can be detected (0.01%). Scale bar 100 μm. **C)** Detection of head and tail specific proteins (tubulin and protamine-1) in extracts of intact sperm, heads and tails fractions. **D)** Representative images of intact and sperm fractions stained for DNA (blue), centrin (green) and α-tubulin (red). In some tails from tails fraction 2 one or two centrioles could still be detected. Scale 10 μm.

C. Sperm tail sample preparation for proteomic analysis:

In order to extract as many centrosomal proteins as possible to then identify them by mass spectrometry, we decided to follow two different protocols. The first approach was based on sequential washes with three different detergent solutions of increasing stringency **(Figure 22A)** (Firat-Karalar et al., 2014b). WB analysis of the three extracts showed that this approach was successful and different human sperm proteins were extracted at each wash step **(Figure 22B)**. We monitored γ-tubulin as a marker of the centrosome fraction and α-tubulin as a marker of axonemes. Anti-centrin antibodies did not detect any positive band and could not be used as a maker of the centrosomes **(data**

not shown). We found that γ-tubulin is enriched in the sample obtained upon the wash with extraction buffer 1 whereas α-tubulin is enriched in the sample obtained after the wash with the extraction buffer 2. None of them were present in the sample obtained after a final wash with extraction buffer 3, suggesting that the cytoskeletal proteins of interest are not present anymore **(Figure 22B)**.

Our results with human sperm are different from those in the literature on bovine spermatozoa. According to these published data, the centrosome enriched fraction from bovine spermatozoa is obtained with the extraction buffer 2 and α-tubulin is mainly found with extraction buffer 3. It seems, therefore, that proteins are extracted more easily from human spermatozoa than from bovine spermatozoa. These differences may be due to different composition and/or complexity of the membranes of the human and bovine sperms and/or the specific sonication conditions.

As an alternative approach we decided to directly solubilize all the proteins in tail fraction 2 by incubation in SDS-PAGE loading buffer (Lammeli Buffer). The resulting soluble fraction was then run in a 4-16% gradient SDS-PAGE gel **(Figure 22C)**. The gel was stained with Coomassie blue staining. In the gel we could appreciate that the sperm proteome is complex, and that the sample is enriched in proteins with a molecular weight of approximately 100 kDa or less (3rd top molecular marker band). Three major bands are highly enriched: one of them corresponding to tubulin (55 kDa) and the two other bands, of unknown proteins, have a molecular weight of approximately 100 and 70 kDa respectively.

For mass spectrometry analysis, 9 fragments of the gel were excised taking into account the abundance and complexity of the proteins. In this way, we separated segments containing highly abundant proteins, such as tubulin, from others with less proteins. The 9 bands were analyzed independently by mass spectrometry.
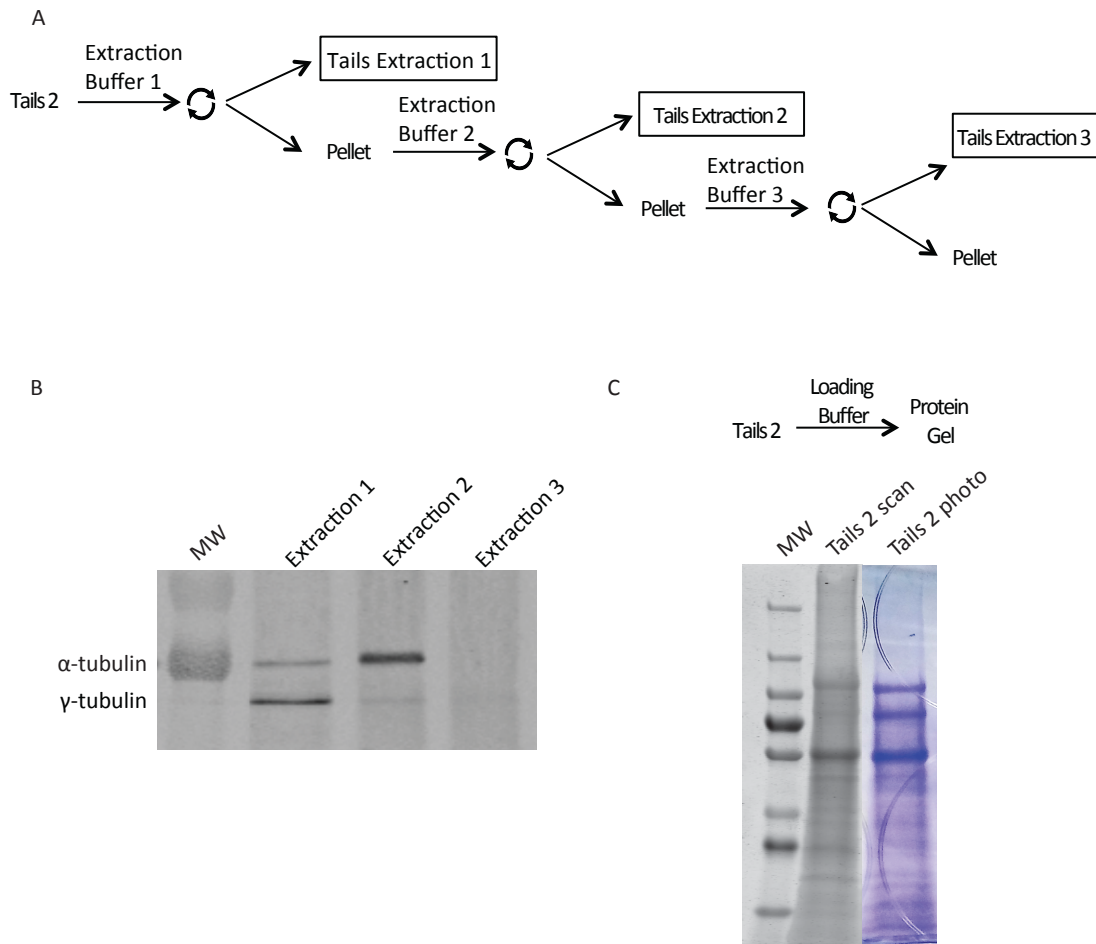
Figure 22: Protein extraction form. A) Protocol used to sequentially extract proteins. This protocol is based on the published protocol from Firat et al., 2014. **B)** Samples from each extraction were run in a gel and blotted to confirm the different protein extraction, and to identify the centrosome enriched fraction. **C)** Protocol of the second approach and protein gel obtained from the solubilized Tails 2 fraction.

D. Mass spectrometry based proteomic analysis of human sperm tails:

Data from the 4 independent experiments resulted in the identification of around 2,000 proteins per experiment using the sequential protein extraction protocol (protocol 1) (experiment 1 to 3) and approximately 4,500 proteins using the tail solubilization approach (protocol 2) (experiment 4) **(Figure 23A)**. In total we identified 4,736 proteins **(Figure 23B)**. To minimize potential contaminants we further considered only proteins identified in at least two independent experiments. This resulted in a human sperm tail proteome of 2,312 proteins. To our knowledge, it is the most complete tail proteome from human spermatozoa. Indeed, our proteome, that includes 82.7% of the proteins

previously reported for human sperm tails, is twice as big **(Figure 23C)** (Amaral et al., 2013). The high number of proteins identified may seem surprising because previous data have suggested that spermatozoon eliminates a large number of proteins during its maturation and it is mostly composed of the genetic material and the centrosome.

To analyze the composition of the sperm tail proteome we performed Gene Ontology (GO) analysis. Based on biological processes, the most abundant proteins are related to metabolic processes as previously described **(Figure 23D)** (Amaral et al., 2013), followed by intracellular transport, cell movement and reproductive processes, as expected. Based on cellular localization, most of the proteins were related to mitochondria or the cytoskeleton **(Figure 23E)**. Note that we emphasized in the graph the proteins allocated to the cytoskeleton cluster because centrosomal proteins should be included there. Many proteins were also associated with the Golgi apparatus, the Endoplasmic Reticulum and to vesicles. These groups had also been described in previous proteomic studies of whole sperm (Wang et al., 2013). The fact that spermatozoa contain a large number of these proteins suggests that the mature spermatozoa is much more dynamic than previously thought. It is also important to mention that the distribution of the GO clusters for each individual experiment was highly similar, demonstrating the robustness and reproducibility of our approaches. Taken together, our data suggest that mature spermatozoa are much more complex cells than previously described. Although many of their proteins are involved in the spermatozoon reproductive function (movement, sperm-oocyte fusion), many metabolic pathways and protein/membrane synthesis processes are also represented.

A

	Number of protein identified by MS
Experiment 1	1900
Experiment 2	1824
Experiment 3	1735
Experiment 4	4401

B

C

D

E
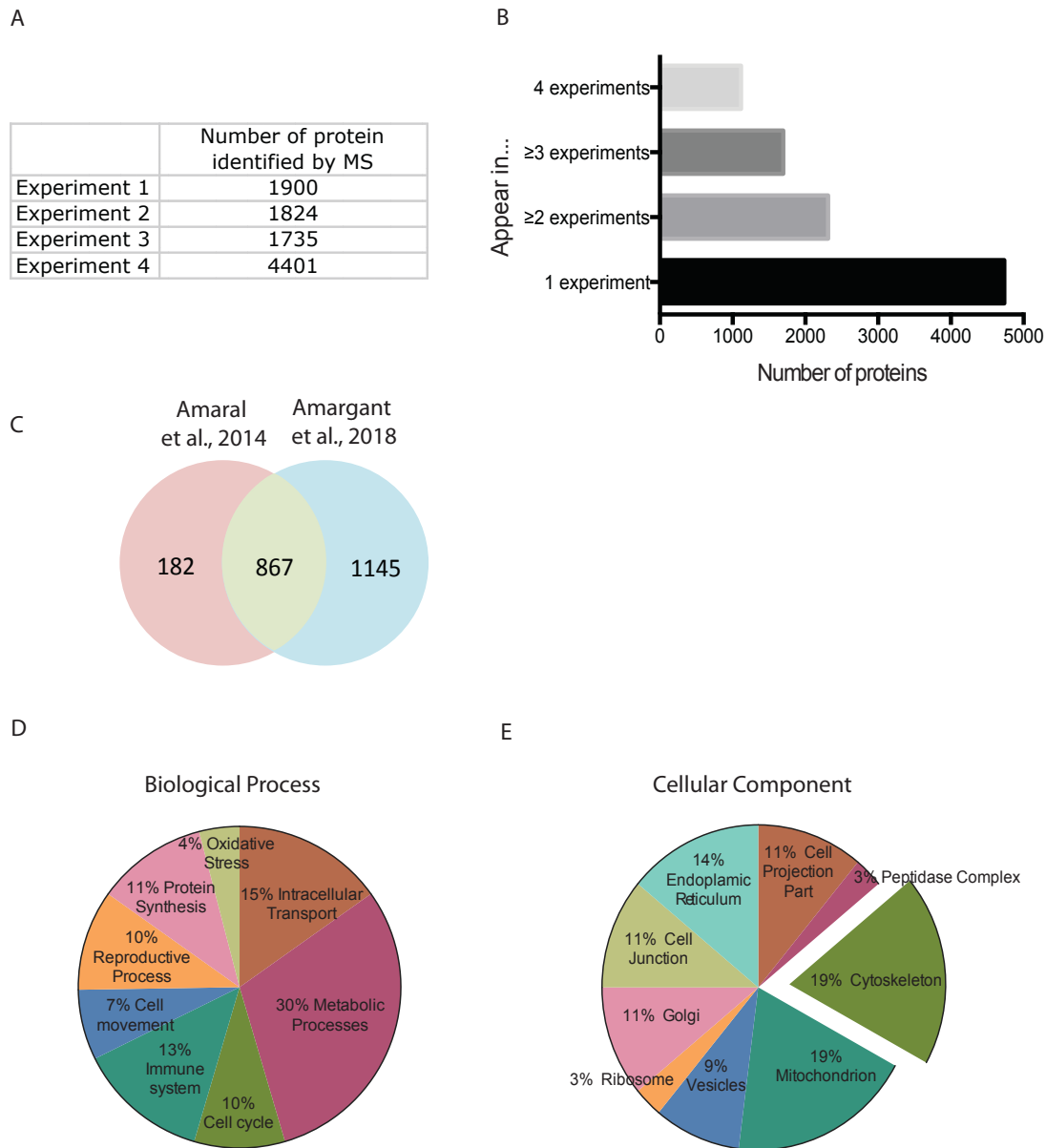
Figure 23: Proteome of the human sperm tail. A) Number of proteins identified in each experiment. Note that the approach in which we identify more proteins was using the gel protein protocol. **B)** Number of proteins identified that appear at least in 1, 2, 3 or in all 4 experiments. **C)** Comparison of the number of proteins identified at least in 2 of our experiments and the previously published human sperm tail proteome. **D)** Gene Ontology of the 2312 proteins related to their biological process. **E)** Gene Ontology of the 2312 proteins related to their cellular localization.

E. The sperm centrosome composition:

To define the proteome of the human sperm basal body we looked for proteins with GO terms such as microtubule organizing center, microtubule organizing center part, centriole, centrosome and spindle pole. We will further on refer to these proteins as PCM proteins. As already exposed, PCM proteins are very low abundant proteins that are difficult to detect. Therefore, we decided to consider all the proteins identified in the

4 experiments without taking into account whether they appeared or not in different experimental replicates. 288 proteins were related to PCM **(Figure 24A)**. Some proteins were centriolar, such as Cep68, Cep135; others were coiled-coil proteins (CCDC146, CCDC151), components of the γ-TuSc (GCP2, GCP3) and protein kinases (Nek9) **(Table 3)**. We then evaluated our results in the view of previously published proteomic data from entire sperm, heads or tails. Until 2014, 6198 different proteins had been described for human spermatozoa (Amaral et al., 2014a). Despite this large number, 22% of the PCM proteins identified in our work are new **(Figure 24B)**.

We evaluated whether we mostly identified abundant centrosomal proteins by looking at published data on centrosomal protein abundance in KE37 isolated centrosomes (Bauer et al., 2016). We have identified 19 out of the 73 proteins for which they characterized their abundance. We were able to detect proteins that are considered to be abundant in KE37 isolated centrosomes like ODF2 (402 average copy number/centrosome, normalized to γ-tubulin) and POC1B (284 average copy number/centrosome, normalized to γ-tubulin); other with a mild abundance such as OFD1 (121 average copy number/centrosome, normalized to γ-tubulin) and Cep76 (113 average copy number/centrosome, normalized to γ-tubulin), and also proteins with low abundance, such as LRRC45 (42 average copy number/centrosome, normalized to γ-tubulin), Cep290 (57 average copy number/centrosome, normalized to γ-tubulin) and Cep170 (58 average copy number/centrosome, normalized to γ-tubulin). These data suggest that the sperm basal body contains a wide range of PCM proteins either characterized by function or by amount, although it may not be accurate to make these direct extrapolations since spermatozoa are highly differentiated cells and the relative abundance of the different proteins is cell-specific.

A

	Centrosomal proteins
Experiment 1	96
Experiment 2	95
Experiment 3	89
Experiment 4	274
Total amount	288

B
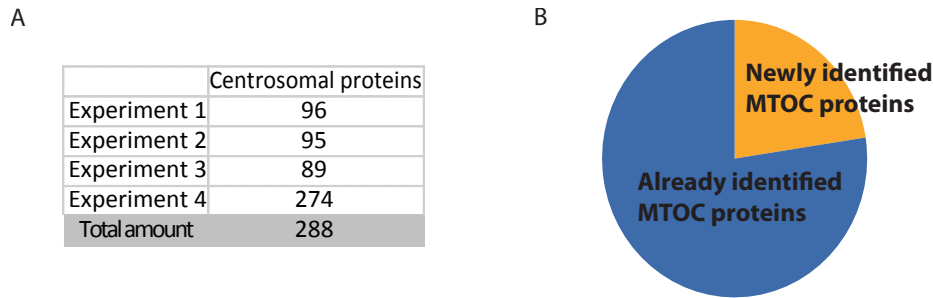
Figure 24: Spermatozoa PCM proteome. A) Number of PCM proteins identified in each experiment. Using the second approach we were able to identify more PCM proteins (experiment 4). **B)** PCM proteins identified here compared to previously published data. 22% of our 288 PCM proteins are, for the first time, described in the human spermatozoa (orange fraction) while 78% of proteins were already published.

Table 3: Spermatozoa PCM proteins identified by mass spectrometry.

Human sperm PCM proteins (Only identified by mass spectrometry)	
P62081	40S ribosomal protein S7
O60733	85/88 kDa calcium-independent phospholipase A2
Q99996	A-kinase anchor protein 9 AKAP9
Q8IZT6	Abnormal spindle-like microcephaly-associated protein
Q15650	Activating signal cointegrator 1
Q9Y6K8	Adenylate kinase isoenzyme 5
P36404	ADP-ribosylation factor-like protein 2
P36405	ADP-ribosylation factor-like protein 3
Q9NRG9	Aladin
P61163	Alpha-centractin
Q8TCU4	Alstrom syndrome protein 1
Q03518	Antigen peptide transporter 1
Q9BZC7	ATP-binding cassette sub-family A member 2
Q08211	ATP-dependent RNA helicase A
Q9UQB9	Aurora kinase C
Q9UPM9	B9 domain-containing protein 1
Q9NR09	Baculoviral IAP repeat-containing protein 6
Q9BXC9	Bardet-Biedl syndrome 2 protein
Q96RK4	Bardet-Biedl syndrome 4 protein
Q8N3I7	Bardet-Biedl syndrome 5 protein
Q8IWZ6	Bardet-Biedl syndrome 7 protein
Q8ND07	Basal body-orientation factor 1
P42025	Beta-centractin
Q8IYS8	Biorientation of chromosomes in cell division protein 1-like 2
Q9P287	BRCA2 and CDKN1A-interacting protein
Q9Y6D5	Brefeldin A-inhibited guanine nucleotide-exchange protein 2
Q15018	BRISC complex subunit Abro1
O60271	C-Jun-amino-terminal kinase-interacting protein 4
Q99828	Calcium and integrin-binding protein 1

P62158	Calmodulin
Q9P1Y5	Calmodulin-regulated spectrin-associated protein 3 CAMPSA3
P17612	cAMP-dependent protein kinase catalytic subunit alpha
P22694	cAMP-dependent protein kinase catalytic subunit beta
P13861	cAMP-dependent protein kinase type II-alpha regulatory subunit
P30622	CAP-Gly domain-containing linker protein 1
P48729	Casein kinase I isoform alpha
P35222	Catenin beta-1
Q96JB5	CDK5 regulatory subunit-associated protein 3
P60953	Cell division control protein 42 homolog
Q13042	Cell division cycle protein 16 homolog CDC16
Q9NXG0	Centlein
Q12798	Centrin-1
O43264	Centromere/kinetochore protein zw10 homolog
Q8N8E3	Centrosomal protein of 112 kDa
Q66GS9	Centrosomal protein of 135 kDa
Q5SW79	Centrosomal protein of 170 kDa
O15078	Centrosomal protein of 290 kDa
Q53EZ4	Centrosomal protein of 55 kDa
Q76N32	Centrosomal protein of 68 kDa
Q8NHQ1	Centrosomal protein of 70 kDa
Q8TAP6	Centrosomal protein of 76 kDa
Q9HD42	Charged multivesicular body protein 1a
Q9Y696	Chloride intracellular channel protein 4
Q5JU67	Cilia- and flagella-associated protein 157
Q9Y6A4	Cilia- and flagella-associated protein 20
O43809	Cleavage and polyadenylation specificity factor subunit 5
Q7Z460	CLIP-associating protein 1
Q96AJ1	Clusterin-associated protein 1
Q8TD31	Coiled-coil alpha-helical rod protein 1
Q9H0I3	Coiled-coil domain-containing protein 113
Q8IYX3	Coiled-coil domain-containing protein 116
Q8IYE0	Coiled-coil domain-containing protein 146
A5D8V7	Coiled-coil domain-containing protein 151
Q502W7	Coiled-coil domain-containing protein 38
Q6ZN84	Coiled-coil domain-containing protein 81
A6NC98	Coiled-coil domain-containing protein 88B
Q2M329	Coiled-coil domain-containing protein 96
O94886	CSC1-like protein 1
Q13618	Cullin-3
P06493	Cyclin-dependent kinase 1
Q14204	Cytoplasmic dynein 1 heavy chain 1
Q13409	Cytoplasmic dynein 1 intermediate chain 2
Q9Y6G9	Cytoplasmic dynein 1 light intermediate chain 1
O43237	Cytoplasmic dynein 1 light intermediate chain 2

Q8IYA6	Cytoskeleton-associated protein 2-like
Q14008	Cytoskeleton-associated protein 5
P53384	Cytosolic Fe-S cluster assembly factor NUBP1
Q9Y5Y2	Cytosolic Fe-S cluster assembly factor NUBP2
Q8TF46	DIS3-like exonuclease 1
Q15398	Disks large-associated protein 5
P11388	DNA topoisomerase 2-alpha
Q02750	Dual specificity mitogen-activated protein kinase kinase 1
Q14203	Dynactin subunit 1
Q13561	Dynactin subunit 2
O75935	Dynactin subunit 3
Q9UJW0	Dynactin subunit 4
Q9BTE1	Dynactin subunit 5
O00399	Dynactin subunit 6
P50570	Dynamin-2
Q9UI46	Dynein intermediate chain 1, axonemal
P63167	Dynein light chain 1, cytoplasmic
Q96FJ2	Dynein light chain 2, cytoplasmic
O75923	Dysferlin
O95714	E3 ubiquitin-protein ligase HERC2
Q86YT6	E3 ubiquitin-protein ligase MIB1
Q5T4S7	E3 ubiquitin-protein ligase UBR4
Q5JVL4	EF-hand domain-containing protein 1 EFHC1
P50402	Emerin
Q5T890	ERCC6L2
Q9UPT5	Exocyst complex component 7
P15311	Ezrin
P08F94	Fibrocystin
O75955	Flotillin-1
P05062	Fructose-bisphosphate aldolase B
P14635	G2/mitotic-specific cyclin-B1
Q9BSJ2	Gamma-tubulin complex component 2
Q96CW5	Gamma-tubulin complex component 3
Q96RT7	Gamma-tubulin complex component 6
Q3V6T2	Girdin
P49841	Glycogen synthase kinase-3 beta
Q08379	Golgin subfamily A member 2
O95995	Growth arrest-specific protein 8
P62826	GTP-binding nuclear protein Ran
P63096	Guanine nucleotide-binding protein G(i) subunit alpha-1
P04899	Guanine nucleotide-binding protein G(i) subunit alpha-2
P08754	Guanine nucleotide-binding protein G(k) subunit alpha
O94927	HAUS augmin-like complex subunit 5
P0DMV8	Heat shock 70 kDa protein 1A
Q00839	Heterogeneous nuclear ribonucleoprotein U

P42858	Huntingtin
Q9Y547	IFT25
Q9HBG6	Intraflagellar transport protein 122 homolog
Q96RY7	Intraflagellar transport protein 140 homolog IFT40
Q9UG01	Intraflagellar transport protein 172 homolog
Q8IY31	Intraflagellar transport protein 20 homolog
Q9H7X7	Intraflagellar transport protein 22 homolog
Q9BW83	Intraflagellar transport protein 27 homolog IFT27
Q9NQC8	Intraflagellar transport protein 46 homolog
Q9Y366	Intraflagellar transport protein 52 homolog
A0AVF1	Intraflagellar transport protein 56
Q9NWB7	Intraflagellar transport protein 57 homolog IFT57
Q96LB3	Intraflagellar transport protein 74 homolog
Q9P2H3	Intraflagellar transport protein 80 homolog
Q8WYA0	Intraflagellar transport protein 81 homolog
Q13099	Intraflagellar transport protein 88 homolog
Q15051	IQ calmodulin-binding motif-containing protein 1
P53990	IST1 homolog
Q14145	Kelch-like ECH-associated protein 1
P05783	Keratin, type I cytoskeletal 18
P33176	Kinesin-1 heavy chain
Q92845	Kinesin-associated protein 3
Q02241	Kinesin-like protein KIF23
O00139	Kinesin-like protein KIF2A
Q8N4N8	Kinesin-like protein KIF2B
Q99661	Kinesin-like protein KIF2C
O15066	Kinesin-like protein KIF3B
Q9BVG8	Kinesin-like protein KIFC3
Q86VQ0	Lebercilin
Q9C099	Leucine-rich repeat and coiled-coil domain-containing protein 1
Q9UFC0	Leucine-rich repeat and WD repeat-containing protein 1
Q96CN5	Leucine-rich repeat-containing protein 45
P46736	Lys-63-specific deubiquitinase BRCC36
P40121	Macrophage-capping protein
Q5HYA8	Meckelin
Q9P2G4	Microtubule-associated protein 10
Q15691	Microtubule-associated protein RP/EB family member 1
P28482	Mitogen-activated protein kinase 1
Q16539	Mitogen-activated protein kinase 14
P53985	Monocarboxylate transporter 1
Q13485	Mothers against decapentaplegic homolog 4
P78406	mRNA export factor
P29966	Myristoylated alanine-rich C-kinase substrate
O95865	N(G),N(G)-dimethylarginine dimethylaminohydrolase 2
Q92597	NDRG1

Q96JN8	Neuralized-like protein 4
Q14980	Nuclear mitotic apparatus protein 1
P57740	Nuclear pore complex protein Nup107
P37198	Nuclear pore glycoprotein p62 NUP62
P06748	Nucleophosmin
Q9Y5B8	Nucleoside diphosphate kinase 7
P15531	Nucleoside diphosphate kinase A
Q8WVJ2	NudC domain-containing protein 2
Q9NTK5	Obg-like ATPase 1
Q9NQR4	Omega-amidase NIT2
O75665	Oral-facial-digital syndrome 1 protein
Q5BJF6	Outer dense fiber protein 2
O95613	Pericentrin
Q15154	Pericentriolar material 1 protein
P43034	Platelet-activating factor acetylhydrolase IB subunit alpha
Q8TC44	POC1 centriolar protein homolog B
O00592	Podocalyxin
P49768	Presenilin-1, PSEN1
Q8WUM4	Programmed cell death 6-interacting protein
P12004	Proliferating cell nuclear antigen
P25786	Proteasome subunit alpha type-1
P28074	Proteasome subunit beta type-5
Q5VYK3	Proteasome-associated protein ECM29 homolog
O43822	Protein C21orf2
Q9P219	Protein Daple
O60610	Protein diaphanous homolog 1
Q3B820	Protein FAM161A
A1XBS5	Protein FAM92A1
Q5VTH2	Protein Flattop
Q13045	Protein flightless-1 homolog
Q9UJC3	Protein Hook homolog 1
Q9ULD6	Protein inturned
O76095	Protein JTB
Q04759	Protein kinase C theta type
O14974	Protein phosphatase 1 regulatory subunit 12A
Q8TCI5	Protein pitchfork
Q3SYG4	Protein PTHB1
O43663	Protein regulator of cytokinesis 1
Q13432	Protein unc-119 homolog A
Q9UBK9	Protein UXT
O75695	Protein XRP2
Q96QF0	Q96QF0
Q9Y3P9	Rab GTPase-activating protein 1
Q9BXF6	Rab11 family-interacting protein 5
P31749	RAC-alpha serine/threonine-protein kinase

P46060	Ran GTPase-activating protein 1
Q86VV4	Ran-binding protein 3-like RANBP3L
P43487	Ran-specific GTPase-activating protein
P62491	Ras-related protein Rab-11A
Q9ULC3	Ras-related protein Rab-23
P51157	Ras-related protein Rab-28
Q9H0N0	Ras-related protein Rab-6C
P61006	Ras-related protein Rab-8A
Q9NRY4	Rho GTPase-activating protein 35
O15013	Rho guanine nucleotide exchange factor 10
Q13464	Rho-associated protein kinase 1
O75116	Rho-associated protein kinase 2
Q9Y3A5	Ribosome maturation protein SBDS
Q9Y265	RuvB-like 1
Q9Y230	RuvB-like 2
P51957	Serine/threonine-protein kinase Nek4
Q8TDX7	Serine/threonine-protein kinase Nek7
Q8TD19	Serine/threonine-protein kinase Nek9
Q15172	Serine/threonine-protein phosphatase 2A 56 kDa regulatory subunit alpha isoform
P67775	Serine/threonine-protein phosphatase 2A catalytic subunit alpha isoform
P62714	Serine/threonine-protein phosphatase 2A catalytic subunit beta isoform
P60510	Serine/threonine-protein phosphatase 4 catalytic subunit
Q9NY27	Serine/threonine-protein phosphatase 4 regulatory subunit 2
Q6IN85	Serine/threonine-protein phosphatase 4 regulatory subunit 3A
Q8TCT7	Signal peptide peptidase-like 2B
O43805	Sjoegren syndrome nuclear autoantigen 1
Q9Y448	Small kinetochore-associated protein
Q76KD6	Speriolin
Q8IYX7	Stabilizer of axonemal microtubules 1
Q9P2P6	StAR-related lipid transfer protein 9
Q6ZVD7	Storkhead-box protein 1
Q14683	Structural maintenance of chromosomes protein 1A
Q9UQE7	Structural maintenance of chromosomes protein 3
O95721	Synaptosomal-associated protein 29
Q96C24	Synaptotagmin-like protein 4
P17987	T-complex protein 1 subunit alpha
P50991	T-complex protein 1 subunit delta
P48643	T-complex protein 1 subunit epsilon
P50990	T-complex protein 1 subunit theta
O95271	Tankyrase-1
Q6IQ55	Tau-tubulin kinase 2
Q9P0N9	TBC1 domain family member 7

Q8WW35	Tctex1 domain-containing protein 2
Q9UIF3	Tektin-2
Q6NXR4	TELO2-interacting protein 2
Q9UJT2	Testis-specific serine kinase substrate
Q96PF2	Testis-specific serine/threonine-protein kinase 2
Q9H892	Tetratricopeptide repeat protein 12
Q6DKK2	Tetratricopeptide repeat protein 19, mitochondrial
Q8TDR0	TRAF3-interacting protein 1
O95359	Transforming acidic coiled-coil-containing protein 2
Q9BVT8	Transmembrane and ubiquitin-like domain-containing protein 1
Q13748	Tubulin alpha-3C/D chain
P23258	Tubulin gamma-1 chain
Q9BTW9	Tubulin-specific chaperone D
Q99816	Tumor susceptibility gene 101 protein
P06239	Tyrosine-protein kinase Lck
Q9H3S7	Tyrosine-protein phosphatase non-receptor type 23
O75604	Ubiquitin carboxyl-terminal hydrolase 2
Q9NQC7	Ubiquitin carboxyl-terminal hydrolase CYLD
Q9BZV1	UBX domain-containing protein 6
Q8IVU9	Uncharacterized protein C10orf107
Q8N865	Uncharacterized protein C7orf31
Q9Y224	UPF0568 protein C14orf166
A7E2U8	UPF0602 protein C4orf47
P07911	Uromodulin
P54725	UV excision repair protein RAD23 homolog A
Q9Y5K8	V-type proton ATPase subunit D
P61421	V-type proton ATPase subunit d 1
Q8NEZ2	Vacuolar protein sorting-associated protein 37A
Q9UN37	Vacuolar protein sorting-associated protein 4A
O75351	Vacuolar protein sorting-associated protein 4B
Q9H1Z4	WD repeat-containing protein 13
Q96EX3	WD repeat-containing protein 34
Q9P2L0	WD repeat-containing protein 35
O43379	WD repeat-containing protein 62
Q14191	Werner syndrome ATP-dependent helicase
Q92834	X-linked retinitis pigmentosa GTPase regulator
O75800	Zinc finger MYND domain-containing protein 10

F. Composition of the early embryonic PCM: a biparental inheritance?

Our data suggest that the sperm basal body is associated with PCM proteins that are most likely transferred upon fertilization to the oocyte. However, additional components are most likely recruited from the oocyte cytoplasm, suggesting that the PCM is

biparentally inherited. A recent work described a human oocyte proteome consisting of 2,154 proteins (Virant-Klun et al., 2016). We found that 88 of the 288 sperm PCM proteins that we identified by mass spectrometry were also identified in oocytes. Surprisingly this represents only 30.6% of the centrosomal proteins we identified in sperm **(Figure 25A)**. We envisage two possible explanations for this low recovery in oocytes. First, the report of Virant-klun et al. is the first and only proteomic study of human oocytes. Centrosomal proteins are often difficult to detect and it is plausible that not all of them were identified. Second, oocytes do not have centrioles and it is possible that the PCM components are stored in the form of mRNAs instead of proteins. To explore this idea, we used data obtained from total RNA extracted from 36 donor oocytes (Barragan et al., 2017) to search for RNAs encoding PCM proteins. We found that 94.4% of the sperm PCM proteins we identified are also present as RNAs in the oocyte. The data from Barragan et al. does not provide any evidence for translation activity of the RNAs since they are based on total RNA. They, however, suggest that centrosomal protein genes are highly transcribed during oocyte growth and maturation **(Figure 25B)**. To elucidate whether this idea is true, we searched for the presence of pericentrin, a PCM component that localizes to the MTOCs and recruits other PCM proteins (Kim and Rhee, 2014) in the human oocytes. Although pericentrin RNA was found in the oocyte (7±0.2 A.U. of intensity), no protein was identified **(Figure 25C)**, while we could detect it in arrested human embryos (after fertilization) **(Figure 25D)**. This suggests that indeed some PCM components are stored in the oocyte in the form of RNA.

To summarize, the human oocyte contains PCM components, some of them as proteins but many as RNAs that are probably translated during early embryogenesis.
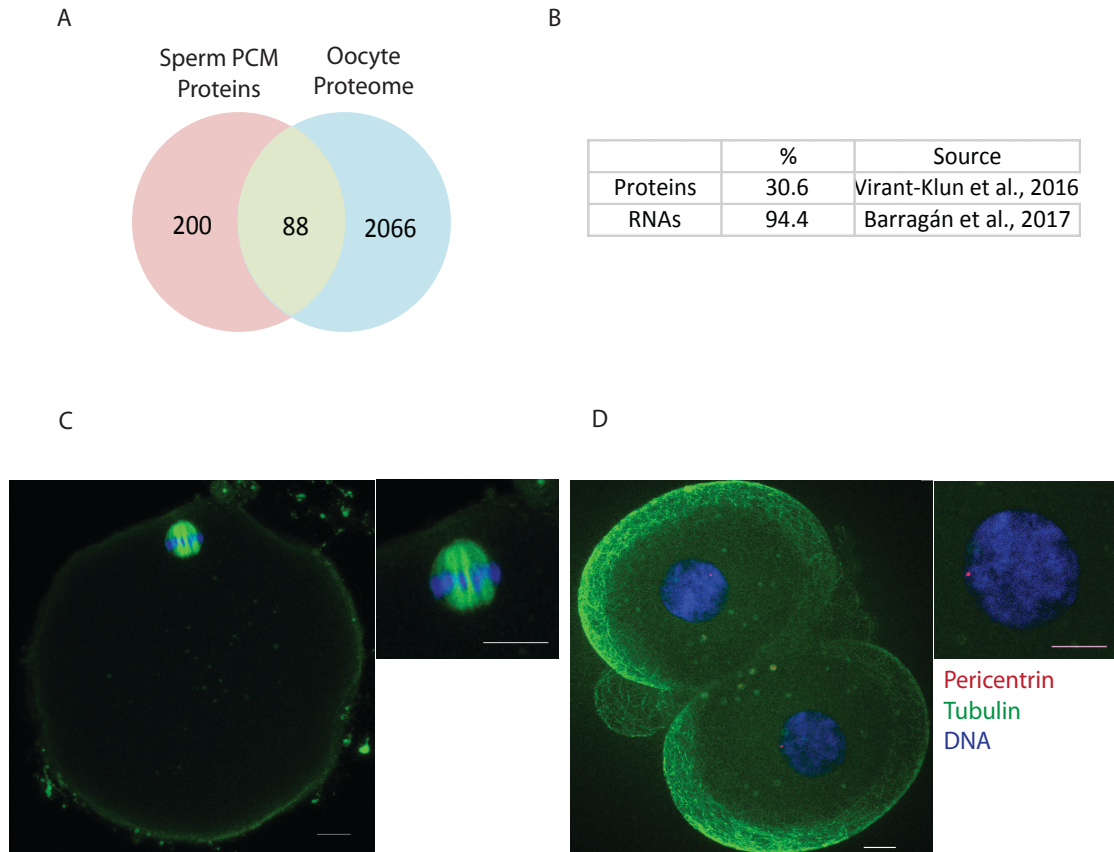
Figure 25: Oocyte PCM material. A) Common oocyte and sperm PCM proteins, both detected by proteomics. **B)** Percentage of detected proteins and RNAs from the sperm PCM in the oocyte. **C)** Representative image of an MII oocyte stained for pericentrin (red) and tubulin (green). **D)** As a positive control, human embryo at D+2 was fixed and stained for pericentrin and tubulin. Scale 10 μm.

G. Identification of novel centrosomal proteins:

Several proteins identified here by mass spectrometry are uncharacterized. 26 were identified in at least 2 independent experiments **(Table 4)**. For most of them, no information is currently available. In very few cases, there is some information about localization mostly based on similarity or obtained through high throughput assays.

Table 4: Uncharacterized proteins identified in the sperm tail proteome

Uniprot code	Name	Uniprot information (localization)
H3BRN8	C15orf65	-
Q53QW1	TEX44	Cytoplasm
Q5JU67	CFAP157	Cilium basal body
Q5T5A4	C1orf194	-
Q5T681	**C10orf62**	-
Q5TEZ5	C6orf163	-
Q5VTT2	C9orf135	Cell membrane and cytoplasm

Q5VU69	C1orf189	-
Q6P656	CFAP161	-
Q6V702	C4orf22	-
Q6ZQR2	CFAP77	Cilium localization
Q8IZ16	C7orf61	Nucleus
Q8N1D5	C1orf158	-
Q8N801	STPG4	Nucleus and cytoplasm
Q8N865	C7orf31	Centrosome in bovine sperm
Q8NA69	TEX45	-
Q8NEP4	C17orf47	-
Q8WW14	C10orf82	-
Q96LM5	C4orf45	-
Q96M34	C3orf30	-
Q9H0B3	KIAA1683	Mitochondrion and Nucleus
Q9H1P6	C20orf85	-
A4D263	C7orf72	-
A4QMS7	C5orf49	-
A6NCJ1	C19orf71	-
B2RV13	C17orf105	-

In order to elucidate whether these proteins could be novel centrosomal proteins, we selected 10 (in bold in the table) to further characterize in culture human cells. We used the protein C7orf31 as a positive control because it was recently identified by mass spectrometry analysis of bovine sperm and validated as a new centrosomal protein in human somatic cells (Firat-Karalar et al., 2014b). We cloned the corresponding cDNA of the 10 candidate proteins to express them with an N-terminal GFP or C-terminal CFP tags. HeLa cells were transfected with the corresponding constructs and the localization of the exogenously expressed proteins monitored by fluorescence microscopy in fixed cells with anti-centrin antibodies. 2 out of the 10 proteins co-localized with centrin, suggesting that they are indeed novel centrosomal proteins (**Figure 26A and B**). C7orf31 also accumulated to the centrosome as previously described (data not shown). The remaining 7 proteins did not co-localize with centrin.

In summary, we have identified two novel centrosomal proteins that will be interesting to further characterize.
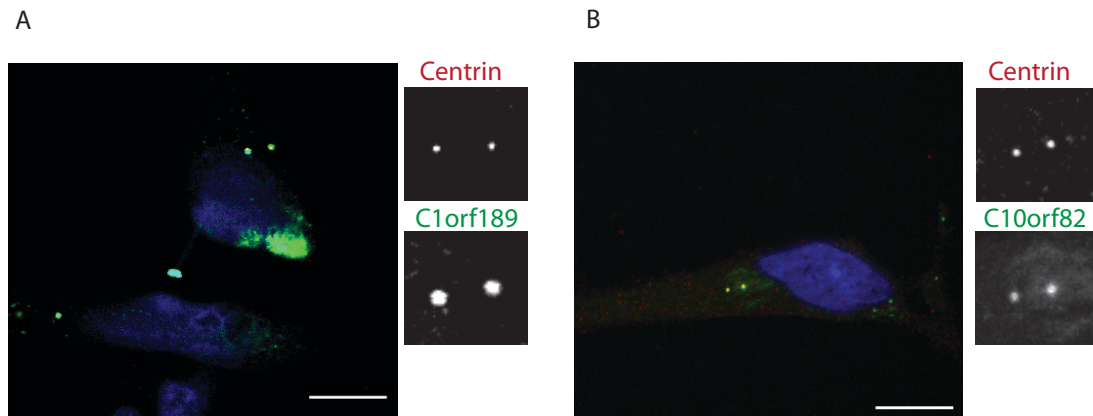
Figure 26: Localization of new centrosomal proteins. A) HeLa cells transfected for 24 h and then fixed with methanol. Centrioles were stained with centrin (red), C1orf189 visualized with CFP (green) and DNA stained with Hoechst (blue). Scale 10 μm. **B)** The same conditions were used to visualize centrin (red) and the C10orf82 (green) protein. Scale 10 μm

H. Conclusions and a short data interpretation:

We used and adapted a previously reported method to obtain a sperm fraction enriched in tails and centrosomes. Two different proteomic approaches to the analysis of this fraction identified more than 2,000 proteins, most of them involved in metabolic and reproductive processes. Additional analysis showed that we identified 289 PCM proteins, suggesting that the sperm basal body is enriched in PCM. We further identified two novel centrosomal proteins. Interestingly, although the distal centriole has a "degenerated" structure, we found that it is associated with centriolar and PCM proteins. An attractive model is that the PCM proteins that the spermatozoon does provides to the fertilized oocyte are important to assemble the first functional centrosome of the zygote, because only around 30% of these proteins are also present in the mature oocyte at the time of fertilization. Therefore, our results could point to a biparental inheritance of PCM during human fertilization.

IV. Chapter 3: The paternal inheritance of the centrosome provides an advantage to support early embryonic development.

In the human species, the centrosome is already present in the zygote, in contrast to other species in which the centrosomes are formed *de novo* during early development. Therefore, are centrosomes really necessary for the first stages of human development? Or is its fertilization inheritance a mechanism only needed in order to regulate the number of centrosomes per cell?

We know that centrosomes are essential for the development of *C. elegans* and *Drosophila* embryos. However, they are not necessary in mice. The centrosomes could be important due to several reasons. For example, they could be important to position the spindle inside the cell during early embryo development. Specifically, in the first cell division when a completely symmetric segregation of the cytoplasmic material must occur. We also hypothesize that centrosomes could be important during embryo compaction, when embryo asymmetry arises. Astral microtubules should play an important role in establishing the asymmetric cell division plane. On the other hand, we know that there are alternative mechanisms of spindle positioning in the cell relying on actin filaments. Also, indispensable for the correct development and survival of the organism is maintaining the correct number of centrosomes per cell. Abnormal centrosome number is associated with many diseases such as cancer and microcephaly. The mechanism of centrosome duplication is cell cycle dependent, as centrosomes duplicate once per cycle and it involves a complex machinery regulated by many cell cycle factors. If the centrosome is inherited during fertilization, centrosome duplication cycle is regulated already in the zygote but, if centrosomes are formed *de novo*, the number of centrosomes per cell tends to be altered.

Aware of the lack of data on this matter in the human species, we tried to establish a methodology to test the role of the paternal centrosome during human preimplantation development. In this chapter, I expose the methodology we developed, as well as our data supporting one of the hypotheses previously described.

A. Individual isolation of the human sperm centrosome:

Our experimental approach is based on the injection of microsurgically isolated sperm tails, containing the centrosome, into mature human oocytes, followed by parthenogenetic activation of the resulting construct. We expect the paternal centrosome in the injected tails to become functional in the resulting parthenote. If the addition of the centrosome provides an advantage to the parthenote, the centrosome-containing ones would develop more efficiently up to later stages of embryo development, the cells would maintain their symmetry up to D+3 post-activation and the ICM and the TE would better segregate, among other characteristics.

To set up the method, we had to take several aspects into consideration: 1) the microsurgical head – tail sperm separation had to be very precise because the sperm centrosome is located very close to the head **(Figure 27A)**. 2) DNA could not remain attached to the tail portion. The introduction of DNA into oocytes, in fact, would equate to fertilization, and the Spanish law and regulations prohibit fertilization of human oocytes for any purpose other than reproduction. 3) Centrosome and mitochondria are the main organelles of the tail. Mitochondria are mostly eliminated soon after sperm entry, therefore, the effect that we would expect to see may be centrosome-specific. 4) Several heterologous ICSIs models (both gametes are from different species) have been proposed to study the human sperm centrosome during fertilization (Terada et al., 2004). However, because they are heterologous, the results obtained might not recapitulate exactly what occurs naturally during human development. Here, we propose to use both male and female human gametes, albeit without paternal DNA, to mimic as much as possible human early development.

As an initial proof of principle, we assessed how many isolated sperm tails contained the centrosome. We used sperm donor samples. Once the sperm tail microsurgical separation was done (see Materials and Methods for an accurate description of the technique), we aspirated and loaded the separated spermatozoa (head + tail) onto a glass microscope slide and stained with an antibody against centrin in order to detect the centrioles, tubulin and DNA **(Figure 27B)**. In an ejaculated normozoospermic sperm sample not microsurgically manipulated, 83,9% of the spermatozoa presented a positive centrin signal, indicating that the staining was robust. We found that 63,1% of the

detached sperm presented either 1 or 2 centrin dots, and no traces of DNA were detected **(Figure 27C)**. In summary, we were able to efficiently isolate sperm tails with most of the centrosomes and no DNA.
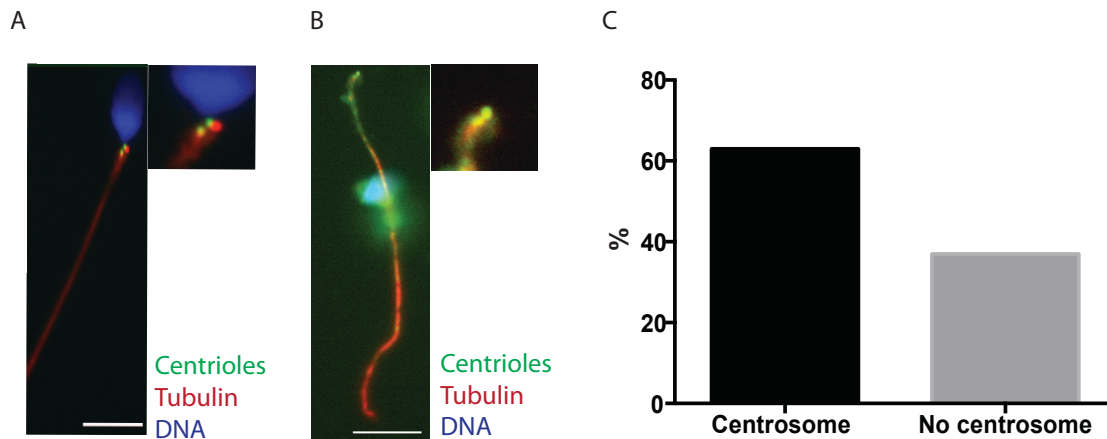
Figure 27: Sperm centrosome localizes to the microsurgically separated tails. A) Intact sperm cell. Centrioles localize close to the head. Scale 7,5 μm. **B)** Head and tail from a manually separated spermatozoon. In the tail, two centrioles and no DNA can be detected. Scale 7,5 μm. **C)** Percentage of isolated tails with centrosomes. Approximately, 60% of the tails, at least, contain one centriole.

B. Functional MTOCs are assembled in tail-injected oocytes:

More than 60% of the sperm tails did contain at least one centriole. Nevertheless, we checked if these centrioles assembled functional centrosomes when they were injected into oocytes that were activated. To assess if functional centrosomes were assembled, we first checked whether our centrosome detection protocol by IF was efficient and reliable. To do that, we used embryos with 1- or ≥3-PN because, although these embryos are incorrectly fertilized and discarded form IVF cycles, the oocytes were activated naturally. We were unable to optimize centrin staining (centriolar marker) in 1- or ≥3-PN embryos, therefore we used pericentrin. Since pericentrin is a PCM component, we cannot refer to the detected structures as centrosomes. For this reason, we decided to refer to them as MTOCs. We stained 1- (n=9) and ≥3- (n=7) PN embryos fixed at the 2- or 4-cell stage to detect pericentrin, tubulin, and DNA. 87% and 100% of the 1- and ≥3-PN embryos, respectively, did contain at least one MTOC **(Figure 28A and B)**. These data suggest that pericentrin can be used as a marker of MTOCs in early embryos and parthenotes.

Then, we analyzed 6 sham– (or Control) and 10 tails– (or Injected) injected and activated oocytes fixed at 2- or 4-cell stage (D+1 or D+2) and stained to visualize

pericentrin, tubulin and DNA. As expected, no pericentrin staining was detected in control oocytes. In contrast, in 20% of the injected-oocytes we detected a pericentrin signal similar to the one in 1- or ≥3-PN embryos, as well as in 2-PN embryos in a previously published (Kai et al., 2015) **(Figure 28C)**. These data also showed that 40% of the injected centrosomes did not become functional into the activated oocyte. One possible explanation is that the mechanical process of sperm head-tail separation affects the centrosome structure and function.
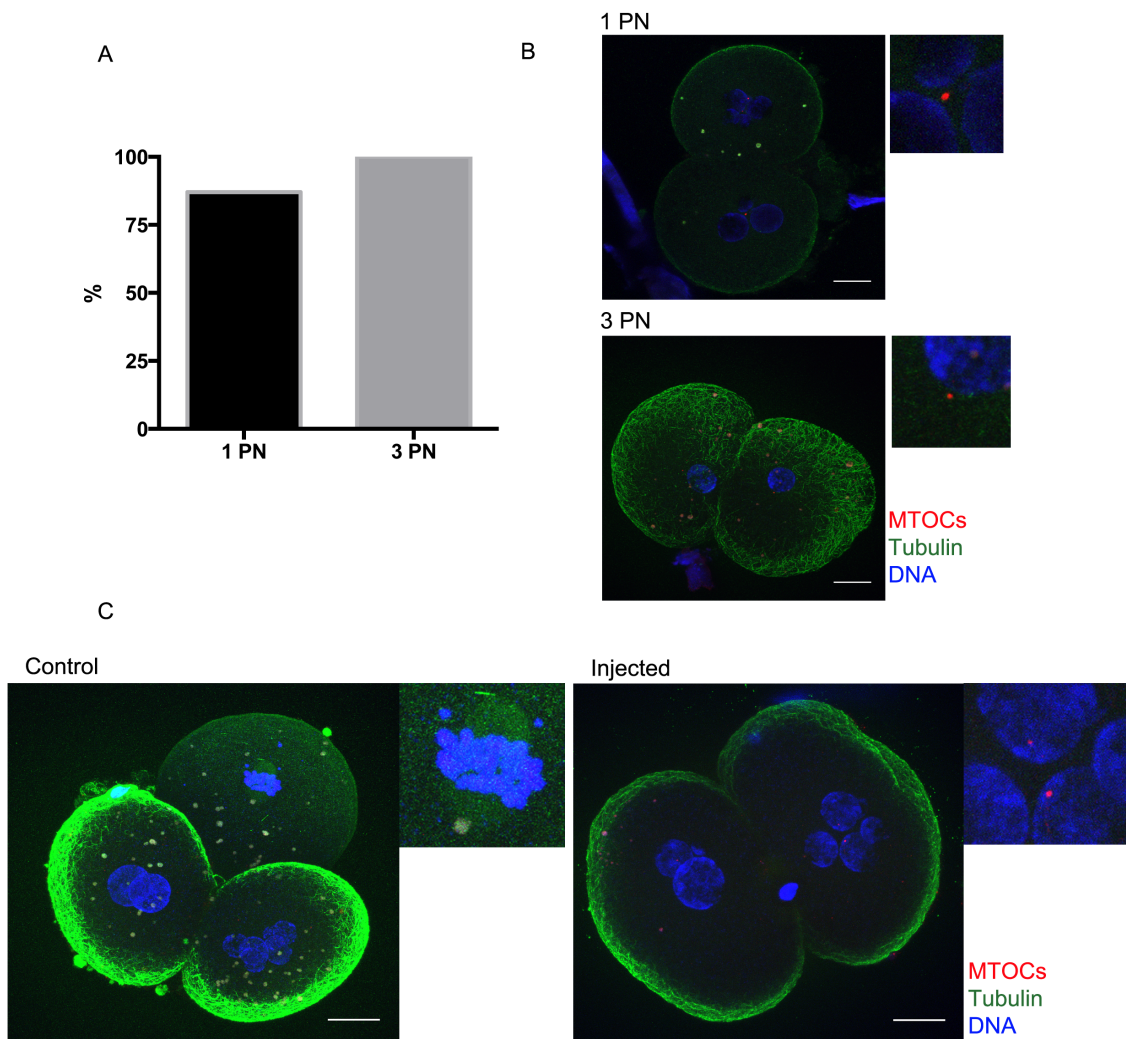
Figure 28: MTOCs are only detected in injected oocytes. A) Percentage of cells that contains at least one MTOC at 2- to 4-cell stage of 1- and ≥3-PN embryos. Our staining is very efficient because in ≥3-PN embryos we detected at least one MTOC per cell. **B)** Representative pictures of 1- and ≥3-PN embryos stained for pericentrin, tubulin and DNA. MTOCs are very small dots that localize close to the nucleus. Scale 20 μm. **C)** Representative image of control and injected oocytes. Control oocytes were sham injected, activated and fixed at D+1 or D+2 to visualize MTOCs, tubulin and DNA. In none of the controls, a MTOC signal was detected. In tail injected oocytes, 20% assembled functional MTOCs. In this particular image, for example, two MTOCs are detected, which also suggests that the sperm centrosome can duplicate. Scale 20 μm.

In summary, 20% of the injected-oocytes formed functional MTOCs at the 2- to 4-cell stage, so if any difference during parthenogenetic development is caused by the presence of MTOCs, it might be difficult to detect. It is worth to mention that this experiment was performed once and the sample size is small, therefore, the percentage of parthenotes with functional MTOCs could be slightly variable among experiments.

C. MTOCs provide an advantage to the embryo to support its early development:

Despite the presence of just 20% of functional MTOCs, we performed two independent experiments with control (n=10) and injected (n=15) oocytes **(Table 5)**. Right after the injections and parthenogenetic activation, we maintained the parthenotes in culture until D+5 or D+6 when we fixed and stained them for pericentrin, tubulin and DNA. During these days of *in vitro* culture, images of the growing parthenotes were taken every 5 minutes to analyze morphokinetically the parthenotes development (time-lapse).

First, we compared the percentage of controls and injected oocytes that reached blastocyst stage as a marker of active development. We found that 20% of controls and 27% of injected oocytes developed up to blastocyst **(Figure 29A and B)**. Although more injected oocytes formed blastocysts, it was not significantly different. This could be due to the samll sample size, not enough to perform robust statistical analyses. The percentage of controls that form blastocyst was previously quantified to be ≈12.8% (Paffoni et al., 2007). Our percentage of control blastocysts is above, which indicated that our system is optimized.

Table 5: Sample size for each experiment. We only took into account oocytes that were activated (PB extrusion and PN formation) in order to avoid oocyte activation problems.

	Control	Injected
Experiment 1	5	8
Experiment 2	6	7
Total	10	15

A

B
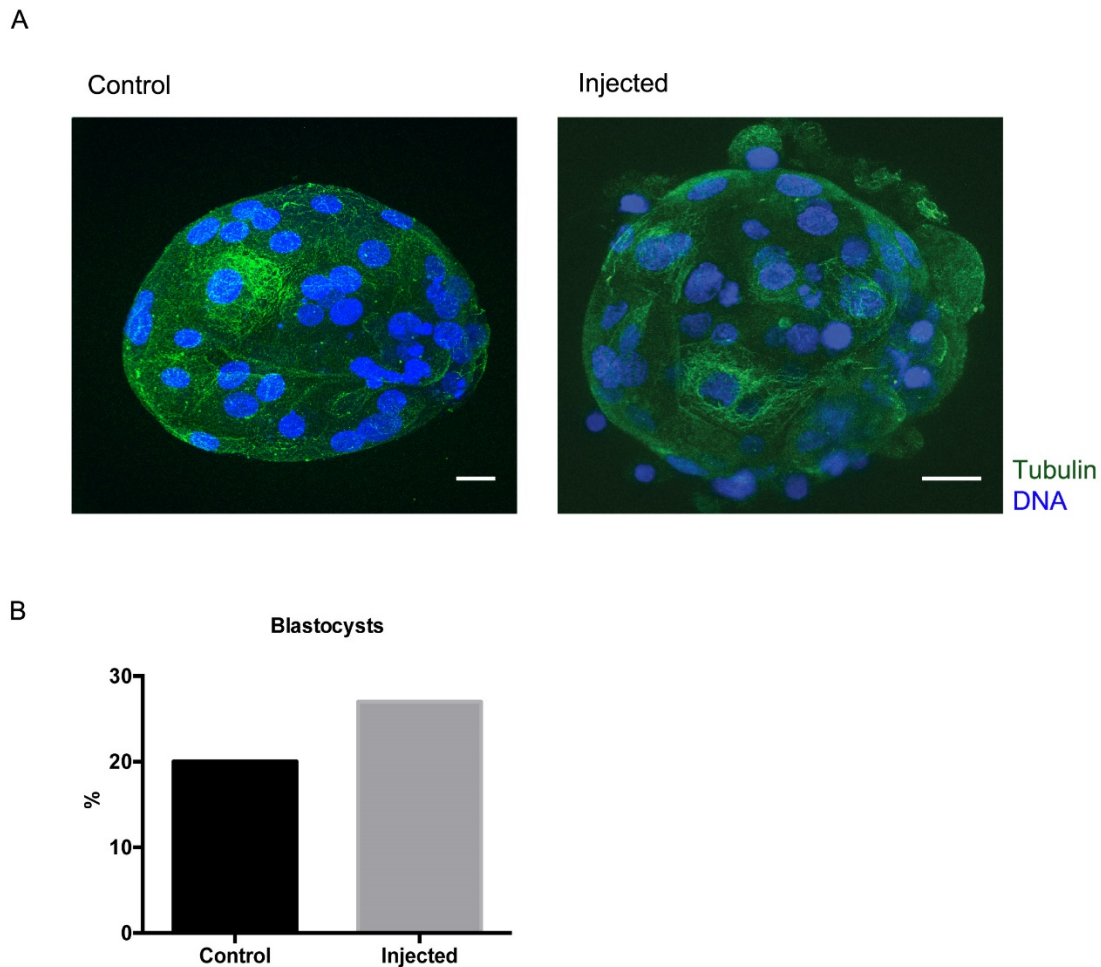
Figure 29: Similar rates of control and injected oocytes reached blastocyst stage. A) Representative images of control and injected blastocysts imaged with tubulin and DNA. Scale 20 μm. **B)** Percentage of blastocysts obtained at D+5 and D+6 in control and injected conditions. The number of blastocysts achieved in both situations is very similar and not statistically different.

When we compared in detail the early development of control *versus* injected oocytes, interesting data were found **(Table 6)**. We quantified the number of parthenotes that achieved the following stages: 1-, 2-, 3-, 4- and 5-cells, compaction, early blastocyst and expanded blastocyst (Martinez et al., 2016) **(Figure 30A)**. In general, control and injected oocytes had a similar developmental progress, but a slightly different pattern was detected in 1- to 2-cell stage transition as well as from 5-cells to early blastocyst transition. To quantify these observations, we measured the different percentage of controls *versus* injected parthenotes at each stage **(Figure 30A and B)** together with the slope between each stage transition **(Figure 30C)**.

Table 6: Time-lapse images analyses. The time needed to achieve each cellular and embryonic stage per sample was annotated in hours. "no data" refer to processes that could not be analyzed due to the low quality of the image. The last two columns refer to whether the sample could be analyzed by IF and if the sample was positive or negative for MTOC signal.

Sample	Pronucleus formation	Pronuclear Break Down	2 cells	3 cells	4 cells	5 cells	Compaction	Early Blastocyst	Expanded Blastocyst	IF	MTOC Signal
EXPERIMENT 1											
Control_1	no data	65	71	104	no data	135	214			YES	NO
Control_2	no data	62	71							YES	NO
Control_3	no data	61	75	81						YES	NO
Control_4	no data	71	81	114	116	161				YES	NO
Control_5	no data	73								NO	
Injected_1	28	57	65	97	106	142				YES	NO
Injected_2	17	36	44							YES	YES
Injected_3	14	33	43	69	71	96	232			YES	YES
Injected_4	16	40	48	73	80	100	218	253	261	YES	YES
Injected_5	15	39	47	51	57	89				YES	NO
Injected_6	18	42	49	80	115	188	219			YES	YES
Injected_7	no data	no data	116	123						YES	NO
Injected_8	13	49	57	79	96	118	182	325	369	YES	NO
EXPERIMENT 2											
Control_1	18	45	54	68						NO	
Control_2	25	43	50	80	107	109	213	307	316	YES	YES
Control_3	24	44	54	71	86	109	259	299		YES	YES
Control_4	16	40	46	78	83	106	223	282	362	YES	YES
Control_5	19	no data	49	110	110	120				NO	
Injected_1	23	55	64	75	91	115	173			YES	NO
Injected_2	20	50	56	88	no data	136	225	320		YES	YES
Injected_3	33	46	53							YES	NO
Injected_4	28	44	58	85	88	125	176			YES	NO
Injected_5	no data	no data	24	39						YES	NO
Injected_6	21	46	52	80	87	109	197	278	301	YES	YES
Injected_7	21	61	67	72	98	105	210	316	338	YES	YES

A
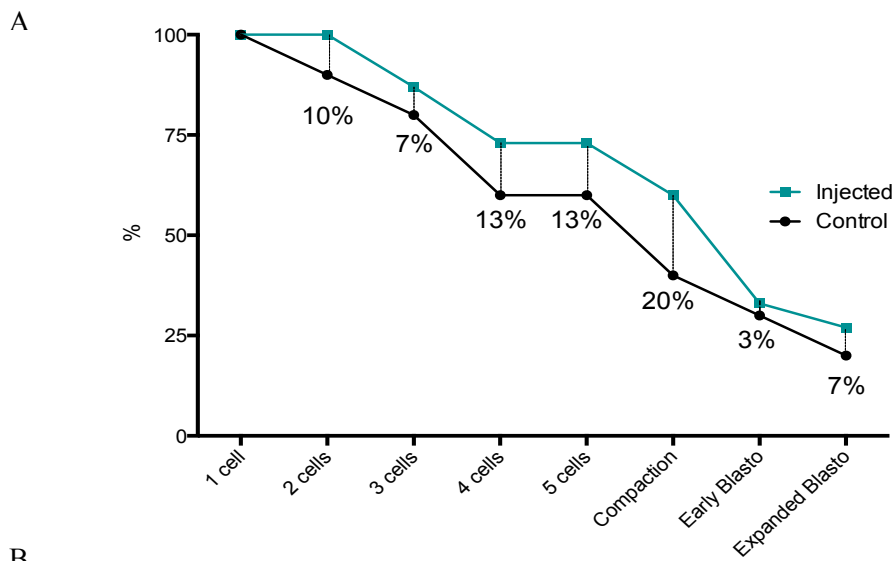
B

1-cell	**0**
2-cells	10
3-cells	7
4-cells	13
5-cells	13
Compaction	**20**
Early Blasto	3
Expanded Blasto	7

C

Stage	Injected slope	Control slope
1- to 2-cells	**0**	**-10**
2- to 3-cells	-13.3	-10
3- to 4-cells	-13.3	-20
4- to 5-cells	0	0
5-cells to Compaction	**-13.3**	**-20**
Compaction to Early Blasto	**-26.6**	**-10**
Early Blasto to Expanded Blasto	-6.6	-10

Figure 30: Developmental progress of control and injected oocytes. A) The graph represents the percentage of parthenotes that continue their development until blastocyst. **B)** Percentage of the different number of injected *versus* control oocytes that achieved each cellular or embryonic stage. **C)** Analysis of the slope between the transition of cells and parthenotes stages.

From 1- to 2-cell stage, 10% of controls did not divide whereas all the injected oocytes formed 2-cells (%= 0; slope=-10). Microtubules from this control oocyte emanated from the DNA but they did not organize into a bipolar structure **(Figure 31A)** what could suggest that MTOCs are important for spindle assembly and bipolarization at the first embryo cell division. The transition from 2- to 5-cells presented a similar pattern in control and injected oocytes **(Figure 30)**. But, whereas control parthenotes mainly arrested at 3- to 4-cell (slope=-20) as previously described (Paffoni et al., 2007), injected oocytes arrested indifferently from 2- to 4-cell stage (slope=-13.3). Nevertheless, in both cases, when a parthenote had 4-cells, it divided to 5-cells (slope=0), indicating that MTOCs are not essential for this division.

An important step during embryo early development is compaction. We hypothesized that centrosomes may play an important role because the embryo symmetry is broken. Indeed, we found the most divergent percentage of control *versus* injected parthenotes at compaction; 20% more oocytes could compact in the injected group compared with controls **(Figure 30A and B)**, while this difference disappeared in early blastocysts (30% of controls and 33% of injected parthenotes). In the same direction of these data, the slope is inverted in control and injected oocytes from 5-cells to compaction (control slope=-20, injected=-13.3) and from compaction to early blastocyst (control slope=-10, injected=-26.6) **(Figure 30B and C)**. So far, these data would suggest that MTOCs might be needed to both start and exit compaction.

To further understand the observed phenotype, we analyzed at which point the arrested parthenotes stopped their development. We formed two groups: parthenotes that arrested before compaction (from 1- to 5-cells) and after compaction (from compacted parthenote to blastocyst). Our functional experiments showed that 75% of the arrested controls (from the 80% of total parthenotes arrested) did so before compaction and 25% after compaction **(Figure 31B and C)**. On the other hand, 55% of the injected oocytes (from the 73% of total parthenotes arrested) arrested before compaction and 45% after it **(Figure 31B and C)**. These data showed that if MTOCs are present during early development, parthenotes arrest similarly during these 5 days whereas parthenotes without MTOCs tend to arrest before compaction.
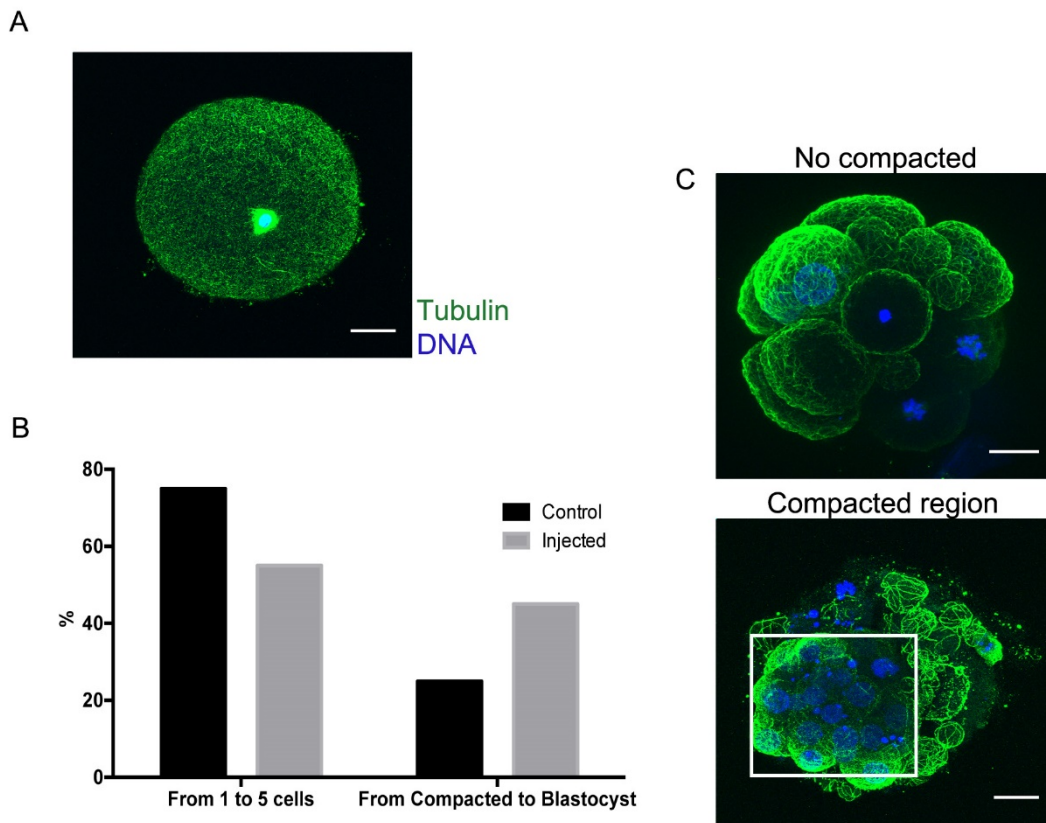
Figure 31: More injected oocytes can compact compared with control oocytes. A) Control oocyte stained with tubulin and DNA. This oocyte was activated but did not divide. Around the DNA, microtubules were assembled but a bipolar spindle was not organized. Scale 20 μm. **B)** Rate of control and injected oocytes that arrested before or after compaction. Most of the control oocytes arrested before compaction (from 1- to 5-cells stage) whereas injected oocytes arrest similarly before and after compaction. **C)** Representative images of parthenotes imaged with tubulin and DNA before compaction and already compacted. Scale 20 μm.

D. Human parthenotes can form *de novo* MTOCs :

To complete our analyses, we checked by IF how many of the injected oocytes had MTOCs signal **(Table 6)**. 46.6% of the injected oocytes had MTOCs signal, from which 85.7% developed at least until compaction while 14.3% arrested before. These data support the previous observation that MTOCs might help to achieve a successful compaction. Surprisingly, we found that in a few cases, MTOCs could also be detected in controls **(Figure 32A)**. MTOCs were only detected in early blastocysts, right after compaction (100% of control blastocysts contained MTOCs). Until now, the presence of MTOCs in human parthenotes was only described once (Brevini et al., 2012). We hypothesized that because centrosomes might be necessary to efficiently bypass compaction, if they are not paternally inherited, centrosomes can be formed *de novo* when the embryonic genome is reactivated. The activation of the genome will lead to an

increase of PCM proteins that may facilitate their clustering thanks to their phase-separation properties (Woodruff et al., 2017). To confirm our hypothesis, we sham-injected oocytes, activated them parthenogenetically, and fixed at D+3 or D+5 to detect pericentrin and tubulin by IF in two independent experiments **(Table 7 and 8)**. None of the control oocytes fixed at D+3 did have MTOC signal, in contrast, 1 out of 5 controls fixed at D+5 progressed until blastocyst and presented MTOCs. This mechanism of MTOC formation at the blastocyst stage highly resembles *de novo* centrosome formation in mice. Since when the centrosomes are formed *de novo* their duplication cycle is altered (Khodjakov et al., 2002), we quantified the number of centrosomes per cell in 1- and ≥3-PN embryos (n of cells=65), in controls (n of cells=116) and in the injected ones (n of cells=116) **(Figure 32B)**. The number of cells with 1 or 2 MTOCs (correct proportion) in injected oocytes highly resembled the ones in embryos (Injected=62.8%; embryos=66.2%). However, in controls where MTOCs are all formed *de novo*, the proportion of cells with no MTOCs is much higher (0 MTOCs=37.9%). We also realized that in control parthenotes, MTOCs are not defined structures like in injected oocytes and embryos. We classify this morphology as "scattered" **(Figure 32A – lower panels)**. We found that almost half of the control MTOCs are scattered whereas most of the 1- and ≥3-PN embryos and injected oocytes had MTOCs with a defined structure (% of scattered MTOCs, embryos=15.4%; Controls =54.2%; Injected=28.3%) **(Figure 32C)**. Our data propose that the paternal inheritance of the centrosome not only supports early embryo development, but also it is a mechanism to ensure the proper structure and number of centrosomes per cell in the developing embryo.

Table 7: Sample size for each experiment. A total of 6 control oocytes were fixed at D+3 and 5 at D+5

	D+3	D+5
Experiment 1	3	2
Experiment 2	3	3
Total	6	5

Table 8: Kinetics and IF analyses of control oocytes fixed at D+3 and D+5 of development. Like in the previous experiment, the time to achieve each cellular and embryonic developmental stage was annotated in hours. "no data" refer to process that could not be analyzed due to the low quality of the image. The last two columns indicate if the sample was analyzed by IF and if MTOC signal was present.

Sample	Pronucleus formation	Pronuclear Break Down	2 cells	3 cells	4 cells	5 cells	Compaction	Early Blastocyst	Expanded Blastocyst	IF	MTOC Signal
FIXED AT D+3											
Control_1	no data	no data	35	51	54	54				NO	
Control_2	12	21	23							YES	NO
Control_3	17	19	22	34	36	48				YES	NO
Control_4	9	17	20	36	39	57				YES	NO
Control_5	7	28	31							YES	NO
Control_6	9	22	25	24						YES	NO
FIXED AT D+5											
Control_1	no data	no data	21	22	46	53	63	93	102	YES	YES
Control_2	10	26	31	44	44	56	83			NO	
Control_3	7	19	22							YES	NO
Control_4	11	23	25	28	43	63				YES	NO
Control_5	no data	22	24							NO	

A

3 PN Embryo   Control   Injected

MTOCs
Tubulin
DNA

B

Sample	0 MTOCs	1 or 2 MTOCs	≥3 MTOCs
1 or 3 PN	20	66.2	13.8
Control	37.9	49.1	12.9
Injected	28.7	62.8	8.5

C

Sample	No	Yes
1 or 3 PN	84.6	15.4
Control	45.8	54.2
Injected	71.7	28.3
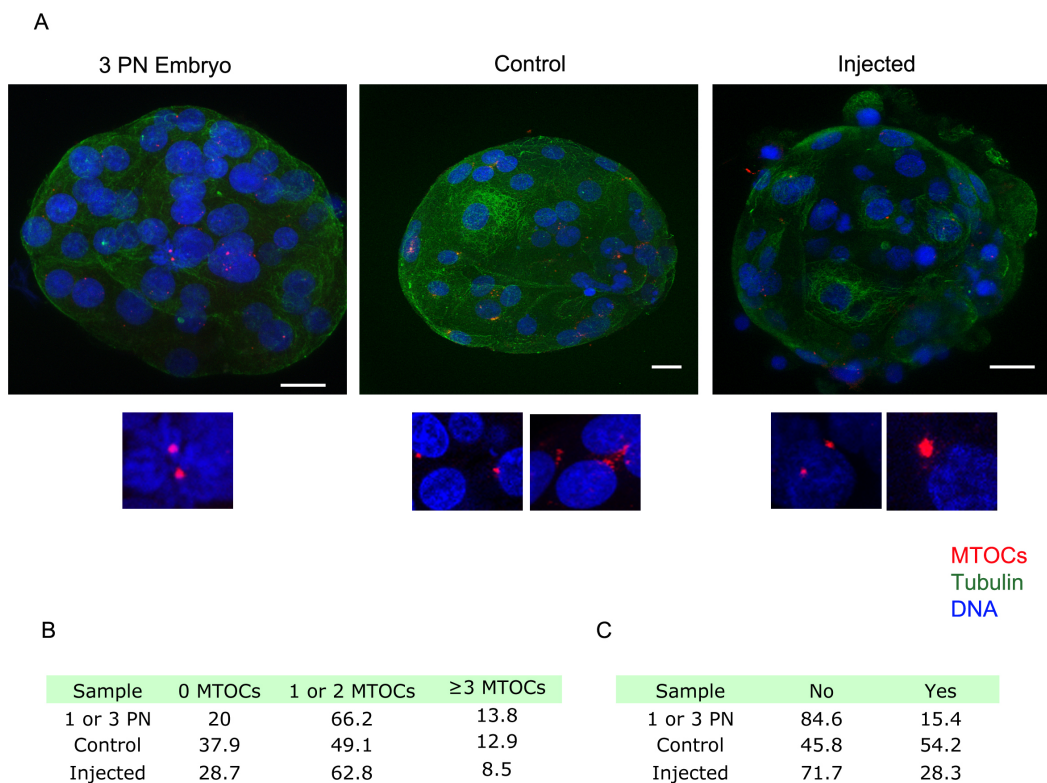
Figure 32: MTOCs can form *de novo* in control blastocyst and after the embryonic genome activation. A) ≥3-PN embryo, control and injected oocytes were fixed at blastocyst stage and analyzed by IF for MTOC, tubulin and DNA. In all the three cases MTOCs are detected, however their morphology is slightly different. MTOCs from ≥3-PN embryos are defined rounds whereas in control and injected oocytes rounded and scattered MTOCs were also visualized (lower panel). Scale 20 μm. **B)** Number of MTOCs per cell in 1- or ≥3-PN embryos, control and injected oocytes. In the controls, where MTOCs are all formed *de novo*, it is frequent to detect aberrant MTOC numbers. **C)** Rate of scattered MTOCs per sample. MTOCs were classified as rounded structures (NO) or scattered (YES). The MTOCs morphology of injected oocytes resembles that of the embryo rather than controls.

We finally analyzed the contribution of the MTOCs to the early embryonic development morphokinetics since centrosomes define the kinetics of the first embryonic spindle bipolarization (Cavazza et al., 2016). To be as accurate as possible, we only included in the injected condition the parthenotes that had MTOCs detected by IF. (**Figure 33 and**

Table 6). Although injected oocytes took less time to achieve each of the previous described cellular or embryonic stages, the differences are not significant, thus, MTOCs did not provide a kinetic advantage when a whole complex cellular structure is analyzed. Probably the differences in the spindle assembly kinetics are not detected due to the small sample size.
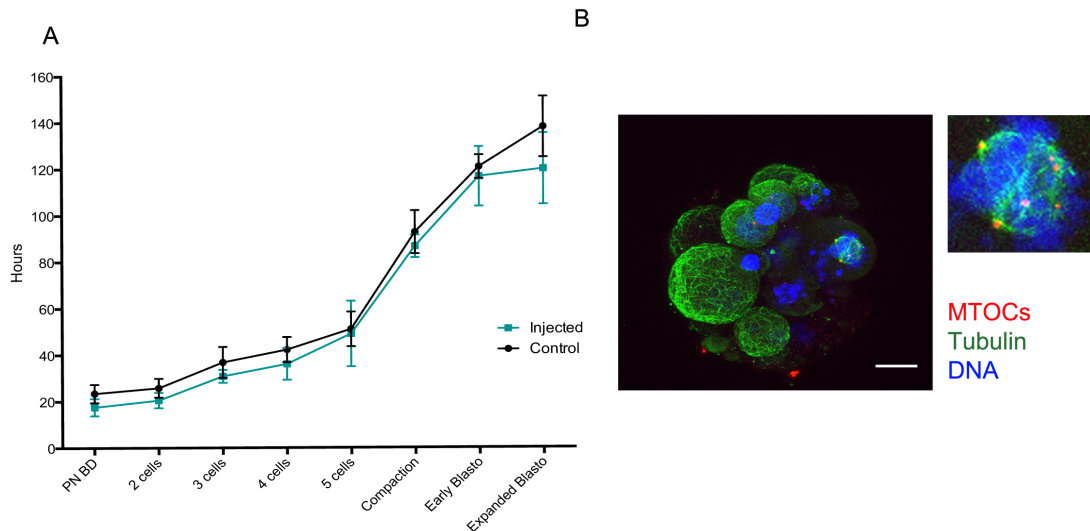
Figure 33: Kinetics of early development is not centrosome-dependent. A) No significant differences are detected in the kinetics of cell division and embryonic stages after tail injection compared with controls. **B)** Representative picture of injected oocytes at D+4. Note that when multiple MTOCs are formed in one cell, the assembled spindle is not functional. Scale 20 μm.

E. Conclusions and a short data interpretation:

We optimized a methodology that enables us to study the contribution of the sperm centrosome to embryo early development. Although our microsurgical separation of the sperm tail from the head was highly efficient, only 20% of the injected centrosomes became functional in the activated oocyte. Nevertheless, we were able to detect that the paternal inheritance of the centrosome provides an advantage to successfully achieve compaction and to ensure the correct number of MTOCs per cell. Surprisingly, we found that when parthenotes do not have MTOCs they can be formed *de novo* after embryonic genome reactivation. This emphasizes that MTOCs must provide a positive cue for the embryo development.
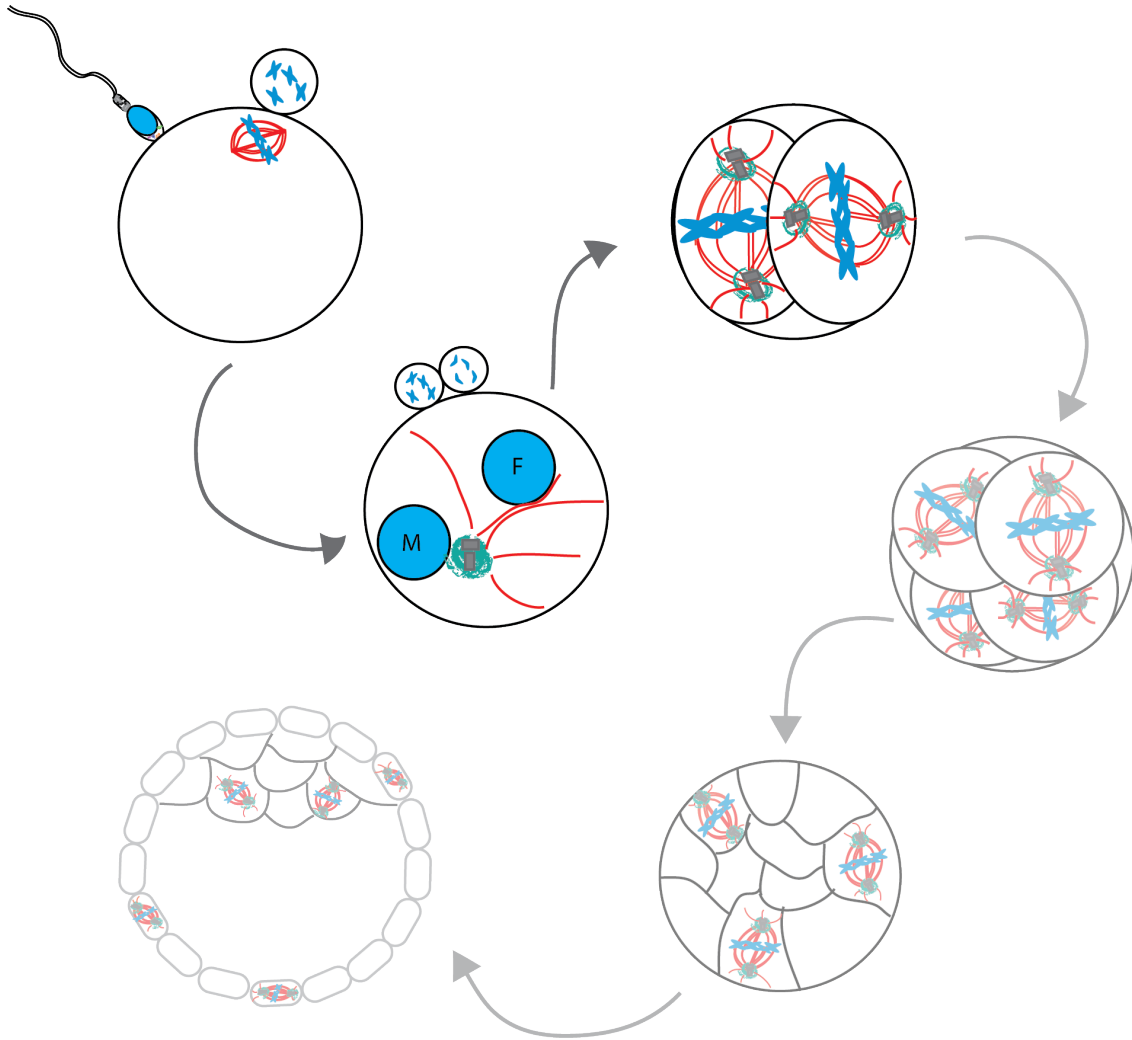
I. Why I think that human infertility treatments fail:

It is estimated that 186 million people worldwide are affected by infertility (Inhorn and Patrizio, 2015). The introduction of ART helped many of them to fulfill their dream of becoming parents, yet, ART is still not available worldwide. Since the birth of Louise Brown in 1978, the number of people conceived by ART has grown exponentially, approaching rapidly to 0.1% of the world population. It is estimated that by 2100, ART children will represent, at least, 1.4% of humanity (Faddy et al., 2018). In some countries such as Denmark, Slovenia and Belgium, ART births already represent 6.1%, 4.9% and 4.6% respectively of the total natality (European et al., 2016), which emphasizes the social impact of ART.

Although ART has witnessed numerous advances, which include the development of several different techniques and equipment as well as the training of highly qualified professionals, ART success rate is still low. From 2009, the pregnancy rate remained almost constant (≈30%) as well as the percentage of ART infants born per cycle (≈21%). However, from 1997 the number of reported ART cycles has increased more than 3-fold (only in Europe 203,225 cycles in 1997 and 686,271 cycles in 2013) (European et al., 2017; European et al., 2016; Ferraretti et al., 2013; Kupka et al., 2014). This suggests that we still miss much knowledge that there is a whole space of research to explore, with the final goal of translating this knowledge to fertility clinics to increase ART success rates and ultimately, social welfare.

So, one can ask what is failing in ART? First, we must take into account that human reproduction is a highly inefficient process. It has been estimated that the chances of getting pregnant on the first menstrual cycle upon the decision of having a child are only 30.1% in a population of young women (Wang et al., 2003b). However, in ART the gametes and embryos to transfer are selected and the women body is monitored to select the best moment for embryo to implant, but the success rate is even lower than in natural human reproduction.

The main bottleneck seems to be during the early stages of development. On average, the fertilization rate is around 75% (Joergensen et al., 2014; Liu et al., 2017)

independently of the technique (IVF *vs* ICSI). The remaining 25% are not fertilized oocytes or fertilized oocytes with abnormal number of PN (1 or ≥3 PN). Although almost 100% of the correctly fertilized oocytes cleave, only 66% of them are considered top-quality day-3 embryos and only between 50 to 60% will form blastocysts by day 5 of *in vitro* culture (Ebner et al., 2012; Jin et al., 2015). As an example to realize the impact of these losses, if a couple has 10 MII oocytes only 4 will become blastocysts (not selected by their quality) and from these 4, less than the half will implant. These data show that during human *in vitro* embryo early development, most of the fertilized oocytes fail to develop up to day 5, reducing the number of embryos available for transfer.

There are many reasons that could explain why *in vitro* development fails; here, there are some of them:

- Human assisted reproduction is a relatively recent area of research and many advances are still made based on observational studies.

- The sample population is very heterogeneous; each gamete, embryo and women body (reproductive system) behave differently because they come from different genetic and environmental conditions, which makes difficult to extrapolate results to all patients.

- Embryos are cultured *in vitro* outside the body. Many studies have been performed to determine the levels of metabolites, oxygen and pH variations during embryo development *in vivo* in order to adjust the *in vitro* conditions as much as possible to the natural ones (Gardner et al., 1996; Morbeck et al., 2017; Sunde et al., 2016). For example, it is known that atmospheric oxygen levels (20% *vs* 5%) can reduce embryo developmental rates and influence the kinetics of embryonic cell divisions (Kirkegaard et al., 2013); on the other hand, embryos are exposed to different metabolite concentrations (such as lactate and glucose) along the oviduct (Gardner et al., 1996). All these transient changes are difficult to reproduce *in vitro* and, most likely, have an effect on the embryo development success.

- Gamete and embryo selection are mainly based on morphological characteristics rather than functional analyses. In ART, the concept of gamete selection is particularly relevant because embryo success only depends on one spermatozoon and an oocyte. If any of the gametes is unable to develop a new organism, no other cell can compensate for its failure. Unfortunately, the development of new selection methods is difficult because human reproduction is a multifactor process and many uncontrolled elements can introduce a bias when trying to correlate gamete quality with reproductive results (Sakkas et al., 2015).

Basic research could aid in understanding the molecular causes of human embryo arrest and provide new concepts and tools to improve ART success. The main limitation of this approach is the difficulty of working with human samples, even though some molecular causes of infertility are already known. These causes that will affect the embryo early development can be divided in whether they come from maternal or paternal origin at the time of fertilization.

Oocytes are prone to aneuploidy, and this is one of the major factors that result in low efficiency in human infertility treatments. Although it has been estimated that 20% of human oocytes are aneuploid (Pacchierotti et al., 2007), some authors detected more than 60% of aneuploid oocytes (Kuliev et al., 2005). The incidence of aneuploidies increases with woman age, as the oocyte spindle becomes aberrant and chromosomes are not well aligned (Eichenlaub-Ritter et al., 1988). On the other hand, the oocyte cytoplasm undergoes a complex process of maturation during oogenesis (Conti and Franciosi, 2018). Although the functional significance of the oocyte cytoplasm maturation is not completely known, it is necessary for the acquisition of the embryo developmental competence. Often the cytoplasm of human oocytes display morphological anomalies (granularity, elongated shape, among others) (Coticchio et al., 2004) and whereas some authors demonstrated that such dysmorphisms have a negative effect on the embryo developmental competence (Serhal et al., 1997), others questioned these findings (Balaban et al., 1998). Molecular data should be obtained to clarify this

controversy and maybe relate these morphological anomalies to aberrant oocyte cytoplasmic maturation.

When we refer to the spermatozoon defects aneuploidies are rare (1 – 4%) but DNA fragmentation is relatively common (in an ejaculate, ≈20% of the cells) (Kishi et al., 2015). DNA fragmentation can refer to either single or double DNA strand damage, or both. When a sperm sample has high levels of DNA fragmentation, it is associated with recurrent pregnancy loss (Carrell et al., 2003; Ribas-Maynou et al., 2012). Other components that the spermatozoon provides to the oocyte, and were molecularly characterized to affect embryo early development, are sperm-borne oocyte activating factors such as PLCζ (Hachem et al., 2017). But, during fertilization the spermatozoon also provides another component that is essential for the development of a new and healthy organism, the centrosome. Therefore, can the sperm centrosome be used as a new functional prognosis tool? Is the centrosome necessary to support human embryo early development? These are few questions that have been discussed in the literature, but no conclusive answers exist yet, and in my opinion, it is mainly due to the lack of methods to address them.

II. The human sperm basal body contributes a complex matrix of proteins important for proper preimplantation development of the oocyte upon fertilization:

Some species degenerate their sperm basal body but others do not; some need the centrosome from the zygote whereas others can develop until the blastocyst stage without them. So, how is the centrosome inherited in humans, and how important is the centrosome to support human embryo early development? In the literature, many authors suggest that the human sperm basal body is partially degenerated and "PCM-naked", but its contribution in human early development has not been directly tested. Here, we used a combination of tools, which includes descriptive and functional analyses to elucidate how the human sperm basal body is converted into a functional centrosome in the fertilized oocyte.

A. Sperm tail proteomics as an approach to identify sperm centrosomal proteins:

Serial sections of electron microscopy in the human sperm basal body showed that some microtubule-triplets are absent in the distal centriole (mother centriole) (Manandhar et al., 2000). Due to this structural particularity, it was hypothesized that the sperm basal body also has a reduced PCM content (centrosome reduction) (Avidor-Reiss et al., 2015; Manandhar et al., 2005). To further test this hypothesis, we analyzed by IF two centrosomal proteins related to centrosome structure (centrin) and centrosome duplication (Cep63), as representative proteins of the centrosome. To our surprise both proteins were found in the sperm basal body and interestingly, centrin localization clearly resembles a centriole when imaged with high-resolution microscopy.

After this first unexpected result we looked for a technique that could provide an overview of the centrosomal protein composition of the spermatozoon. Although the spermatozoon is one of the most specialized cells in the human body, it is not just a simple carrier of half of the genetic material to the oocyte; it also provides proteins, mRNAs and the centrosome. Indeed, when all the proteomic analyses of human sperm were analyzed, more than 6,198 different proteins were identified (Amaral et al., 2014a), demonstrating the complex composition of this cell.

We know from somatic cell studies that the identification of centrosomal proteins by proteomics (and with many other techniques) is difficult because they are present with low abundance (Bauer et al., 2016). But here, we faced an extra challenge; spermatozoa from many species suffer a process of centrosome reduction. It has been proposed that centrosome reduction also occurs in human spermatozoa. Therefore, it is expected that centrosomal proteins are even less abundant. Proteomics could be a useful tool to identify low abundant proteins but only when the sample is sufficiently enriched in centrosomal proteins; if not, other more abundant proteins would mask their detection. In order to simplify as much as possible our sample, we decided to perform cellular fractionation, which allowed us to analyze only sperm tails containing centrosomes. Using this approach, we identified the most complex sperm tail proteome, which covers more than 2,300 proteins. Most of the proteins are cytoskeleton or mitochondrion

related proteins, as expected of a structure whose main function is to provide energy to promote sperm motility.

When we focused on the cytoskeleton cluster we identified 288 MTOC related proteins. We were truly surprised about this finding because our results suggest that the sperm basal body is formed by a complex matrix of proteins and, more interestingly, that these proteins will be included in the fertilized oocyte. We think that we obtained a good representation of the sperm centrosomal proteins because we found proteins related to many centrosome cycle events such as centriole duplication and centriolar length regulation; but also, PCM components with structural roles like pericentrin or nucleating roles like GCPs, as well as motor proteins and kinases. Most of them, when compared with a quantitative somatic centrosome proteome (Bauer et al., 2016) are included in the abundant centrosomal proteins although we could also detect some very low abundant proteins. However, we also missed some components essential for the centrosome function and cycle like PLK4 and PLK1 (Bettencourt-Dias et al., 2004).

Altogether, the combination of proteomics and other techniques such as IF was sufficient to demonstrate that although the sperm basal body is microtubule-degenerated, it contains more centrosomal proteins than expected, and the distal centriole has the capacity to recruit them.

B. A proposed mechanism for human sperm basal body biparental inheritance:

The identification of 289 different centrosomal proteins in the human spermatozoa, the capacity of some of them to localize to the "degenerated" centriole, and the fact that some of these centrosomal proteins are also present in the oocyte opens a completely new view about how the human sperm basal body is converted into a fully functional centrosome in the fertilized oocyte.

As explained previously, several hypotheses exist around this topic (Introduction – IV.C). Nevertheless, certain aspects of our results are reminiscent of the proposed model for *Drosophila* sperm basal body inheritance (Khire et al., 2016). *Drosophila* sperm basal body is composed of a giant centriole and a PCL, which is an atypical centriole. This PCL is remodeled during spermatogenesis and is only formed by an

electrodense material in mature spermatozoa. Despite missing microtubules, this centriole-like structure is able to recruit centrosomal proteins. Its PCM composition (containing proteins such as Poc1 and Asterless) at the time of fertilization is essential for the recruitment of other oocyte centrosomal proteins and therefore, to ensure the correct basal body to centrosome transition. Our results point in a similar direction, but with some variations. The distal centriole has been described to be "microtubule-degenerated" but it is enriched in PCM proteins, suggesting that "centrosome reduction" is less severe in the human species. It seems plausible that the human sperm basal body is indeed a functional centrosome, and that its centrosomal proteins serve as a platform to recruit more PCM proteins in the oocyte, as it happens in *Drosophila*. Therefore, we propose that the sperm basal body is remodeled rather than degenerated, because although the distal centriole has a particular microtubule structure, it retains many PCM proteins.

This model also opens other questions related to the basic biology of the centrosome cycle. If the centrosome microtubule structure is not maintained, how does duplication occur? How is the mechanism of cartwheel formation? For the first question, the centriole walls serve as a platform to initiate centriole duplication. How does the centrosome duplication occur if the centriolar microtubules are so remodeled? Does it follow a mechanism of *de novo* centrosome formation? Regarding the second question, it has been proposed that the cartwheel can be formed either directly at the centrosome surface or it is assembled first in the centriolar lumen to then be placed at the centriole surface (Fong et al., 2014; Guichard et al., 2017). In the case of the sperm basal body it seems more feasible that the cartwheel structure assembles directly on the centriole wall without the need of a full-length centriole.

C. Functional assays to elucidate the importance of the human sperm basal body in supporting human embryo early development:

Proteomic studies are useful to identify new components, but it is necessary to supplement these studies with functional analysis to understand the magnitude of the results. To do that, we set up a challenging method in which sperm tails microsurgically separated from the DNA containing heads were injected into an oocyte that was then parthenogenetically activated.

Spanish law does not allow the fertilization of oocytes to create human embryos for research purposes. However, to study the first embryonic events we can take advantage of the oocyte parthenogenetic development. Parthenogenesis is defined as the formation of a pseudo-embryo without the contribution of the paternal genome. In order to induce human oocytes to develop parthenogenetically, only few pulses of calcium are necessary (Paffoni et al., 2007). However, these pseudo-embryos fail to develop easily because they do not have the paternal content. The injection of sperm tails containing the basal body in parthenogenetically activated oocytes offered a unique system to test the role of the sperm basal body in supporting human embryo early development independently of other sperm components such as the paternal genome.

In spite of the high efficiency in separating sperm tails containing the centrosome from the heads, only 20% of these centrosomes became functional in the activated oocyte. This is a low percentage, and the main limitation of our system. However, because the only difference between our control oocytes and the injected oocytes is the tail, whose main organelle is the centrosome, we were able to detect differences. Nevertheless, this 20% forces us to use big sample sizes to detect significant differences, and this is extremely difficult when working with human gametes. In order to reduce sample variability and phenotypes derived from infertility, we decided to only use donor oocytes and spermatozoa. To visualize the sperm centrosome in the parthenotes we used pericentrin staining because we were unable to optimize centriole-specific staining. Therefore, it is important to specify that all pericentrin positive structures identified have to be referred as MTOCs rather than centrosomes, as we can not assume that they are centriole positive. Despite this, we are convinced that pericentrin staining in tails-injected oocytes recognize the sperm derived centrosome because sham injected controls did not show any positive signal before the embryonic genome reactivation.

D. Fertilization inheritance of the sperm basal body increases the likelihood of human embryo compaction:

We observed that when MTOCs are inherited during fertilization they favor parthenotes compaction. But, why are the centrosomes important to support compaction? Compaction is characterized by a high cellular and embryonic reorganization, and in these and other events centrosomes could play an important role. For instance, the

symmetry of the embryo is broken to favor cell internalization (Maitre et al., 2016), a prelude of cell specification. In mice, many different mechanisms have been proposed to mediate cell internalization, but the orientation of the cell division is a key point in most of them. If the orientation of cell division is parallel to the embryo surface, a cell is already internalized. On the other hand, if cell division is perpendicular to the embryo surface, the localization of the spindle is responsible for the distribution of the apical membrane generating different membrane tensions, which in turn drives cell internalization. In the *Drosophila* male germ line, the asymmetric behavior and inheritance of the mother centrosome *versus* the daughter centrosome determines the spindle orientation and daughter cells fate (Yamashita et al., 2007). In humans, a similar mechanism could exist. The mother and daughter centrosomes have different properties. The mother centrosome is a completely mature centrosome with all the appendages and much more enriched in PCM compared with the daughter centrosome. The different mother and daughter centrosome properties could not only define the orientation of the spindle but also the asymmetric distribution of the cellular components between the two daughter cells, mediating symmetry breaking.

E. Genome activation drives *de novo* MTOC formation by a phase-separation mechanism:

An interesting and completely unexpected result was the visualization of MTOCs in control blastocysts, and we wondered how they could be formed. In humans, embryonic genome reactivation starts as early as the 4-cell stage (D+2 of embryo development) but, the maximum protein expression occurs when the embryo is at morula stage (compaction) (Vassena et al., 2011). Control parthenotes stopped at D+3 never showed MTOCs whereas control D+5 parthenotes (blastocyst-like stage) did. The only possible mechanism that could explain *de novo* MTOC formation is the embryonic genome reactivation. Our results suggest that when the genome is active, the production of PCM proteins increases considerably after D+3. PCM proteins may cluster and form independent identities thanks to their phase separation properties. Their ability to accumulate tubulin triggers microtubule nucleation. Therefore, we also must take into account when interpreting the IF data of tail injected oocytes that some of the pericentrin positive MTOCs could be formed *de novo* instead of "real" centrosomes derived from the sperm basal body.

The appearance of MTOCs at the blastocyst stage is kinetically similar to *de novo* centrosome formation in mice, however, in our case we cannot assume that they are centriolar MTOCs, but it suggests that MTOCs activity is important for the development of complex organisms.

F. Model for sperm basal body to functional centrosome transition during development:

Taking into account both descriptive and functional analyses, we propose the following model **(Figure 34)**: the human spermatozoon provides the oocyte with a basal body that is a remodeled centrosome, which has not suffered a dramatic "centrosome reduction" during spermatogenesis. Although the distal centriole is microtubule-remodeled, it still has the capacity to recruit proteins, which suggests that despite being structurally cell-specific, it is still a functional centrosome. On the other hand, the human oocyte does not have centrioles because they are eliminated during oogenesis. However, centrosomal proteins or their RNA are present in the oocyte cytoplasm. One of the most important PCM proteins, pericentrin, is not expressed in the oocyte (we could not detect it by IF) but it is present in the spermatozoon. When the oocyte is fertilized, the sperm centrosome can recruit oocyte-derived centrosomal proteins that are not recruited without the activity of the centrosome as a protein hub. We think that the fact that the sperm centrosome is inherited with a good PCM composition could be important to mediate oocyte proteins recruitment and to perform its microtubule organization functions right after fertilization. This model is reinforced by the fact that no MTOC foci are observed in parthenotes. Since the sperm basal body has the capacity to maintain centrosomal proteins despite its unconventional structure, we think that it could also duplicate. Later, during the embryo early development, the centrosomes provide an advantage during compaction. Probably centrosomes can also play a role in driving cell internalization defining the axis of the cell division. When centrosomes are not present, this process is highly inefficient as 75% of the pseudo-embryos that arrest, do it before compaction. In the case that activated oocytes start compaction, MTOCs can be formed *de novo* due to the increase in centrosomal proteins expression after the reactivation of the embryonic genome. When centrosomal proteins are highly expressed, their structure favors their accumulation assembling clusters that are phase separated

from the cytoplasm favoring tubulin recruitment and microtubule nucleation and organization. However, the number and morphology of these MTOCs are not the correct one, suggesting that sperm basal body inheritance also ensures the correct number of centrosomes per cell. This process of MTOC formation is similar in mice, no centrosomes are inherited during fertilization rather they are formed *de novo* at the blastocyst stage. We cannot answer if MTOC formation is the consequence of embryo compaction or its cause, what we can say is that it should be important to have MTOCs at that stage because they favor embryo compaction. Together our results demonstrate that the inheritance of the sperm basal body and its associated PCM during fertilization is biparental and that having the centrosome provides an advantage to the embryo to compact and to ensure the correct number of MTOCs per cell in the future organism.
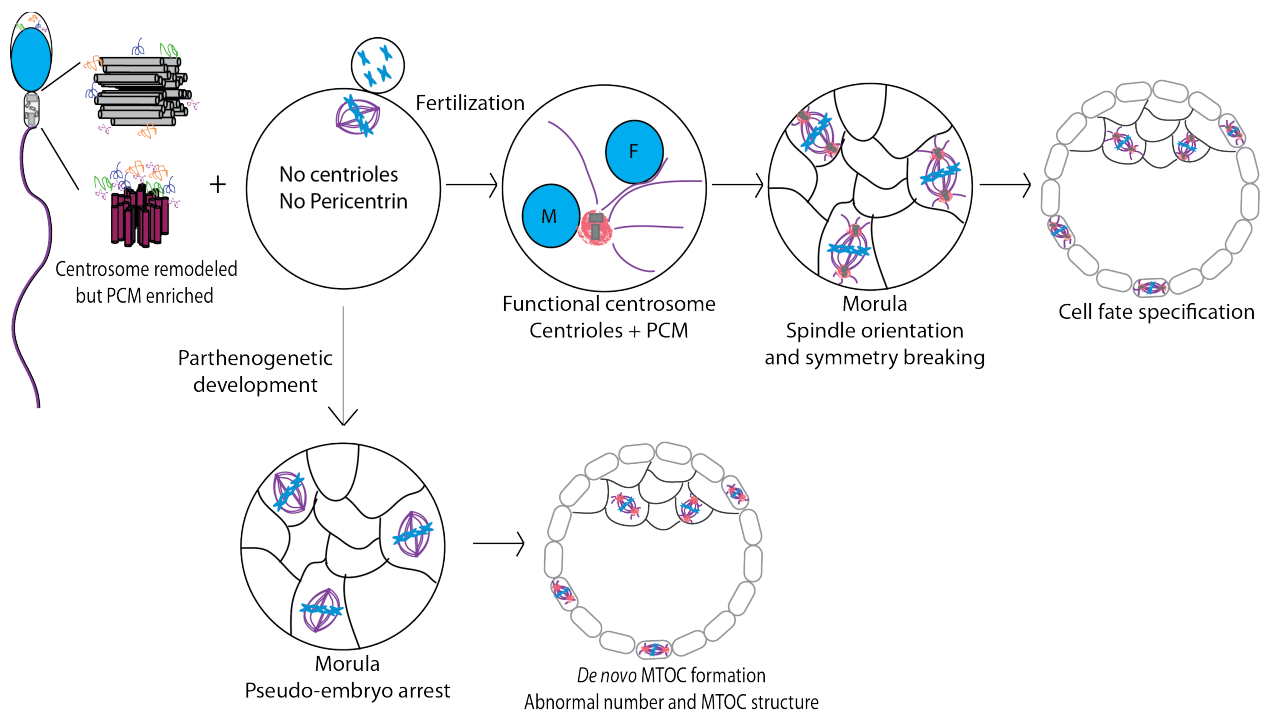
Figure 34: Model for the human sperm basal body to functional centrosome transition during human embryo early development. Our results point out to a model in which the sperm basal body is remodeled rather than a degenerated centrosome because it suffered a modest "centrosome reduction" process. In the fertilized oocyte the centrosome is biparentally inherited as the PCM is provided by both gametes. The presence of centrosomes during compaction favors the embryo to bypass this process. However if the embryos do not have centrosomes they can form MTOCs *de novo* after the embryonic genome is reactivated, although their number and morphology is not optimal, suggesting that not only the inheritance of the centrosomes during fertilization provides an advantage to compact but also ensures the correct number of MTOCs per cell to develop a healthy organism.

III. Development of a new *ex vivo* system to study the processes that the human spermatozoon triggers during fertilization:

One of the main concerns in human *in vitro* reproduction is the selection of functional gametes to improve the chances of success. Nowadays male gamete selection is mainly based on observational analysis, but the low ART success rate suggests that selection by morphology, motility and concentration are not sufficient to select the right spermatozoon. Other observations, either in humans or in animal models, reinforce this previous statement:

- Men with a good percentage of motile spermatozoa (from 54 to 92% of progressive motility) differ in the fecundity rate (from less than 5% to almost 40% of fecundity) (Barratt et al., 1998).

- Rat spermatozoa with abnormal morphology and motility can also arrive to the oocyte (van der Horst et al., 2011).

Therefore, it is important to establish new sperm quality indicators. Some new technologies emerged these last years such as the hyaluronic acid binding capacity, but its correlation with clinical outcomes is still not confirmed (Sakkas et al., 2015). One can think that having a technology that mimics as much as possible the natural sperm selection will increase the chances of having a successful ART, but we know that natural fertilization is also inefficient. What I think we need is a method that reproduces the spermatozoon triggering molecular events during fertilization to evaluate not only the whole sperm sample fitness in the fertilized oocyte, but also to understand at the molecular level the process of fertilization.

A. The use of *Xenopus* egg extract system to study human fertilization:

Relatively little information is known about human fertilization due to ethical and technical reasons, and most of our knowledge comes from animal models. However, species-specific differences in basic reproductive biology make conclusions difficult. With the purpose of gaining knowledge of the events that the human spermatozoon

triggers during fertilization, we set up a quantitative system based on the use of XEE and human spermatozoa.

The XEE system is a powerful tool to study not only microtubule related processes but also other mechanisms such as DNA damage and repair pathways (Hoogenboom et al., 2017). This system has numerous advantages, for example it contains enough cytoplasmic material to complete 12 cell cycle events and it allows the study of proteins translation independently of transcription. Another property that is especially important is that most of the mechanisms studied XEE are conserved in humans. In the laboratory of Dr. Vernos, the XEE system has been widely used to study the different microtubule assembly pathways. We decided to use the XEE as a system to mimic human fertilization and the processes that the human spermatozoon triggers during fertilization.

Our system can reproduce most the processes expected to occur during human fertilization: DNA decondensation and replication, centrosome reconstitution and duplication, and spindle assembly. Because we checked that all these previous processes are at the molecular level correctly performed and resemble what has been described in human fertilization, we think that our system could be a powerful tool to study molecular details that could not be addressed until now. Some of the mechanisms that we would like to address with our system are: identification of new sperm proteins that trigger oocyte activation and their mechanism, the kinetics of protamines' substitution with histones in the sperm DNA, and the temporal mechanism of basal body to centrosome reconstitution.

We further wanted to provide a clinical application to our system. We know that defects in microtubule nucleation and organization are detected in almost 25% of fertilization failures observed in ART cycles (Simerly et al., 1995), and that human embryos that arrest during they early development had more abnormal spindles when compared with human developing embryos (Chatzimeletiou et al., 2005). Therefore, we decided to test if our system could be used as a prognosis tool testing sperm sample capacity to assemble a functional spindle, as a marker of spermatozoa functionality. Indeed we validated our system by correlating spindle capacity with semen parameters. Therefore, our system can be used to analyze the behavior of a sperm sample population in the oocyte to provide a complementary functional test for sperm fitness. The functional

results will be useful in order to decide with is the best ART treatment for each patient. For instance, an example of how our system can be used in setting up a personalized assisted reproduction treatment is to test sperm samples with idiopathic infertility. Testing sperm performance in *Xenopus* oocytes could indicate the use of sperm donation in specific IVF/ICSI cycles.

But the applicability of our system in clinical research is probably beyond a functional sperm prognosis tool before performing IVF/ICSI cycles. We would like to test, for instance, how the environment, the radiations or some habits like smoking or doing sport can affect sperm functionality.

IV. The importance of developing new approaches to answer old questions:

The questions that I have tried to answer in this thesis are not new; what is new is the development of different methodologies to answer them. The hypothesis that the sperm basal body can be the cause of some infertility cases was first postulated in the eighties (Holstein et al., 1986). Still, there is little information on the importance of the sperm centrosome for early embryo development, which prevents the development of functional tools based on microtubule nucleation and organization.

We decided to answer these questions setting up new methodologies. Indeed, an important part of this thesis was destined to optimize the sperm head-tail microsurgical separation as well as our XEE heterologous system. With these methodologies we were able to demonstrate that the sperm basal body is a complex organelle, whose PCM is biparentally inherited during fertilization and its function is important to support embryo compaction. But we were also able to predict the functionally of the human spermatozoa in the oocyte in terms of microtubule nucleation and spindle assembly.

As future directions to gain a better understanding of the role of the centrosome during fertilization and development, I would like to know if centrosomes are involved in the process of embryo symmetry breaking, and by which mechanism. Later in implantation, are the centrosomal microtubules playing a key role in mediating embryo-uterus

invasion? Are semen samples with DNA fragmentation able to reproduce a normal fertilization process in XEE? Are mutations in sperm basal body proteins responsible for altered sperm motility and morphology? These are only some general questions that should be addressed in the next future.
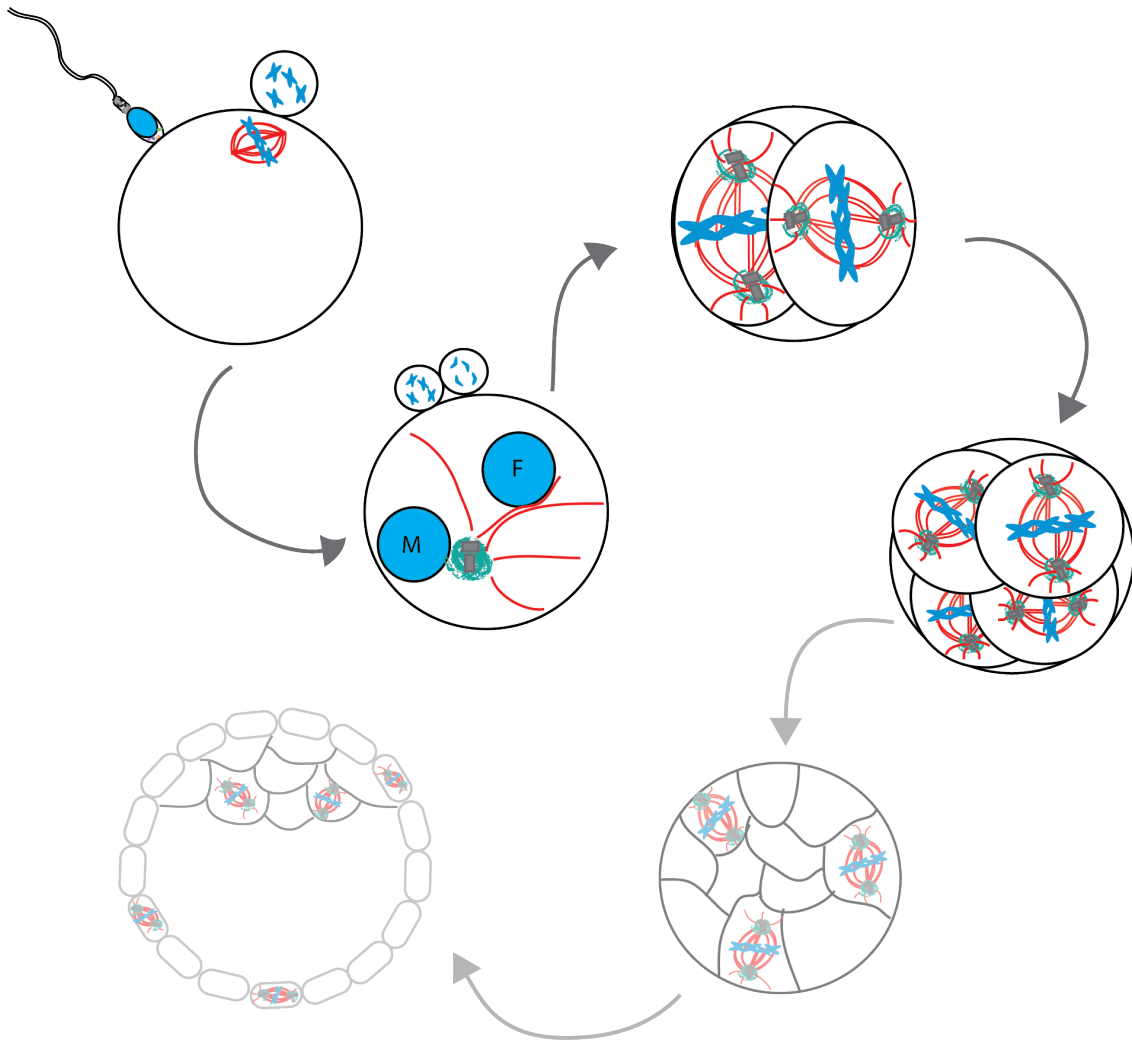
CONCLUSIONS

1) We set up a method based on the use of *Xenopus* egg extract and human spermatozoa to mimic the molecular processes that occur during fertilization.

2) Human sperm samples decondense and replicate their DNA as well as duplicate their basal body in our heterologous system independently of the sperm diagnosis.

3) However, although all the sperm samples can trigger spindle assembly, their positively correlate with some sperm sample diagnosis parameters, a correlation that validates functionally our system.

4) We defined the most extensive human sperm tail proteome, which includes 2,312 proteins. Many of them are functionally related to the cytoskeleton or mitochondria.

5) The sperm basal body contains, at least, 289 centrosomal proteins, therefore, it does not undergo a full process of centrosome reduction.

6) The sperm distal centriole can recruit centrosomal proteins although it has incomplete microtubules triplets.

7) Many of the sperm centrosomal proteins are not found in human oocytes, they are rather stored in an RNA form.

8) We identified a subset of uncharacterized proteins present in sperm tails; 2 of them are new centrosomal proteins.

9) We set up a functional method to incorporate isolated human sperm centrosomes into human oocytes to study how the sperm basal body supports human pre-implantation development.

10) MTOCs seem to be necessary to initiate and complete embryo compaction efficiently.

11) Pseudo-embryos not injected with centrosomes can assemble *de novo* MTOCs after embryonic genome reactivation and during early blastocyst formation.
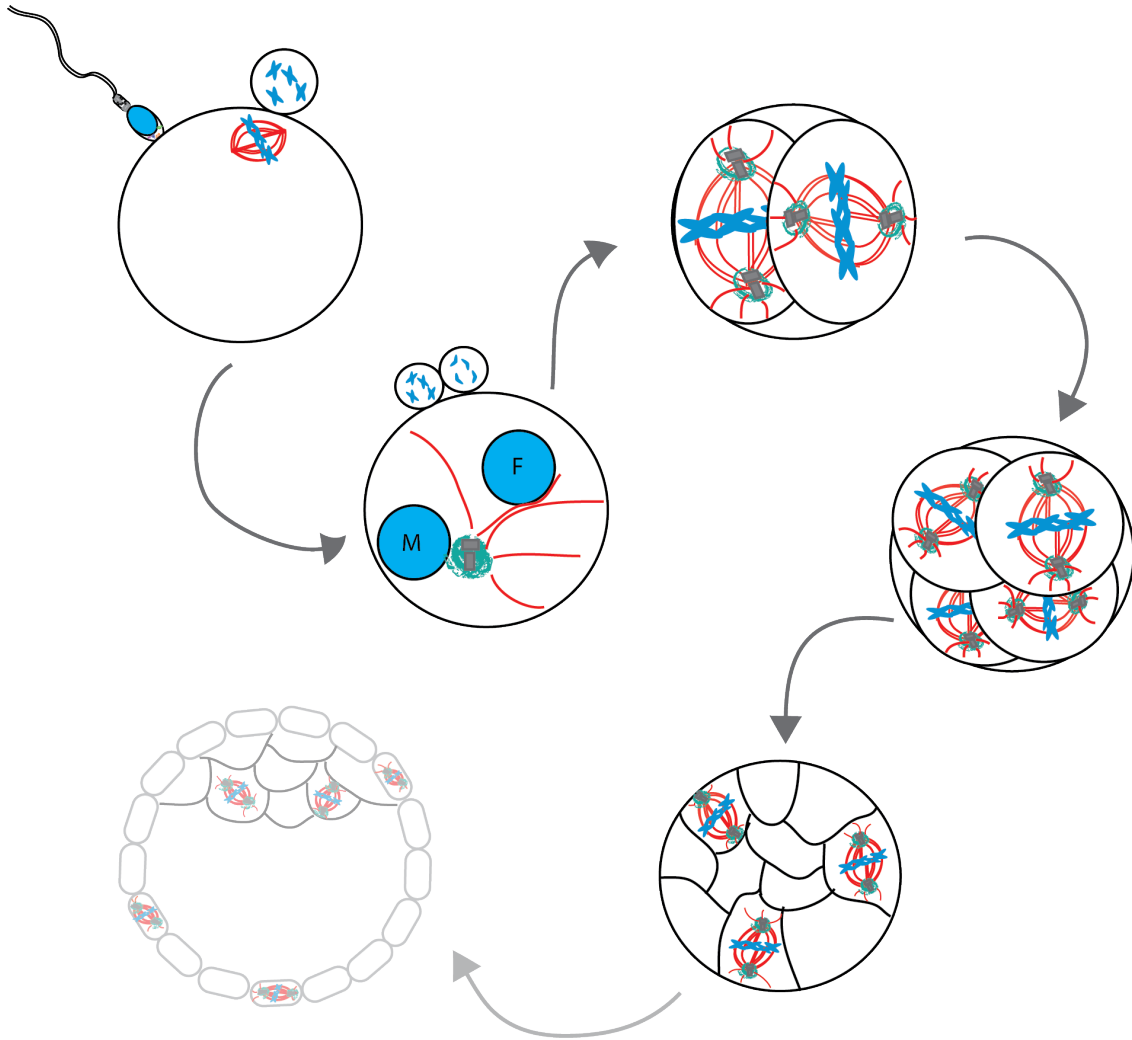
FUTURE PERSPECTIVES

In the discussion, I already mentioned some general questions that scientists are interested in answering. Here, I provide some specific questions that came up during the development of my thesis, and how I would like to address them.

I divided them in the following 4 main topics:

1. ***Xenopus* egg extract system:** our heterologous system could be a powerful tool to study the human sperm basal body reconstitution during fertilization. High-resolution microscopy could be performed to visualize and analyze centriole length, to answer whether sperm distal centriole is regenerated. But we could also assess which are the first proteins recruited to the centriole, for instance.

2. **Centrosome reduction:** how severe and important is the centrosome reduction process in human spermatozoa? We could analyze it by quantitative proteomics of ejaculated *versus* biopsied (less matured) patient sperm tails. If centrosome reduction is important for embryo early development, we could inject microsurgically separated tails from both sample populations in donor oocytes and analyze their microtubule configuration and dynamics.

3. **Tails injection approach:** using this methodology several aspects can be studied. For example, I would like to perform live imaging of tails injected and activated oocytes in which labeled tubulin and centrin are added. This will allow us to analyze how are the microtubule dynamics in human pseudo-zygotes. Is actin also playing a role in pronuclear apposition? Inhibitors of actin could also be included in these experiments. Using time-lapse microscopy, is the cytoplasmic wave at D+0 post-fertilization centrosome dependent? Maybe this cytoplasmic wave can be used as a marker of centrosome functionality.

4. **Mechanism of *de novo* MTOC formation in human parthenotes:** the study of molecular mechanisms in human gametes and embryos is difficult but, recently, a powerful tool was developed: the Trim-Away system. This system allows protein depletion within minutes (Clift et al., 2017). Depleting centrosomal proteins such as PLK4 or pericentrin, could provide some hints on

the mechanism by which MTOCs are formed *de novo*. This analysis could be complemented by a study of the pattern of centrosomal proteins expression.
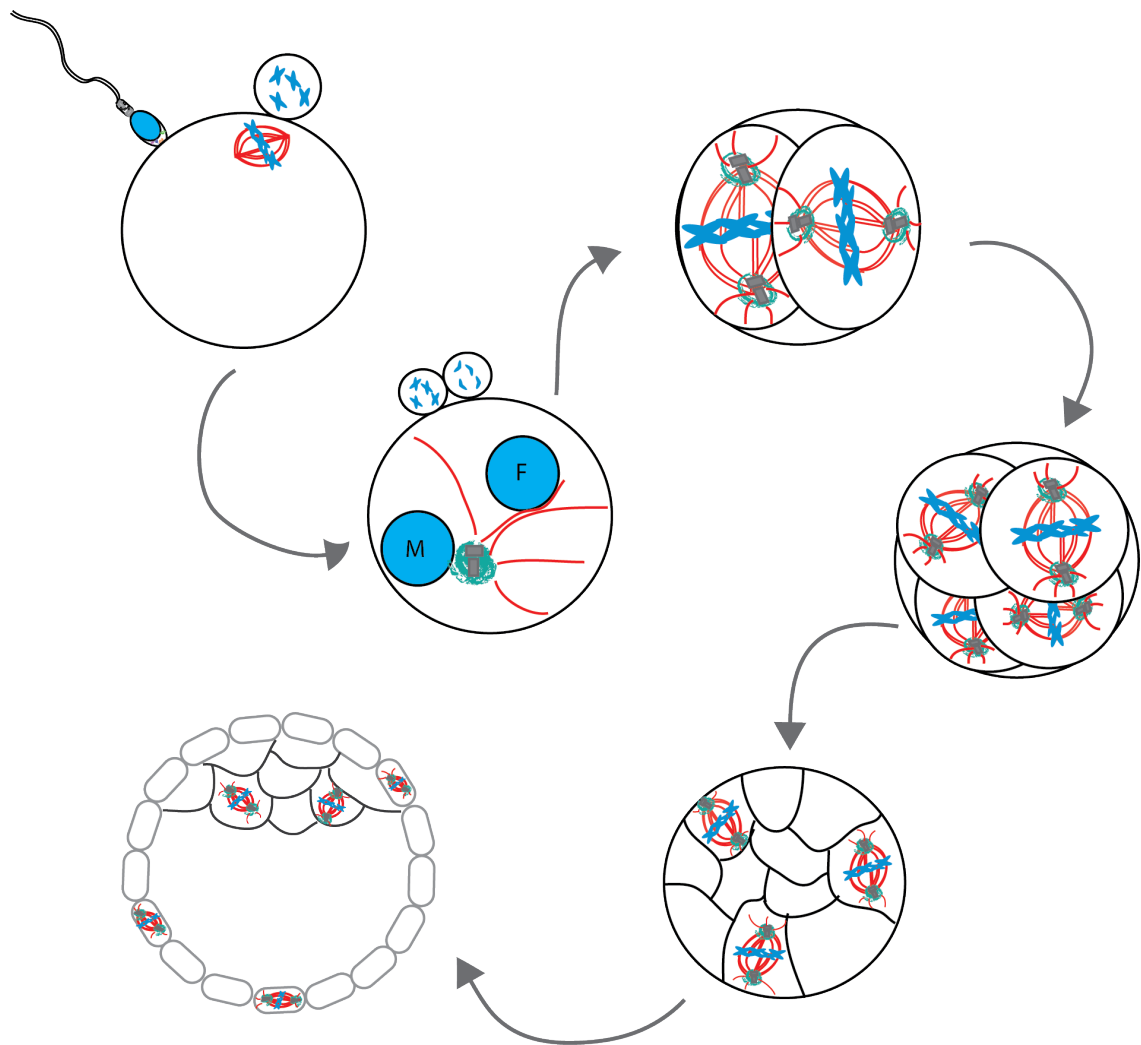
MATERIALS AND METHODS

I. Ethics:

Approval to conduct these studies was obtained from the local Ethical Committee for Clinical Research. All procedures performed were in accordance with the ethical standards of the institutional research committees and with the 1964 Helsinki declaration of the Ethical principles for medical research involving human subjects, as revised in 2013 in Fortaleza (World Medical, 2013). Written informed consents to participate were obtained from all participants prior to their inclusions in the studies.

II. Specific techniques:

A. *Xenopus* egg extract:

CSF-arrested XEE (CSF-EE) were prepared as previously described (Desai et al., 1999). Briefly, to visualize microtubules, $\approx$0.2 mg/ml final concentration of rhodamine-labelled tubulin was added. For cycled spindle assembly, 0.4 mM of calcium and 3,000 sperm nuclei (*Xenopus* or human) were added to the CSF-EE and placed at 20°C for 90 minutes. Then, interphase extracts were cycled back into mitosis by adding the same volume of CSF-EE. After 60 minutes, the assembled spindles were centrifuged through a 40% glycerol cushion onto a 12mm diameter coverslip, and fixed with cold methanol for 10 minutes. For spindles treated with nocodazole (centrosome immunodetection), after the spindles were assembled, 0.5 μM of the compound were added for 20 minutes. For decondensation dynamic analyses, 2 μl of cycling XEE and 4 μl of fixing solution were squashed below an 18x18mm coverslip at the indicated time points. DNA replication was analyzed by adding 40 μM of biotin-dUTPs to the cycling XEE. At each indicated time point, 10 μl of XEE was retrieved and fixed with 4% formaldehyde.

B. Sperm preparation for XEE:

Xenopus spermatozoa were treated with lysolecithin 50 mg/ml for 10 minutes at room temperature. Then, the sample was washed with HSPP buffer containing decreasing amounts of BSA (HSPP 3% BSA and HSPP 0.3% BSA). Human sperm samples were first washed with HSPP buffer. Then, samples were mixed with 1 mM of DTT at room temperature for 10 minutes. Right after these 10 minutes, 0.25% of Triton X-100 final

concentration was added to the samples and they were kept under movement for 30 minutes at room temperature. Like *Xenopus* spermatozoa, human samples were washed with decreasing BSA concentrations. Both samples were finally diluted with HSPP 0.3% BSA, 30% glycerol and their concentration were adjusted at $2x10^7$ cells/ml before freezing.

C. Centrosome complementation assay:

Centrosome complementation assay was performed as previously described (Moritz et al., 1998) with minor modifications. *Xenopus* and human spermatozoa were incubated with 4 M KI (potassium iodide) and then applied onto a 12mm diameter poly-lysine coated glass coverslip. After blocking the samples with 60 μl of HEPES blocking buffer, 60 μl of XEE were incubated for 10 minutes at 30°C. After several washes, 2 mg/ml of pure tubulin were incubated 10 minutes also at 30ºC. Samples were fixed with 1% glutaraldehyde and post-fixed 3 more minutes with cold methanol. Finally, the samples were processed by IF to detect tubulin and centrosomes.

D. Sperm freezing and thawing:

To freeze sperm, specific commercial products were used. 0.5 ml of Sperm Rinse (bicarbonate and HEPES buffered medium with BSA; Vitrolife) was added to a human sperm pellet (previously centrifuged at 300xg, 5 minutes). To the 0.5 ml of sperm sample, 177 μl of Sperm Cryoprotect (contains ingredients to reduce intracellular water and cryoprotectants; Nidacon) were added drop by drop. The mix was incubated 1h at 4°C and then 30 minutes at nitrogen vapors.

To thaw sperm samples, straws were incubated at 37°C for 5 minutes. To remove the sperm cyroprotectant, the sample was centrifuged for 5 minutes at 300xg.

E. Sperm swim-up:

Freshly ejaculated sperm samples were liquated and washed by diluting the samples with the same volume of Sperm Rinse. The diluted samples were pelleted at 372xg, 5 minutes at room temperature. After the elimination of the supernatants, 0.1 ml of Sperm Rinse was carefully loaded on the top of the pellets. The tubes were oriented at 45° for 10 minutes. During this time, the motile spermatozoa swam to the Sperm Rinse fraction.

Finally, the Sperm Rinse fractions were carefully taken avoiding the aspiration of the pellet.

F. Proteomics:

Two different methods were used to analyze spermatozoa centrosomal composition. Only normozoospermic samples with >50% of A+B motility were used. The first approach was based on a previously published protocol (Firat-Karalar et al., 2014b) but with some changes. Frozen samples were thawed and washed two times with PBS and checked under the microscope for any defects caused by the freezing and/or thawing cycles (if any defect was detected, they were discarded). The total amount of cells used at each experiment was of ≈60 millions. Washed samples were pelleted at 850xg, 10 minutes, and resuspended with 350 μl of PBS. Then, samples were sonicated 5 times at 70% output for 15 seconds with 30 seconds intervals (Bioruptor). 1 μl of each sample was taken to check the sonication efficiency under a bright-field microscope. Sperm tails were separated from the heads through a 30% sucrose cushion (centrifugation at 200xg for 10 minutes at 4°C). 1 μl of the tails fraction was taken and squashed in an 18x18 mm coverslip to check its purity. Tails were diluted with the same volume of Buffer 1 (NP40, ß-mercaptoethanol, DTT. See exact composition at the buffers table) and incubated 1h at 4°C under movement. After this incubation, the sample was centrifuged at maximum velocity for 10 minutes at 4°C. The pellet and the supernatant were separated in two different tubes to be treated differentially. In the supernatant, the proteins solubilized by buffer 1 are found. 125 μl of 100% TCA was added to the supernatant and kept at 4°C for 10 minutes. To pellet all the precipitated proteins, the sample was centrifuged at maximum velocity at 4°C, 5 minutes. The supernatant was removed and the pellet washed twice with cold acetone and dried at 95°C to remove the remnants of acetone. Finally, it was diluted with 6M urea and 200mM of ABC (ammonium bicarbonate) in ddH$_2$O. Exactly the same process was performed for the pellet obtained after Buffer 1 incubation, first resuspending it with 500 μl of Buffer 2 (KSCN, DTT) and then with Buffer 3 (urea). 3 different extractions diluted in urea and ABC were finally obtained and analyzed by mass spectrometry.

For the second approach, sonicated tails were pelleted at 4°C at the maximum velocity and diluted with LB (loading buffer). Samples were run in a 4 – 16% gradient gel and each row cut in 9 different bands that were analyzed by mass spectrometry.

G. Oocyte warming:

Warming oocytes is a much more delicate process than thawing spermatozoa. Three different media (all of them commercial) were needed: TS, DS and WS (Kitazato). TS had to be prewarmed at 37°C at least 1.5h prior to use. DS and WS were used at room temperature. Oocyte straws need to be always submerged in liquid nitrogen. The straw cap was carefully removed and the straw quickly immersed in a dish with 500 μl of TS solution located on the microscope stage. This process needs to be as fast as possible. During this minute, oocytes should be release from the straw to the TS medium. After this minute, oocytes were changed from the TS to the DS medium and kept them in DS for 3 minutes. Finally, oocytes were placed to the WS medium 5 more minutes before incubating them 2h at 37°C, 6% CO_2 atmosphere to let them recover from the warming.

H. Tails injection:

In an ICSI dish of 60mm of diameter, drops of G-MOPS plus (containing each one an oocyte, Vitrolife) surrounded a PVP drop (polyvinylpyrrolidone; Origio) containing the sperm swim-up sample. The plate was filled with oil (ovoil, Vitrolife) to prevent the evaporation of the drops. This plate has to be prepared on the same day, and maintained at 37°C (at least for 15 minutes) to temperate the solutions. Once the plate is at 37°C, the oocytes and the sperm sample can be added and placed on the ICSI microscope (Olympus IX50).

Two different pipettes were needed to perform tails separation and injection into oocytes. The pipette used for the sperm head-tail separation was a PZD (Partial Zona Dissection, Vitrolife) pipette, and the one for tails injection was an ICSI micropipette (Vitrolife). Both pipettes were located in a double needle holder. Then, the PZD pipette was located in the interface between the sperm head and the midpiece. With a sharp but accurate blow the separation of both parts was achieved. To collect these tails it is better to do it immediately because the tails can get attached to the plate surface. To known whether the separated tails had the centrosome but not DNA, tails were collected with the ICSI micropipette and loaded to a glass microscope slide (25 mm x 75 mm) and

fixed with 4% PFA to immunodetect centrosomes and DNA. If the tails were injected into oocytes (ICSI), they were collected with the micropipette and microinjected into an oocyte. In all the cases, only one tail was injected per oocyte. We realized that when the tail was aspirated in the micropipette it was very difficult to visualize it. To be sure that the tail was incorporated into the oocyte, in all the cases, we microinjected more PVP containing the tail that the one we aspirated.

I. Oocyte activation:

Right after the ICSI, oocytes were mixed and washed 4 times with G1-Plus medium (Vitrolife) (higher content of calcium compared with other media) and we let them recover from ICSI during 30 minutes at 37°C, 6% CO_2. Oocyte activation protocol or AOA included 3 incubations with 10 μl of 1 mM ionomycin (calcium ionophore, MP Biomedical) diluted in 990 μl of G1 medium and 3 washes with G1 medium alone. All the plates were covered with oil. After the first 30 minutes of G1 incubation, oocytes were transferred into an ionomycin plate and incubated 10 minutes at 37°C. Then, oocytes were washed 10 times in G1 drops and incubated 30 minutes at 37°C. This protocol was repeated 2 more times. When the protocol was finished, oocytes were transferred in a plate with SAGE medium (continuous medium for embryo development, Origio) to be placed at the Primovision or Embryoscope (Vitrolife). These two equipments maintain the embryo (in our case parthenotes) developmental conditions (37°C, 6% CO_2) but they also take images of each sample every 5 minutes, allowing the morphologic and the kinetic analyses of each sample without moving them out from the incubator.

J. Cell culture:

HeLa cells were grown at 37°C in a 5% CO_2 atmosphere. The culture medium was DMEM 4,5 g/L glucose, supplemented with Ultraglutamine (Lonza), with 10% fetal bovine serum (Invitrogen), 100 μg/ml streptomycin and 100 units/ml penicillin.

K. DNA cloning and transfection:

DNA sequences of the 10 uncharacterized proteins were obtained from the ORFeome service (Centre for Genomic Regulation). These sequences were cloned into a pDEST

vector that contained either CFP at the N-terminus (Kanamycin resistant) or GFP at the C-terminus (Ampicillin resistant).

DNA were transfected with the same volume of X-tremeGENE (Sigma) and 100 μl of Opti-MEM (Thermofisher) using 500ng of DNA per well in a 12 well plate (150,000 cells/well) of HeLa cells already attached to a glass coverslip (18 mm diameter). After 24h of protein expression (at 37°C in a 5% CO_2 atmosphere), cells were collected and washed twice with 1 ml of PBS prior fixation with cold methanol (10 minutes) or 4% PFA (15 minutes). To visualize the centrioles, an immunfluorescence was performed against centrin (centrin antibody-Merck Millipore) and DNA (Hoechst, 1 μg/ml).

III. Common techniques:

A. Immunofluorescence:

In this section, I detail the IF conditions for each experiment. You will notice that, although it is the same technique, it is performed differentially depending on the cell type and the protein I wanted to detect. In most of the cases (if not, it is detailed) the images were acquired on an inverted DMI-6000 Leica wide-field fluorescent microscope, and the images processed using Adobe Photoshop CS5.1.

1. XEE immunofluorescence:

Spindles assembled in XEE were diluted with 500 μl of spindle dilution. The mixed sample was spinned down on a glass coverslip through a 4 ml spindle cushion (4000xg, 20 minutes at room temperature) and fixed 10 minutes with cold methanol. After several PBS washes, DNA was stained with Hoechst, and the slides mounted in Mowiol. Samples were visualized with a 40X objective.

For centrin staining, treated spindles with 0.5 μM of Nocodazole were spinned down as described above. Samples were fixed with cold methanol for 4 minutes and the blocking was carried out for 50 minutes with 5% BSA and 0,1% Triton. To incubate the primary and the secondary antibody, the same blocking solution was used adding centrin (20H5,

Merck Millipore) or Alexa-conjugated antibodies. Samples were visualized with a 63X objective.

To immunodetect centrin in the asters formed by the centrosome complementation assay, samples were first fixed with 1% of glutaraldehyde for 3 minutes and post-fixed 3 more minute with cold methanol. After rehydrating the samples with 2 washes of 10 minutes in TBS, they were incubated with small amounts of sodium borohydride diluted with TBS for 7 minutes, and then extensively washed with TBS. Detection of centrin was carried out as described in the previous paragraph but also adding tubulin antibody (ß-tubulin, Abcam). Samples were visualized with a 63X objective.

In the XEE with dUTPs to study chromatin replication dynamics, every 30 minutes 10 μl of XEE were retrieved and fixed 1 hour at room temperature in 200 μl of XB containing 4% formaldehyde. Right after this hour, the sample was spinned down at 2500xg through a 0.7 M sucrose cushion prepared in XB onto a 12 mm diameter glass coverslip, and post-fixed 4 more minutes with cold ethanol. Samples were rehydrated with several washes in PBS and incubated 1 hour in PBS 1%BSA to block non-specific interactions. Then 50 μl of Streptavidin-Alexa Fluor 488 conjugate antibody (ThermoFisher) and Hoechst were used to detect replicated and total amount of DNA. Samples were visualized with a 40X objective.

2. Sperm immunofluorescence:

Thawed samples were washed twice with PBS and then loaded onto a poly-L-lysine coated glass coverslip (12 mm of diameter – from 50,000 to 100,000 cells). After 30 minutes (sperm cells got attached to the glass), the supernatant was removed and the cells were fixed with either 4% PFA 1 hour, or methanol for 10 minutes, depending on the antibody I used. After several washes with PBS, samples were permeabilized with 0,5% Triton X-100 PBS 15 minutes at room temperature. Samples were loaded with 5% BSA in PBS to block unspecific interactions for 2 hours. The same blocking solution was used to incubate the primary and the secondary antibody for 1 hour and 45 minutes respectively. Samples were visualized with a 63X objective.

3. Oocyte and embryos immunofluorescence:

In a prewarmed plate (37°C) oocytes and embryos were mixed with Tyrode's (Sigma) to remove the zona pellucida. This is a critical step because incubating too long with Tyrode's can affect the sample, however when the zona pellucida was not removed, I could not detect MTOCs by IF. It is very important from this step on to wash all the plates and tips with Tween because oocytes and embryos without zona pellucida are very sticky. When the zona pellucida had disappeared, I performed a quick wash with prewarmed PBS. Quickly after this wash, samples were fixed with prewarmed 4% of PFA, 15 minutes. Once the samples are fixed, we can work at room temperature. Permeabilization was done incubating the samples in PBS 0.2% of Triton X-100 during 15 minutes. After washing the samples once with PBS-T and 3 more times with PBS-TB (20 minutes each), samples were blocked with 5% normal goat serum in PBS-TB (freshly prepared) for 3 hours. All primary antibodies were incubated over-night at 4°C with the blocking solution. The next day, 3 washes of 20 minutes in PBS-TB were done while shacking to eliminate the remaining primary antibody. The secondary antibody was only incubated 1 hour at room temperature in PBS-TB together with 1 μg/ml of Hoechst. Samples were mounted with Vectashield (Vector) and visualized at the Zeiss 780 confocal/multiphoton microscopy at 63X with 80% glycerol.

4. Cell culture:

HeLa transfected cells were collected and washed twice with PBS before fixing 10 minutes with cold methanol or 15 minutes with 4% PFA. Cells were block and permeabilized at the same time with IF medium (0.1% Triton X-100, 2% BSA in PBS 1x) during 30 minutes. The primary and the secondary antibodies diluted in IF medium were placed onto the samples for 50 and 45 minutes, respectively. Finally, the samples were visualized at 63X or with the Leica TCS SP5 upright microscope.

B. SDS-PAGE, coomassie and Western Blot:

Sperm cell extracts were obtained diluting the samples with 1x LB and freezing and boiling them 3 times. Then, samples were run in a SDS-PAGE gel. Protein gels were prepared differently whether they were used to analyze tubulin PTMs or sperm proteins (see buffer composition). Nevertheless, they were run at 120V for 90 minutes. Protein gels were stained using Coomassie solution for 15 minutes and distained over-night. To

transfer proteins, the iBlot dry system (ThermoFisher) was used. PVDF membranes were blocked with TBS 5% milk 1 hour. The primary and secondary antibodies were diluted with 2% milk in TBS and incubated over-night at 4ºC and 1 hour at room temperature, respectively. Blots were developed using Alexa Fluor 680 (Invitrogen) and/or IRdye 800 (Li-cor) labeled antibodies at the Odyssey Infrared imaging system (Li-cor).

C. Quantifications and statistics:

To quantify the spindle assembly of individual human and *Xenopus* sperm samples in XEE, 200 and 100 sperm nuclei were counted, respectively, in 4 independent XEE (total amount of structures: 800 per human sample and 400 per *Xenopus* sample). To compare the spindle assembly capacity of samples with different diagnosis, the t-test in Prism 6 (GraphPad Software, La Jolla, CA) was applied. To correlate spindle assembly values with clinical values, % of bipolar spindles for each human sample was divided by the % of *Xenopus* bipolar spindles obtained in the same XEEs. Semen diagnoses and fertilization rates were described for each sperm patient sample and associated IVF/ICSI cycle. Pearson's R coefficient was calculated to evaluate the lineal association between the previous parameters and bipolar spindle assembly. All statistical analyses were performed using the Statistical Package for the Social Sciences (SPSS, version 22). A Pearson's R coefficient between 0.3 and 0.7 was considered as a moderate correlation. For spindle length measurement, a straight line from spindle pole to pole was manually drawn using the ImageJ software in 40 spindles per sample. A nonparametrical Mann-Whitney test was applied with the Prism 6 program to find significant differences.

Tubulin PTMs distribution along the spermatozoa tail was quantified using the Fiji Program (Schindelin et al., 2012). By drawing a line on top of the sperm tail, the tubulin and tubulin PTM intensity was measured at each 0.1 μm. Then, each 0.1 μm was divided by the total length of the sperm tail, to standardize the tail length to 1. The mathematical equation of lineal regression was used to calculate the new intensity (y) for each new 0.001 relative unit of length (x) (y= $y_1 + (x - x_1)\frac{y_2 - y_1}{x_2 - x_1}$), where (x_1,y_1) and (x_2,y_2) are the known values. To calculate the tubulin PTM/tubulin intensity ratio, the intensity at each 0.001 relative units of lengths of tubulin PTM intensity was divided

by the tubulin intensity. Finally all the 1,000 values were represented using the Prism 6 program.

D. Primo-vision analysis:

To analyze the kinetics of parthenotes development, we measured the time of cell division. At day 3 and 5 post activation we graded the parthenotes as explained in the introduction.

E. Gene Ontology enrichment analysis:

The Gene Ontology analyses were performed using the "Gene Ontology Consortium".
http://geneontology.org/page/go-enrichment-analysis

F. Venn diagrams:

A bioinformatic tool form CSIC was used to generate Venn diagrams.
http://bioinfogp.cnb.csic.es/tools/venny/index.html)

IV. Tools:

ANTIBODIES				
PROTEIN	RAISED IN	IF DILUTION	WB DILUTION	COMPANY
Δ2-tubulin	Rabbit	1:200	1:2000	Merck Millipore AB3203
1D5	Mouse	1:200	1:2000	Synaptic systems 302 011
Acetylated tubulin	Mouse	1:1000	1:10000	Sigma T7451
B3	Mouse	1:200	1:2000	Sigma T9822
Centrin	Rabbit	1:2000	-	Millipore, 20H5
Cep63	Rabbit	1:100	-	Merck Millipore, 06-1292

Glu-tubulin	Rabbit	1:1000	1:500	Merck Millipore AB3201
GT335	Mouse	1:200	1:2000	ENZO life sciences ALX-804-885
MonoGly	Mouse	1:200	1:2000	Merck Millipore MABS277
Pericentrin	Rabbit	1:500	-	Abcam, ab448
PLK4	Rabbit	1:500	-	Dr. Bettencourt gift
PolyE tubulin	Rabbit	1:1000	1:500	Home-made
Protamines	Mouse	1:100	1:100	Novus Biologicals H00005619
Tyr-tubulin	Rat	1:1000	1:2000	Merck Millipore MAB1864
α-tubulin	Mouse	1:1000 sperm and culture cell 1:100 in oocytes and embryos	1:20,000	Sigma, T6199
B-tubulin	Rabbit	1:200 sperm and culture cells 1:100 in oocytes and embryos	1:10,000	Abcam, ab6046
γ-tubulin	Mouse	1:100	1:1000	Sigma, GTU-488

DRUGS				
DRUG	EFFECT	STOCK []	WORKING []	COMPANY
Nocodazole	Mt destabilization	20 mM	0.5 μM	Sigma M1404

BUFFERS	
BUFFER	COMPOSITION
50X Calcium solution	20 mM $CaCl_2$, 500 mM KCl, 5 mM $MgCl_2$ p.H. 7.7
Aster cushion	40% glycerol in BRB80
Aster dilution	30% Glycerol, 0.25% glutaraldehyde, 0.1% Triton X-100 in BRB80
BRB80	80 mM K-pipes, pH 6.8, 1 mM $MgCl_2$, 1 mM EGTA
Coomassie	Coomassie Brillant Blue R250, 10% acetic acid, 50% Methanol
CSF-XB	XB, 2 mM $MgCl_2$, 5 mM EGTA, p.H. 7.7
Dejellying	2% cysteine (in water) p.H 7.8 with NaOH
Distaining	10% methanol, 10% acetic acid
Fixing	11% formaldehyde, 48% glycerol, 1 μg/ml Hoechst in CSF-XB buffer
Hepes block	100 mM KCl, 10 mg/ml BSA, 1 mM β-mercaptoethanol
HSPP	250 mM sucrose, 15 mM Hepes pH 7.4, 0.5 mM spermidine, 0.2 mM spermine and protease inhibitors
Lammeli Buffer	2% w/v SDS, 10% Glycerol, 50 mM Tris-HCl p.H. 6.8, 5% ß-mercaptoethanol
MMR	5 mM Hepes, 1000 mM NaCl, 2 mM KCl, 1 mM $MgCl_2$, 2 mM $CaCl_2$, 0.1 mM EDTA, p.H. 7.8 with NaOH
Mowiol	0.1 M Tris p.H 8.5, 10% Mowiol 4-88, 25% Glycerol
PBS 10X	80.6 mM sodium phosphate, 19.4 mM potassium phosphate, 27 mM KCl and 1.37 M NaCl in 1ml of dH_2O p.H 7,4
PBS-T	PBS, 0.1% Tween20
PBS-TB	PBS, 0.1% Tween20, 2% BSA Fraction V
Proteomics Buffer 1	100 mM Tris HCl p.H. 8, 4 mM EGTA, 4 mM EDTA, 1000 mM NaCl, 2% NP40, 0.2% ß-mercaptoethanol, 2mM DTT, protease inhibitors in dH_2O
Proteomics Buffer 2	50 mM Tris HCl p.H. 8, 600 mM KSCN, 2 mM DTT, protease inhibitors in dH_2O
Proteomics Buffer 3	50 mM Tris HCl p.H. 8, 4 M urea, protease inhibitors in dH_2O

Resolving gel (tub PTMs)	7.5% acrylamide, 5 M Tris-HCl pH 9.8, 0.1% SDS (95% Pure, Sigma L5750), 0.07% ammonium persulfate, 0.1% TEMED in ddH$_2$O
Running Buffer	25 mM Tris base, 200 mM glycine, 0.1% SDS
Running Buffer (tub PTMs)	0.1% SDS (95% Pure, Sigma L5750), 0.025 M Tris-HCl p.H. 8.3, 0.192 M glycine
SDS Protein Loading Buffer	10% glycerol, 3% SDS, 10 mM Tris-HC, pH 6.8, 5 mM DTT, 0.2% Bromophenolblue
Spindle Cushion	40% glycerol in 1x BRB80
Spindle dilution	BRB80 1X, 30% glycerol, 0.25% glutaraldehyde, 0.1% Triton X-100
Stacking gel	4% acrylamide (30% acrylamide BioRad), 125 mM Tris-HCl p.H. 6.8, 0.1% SDS, 0.07% ammonium persulfate, 0.1% TEMED
Stacking gel (tub PTMs)	6% acrylamide (30% acrylamide BioRad), 2.5 M of stacking solution (0.5 M Tris-HCl pH 6.8), 0.1% SDS (95% Pure, Sigma L5750), 0.07% ammonium persulfate, 0.1% TEMED in ddH$_2$O
TDB	1x BRB80, 10% Glycerol, 1 mM GTP
TDB wash	1x BRB80, 10% Glycerol, 1 mM GTP and 10 mg/ml BSA
XB	10 mM Hepes, 100 mM KCl, 0.1 mM CaCl$_2$, 1 mM MgCl$_2$, 50 mM sucrose

IMPLANTATION
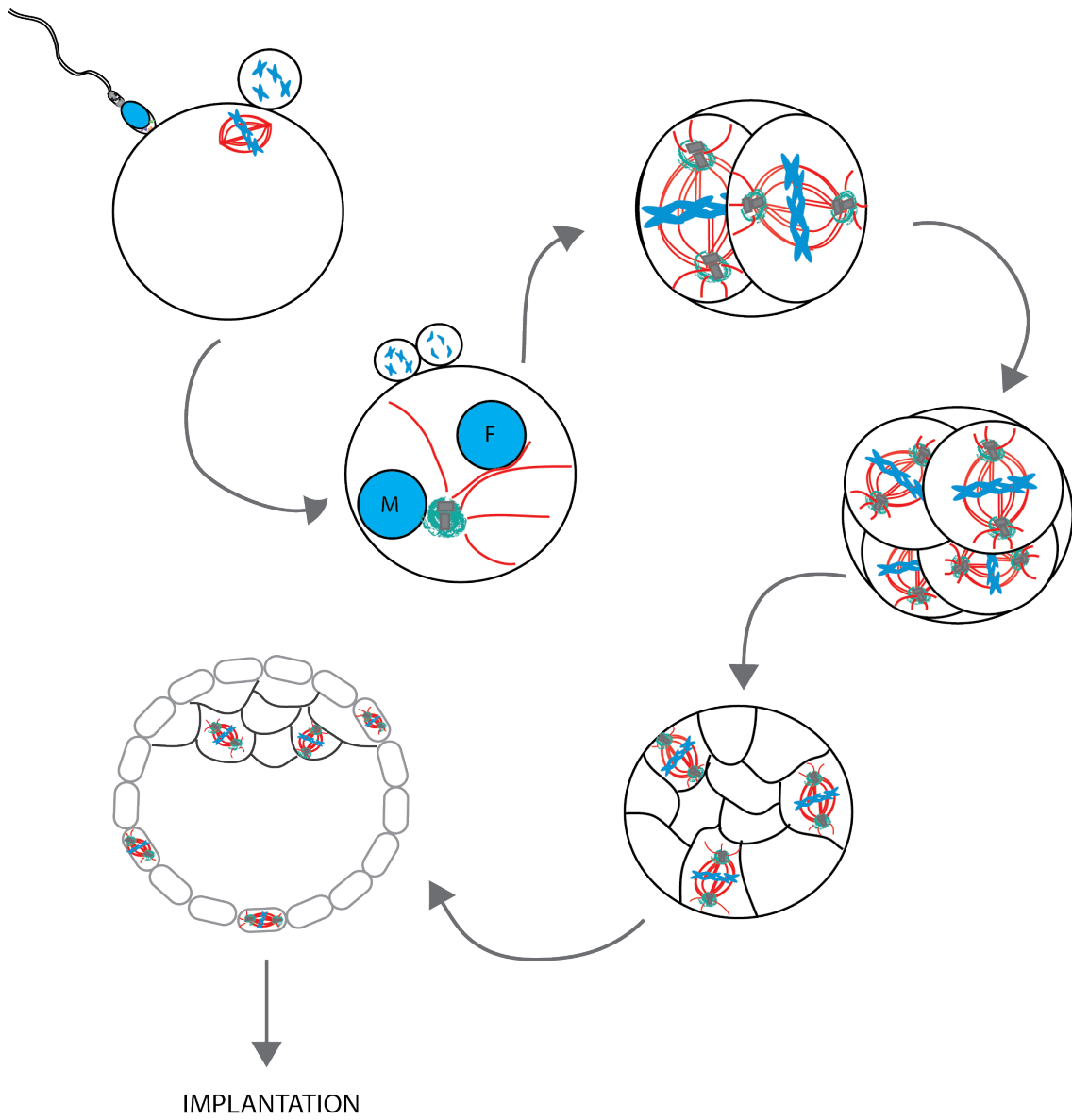
BIBLIOGRAPHY

Ajduk, A., S. Biswas Shivhare, and M. Zernicka-Goetz. 2014. The basal position of nuclei is one pre-requisite for asymmetric cell divisions in the early mouse embryo. *Dev Biol*. 392:133-140.

Ajduk, A., and M. Zernicka-Goetz. 2016. Polarity and cell division orientation in the cleavage embryo: from worm to human. *Mol Hum Reprod*. 22:691-703.

Alpha Scientists in Reproductive, M., and E.S.I.G.o. Embryology. 2011. The Istanbul consensus workshop on embryo assessment: proceedings of an expert meeting. *Hum Reprod*. 26:1270-1283.

Alushin, G.M., G.C. Lander, E.H. Kellogg, R. Zhang, D. Baker, and E. Nogales. 2014. High-resolution microtubule structures reveal the structural transitions in alphabeta-tubulin upon GTP hydrolysis. *Cell*. 157:1117-1129.

Amann, R.P., and S.S. Howards. 1980. Daily spermatozoal production and epididymal spermatozoal reserves of the human male. *J Urol*. 124:211-215.

Amaral, A., J. Castillo, J.M. Estanyol, J.L. Ballesca, J. Ramalho-Santos, and R. Oliva. 2013. Human sperm tail proteome suggests new endogenous metabolic pathways. *Mol Cell Proteomics*. 12:330-342.

Amaral, A., J. Castillo, J. Ramalho-Santos, and R. Oliva. 2014a. The combined human sperm proteome: cellular pathways and implications for basic and clinical science. *Hum Reprod Update*. 20:40-62.

Amaral, A., C. Paiva, C. Attardo Parrinello, J.M. Estanyol, J.L. Ballesca, J. Ramalho-Santos, and R. Oliva. 2014b. Identification of proteins involved in human sperm motility using high-throughput differential proteomics. *J Proteome Res*. 13:5670-5684.

Andersen, J.S., C.J. Wilkinson, T. Mayor, P. Mortensen, E.A. Nigg, and M. Mann. 2003. Proteomic characterization of the human centrosome by protein correlation profiling. *Nature*. 426:570-574.

Arikan, II, B. Demir, G. Bozdag, I. Esinler, L.K. Sokmensuer, and S. Gunalp. 2012. ICSI cycle outcomes in oligozoospermia. *Clin Exp Obstet Gynecol*. 39:280-282.

Arquint, C., A.M. Gabryjonczyk, and E.A. Nigg. 2014. Centrosomes as signalling centres. *Philos Trans R Soc Lond B Biol Sci*. 369.

Austin, C.R. 1951. Observations on the penetration of the sperm in the mammalian egg. *Aust J Sci Res B*. 4:581-596.

Austin, C.R. 1952. The capacitation of the mammalian sperm. *Nature*. 170:326.

Avasthi, P., J.F. Scheel, G. Ying, J.M. Frederick, W. Baehr, and U. Wolfrum. 2013. Germline deletion of Cetn1 causes infertility in male mice. *J Cell Sci*. 126:3204-3213.

Avidor-Reiss, T., A. Khire, E.L. Fishman, and K.H. Jo. 2015. Atypical centrioles during sexual reproduction. *Front Cell Dev Biol*. 3:21.

Azoury, J., K.W. Lee, V. Georget, P. Rassinier, B. Leader, and M.H. Verlhac. 2008. Spindle positioning in mouse oocytes relies on a dynamic meshwork of actin filaments. *Curr Biol*. 18:1514-1519.

Bahe, S., Y.D. Stierhof, C.J. Wilkinson, F. Leiss, and E.A. Nigg. 2005. Rootletin forms centriole-associated filaments and functions in centrosome cohesion. *J Cell Biol*. 171:27-33.

Balaban, B., B. Urman, A. Sertac, C. Alatas, S. Aksoy, and R. Mercan. 1998. Oocyte morphology does not affect fertilization rate, embryo quality and implantation rate after intracytoplasmic sperm injection. *Hum Reprod*. 13:3431-3433.

Balhorn, R., S. Reed, and N. Tanphaichitr. 1988. Aberrant protamine 1/protamine 2 ratios in sperm of infertile human males. *Experientia*. 44:52-55.

Barragan, M., J. Pons, A. Ferrer-Vaquer, D. Cornet-Bartolome, A. Schweitzer, J. Hubbard, H. Auer, A. Rodolosse, and R. Vassena. 2017. The transcriptome of human oocytes is related to age and ovarian reserve. *Mol Hum Reprod*. 23:535-548.

Barratt, C.L., S. Clements, and E. Kessopoulou. 1998. Semen characteristics and fertility tests required for storage of spermatozoa. *Hum Reprod*. 13 Suppl 2:1-7; discussion 8-11.

Barratt, C.L., S. Mansell, C. Beaton, S. Tardif, and S.K. Oxenham. 2011. Diagnostic tools in male infertility-the question of sperm dysfunction. *Asian J Androl*. 13:53-58.

Barrett, S.L., and D.F. Albertini. 2010. Cumulus cell contact during oocyte maturation in mice regulates meiotic spindle positioning and enhances developmental competence. *J Assist Reprod Genet*. 27:29-39.

Basto, R., J. Lau, T. Vinogradova, A. Gardiol, C.G. Woods, A. Khodjakov, and J.W. Raff. 2006. Flies without centrioles. *Cell*. 125:1375-1386.

Bauer, M., F. Cubizolles, A. Schmidt, and E.A. Nigg. 2016. Quantitative analysis of human centrosome architecture by targeted proteomics and fluorescence imaging. *EMBO J*. 35:2152-2166.

Baumann, C., X. Wang, L. Yang, and M.M. Viveiros. 2017. Error-prone meiotic division and subfertility in mice with oocyte-conditional knockdown of pericentrin. *J Cell Sci*. 130:1251-1262.

Benadiva, C.A., J. Nulsen, L. Siano, J. Jennings, H.B. Givargis, and D. Maier. 1999. Intracytoplasmic sperm injection overcomes previous fertilization failure with conventional in vitro fertilization. *Fertil Steril*. 72:1041-1044.

Bettencourt-Dias, M., R. Giet, R. Sinka, A. Mazumdar, W.G. Lock, F. Balloux, P.J. Zafiropoulos, S. Yamaguchi, S. Winter, R.W. Carthew, M. Cooper, D. Jones, L. Frenz, and D.M. Glover. 2004. Genome-wide survey of protein kinases required for cell cycle progression. *Nature*. 432:980-987.

Bettencourt-Dias, M., and D.M. Glover. 2007. Centrosome biogenesis and function: centrosomics brings new understanding. *Nat Rev Mol Cell Biol*. 8:451-463.

Bettencourt-Dias, M., and D.M. Glover. 2009. SnapShot: centriole biogenesis. *Cell*. 136:188-188 e181.

Bettencourt-Dias, M., F. Hildebrandt, D. Pellman, G. Woods, and S.A. Godinho. 2011. Centrosomes and cilia in human disease. *Trends Genet*. 27:307-315.

Bettencourt-Dias, M., A. Rodrigues-Martins, L. Carpenter, M. Riparbelli, L. Lehmann, M.K. Gatt, N. Carmo, F. Balloux, G. Callaini, and D.M. Glover. 2005. SAK/PLK4 is required for centriole duplication and flagella development. *Curr Biol*. 15:2199-2207.

Blachon, S., X. Cai, K.A. Roberts, K. Yang, A. Polyanovsky, A. Church, and T. Avidor-Reiss. 2009. A proximal centriole-like structure is present in Drosophila spermatids and can serve as a model to study centriole duplication. *Genetics*. 182:133-144.

Blachon, S., A. Khire, and T. Avidor-Reiss. 2014. The origin of the second centriole in the zygote of Drosophila melanogaster. *Genetics*. 197:199-205.

Bobinnec, Y., A. Khodjakov, L.M. Mir, C.L. Rieder, B. Edde, and M. Bornens. 1998a. Centriole disassembly in vivo and its effect on centrosome structure and function in vertebrate cells. *J Cell Biol*. 143:1575-1589.

Boke, E., M. Ruer, M. Wuhr, M. Coughlin, R. Lemaitre, S.P. Gygi, S. Alberti, D. Drechsel, A.A. Hyman, and T.J. Mitchison. 2016. Amyloid-like Self-Assembly of a Cellular Compartment. *Cell*. 166:637-650.

Bornens, M., M. Paintrand, J. Berges, M.C. Marty, and E. Karsenti. 1987. Structural and chemical characterization of isolated centrosomes. *Cell Motil Cytoskeleton*. 8:238-249.

Borrego-Pinto, J., K. Somogyi, M.A. Karreman, J. Konig, T. Muller-Reichert, M. Bettencourt-Dias, P. Gonczy, Y. Schwab, and P. Lenart. 2016. Distinct mechanisms eliminate mother and daughter centrioles in meiosis of starfish oocytes. *J Cell Biol*. 212:815-827.

Boryshpolets, S., S. Perez-Cerezales, and M. Eisenbach. 2015. Behavioral mechanism of human sperm in thermotaxis: a role for hyperactivation. *Hum Reprod*. 30:884-892.

Braun, R.E. 2001. Packaging paternal chromosomes with protamine. *Nat Genet*. 28:10-12.

Brevini, T.A., G. Pennarossa, S. Maffei, G. Tettamanti, A. Vanelli, S. Isaac, A. Eden, S. Ledda, M. de Eguileor, and F. Gandolfi. 2012. Centrosome amplification and chromosomal instability in human and animal parthenogenetic cell lines. *Stem Cell Rev*. 8:1076-1087.

Brinsden, P.R., and Bourn Hall Clinic. 1999. A textbook of in vitro fertilization and assisted reproduction : the Bourn Hall guide to clinical and laboratory practice. Parthenon Pub. Group, New York. xii, 564 p. pp.

Brodu, V., A.D. Baffet, P.M. Le Droguen, J. Casanova, and A. Guichet. 2010. A developmentally regulated two-step process generates a noncentrosomal microtubule network in Drosophila tracheal cells. *Dev Cell*. 18:790-801.

Burbank, K.S., and T.J. Mitchison. 2006. Microtubule dynamic instability. *Curr Biol*. 16:R516-517.

Cakmak, H., and H.S. Taylor. 2011. Implantation failure: molecular mechanisms and clinical treatment. *Hum Reprod Update*. 17:242-253.

Calarco-Gillam, P.D., M.C. Siebert, R. Hubble, T. Mitchison, and M. Kirschner. 1983. Centrosome development in early mouse embryos as defined by an autoantibody against pericentriolar material. *Cell*. 35:621-629.

Carabatsos, M.J., C.M. Combelles, S.M. Messinger, and D.F. Albertini. 2000. Sorting and reorganization of centrosomes during oocyte maturation in the mouse. *Microsc Res Tech*. 49:435-444.

Carazo-Salas, R.E., O.J. Gruss, I.W. Mattaj, and E. Karsenti. 2001. Ran-GTP coordinates regulation of microtubule nucleation and dynamics during mitotic-spindle assembly. *Nat Cell Biol*. 3:228-234.

Carazo-Salas, R.E., G. Guarguaglini, O.J. Gruss, A. Segref, E. Karsenti, and I.W. Mattaj. 1999. Generation of GTP-bound Ran by RCC1 is required for chromatin-induced mitotic spindle formation. *Nature*. 400:178-181.

Carrell, D.T., B.R. Emery, and S. Hammoud. 2007. Altered protamine expression and diminished spermatogenesis: what is the link? *Hum Reprod Update*. 13:313-327.

Carrell, D.T., L. Liu, C.M. Peterson, K.P. Jones, H.H. Hatasaka, L. Erickson, and B. Campbell. 2003. Sperm DNA fragmentation is increased in couples with unexplained recurrent pregnancy loss. *Arch Androl*. 49:49-55.

Castilla, J.A., C. Alvarez, J. Aguilar, C. Gonzalez-Varea, M.C. Gonzalvo, and L. Martinez. 2006. Influence of analytical and biological variation on the clinical interpretation of seminal parameters. *Hum Reprod*. 21:847-851.

Cavazza, T., I. Peset, and I. Vernos. 2016. From meiosis to mitosis - the sperm centrosome defines the kinetics of spindle assembly after fertilization in Xenopus. *J Cell Sci*. 129:2538-2547.

Chabin-Brion, K., J. Marceiller, F. Perez, C. Settegrana, A. Drechou, G. Durand, and C. Pous. 2001. The Golgi complex is a microtubule-organizing organelle. *Mol Biol Cell*. 12:2047-2060.

Chaigne, A., C. Campillo, R. Voituriez, N.S. Gov, C. Sykes, M.H. Verlhac, and M.E. Terret. 2016. F-actin mechanics control spindle centring in the mouse zygote. *Nat Commun*. 7:10253.

Chang, M.C. 1951. Fertilizing capacity of spermatozoa deposited into the fallopian tubes. *Nature*. 168:697-698.

Chang, M.C. 1959. Fertilization of rabbit ova in vitro. *Nature*. 184(Suppl 7):466-467.

Chatzimeletiou, K., E.E. Morrison, N. Prapas, Y. Prapas, and A.H. Handyside. 2005. Spindle abnormalities in normally developing and arrested human preimplantation embryos in vitro identified by confocal laser scanning microscopy. *Hum Reprod*. 20:672-682.

Chen, D.T., M. Heymann, S. Fraden, D. Nicastro, and Z. Dogic. 2015. ATP Consumption of Eukaryotic Flagella Measured at a Single-Cell Level. *Biophys J*. 109:2562-2573.

Chen, J.V., R.A. Buchwalter, L.R. Kao, and T.L. Megraw. 2017. A Splice Variant of Centrosomin Converts Mitochondria to Microtubule-Organizing Centers. *Curr Biol*. 27:1928-1940 e1926.

Cho, C., W.D. Willis, E.H. Goulding, H. Jung-Ha, Y.C. Choi, N.B. Hecht, and E.M. Eddy. 2001. Haploinsufficiency of protamine-1 or -2 causes infertility in mice. *Nat Genet*. 28:82-86.

Chretien, D., and R.H. Wade. 1991. New data on the microtubule surface lattice. *Biol Cell*. 71:161-174.

Claw, K.G., and W.J. Swanson. 2012. Evolution of the egg: new findings and challenges. *Annu Rev Genomics Hum Genet*. 13:109-125.

Clift, D., and M. Schuh. 2013. Restarting life: fertilization and the transition from meiosis to mitosis. *Nat Rev Mol Cell Biol*. 14:549-562.

Clift, D., and M. Schuh. 2015. A three-step MTOC fragmentation mechanism facilitates bipolar spindle assembly in mouse oocytes. *Nat Commun*. 6:7217.

Clift, D., W.A. McEwan, L.I. Labzin, V. Konieczny, B. Mogessie, L.C. James and M. Schuh. 2017. A method for the acute and rapid degradation of endogenous proteins. *Cell*. 171(7):1692-1706.

Combelles, C.M., N.A. Cekleniak, C. Racowsky, and D.F. Albertini. 2002. Assessment of nuclear and cytoplasmic maturation in in-vitro matured human oocytes. *Hum Reprod*. 17:1006-1016.

Conduit, P.T., K. Brunk, J. Dobbelaere, C.I. Dix, E.P. Lucas, and J.W. Raff. 2010. Centrioles regulate centrosome size by controlling the rate of Cnn incorporation into the PCM. *Curr Biol*. 20:2178-2186.

Conduit, P.T., Z. Feng, J.H. Richens, J. Baumbach, A. Wainman, S.D. Bakshi, J. Dobbelaere, S. Johnson, S.M. Lea, and J.W. Raff. 2014. The centrosome-specific phosphorylation of Cnn by Polo/Plk1 drives Cnn scaffold assembly and centrosome maturation. *Dev Cell*. 28:659-669.

Conti, M., and F. Franciosi. 2018. Acquisition of oocyte competence to develop as an embryo: integrated nuclear and cytoplasmic events. *Hum Reprod Update*. 24:245-266.

Cooper, T.G., E. Noonan, S. von Eckardstein, J. Auger, H.W. Baker, H.M. Behre, T.B. Haugen, T. Kruger, C. Wang, M.T. Mbizvo, and K.M. Vogelsong. 2010. World Health Organization reference values for human semen characteristics. *Hum Reprod Update*. 16:231-245.

Cota, R.R., N. Teixido-Travesa, A. Ezquerra, S. Eibes, C. Lacasa, J. Roig, and J. Luders. 2017. MZT1 regulates microtubule nucleation by linking gammaTuRC assembly to adapter-mediated targeting and activation. *J Cell Sci*. 130:406-419.

Coticchio, G., M. Dal Canto, M. Mignini Renzini, M.C. Guglielmo, F. Brambillasca, D. Turchi, P.V. Novara, and R. Fadini. 2015. Oocyte maturation: gamete-somatic cells interactions, meiotic resumption, cytoskeletal dynamics and cytoplasmic reorganization. *Hum Reprod Update*. 21:427-454.

Coticchio, G., M.C. Guglielmo, M. Dal Canto, R. Fadini, M. Mignini Renzini, E. De Ponti, F. Brambillasca, and D.F. Albertini. 2013. Mechanistic foundations of the metaphase II spindle of human oocytes matured in vivo and in vitro. *Hum Reprod*. 28:3271-3282.

Coticchio, G., M. Mignini Renzini, P.V. Novara, M. Lain, E. De Ponti, D. Turchi, R. Fadini, and M. Dal Canto. 2018. Focused time-lapse analysis reveals novel aspects of human fertilization and suggests new parameters of embryo viability. *Hum Reprod*. 33:23-31.

Coticchio, G., E. Sereni, L. Serrao, S. Mazzone, I. Iadarola, and A. Borini. 2004. What criteria for the definition of oocyte quality? *Ann N Y Acad Sci*. 1034:132-144.

Courtois, A., M. Schuh, J. Ellenberg, and T. Hiiragi. 2012. The transition from meiotic to mitotic spindle assembly is gradual during early mammalian development. *J Cell Biol*. 198:357-370.

Crowder, M.E., M. Strzelecka, J.D. Wilbur, M.C. Good, G. von Dassow, and R. Heald. 2015. A comparative analysis of spindle morphometrics across metazoans. *Curr Biol*. 25:1542-1550.

D'Angelo, M.A. 2018. Nuclear pore complexes as hubs for gene regulation. *Nucleus*. 9:142-148.

de Mateo, S., J. Castillo, J.M. Estanyol, J.L. Ballesca, and R. Oliva. 2011. Proteomic characterization of the human sperm nucleus. *Proteomics*. 11:2714-2726.

Delattre, M., S. Leidel, K. Wani, K. Baumer, J. Bamat, H. Schnabel, R. Feichtinger, R. Schnabel, and P. Gonczy. 2004. Centriolar SAS-5 is required for centrosome duplication in C. elegans. *Nat Cell Biol*. 6:656-664.

Desai, A., A. Murray, T.J. Mitchison, and C.E. Walczak. 1999. The use of Xenopus egg extracts to study mitotic spindle assembly and function in vitro. *Methods Cell Biol*. 61:385-412.

Dos Santos, H.G., D. Abia, R. Janowski, G. Mortuza, M.G. Bertero, M. Boutin, N. Guarin, R. Mendez-Giraldez, A. Nunez, J.G. Pedrero, P. Redondo, M. Sanz, S. Speroni, F. Teichert, M. Bruix, J.M. Carazo, C. Gonzalez, J. Reina, J.M. Valpuesta, I. Vernos, J.C. Zabala, G. Montoya, M. Coll, U. Bastolla, and L. Serrano. 2013. Structure and non-structure of centrosomal proteins. *PLoS One*. 8:e62633.

Ebner, T., M. Maurer, O. Shebl, M. Moser, R.B. Mayer, H.C. Duba, and G. Tews. 2012. Planar embryos have poor prognosis in terms of blastocyst formation and implantation. *Reprod Biomed Online*. 25:267-272.

Eichenlaub-Ritter, U., A. Stahl, and J.M. Luciani. 1988. The microtubular cytoskeleton and chromosomes of unfertilized human oocytes aged in vitro. *Hum Genet*. 80:259-264.

Esposito, G., B.S. Jaiswal, F. Xie, M.A. Krajnc-Franken, T.J. Robben, A.M. Strik, C. Kuil, R.L. Philipsen, M. van Duin, M. Conti, and J.A. Gossen. 2004. Mice deficient for soluble adenylyl cyclase are infertile because of a severe sperm-motility defect. *Proc Natl Acad Sci U S A*. 101:2993-2998.

Etienne-Manneville, S. 2004. Actin and microtubules in cell motility: which one is in control? *Traffic*. 5:470-477.

European Society of Human, Embryology, C. Calhaz-Jorge, C. De Geyter, M.S. Kupka, J. de Mouzon, K. Erb, E. Mocanu, T. Motrenko, G. Scaravelli, C. Wyns, and V. Goossens. 2017. Assisted reproductive technology in Europe, 2013: results generated from European registers by ESHRE. *Hum Reprod*. 32:1957-1973.

European Society of Human, Embryology, C. Calhaz-Jorge, C. de Geyter, M.S. Kupka, J. de Mouzon, K. Erb, E. Mocanu, T. Motrenko, G. Scaravelli, C. Wyns, and V. Goossens. 2016. Assisted reproductive technology in Europe, 2012: results generated from European registers by ESHRE. *Hum Reprod*. 31:1638-1652.

Faddy, M.J., M.D. Gosden, and R.G. Gosden. 2018. A demographic projection of the contribution of assisted reproductive technologies to world population growth. *Reprod Biomed Online*. 36:455-458.

Feng, S., Y. Song, M. Shen, S. Xie, W. Li, Y. Lu, Y. Yang, G. Ou, J. Zhou, F. Wang, W. Liu, X. Yan, X. Liang, and T. Zhou. 2017a. Microtubule-binding protein FOR20 promotes microtubule depolymerization and cell migration. *Cell Discov*. 3:17032.

Feng, Z., A. Caballe, A. Wainman, S. Johnson, A.F.M. Haensele, M.A. Cottee, P.T. Conduit, S.M. Lea, and J.W. Raff. 2017b. Structural Basis for Mitotic Centrosome Assembly in Flies. *Cell*. 169:1078-1089 e1013.

Ferramosca, A., S.P. Provenzano, L. Coppola, and V. Zara. 2012. Mitochondrial respiratory efficiency is positively correlated with human sperm motility. *Urology*. 79:809-814.

Ferraretti, A.P., V. Goossens, M. Kupka, S. Bhattacharya, J. de Mouzon, J.A. Castilla, K. Erb, V. Korsak, A. Nyboe Andersen. European Ivf-Monitoring Consortioum, and Embryology. 2013. Assisted reproductive technology in Europe, 2009: results generated from European registers by ESHRE. *Hum Reprod*. 28:2318-2331.

Ferrer-Vaquer, A., M. Barragan, T. Freour, V. Vernaeve, and R. Vassena. 2016. PLCzeta sequence, protein levels, and distribution in human sperm do not correlate with semen characteristics and fertilization rates after ICSI. *J Assist Reprod Genet*. 33:747-756.

Findlay, J.K., M.L. Gear, P.J. Illingworth, S.M. Junk, G. Kay, A.H. Mackerras, A. Pope, H.S. Rothenfluh, and L. Wilton. 2007. Human embryo: a biological definition. *Hum Reprod*. 22:905-911.

Fiorentino, A., M.C. Magli, D. Fortini, E. Feliciani, A.P. Ferraretti, B. Dale, and L. Gianaroli. 1994. Sperm:oocyte ratios in an in vitro fertilization (IVF) program. *J Assist Reprod Genet*. 11:97-103.

Firat-Karalar, E.N., N. Rauniyar, J.R. Yates, 3rd, and T. Stearns. 2014a. Proximity interactions among centrosome components identify regulators of centriole duplication. *Curr Biol*. 24:664-670.

Firat-Karalar, E.N., J. Sante, S. Elliott, and T. Stearns. 2014b. Proteomic analysis of mammalian sperm cells identifies new components of the centrosome. *J Cell Sci*. 127:4128-4133.

Flemming, R. 2013. The invention of infertility in the classical Greek world: medicine, divinity, and gender. *Bull Hist Med*. 87:565-590.

Fong, C.S., M. Kim, T.T. Yang, J.C. Liao, and M.F. Tsou. 2014. SAS-6 assembly templated by the lumen of cartwheel-less centrioles precedes centriole duplication. *Dev Cell*. 30:238-245.

Fu, J., Z. Lipinszki, H. Rangone, M. Min, C. Mykura, J. Chao-Chu, S. Schneider, N.S. Dzhindzhev, M. Gottardo, M.G. Riparbelli, G. Callaini, and D.M. Glover. 2016. Conserved molecular interactions in centriole-to-centrosome conversion. *Nat Cell Biol*. 18:87-99.

Gannon, J.R., B.R. Emery, T.G. Jenkins, and D.T. Carrell. 2014. The sperm epigenome: implications for the embryo. *Adv Exp Med Biol*. 791:53-66.

Garcia-Mayoral, M.F., R. Castano, M.L. Fanarraga, J.C. Zabala, M. Rico, and M. Bruix. 2011. The solution structure of the N-terminal domain of human tubulin binding cofactor C reveals a platform for tubulin interaction. *PLoS One*. 6:e25912.

Gard, D.L., and M.W. Kirschner. 1987. Microtubule assembly in cytoplasmic extracts of Xenopus oocytes and eggs. *J Cell Biol*. 105:2191-2201.

Gardner, D.K., M. Lane, I. Calderon, and J. Leeton. 1996. Environment of the preimplantation human embryo in vivo: metabolite analysis of oviduct and uterine fluids and metabolism of cumulus cells. *Fertil Steril*. 65:349-353.

Garrido, G., and I. Vernos. 2016. Non-centrosomal TPX2-Dependent Regulation of the Aurora A Kinase: Functional Implications for Healthy and Pathological Cell Division. *Front Oncol*. 6:88.

Gervasi, M.G., and P.E. Visconti. 2016. Chang's meaning of capacitation: A molecular perspective. *Mol Reprod Dev*. 83:860-874.

Gibbons, I.R., and A.J. Rowe. 1965. Dynein: A Protein with Adenosine Triphosphatase Activity from Cilia. *Science*. 149:424-426.

Gilbert, S.F., S.R. Singer, M.S. Tyler, and R.N. Kozlowski. 2000. Developmental biology. Sinauer Associates,, Sunderland, Mass. xviii, 749 p. ill. (some col.) 729 cm. + 741 computer optical disc (744 743/744 in.).

Good, M.C., M.D. Vahey, A. Skandarajah, D.A. Fletcher, and R. Heald. 2013. Cytoplasmic volume modulates spindle size during embryogenesis. *Science*. 342:856-860.

Gordon, K., D.B. Brown, and F.H. Ruddle. 1985. In vitro activation of human sperm induced by amphibian egg extract. *Exp Cell Res*. 157:409-418.

Gosden, R.G. 2013. Oocyte development and loss. *Semin Reprod Med*. 31:393-398.

Graser, S., Y.D. Stierhof, and E.A. Nigg. 2007. Cep68 and Cep215 (Cdk5rap2) are required for centrosome cohesion. *J Cell Sci*. 120:4321-4331.

Grimes, S.R., Jr., M.L. Meistrich, R.D. Platz, and L.S. Hnilica. 1977. Nuclear protein transitions in rat testis spermatids. *Exp Cell Res*. 110:31-39.

Gruss, O.J., R.E. Carazo-Salas, C.A. Schatz, G. Guarguaglini, J. Kast, M. Wilm, N. Le Bot, I. Vernos, E. Karsenti, and I.W. Mattaj. 2001. Ran induces spindle assembly by reversing the inhibitory effect of importin alpha on TPX2 activity. *Cell*. 104:83-93.

Gruss, O.J., M. Wittmann, H. Yokoyama, R. Pepperkok, T. Kufer, H. Sillje, E. Karsenti, I.W. Mattaj, and I. Vernos. 2002. Chromosome-induced microtubule assembly mediated by TPX2 is required for spindle formation in HeLa cells. *Nat Cell Biol*. 4:871-879.

Guarguaglini, G., L. Renzi, F. D'Ottavio, B. Di Fiore, M. Casenghi, E. Cundari, and P. Lavia. 2000. Regulated Ran-binding protein 1 activity is required for organization and function of the mitotic spindle in mammalian cells in vivo. *Cell Growth Differ*. 11:455-465.

Gueth-Hallonet, C., C. Antony, J. Aghion, A. Santa-Maria, I. Lajoie-Mazenc, M. Wright, and B. Maro. 1993. gamma-Tubulin is present in acentriolar MTOCs during early mouse development. *J Cell Sci*. 105 (Pt 1):157-166.

Guichard, P., and P. Gonczy. 2016. Basal body structure in Trichonympha. *Cilia*. 5:9.

Guichard, P., V. Hamel, M. Le Guennec, N. Banterle, I. Iacovache, V. Nemcikova, I. Fluckiger, K.N. Goldie, H. Stahlberg, D. Levy, B. Zuber, and P. Gonczy. 2017. Cell-free reconstitution reveals centriole cartwheel assembly mechanisms. *Nat Commun*. 8:14813.

Habedanck, R., Y.D. Stierhof, C.J. Wilkinson, and E.A. Nigg. 2005. The Polo kinase Plk4 functions in centriole duplication. *Nat Cell Biol*. 7:1140-1146.

Hachem, A., J. Godwin, M. Ruas, H.C. Lee, M. Ferrer Buitrago, G. Ardestani, A. Bassett, S. Fox, F. Navarrete, P. de Sutter, B. Heindryckx, R. Fissore, and J. Parrington. 2017. PLCzeta is the physiological trigger of the Ca(2+) oscillations that induce embryogenesis in mammals but conception can occur in its absence. *Development*. 144:2914-2924.

Haimov-Kochman, R., Y. Sciaky-Tamir, and A. Hurwitz. 2005. Reproduction concepts and practices in ancient Egypt mirrored by modern medicine. *Eur J Obstet Gynecol Reprod Biol*. 123:3-8.

Hamdine, O., F.J. Broekmans, and B.C. Fauser. 2014. Ovarian stimulation for IVF: mild approaches. *Methods Mol Biol*. 1154:305-328.

Hannak, E., and R. Heald. 2006. Investigating mitotic spindle assembly and function in vitro using Xenopus laevis egg extracts. *Nat Protoc*. 1:2305-2314.

Hardy, K., A.H. Handyside, and R.M. Winston. 1989. The human blastocyst: cell number, death and allocation during late preimplantation development in vitro. *Development*. 107:597-604.

Hazel, J., K. Krutkramelis, P. Mooney, M. Tomschik, K. Gerow, J. Oakey, and J.C. Gatlin. 2013. Changes in cytoplasmic volume are sufficient to drive spindle scaling. *Science*. 342:853-856.

Heald, R., and A. Khodjakov. 2015. Thirty years of search and capture: The complex simplicity of mitotic spindle assembly. *J Cell Biol*. 211:1103-1111.

Heald, R., R. Tournebize, T. Blank, R. Sandaltzopoulos, P. Becker, A. Hyman, and E. Karsenti. 1996. Self-organization of microtubules into bipolar spindles around artificial chromosomes in Xenopus egg extracts. *Nature*. 382:420-425.

Heald, R., R. Tournebize, A. Habermann, E. Karsenti, and A. Hyman. 1997. Spindle assembly in Xenopus egg extracts: respective roles of centrosomes and microtubule self-organization. *J Cell Biol*. 138:615-628.

Helmke, K.J., and R. Heald. 2014. TPX2 levels modulate meiotic spindle size and architecture in Xenopus egg extracts. *J Cell Biol*. 206:385-393.

Hess, K.C., B.H. Jones, B. Marquez, Y. Chen, T.S. Ord, M. Kamenetsky, C. Miyamoto, J.H. Zippin, G.S. Kopf, S.S. Suarez, L.R. Levin, C.J. Williams, J. Buck, and S.B. Moss. 2005. The "soluble" adenylyl cyclase in sperm mediates multiple signaling events required for fertilization. *Dev Cell*. 9:249-259.

Hewitson, L., C. Simerly, and G. Schatten. 1997. Inheritance defects of the sperm centrosome in humans and its possible role in male infertility. *Int J Androl*. 20 Suppl 3:35-43.

Hilbert, M., A. Noga, D. Frey, V. Hamel, P. Guichard, S.H. Kraatz, M. Pfreundschuh, S. Hosner, I. Fluckiger, R. Jaussi, M.M. Wieser, K.M. Thieltges, X. Deupi, D.J. Muller, R.A. Kammerer, P. Gonczy, M. Hirono, and M.O. Steinmetz. 2016. SAS-6 engineering reveals interdependence between cartwheel and microtubules in determining centriole architecture. *Nat Cell Biol*. 18:393-403.

Hinduja, I., N.B. Baliga, and K. Zaveri. 2010. Correlation of human sperm centrosomal proteins with fertility. *J Hum Reprod Sci*. 3:95-101.

Hiramoto, Y. 1962. Microinjection of the live spermatozoa into sea urchin eggs. *Exp Cell Res*. 27:416-426.

Holstein, A.F., W.B. Schill, and H. Breucker. 1986. Dissociated centriole development as a cause of spermatid malformation in man. *J Reprod Fertil*. 78:719-725.

Holubcova, Z., M. Blayney, K. Elder, and M. Schuh. 2015. Human oocytes. Error-prone chromosome-mediated spindle assembly favors chromosome segregation defects in human oocytes. *Science*. 348:1143-1147.

Holubcova, Z., G. Howard, and M. Schuh. 2013. Vesicles modulate an actin network for asymmetric spindle positioning. *Nat Cell Biol*. 15:937-947.

Hoogenboom, W.S., D. Klein Douwel, and P. Knipscheer. 2017. Xenopus egg extract: A powerful tool to study genome maintenance mechanisms. *Dev Biol*. 428:300-309.

Horio, T., and H. Hotani. 1986. Visualization of the dynamic instability of individual microtubules by dark-field microscopy. *Nature*. 321:605-607.

Howe, K., and G. FitzHarris. 2013. A non-canonical mode of microtubule organization operates throughout pre-implantation development in mouse. *Cell Cycle*. 12:1616-1624.

Hud, N.V., M.J. Allen, K.H. Downing, J. Lee, and R. Balhorn. 1993. Identification of the elemental packing unit of DNA in mammalian sperm cells by atomic force microscopy. *Biochem Biophys Res Commun*. 193:1347-1354.

Hudson, J.W., A. Kozarova, P. Cheung, J.C. Macmillan, C.J. Swallow, J.C. Cross, and J.W. Dennis. 2001. Late mitotic failure in mice lacking Sak, a polo-like kinase. *Curr Biol*. 11:441-446.

Inhorn, M.C., and P. Patrizio. 2015. Infertility around the globe: new thinking on gender, reproductive technologies and global movements in the 21st century. *Hum Reprod Update*. 21:411-426.

Inoue, N., M. Ikawa, A. Isotani, and M. Okabe. 2005. The immunoglobulin superfamily protein Izumo is required for sperm to fuse with eggs. *Nature*. 434:234-238.

Izquierdo, D., W.J. Wang, K. Uryu, and M.F. Tsou. 2014. Stabilization of cartwheel-less centrioles for duplication requires CEP295-mediated centriole-to-centrosome conversion. *Cell Rep*. 8:957-965.

Jedrusik, A., D.E. Parfitt, G. Guo, M. Skamagki, J.B. Grabarek, M.H. Johnson, P. Robson, and M. Zernicka-Goetz. 2008. Role of Cdx2 and cell polarity in cell allocation and specification of trophectoderm and inner cell mass in the mouse embryo. *Genes Dev*. 22:2692-2706.

Jin, H.X., S.J. Dai, W.Y. Song, G.D. Yao, S.L. Shi, and Y.P. Sun. 2015. Embryo developmental potential of microsurgically corrected human three-pronuclear zygotes. *Syst Biol Reprod Med*. 61:96-102.

Joergensen, M.W., I. Agerholm, J. Hindkjaer, L. Bolund, L. Sunde, H.J. Ingerslev, and K. Kirkegaard. 2014. Altered cleavage patterns in human tripronuclear embryos and their association to fertilization method: a time-lapse study. *J Assist Reprod Genet*. 31:435-442.

Johnson, G.D., C. Lalancette, A.K. Linnemann, F. Leduc, G. Boissonneault, and S.A. Krawetz. 2011. The sperm nucleus: chromatin, RNA, and the nuclear matrix. *Reproduction*. 141:21-36.

Joseph, J. 2006. Ran at a glance. *J Cell Sci*. 119:3481-3484.

Kai, Y., K. Iwata, Y. Iba, and Y. Mio. 2015. Diagnosis of abnormal human fertilization status based on pronuclear origin and/or centrosome number. *J Assist Reprod Genet*. 32:1589-1595.

Kaji, K., S. Oda, T. Shikano, T. Ohnuki, Y. Uematsu, J. Sakagami, N. Tada, S. Miyazaki, and A. Kudo. 2000. The gamete fusion process is defective in eggs of Cd9-deficient mice. *Nat Genet*. 24:279-282.

Kalab, P., A. Pralle, E.Y. Isacoff, R. Heald, and K. Weis. 2006. Analysis of a RanGTP-regulated gradient in mitotic somatic cells. *Nature*. 440:697-701.

Kalab, P., R.T. Pu, and M. Dasso. 1999. The ran GTPase regulates mitotic spindle assembly. *Curr Biol*. 9:481-484.

Kamel, R.M. 2013. Assisted reproductive technology after the birth of louise brown. *J Reprod Infertil*. 14:96-109.

Karsenti, E., J. Newport, R. Hubble, and M. Kirschner. 1984a. Interconversion of metaphase and interphase microtubule arrays, as studied by the injection of centrosomes and nuclei into Xenopus eggs. *J Cell Biol*. 98:1730-1745.

Karsenti, E., J. Newport, and M. Kirschner. 1984b. Respective roles of centrosomes and chromatin in the conversion of microtubule arrays from interphase to metaphase. *J Cell Biol*. 99:47s-54s.

Karsenti, E., and I. Vernos. 2001. The mitotic spindle: a self-made machine. *Science*. 294:543-547.

Khire, A., K.H. Jo, D. Kong, T. Akhshi, S. Blachon, A.R. Cekic, S. Hynek, A. Ha, J. Loncarek, V. Mennella, and T. Avidor-Reiss. 2016. Centriole Remodeling during Spermiogenesis in Drosophila. *Curr Biol*. 26:3183-3189.

Khire, A., A.A. Vizuet, E. Davila, and T. Avidor-Reiss. 2015. Asterless Reduction during Spermiogenesis Is Regulated by Plk4 and Is Essential for Zygote Development in Drosophila. *Curr Biol*. 25:2956-2963.

Khodjakov, A., R.W. Cole, B.R. Oakley, and C.L. Rieder. 2000. Centrosome-independent mitotic spindle formation in vertebrates. *Curr Biol*. 10:59-67.

Khodjakov, A., and C.L. Rieder. 2001. Centrosomes enhance the fidelity of cytokinesis in vertebrates and are required for cell cycle progression. *J Cell Biol*. 153:237-242.

Khodjakov, A., C.L. Rieder, G. Sluder, G. Cassels, O. Sibon, C.L. Wang. 2002. De novo formation of centrosomes in vertebrates cells arrested during S phase. *J Cell Biol*. 158:1171-81.

Kim, M., B.P. O'Rourke, R.K. Soni, P.V. Jallepalli, R.C. Hendrickson, and M.B. Tsou. 2016. Promotion and Suppression of Centriole Duplication Are Catalytically Coupled through PLK4 to Ensure Centriole Homeostasis. *Cell Rep*. 16:1195-1203.

Kim, S., and K. Rhee. 2014. Importance of the CEP215-pericentrin interaction for centrosome maturation during mitosis. *PLoS One*. 9:e87016.

Kim, Y.J., C.W. Park, and S.Y. Ku. 2014. Indications of intrauterine insemination for male and non-male factor infertility. *Semin Reprod Med*. 32:306-312.

Kimura, A., and S. Onami. 2005. Computer simulations and image processing reveal length-dependent pulling force as the primary mechanism for C. elegans male pronuclear migration. *Dev Cell*. 8:765-775.

Kimura, K., and A. Kimura. 2011. Intracellular organelles mediate cytoplasmic pulling force for centrosome centration in the Caenorhabditis elegans early embryo. *Proc Natl Acad Sci U S A*. 108:137-142.

Kirschner, M.W., T. Mitchison. 1986. Microtubule dynamics. *Nature*. 324(6098):621.

Kirkegaard, K., J.J. Hindkjaer, and H.J. Ingerslev. 2013. Effect of oxygen concentration on human embryo development evaluated by time-lapse monitoring. *Fertil Steril*. 99:738-744 e734.

Kirkham, M., T. Muller-Reichert, K. Oegema, S. Grill, and A.A. Hyman. 2003. SAS-4 is a C. elegans centriolar protein that controls centrosome size. *Cell*. 112:575-587.

Kishi, K., H. Ogata, S. Ogata, Y. Mizusawa, E. Okamoto, Y. Matsumoto, S. Kokeguchi, and M. Shiotani. 2015. Frequency of Sperm DNA Fragmentation According to Selection Method: Comparison and Relevance of a Microfluidic Device and a Swim-up Procedure. *J Clin Diagn Res*. 9:QC14-16.

Klitzman, R. 2016. Deciding how many embryos to transfer: ongoing challenges and dilemmas. *Reprod Biomed Soc Online*. 3:1-15.

Ko, M.A., C.O. Rosario, J.W. Hudson, S. Kulkarni, A. Pollett, J.W. Dennis, and C.J. Swallow. 2005. Plk4 haploinsufficiency causes mitotic infidelity and carcinogenesis. *Nat Genet*. 37:883-888.

Kochanski, R.S., and G.G. Borisy. 1990. Mode of centriole duplication and distribution. *J Cell Biol*. 110:1599-1605.

Kollman, J.M., A. Merdes, L. Mourey, and D.A. Agard. 2011. Microtubule nucleation by gamma-tubulin complexes. *Nat Rev Mol Cell Biol*. 12:709-721.

Kollman, J.M., J.K. Polka, A. Zelter, T.N. Davis, and D.A. Agard. 2010. Microtubule nucleating gamma-TuSC assembles structures with 13-fold microtubule-like symmetry. *Nature*. 466:879-882.

Koot, Y.E., and N.S. Macklon. 2013. Embryo implantation: biology, evaluation, and enhancement. *Curr Opin Obstet Gynecol*. 25:274-279.

Korotkevich, E., R. Niwayama, A. Courtois, S. Friese, N. Berger, F. Buchholz, and T. Hiiragi. 2017. The Apical Domain Is Required and Sufficient for the First Lineage Segregation in the Mouse Embryo. *Dev Cell*. 40:235-247 e237.

Kramer, J.A., and S.A. Krawetz. 1996. Nuclear matrix interactions within the sperm genome. *J Biol Chem*. 271:11619-11622.

Krawetz, S.A. 2005. Paternal contribution: new insights and future challenges. *Nat Rev Genet*. 6:633-642.

Kuliev, A., J. Cieslak, and Y. Verlinsky. 2005. Frequency and distribution of chromosome abnormalities in human oocytes. *Cytogenet Genome Res*. 111:193-198.

Kupka, M.S., A.P. Ferraretti, J. de Mouzon, K. Erb, T. D'Hooghe, J.A. Castilla, C. Calhaz-Jorge, C. De Geyter, V. Goossens. European Ivf-Monitoring Consortium, and Embryology. 2014. Assisted reproductive technology in Europe, 2010: results generated from European registers by ESHREdagger. *Hum Reprod*. 29:2099-2113.

Kyogoku, H., and T.S. Kitajima. 2017. Large Cytoplasm Is Linked to the Error-Prone Nature of Oocytes. *Dev Cell*. 41:287-298 e284.

Lane, H.A., and E.A. Nigg. 1996. Antibody microinjection reveals an essential role for human polo-like kinase 1 (Plk1) in the functional maturation of mitotic centrosomes. *J Cell Biol*. 135:1701-1713.

Lawo, S., M. Bashkurov, M. Mullin, M.G. Ferreria, R. Kittler, B. Habermann, A. Tagliaferro, I. Poser, J.R. Hutchins, B. Hegemann, D. Pinchev, F. Buchholz, J.M. Peters, A.A. Hyman, A.C. Gingras, and L. Pelletier. 2009. HAUS, the 8-subunit human Augmin complex, regulates centrosome and spindle integrity. *Curr Biol*. 19:816-826.

Lawo, S., M. Hasegan, G.D. Gupta, and L. Pelletier. 2012. Subdiffraction imaging of centrosomes reveals higher-order organizational features of pericentriolar material. *Nat Cell Biol*. 14:1148-1158.

Le Naour, F., E. Rubinstein, C. Jasmin, M. Prenant, and C. Boucheix. 2000. Severely reduced female fertility in CD9-deficient mice. *Science*. 287:319-321.

Leader, B., H. Lim, M.J. Carabatsos, A. Harrington, J. Ecsedy, D. Pellman, R. Maas, and P. Leder. 2002. Formin-2, polyploidy, hypofertility and positioning of the meiotic spindle in mouse oocytes. *Nat Cell Biol*. 4:921-928.

Leonardo, C.D. O'Malley, and J.B.d.M. Saunders. 1952. Leonardo da Vinci on the human body: the anatomical, physiological, and embryological drawings of Leonardo da Vinci. H. Schuman, New York,. 506 p. pp.

Li, B., Y. Ma, J. Huang, X. Xiao, L. Li, C. Liu, Y. Shi, D. Wang, and X. Wang. 2014. Probing the effect of human normal sperm morphology rate on cycle outcomes and assisted reproductive methods selection. *PLoS One*. 9:e113392.

Li, K., E.Y. Xu, J.K. Cecil, F.R. Turner, T.L. Megraw, and T.C. Kaufman. 1998. Drosophila centrosomin protein is required for male meiosis and assembly of the flagellar axoneme. *J Cell Biol*. 141:455-467.

Li, R., and D.F. Albertini. 2013. The road to maturation: somatic cell interaction and self-organization of the mammalian oocyte. *Nat Rev Mol Cell Biol*. 14:141-152.

Li, Y., and H. Sasaki. 2011. Genomic imprinting in mammals: its life cycle, molecular mechanisms and reprogramming. *Cell Res*. 21:466-473.

Liao, G., T. Nagasaki, and G.G. Gundersen. 1995. Low concentrations of nocodazole interfere with fibroblast locomotion without significantly affecting microtubule level: implications for the role of dynamic microtubules in cell locomotion. *J Cell Sci*. 108 (Pt 11):3473-3483.

Liguori, L., E. de Lamirande, A. Minelli, and C. Gagnon. 2005. Various protein kinases regulate human sperm acrosome reaction and the associated phosphorylation of Tyr residues and of the Thr-Glu-Tyr motif. *Mol Hum Reprod*. 11:211-221.

Lishko, P.V., I.L. Botchkina, and Y. Kirichok. 2011. Progesterone activates the principal Ca2+ channel of human sperm. *Nature*. 471:387-391.

Liu, D.Y., and H.W. Baker. 1992. Morphology of spermatozoa bound to the zona pellucida of human oocytes that failed to fertilize in vitro. *J Reprod Fertil*. 94:71-84.

Liu, L., J. Cai, P. Li, X. Jiang, and J. Ren. 2017. Clinical outcome of cycles with oocyte degeneration after intracytoplasmic sperm injection. *Syst Biol Reprod Med*. 63:113-119.

Locatelli, L., A. Nespoli, and M.A. Riva. 2015. .Letter to the editor: Dante and human reproduction: concept of embryogenesis in the Middle Ages. *Rom J Morphol Embryol*. 56:325-326.

Lohka, M.J., and J.L. Maller. 1988. Induction of metaphase chromosome condensation in human sperm by Xenopus egg extracts. *Exp Cell Res*. 179:303-309.

Loughlin, R., J.D. Wilbur, F.J. McNally, F.J. Nedelec, and R. Heald. 2011. Katanin contributes to interspecies spindle length scaling in Xenopus. *Cell*. 147:1397-1407.

Luders, J., U.K. Patel, and T. Stearns. 2006. GCP-WD is a gamma-tubulin targeting factor required for centrosomal and chromatin-mediated microtubule nucleation. *Nat Cell Biol*. 8:137-147.

Magli, M.C., G.M. Jones, K. Lundin, and E. van den Abbeel. 2012. Atlas of human embryology: from oocytes to preimplantation embryos. Preface. *Hum Reprod*. 27 Suppl 1:i1.

Maiato, H., and E. Logarinho. 2014. Mitotic spindle multipolarity without centrosome amplification. *Nat Cell Biol*. 16:386-394.

Maitre, J.L., H. Turlier, R. Illukkumbura, B. Eismann, R. Niwayama, F. Nedelec, and T. Hiiragi. 2016. Asymmetric division of contractile domains couples cell positioning and fate specification. *Nature*. 536:344-348.

Manandhar, G., and G. Schatten. 2000. Centrosome reduction during Rhesus spermiogenesis: gamma-tubulin, centrin, and centriole degeneration. *Mol Reprod Dev*. 56:502-511.

Manandhar, G., H. Schatten, and P. Sutovsky. 2005. Centrosome reduction during gametogenesis and its significance. *Biol Reprod*. 72:2-13.

Manandhar, G., C. Simerly, J.L. Salisbury, and G. Schatten. 1999. Centriole and centrin degeneration during mouse spermiogenesis. *Cell Motil Cytoskeleton*. 43:137-144.

Manandhar, G., C. Simerly, and G. Schatten. 2000. Highly degenerated distal centrioles in rhesus and human spermatozoa. *Hum Reprod*. 15:256-263.

Manandhar, G., P. Sutovsky, H.C. Joshi, T. Stearns, and G. Schatten. 1998. Centrosome reduction during mouse spermiogenesis. *Dev Biol*. 203:424-434.

Mandelkow, E.M., E. Mandelkow, and R.A. Milligan. 1991. Microtubule dynamics and microtubule caps: a time-resolved cryo-electron microscopy study. *J Cell Biol*. 114:977-991.

Martinez, M., A. Obradors, V. Vernaeve, J. Santalo, and R. Vassena. 2016. Oocyte vitrification does not affect early developmental timings after intracytoplasmic sperm injection for women younger than 30 years old. *Mol Reprod Dev*. 83:624-629.

Mascarenhas, M.N., S.R. Flaxman, T. Boerma, S. Vanderpoel, and G.A. Stevens. 2012. National, regional, and global trends in infertility prevalence since 1990: a systematic analysis of 277 health surveys. *PLoS Med*. 9:e1001356.

Matorras, R., K. Rubio, M. Iglesias, I. Vara, and A. Exposito. 2018. Risk of pelvic inflammatory disease after intrauterine insemination: a systematic review. *Reprod Biomed Online*. 36:164-171.

McIntosh, J.R., M.K. Morphew, P.M. Grissom, S.P. Gilbert, and A. Hoenger. 2009. Lattice structure of cytoplasmic microtubules in a cultured Mammalian cell. *J Mol Biol*. 394:177-182.

Meetei, A.R., K.S. Ullas, V. Vasupradha, and M.R. Rao. 2002. Involvement of protein kinase A in the phosphorylation of spermatidal protein TP2 and its effect on DNA condensation. *Biochemistry*. 41:185-195.

Menkveld, R., and T.F. Kruger. 1992. Sperm morphology--predictive value? *Fertil Steril*. 57:942-943.

Mennella, V., B. Keszthelyi, K.L. McDonald, B. Chhun, F. Kan, G.C. Rogers, B. Huang, and D.A. Agard. 2012. Subdiffraction-resolutioin fluorescence microscopy reveals a domian of the centrosome critical for pericentriolar material organization. *Nat Cell Biol*. 14:1159-1168.

Meunier, S., M. Shvedunova, N. Van Nguyen, L. Avila, I. Vernos, and A. Akhtar. 2015. An epigenetic regulator emerges as microtubule minus-end binding and stabilizing factor in mitosis. *Nat Commun*. 6:7889.

Meunier, S., and I. Vernos. 2011. K-fibre minus ends are stabilized by a RanGTP-dependent mechanism essential for functional spindle assembly. *Nat Cell Biol*. 13:1406-1414.

Middendorp, S., T. Kuntziger, Y. Abraham, S. Holmes, N. Bordes, M. Paintrand, A. Paoletti, and M. Bornens. 2000. A role for centrin 3 in centrosome reproduction. *J Cell Biol*. 148:405-416.

Miki, K., and D.E. Clapham. 2013. Rheotaxis guides mammalian sperm. *Curr Biol*. 23:443-452.

Mills, N.C., and A.R. Means. 1977. Nonhistone chromosomal proteins of the developing rat testis. *Biol Reprod*. 17:769-779.

Mitchison, T., and M. Kirschner. 1984. Dynamic instability of microtubule growth. *Nature*. 312:237-242.

Mitchison, T.J. 2014. The engine of microtubule dynamics comes into focus. *Cell*. 157:1008-1010.

Miyado, K., G. Yamada, S. Yamada, H. Hasuwa, Y. Nakamura, F. Ryu, K. Suzuki, K. Kosai, K. Inoue, A. Ogura, M. Okabe, and E. Mekada. 2000. Requirement of CD9 on the egg plasma membrane for fertilization. *Science*. 287:321-324.

Mogessie, B., and M. Schuh. 2017. Actin protects mammalian eggs against chromosome segregation errors. *Science*. 357.

Morbeck, D.E., N.A. Baumann, and D. Oglesbee. 2017. Composition of single-step media used for human embryo culture. *Fertil Steril*. 107:1055-1060 e1051.

Morice, P., P. Josset, C. Chapron, and J.B. Dubuisson. 1995. History of infertility. *Hum Reprod Update*. 1:497-504.

Moritz, M., M.B. Braunfeld, J.W. Sedat, B. Alberts, and D.A. Agard. 1995. Microtubule nucleation by gamma-tubulin-containing rings in the centrosome. *Nature*. 378:638-640.

Moritz, M., Y. Zheng, B.M. Alberts, and K. Oegema. 1998. Recruitment of the gamma-tubulin ring complex to Drosophila salt-stripped centrosome scaffolds. *J Cell Biol*. 142:775-786.

Morris, S.A., R.T. Teo, H. Li, P. Robson, D.M. Glover, and M. Zernicka-Goetz. 2010. Origin and formation of the first two distinct cell types of the inner cell mass in the mouse embryo. *Proc Natl Acad Sci U S A*. 107:6364-6369.

Murray, A.W. 1991. Cell cycle extracts. *Methods Cell Biol*. 36:581-605.

Navara, C.S., C. Simerly, S. Zoran, and G. Schatten. 1995. The sperm centrosome during fertilization in mammals: implications for fertility and reproduction. *Reprod Fertil Dev*. 7:747-754.

Neto, F.T., P.V. Bach, B.B. Najari, P.S. Li, and M. Goldstein. 2016. Spermatogenesis in humans and its affecting factors. *Semin Cell Dev Biol*. 59:10-26.

Niakan, K.K., J. Han, R.A. Pedersen, C. Simon, and R.A. Pera. 2012. Human pre-implantation embryo development. *Development*. 139:829-841.

Nigg, E.A., and A.J. Holland. 2018. Once and only once: mechanisms of centriole duplication and their deregulation in disease. *Nat Rev Mol Cell Biol*. 19:297-312.

Nogales, E., M. Whittaker, R.A. Milligan, and K.H. Downing. 1999. High-resolution model of the microtubule. *Cell*. 96:79-88.

Nogales, E., S.G. Wolf, and K.H. Downing. 1998. Structure of the alpha beta tubulin dimer by electron crystallography. *Nature*. 391:199-203.

Nomikos, M., Y. Yu, K. Elgmati, M. Theodoridou, K. Campbell, V. Vassilakopoulou, C. Zikos, E. Livaniou, N. Amso, G. Nounesis, K. Swann, and F.A. Lai. 2013. Phospholipase Czeta rescues failed oocyte activation in a prototype of male factor infertility. *Fertil Steril*. 99:76-85.

Oegema, K., C. Wiese, O.C. Martin, R.A. Milligan, A. Iwamatsu, T.J. Mitchison, and Y. Zheng. 1999. Characterization of two related Drosophila gamma-tubulin complexes that differ in their ability to nucleate microtubules. *J Cell Biol*. 144:721-733.

Ohba, T., M. Nakamura, H. Nishitani, and T. Nishimoto. 1999. Self-organization of microtubule asters induced in Xenopus egg extracts by GTP-bound Ran. *Science*. 284:1356-1358.

Ohsumi, K., C. Katagiri, and R. Yanagimachi. 1988. Human sperm nuclei can transform into condensed chromosomes in Xenopus egg extracts. *Gamete Res*. 20:1-9.

Okabe, M. 2013. The cell biology of mammalian fertilization. *Development*. 140:4471-4479.

Oliva, R., and G.H. Dixon. 1991. Vertebrate protamine genes and the histone-to-protamine replacement reaction. *Prog Nucleic Acid Res Mol Biol*. 40:25-94.

Ortega, C., G. Verheyen, D. Raick, M. Camus, P. Devroey, and H. Tournaye. 2011. Absolute asthenozoospermia and ICSI: what are the options? *Hum Reprod Update*. 17:684-692.

Pacchierotti, F., I.D. Adler, U. Eichenlaub-Ritter, and J.B. Mailhes. 2007. Gender effects on the incidence of aneuploidy in mammalian germ cells. *Environ Res*. 104:46-69.

Paffoni, A., T.A. Brevini, E. Somigliana, L. Restelli, F. Gandolfi, and G. Ragni. 2007. In vitro development of human oocytes after parthenogenetic activation or intracytoplasmic sperm injection. *Fertil Steril*. 87:77-82.

Palacios, M.J., H.C. Joshi, C. Simerly, and G. Schatten. 1993. Gamma-tubulin reorganization during mouse fertilization and early development. *J Cell Sci*. 104 (Pt 2):383-389.

Palermo, G., H. Joris, M.P. Derde, M. Camus, P. Devroey, and A. Van Steirteghem. 1993. Sperm characteristics and outcome of human assisted fertilization by subzonal insemination and intracytoplasmic sperm injection. *Fertil Steril*. 59:826-835.

Palermo, G., H. Joris, P. Devroey, and A.C. Van Steirteghem. 1992. Pregnancies after intracytoplasmic injection of single spermatozoon into an oocyte. *Lancet*. 340:17-18.

Pang, P.C., P.C. Chiu, C.L. Lee, L.Y. Chang, M. Panico, H.R. Morris, S.M. Haslam, K.H. Khoo, G.F. Clark, W.S. Yeung, and A. Dell. 2011. Human sperm binding is mediated by the sialyl-Lewis(x) oligosaccharide on the zona pellucida. *Science*. 333:1761-1764.

Paoletti, A., M. Moudjou, M. Paintrand, J.L. Salisbury, and M. Bornens. 1996. Most of centrin in animal cells is not centrosome-associated and centrosomal centrin is confined to the distal lumen of centrioles. *J Cell Sci*. 109 (Pt 13):3089-3102.

Payne, C., J.C. St John, J. Ramalho-Santos, and G. Schatten. 2003. LIS1 association with dynactin is required for nuclear motility and genomic union in the fertilized mammalian oocyte. *Cell Motil Cytoskeleton*. 56:245-251.

Paz, J., and J. Luders. 2018. Microtubule-Organizing Centers: Towards a Minimal Parts List. *Trends Cell Biol*. 28:176-187.

Pelletier, L., N. Ozlu, E. Hannak, C. Cowan, B. Habermann, M. Ruer, T. Muller-Reichert, and A.A. Hyman. 2004. The Caenorhabditis elegans centrosomal protein SPD-2 is required for both pericentriolar material recruitment and centriole duplication. *Curr Biol*. 14:863-873.

Piehl, M., U.S. Tulu, P. Wadsworth, and L. Cassimeris. 2004. Centrosome maturation: measurement of microtubule nucleation throughout the cell cycle by using GFP-tagged EB1. *Proc Natl Acad Sci U S A*. 101:1584-1588.

Piel, M., P. Meyer, A. Khodjakov, C.L. Rieder, and M. Bornens. 2000. The respective contributions of the mother and daughter centrioles to centrosome activity and behavior in vertebrate cells. *J Cell Biol*. 149:317-330.

Pimenta-Marques, A., I. Bento, C.A. Lopes, P. Duarte, S.C. Jana, and M. Bettencourt-Dias. 2016. A mechanism for the elimination of the female gamete centrosome in Drosophila melanogaster. *Science*. 353:aaf4866.

Practice Committees of the American Society for Reproductive, M., and T. Society for Assisted Reproductive. 2012. Intracytoplasmic sperm injection (ICSI) for non-male factor infertility: a committee opinion. *Fertil Steril*. 98:1395-1399.

Ravelli, R.B., B. Gigant, P.A. Curmi, I. Jourdain, S. Lachkar, A. Sobel, and M. Knossow. 2004. Insight into tubulin regulation from a complex with colchicine and a stathmin-like domain. *Nature*. 428:198-202.

Rawe, V.Y., S.B. Olmedo, F.N. Nodar, G.D. Doncel, A.A. Acosta, and A.D. Vitullo. 2000. Cytoskeletal organization defects and abortive activation in human oocytes after IVF and ICSI failure. *Mol Hum Reprod*. 6:510-516.

Rawe, V.Y., Y. Terada, S. Nakamura, C.F. Chillik, S.B. Olmedo, and H.E. Chemes. 2002. A pathology of the sperm centriole responsible for defective sperm aster formation, syngamy and cleavage. *Hum Reprod*. 17:2344-2349.

Rawson, B., and Australian National University. 1986. The Family in ancient Rome : new perspectives. Cornell University Press, Ithaca, N.Y. 279 p. pp.

Reck-Peterson, S.L., W.B. Redwine, R.D. Vale, and A.P. Carter. 2018. The cytoplasmic dynein transport machinery and its many cargoes. *Nat Rev Mol Cell Biol*.

Reed, N.A., D. Cai, T.L. Blasius, G.T. Jih, E. Meyhofer, J. Gaertig, and K.J. Verhey. 2006. Microtubule acetylation promotes kinesin-1 binding and transport. *Curr Biol*. 16:2166-2172.

Reinsch, S., and P. Gonczy. 1998. Mechanisms of nuclear positioning. *J Cell Sci*. 111 (Pt 16):2283-2295.

Reinsch, S., and E. Karsenti. 1997. Movement of nuclei along microtubules in Xenopus egg extracts. *Curr Biol*. 7:211-214.

Ren, D., B. Navarro, G. Perez, A.C. Jackson, S. Hsu, Q. Shi, J.L. Tilly, and D.E. Clapham. 2001. A sperm ion channel required for sperm motility and male fertility. *Nature*. 413:603-609.

Ribas-Maynou, J., A. Garcia-Peiro, A. Fernandez-Encinas, M.J. Amengual, E. Prada, P. Cortes, J. Navarro, and J. Benet. 2012. Double stranded sperm DNA breaks, measured by Comet assay, are associated with unexplained recurrent miscarriage in couples without a female factor. *PLoS One*. 7:e44679.

Rusan, N.M., and G.C. Rogers. 2009. Centrosome function: sometimes less is more. *Traffic*. 10:472-481.

Sakkas, D., M. Ramalingam, N. Garrido, and C.L. Barratt. 2015. Sperm selection in natural conception: what can we learn from Mother Nature to improve assisted reproduction outcomes? *Hum Reprod Update*. 21:711-726.

Salisbury, J.L., K.M. Suino, R. Busby, and M. Springett. 2002. Centrin-2 is required for centriole duplication in mammalian cells. *Curr Biol*. 12:1287-1292.

Sanchez, F., and J. Smitz. 2012. Molecular control of oogenesis. *Biochim Biophys Acta*. 1822:1896-1912.

Santi, C.M., P. Martinez-Lopez, J.L. de la Vega-Beltran, A. Butler, A. Alisio, A. Darszon, and L. Salkoff. 2010. The SLO3 sperm-specific potassium channel plays a vital role in male fertility. *FEBS Lett*. 584:1041-1046.

Sathananthan, A.H. 1998. Paternal centrosomal dynamics in early human development and infertility. *J Assist Reprod Genet*. 15:129-139.

Sathananthan, A.H., I. Kola, J. Osborne, A. Trounson, S.C. Ng, A. Bongso, and S.S. Ratnam. 1991. Centrioles in the beginning of human development. *Proc Natl Acad Sci U S A*. 88:4806-4810.

Sathananthan, A.H., S.S. Ratnam, S.C. Ng, J.J. Tarin, L. Gianaroli, and A. Trounson. 1996. The sperm centriole: its inheritance, replication and perpetuation in early human embryos. *Hum Reprod*. 11:345-356.

Sato, M., and K. Sato. 2011. Degradation of paternal mitochondria by fertilization-triggered autophagy in C. elegans embryos. *Science*. 334:1141-1144.

Satouh, Y., N. Inoue, M. Ikawa, and M. Okabe. 2012. Visualization of the moment of mouse sperm-egg fusion and dynamic localization of IZUMO1. *J Cell Sci*. 125:4985-4990.

Satzinger, H. 2008. Theodor and Marcella Boveri: chromosomes and cytoplasm in heredity and development. *Nat Rev Genet*. 9:231-238.

Scheer, U. 2014. Historical roots of centrosome research: discovery of Boveri's microscope slides in Wurzburg. *Philos Trans R Soc Lond B Biol Sci*. 369.

Schindelin, J., I. Arganda-Carreras, E. Frise, V. Kaynig, M. Longair, T. Pietzsch, S. Preibisch, C. Rueden, S. Saalfeld, B. Schmid, J.Y. Tinevez, D.J. White, V. Hartenstein, K. Eliceiri, P. Tomancak, and A. Cardona. 2012. Fiji: an open-source platform for biological-image analysis. *Nat Methods*. 9:676-682.

Schuh, M., and J. Ellenberg. 2007. Self-organization of MTOCs replaces centrosome function during acentrosomal spindle assembly in live mouse oocytes. *Cell*. 130:484-498.

Schuh, M., and J. Ellenberg. 2008. A new model for asymmetric spindle positioning in mouse oocytes. *Curr Biol*. 18:1986-1992.

Serhal, P.F., D.M. Ranieri, A. Kinis, S. Marchant, M. Davies, and I.M. Khadum. 1997. Oocyte morphology predicts outcome of intracytoplasmic sperm injection. *Hum Reprod*. 12:1267-1270.

Simerly, C., G.J. Wu, S. Zoran, T. Ord, R. Rawlins, J. Jones, C. Navara, M. Gerrity, J. Rinehart, Z. Binor, R. Asch, and G. Schatten. 1995. The paternal inheritance of the centrosome, the cell's microtubule-organizing center, in humans, and the implications for infertility. *Nat Med*. 1:47-52.

Simerly, C., S.S. Zoran, C. Payne, T. Dominko, P. Sutovsky, C.S. Navara, J.L. Salisbury, and G. Schatten. 1999. Biparental inheritance of gamma-tubulin during human fertilization: molecular reconstitution of functional zygotic centrosomes in inseminated human oocytes and in cell-free extracts nucleated by human sperm. *Mol Biol Cell*. 10:2955-2969.

Simon, L., K. Murphy, M.B. Shamsi, L. Liu, B. Emery, K.I. Aston, J. Hotaling, and D.T. Carrell. 2014. Paternal influence of sperm DNA integrity on early embryonic development. *Hum Reprod*. 29:2402-2412.

Skamagki, M., K.B. Wicher, A. Jedrusik, S. Ganguly, and M. Zernicka-Goetz. 2013. Asymmetric localization of Cdx2 mRNA during the first cell-fate decision in early mouse development. *Cell Rep*. 3:442-457.

Sonnen, K.F., A.M. Gabryjonczyk, E. Anselm, Y.D. Stierhof, and E.A. Nigg. 2013. Human Cep192 and Cep152 cooperate in Plk4 recruitment and centriole duplication. *J Cell Sci*. 126:3223-3233.

Sorokin, A.V., E.R. Kim, and L.P. Ovchinnikov. 2007. Nucleocytoplasmic transport of proteins. *Biochemistry (Mosc)*. 72:1439-1457.

Stearns, T., and M. Kirschner. 1994. In vitro reconstitution of centrosome assembly and function: the central role of gamma-tubulin. *Cell*. 76:623-637.

Steptoe, P.C., and R.G. Edwards. 1978. Birth after the reimplantation of a human embryo. *Lancet*. 2:366.

Strambio-De-Castillia, C., M. Niepel, and M.P. Rout. 2010. The nuclear pore complex: bridging nuclear transport and gene regulation. *Nat Rev Mol Cell Biol*. 11:490-501.

Suarez, S.S., and M. Wu. 2017. Microfluidic devices for the study of sperm migration. *Mol Hum Reprod*. 23:227-234.

Sullivan, R., and R. Mieusset. 2016. The human epididymis: its function in sperm maturation. *Hum Reprod Update*. 22:574-587.

Sunde, A., D. Brison, J. Dumoulin, J. Harper, K. Lundin, M.C. Magli, E. Van den Abbeel, and A. Veiga. 2016. Time to take human embryo culture seriously. *Hum Reprod*. 31:2174-2182.

Sutovsky, P. 2011. Sperm proteasome and fertilization. *Reproduction*. 142:1-14.

Teixido-Travesa, N., J. Villen, C. Lacasa, M.T. Bertran, M. Archinti, S.P. Gygi, C. Caelles, J. Roig, and J. Luders. 2010. The gammaTuRC revisited: a comparative analysis of interphase and mitotic human gammaTuRC redefines the set of core components and identifies the novel subunit GCP8. *Mol Biol Cell*. 21:3963-3972.

Templado, C., L. Uroz, and A. Estop. 2013. New insights on the origin and relevance of aneuploidy in human spermatozoa. *Mol Hum Reprod*. 19:634-643.

Terada, Y., S. Nakamura, J. Morita, M. Tachibana, Y. Morito, K. Ito, T. Murakami, N. Yaegashi, and K. Okamura. 2004. Use of Mammalian eggs for assessment of human sperm function: molecular and cellular analyses of fertilization by intracytoplasmic sperm injection. *Am J Reprod Immunol*. 51:290-293.

Terada, Y., C.R. Simerly, L. Hewitson, and G. Schatten. 2000. Sperm aster formation and pronuclear decondensation during rabbit fertilization and development of a functional assay for human sperm. *Biol Reprod*. 62:557-563.

Tournier, F., E. Karsenti, and M. Bornens. 1989. Parthenogenesis in Xenopus eggs injected with centrosomes from synchronized human lymphoid cells. *Dev Biol*. 136:321-329.

Tsou, M.F., and T. Stearns. 2006. Mechanism limiting centrosome duplication to once per cell cycle. *Nature*. 442:947-951.

Ugajin, T., Y. Terada, H. Hasegawa, H. Nabeshima, K. Suzuki, and N. Yaegashi. 2010. The shape of the sperm midpiece in intracytoplasmic morphologically selected sperm injection relates sperm centrosomal function. *J Assist Reprod Genet*. 27:75-81.

Vadnais, M.L., W. Cao, H.K. Aghajanian, L. Haig-Ladewig, A.M. Lin, O. Al-Alao, and G.L. Gerton. 2014. Adenine nucleotide metabolism and a role for AMP in modulating flagellar waveforms in mouse sperm. *Biol Reprod*. 90:128.

Vale, R.D., T.S. Reese, and M.P. Sheetz. 1985. Identification of a novel force-generating protein, kinesin, involved in microtubule-based motility. *Cell*. 42:39-50.

Vallee, R.B., J.S. Wall, B.M. Paschal, and H.S. Shpetner. 1988. Microtubule-associated protein 1C from brain is a two-headed cytosolic dynein. *Nature*. 332:561-563.

Van Blerkom, J., P. Davis, and S. Alexander. 2004. Occurrence of maternal and paternal spindles in unfertilized human oocytes: possible relationship to nucleation defects after silent fertilization. *Reprod Biomed Online*. 8:454-459.

van der Horst, G., L. Maree, S.H. Kotze, and M.J. O'Riain. 2011. Sperm structure and motility in the eusocial naked mole-rat, Heterocephalus glaber: a case of degenerative orthogenesis in the absence of sperm competition? *BMC Evol Biol*. 11:351.

Van Voorhis, B.J. 2007. Clinical practice. In vitro fertilization. *N Engl J Med*. 356:379-386.

Vasquez, R.J., D.L. Gard, and L. Cassimeris. 1994. XMAP from Xenopus eggs promotes rapid plus end assembly of microtubules and rapid microtubule polymer turnover. *J Cell Biol*. 127:985-993.

Vassena, R., S. Boue, E. Gonzalez-Roca, B. Aran, H. Auer, A. Veiga, and J.C. Izpisua Belmonte. 2011. Waves of early transcriptional activation and pluripotency program initiation during human preimplantation development. *Development*. 138:3699-3709.

Verde, F., M. Dogterom, E. Stelzer, E. Karsenti, and S. Leibler. 1992. Control of microtubule dynamics and length by cyclin A- and cyclin B-dependent kinases in Xenopus egg extracts. *J Cell Biol*. 118:1097-1108.

Vinot, S., T. Le, S. Ohno, T. Pawson, B. Maro, and S. Louvet-Vallee. 2005. Asymmetric distribution of PAR proteins in the mouse embryo begins at the 8-cell stage during compaction. *Dev Biol*. 282:307-319.

Virant-Klun, I., S. Leicht, C. Hughes, and J. Krijgsveld. 2016. Identification of Maturation-Specific Proteins by Single-Cell Proteomics of Human Oocytes. *Mol Cell Proteomics*. 15:2616-2627.

Visconti, P.E. 2009. Understanding the molecular basis of sperm capacitation through kinase design. *Proc Natl Acad Sci U S A*. 106:667-668.

Visconti, P.E., D. Krapf, J.L. de la Vega-Beltran, J.J. Acevedo, and A. Darszon. 2011. Ion channels, phosphorylation and mammalian sperm capacitation. *Asian J Androl*. 13:395-405.

Wang, D., J. Hu, I.A. Bobulescu, T.A. Quill, P. McLeroy, O.W. Moe, and D.L. Garbers. 2007. A sperm-specific Na+/H+ exchanger (sNHE) is critical for expression and in vivo bicarbonate regulation of the soluble adenylyl cyclase (sAC). *Proc Natl Acad Sci U S A*. 104:9325-9330.

Wang, D., S.M. King, T.A. Quill, L.K. Doolittle, and D.L. Garbers. 2003a. A new sperm-specific Na+/H+ exchanger required for sperm motility and fertility. *Nat Cell Biol*. 5:1117-1122.

Wang, G., Y. Guo, T. Zhou, X. Shi, J. Yu, Y. Yang, Y. Wu, J. Wang, M. Liu, X. Chen, W. Tu, Y. Zeng, M. Jiang, S. Li, P. Zhang, Q. Zhou, B. Zheng, C. Yu, Z. Zhou, X. Guo, and J. Sha. 2013. In-depth proteomic analysis of the human sperm reveals complex protein compositions. *J Proteomics*. 79:114-122.

Wang, G., Q. Jiang, and C. Zhang. 2014. The role of mitotic kinases in coupling the centrosome cycle with the assembly of the mitotic spindle. *J Cell Sci*. 127:4111-4122.

Wang, H., and S.K. Dey. 2006. Roadmap to embryo implantation: clues from mouse models. *Nat Rev Genet*. 7:185-199.

Wang, J.T., D. Kong, C.R. Hoerner, J. Loncarek, and T. Stearns. 2017. Centriole triplet microtubules are required for stable centriole formation and inheritance in human cells. *Elife*. 6.

Wang, W.J., D. Acehan, C.H. Kao, W.N. Jane, K. Uryu, and M.F. Tsou. 2015. De novo centriole formation in human cells is error-prone and does not require SAS-6 self-assembly. *Elife*. 4.

Wang, X., C. Chen, L. Wang, D. Chen, W. Guang, and J. French. 2003b. Conception, early pregnancy loss, and time to clinical pregnancy: a population-based prospective study. *Fertil Steril*. 79:577-584.

Watanabe, T., J.S. Biggins, N.B. Tannan, and S. Srinivas. 2014. Limited predictive value of blastomere angle of division in trophectoderm and inner cell mass specification. *Development*. 141:2279-2288.

Wei, J.H., Z.C. Zhang, R.M. Wynn, and J. Seemann. 2015. GM130 Regulates Golgi-Derived Spindle Assembly by Activating TPX2 and Capturing Microtubules. *Cell*. 162:287-299.

White, R.A., Z. Pan, and J.L. Salisbury. 2000. GFP-centrin as a marker for centriole dynamics in living cells. *Microsc Res Tech*. 49:451-457.

Wilde, A., and Y. Zheng. 1999. Stimulation of microtubule aster formation and spindle assembly by the small GTPase Ran. *Science*. 284:1359-1362.

Williams, H.L., S. Mansell, W. Alasmari, S.G. Brown, S.M. Wilson, K.A. Sutton, M.R. Miller, P.V. Lishko, C.L. Barratt, S.J. Publicover, and S. Martins da Silva. 2015. Specific loss of CatSper function is sufficient to compromise fertilizing capacity of human spermatozoa. *Hum Reprod*. 30:2737-2746.

Winey, M., and E. O'Toole. 2014. Centriole structure. *Philos Trans R Soc Lond B Biol Sci*. 369.

Wolf, N., D. Hirsh, and J.R. McIntosh. 1978. Spermatogenesis in males of the free-living nematode, Caenorhabditis elegans. *J Ultrastruct Res*. 63:155-169.

Woodruff, J.B., B. Ferreira Gomes, P.O. Widlund, J. Mahamid, A. Honigmann, and A.A. Hyman. 2017. The Centrosome Is a Selective Condensate that Nucleates Microtubules by Concentrating Tubulin. *Cell*. 169:1066-1077 e1010.

Woodruff, J.B., A.A. Hyman, and E. Boke. 2018. Organization and Function of Non-dynamic Biomolecular Condensates. *Trends Biochem Sci*. 43:81-94.

Woodruff, J.B., O. Wueseke, and A.A. Hyman. 2014. Pericentriolar material structure and dynamics. *Philos Trans R Soc Lond B Biol Sci*. 369.

Woodruff, J.B., O. Wueseke, V. Viscardi, J. Mahamid, S.D. Ochoa, J. Bunkenborg, P.O. Widlund, A. Pozniakovsky, E. Zanin, S. Bahmanyar, A. Zinke, S.H. Hong, M. Decker, W. Baumeister, J.S. Andersen, K. Oegema, and A.A. Hyman. 2015. Centrosomes. Regulated assembly of a supramolecular centrosome scaffold in vitro. *Science*. 348:808-812.

World Health Organization. 2010. WHO laboratory manual for the examination of human semen and sperm-cervical mucus interaction. Published on behalf of the World Health Organization by Cambridge University Press, Cambridge, UK ; New York, NY. x, 128 p. pp.

World Medical, A. 2013. World Medical Association Declaration of Helsinki: ethical principles for medical research involving human subjects. *JAMA*. 310:2191-2194.

Wu, H.Y., Y. Rong, K. Correia, J. Min, and J.I. Morgan. 2015. Comparison of the enzymatic and functional properties of three cytosolic carboxypeptidase family members. *J Biol Chem*. 290:1222-1232.

Wu, J., and A. Akhmanova. 2017. Microtubule-Organizing Centers. *Annu Rev Cell Dev Biol*. 33:51-75.

Wu, J., C. de Heus, Q. Liu, B.P. Bouchet, I. Noordstra, K. Jiang, S. Hua, M. Martin, C. Yang, I. Grigoriev, E.A. Katrukha, A.F.M. Altelaar, C.C. Hoogenraad, R.Z. Qi, J. Klumperman, and A. Akhmanova. 2016. Molecular Pathway of Microtubule Organization at the Golgi Apparatus. *Dev Cell*. 39:44-60.

Wu, J.Y., T.J. Ribar, D.E. Cummings, K.A. Burton, G.S. McKnight, and A.R. Means. 2000. Spermiogenesis and exchange of basic nuclear proteins are impaired in male germ cells lacking Camk4. *Nat Genet*. 25:448-452.

Wunderlich, V. 2002. JMM---past and present. Chromosomes and cancer: Theodor Boveri's predictions 100 years later. *J Mol Med (Berl)*. 80:545-548.

Wykes, S.M., and S.A. Krawetz. 2003. The structural organization of sperm chromatin. *J Biol Chem*. 278:29471-29477.

Yamashita, Y.M., A.P. Mahowald, J.R. Perlin, and M.T. Fuller. 2007. Asymmetric inheritance of mother versus daughter centrosome in stem cell division. *Science*. 315:518-521.

Yao, R., C. Ito, Y. Natsume, Y. Sugitani, H. Yamanaka, S. Kuretake, K. Yanagida, A. Sato, K. Toshimori, and T. Noda. 2002. Lack of acrosome formation in mice lacking a Golgi protein, GOPC. *Proc Natl Acad Sci U S A*. 99:11211-11216.

Yoshimoto-Kakoi, T., Y. Terada, M. Tachibana, T. Murakami, N. Yaegashi, and K. Okamura. 2008. Assessing centrosomal function of infertile males using heterologous ICSI. *Syst Biol Reprod Med*. 54:135-142.

Young, C., P. Grasa, K. Coward, L.C. Davis, and J. Parrington. 2009. Phospholipase C zeta undergoes dynamic changes in its pattern of localization in sperm during capacitation and the acrosome reaction. *Fertil Steril*. 91:2230-2242.

Yu, Y.E., Y. Zhang, E. Unni, C.R. Shirley, J.M. Deng, L.D. Russell, M.M. Weil, R.R. Behringer, and M.L. Meistrich. 2000. Abnormal spermatogenesis and reduced fertility in transition nuclear protein 1-deficient mice. *Proc Natl Acad Sci U S A*. 97:4683-4688.

Zegers-Hochschild, F., G.D. Adamson, S. Dyer, C. Racowsky, J. de Mouzon, R. Sokol, L. Rienzi, A. Sunde, L. Schmidt, I.D. Cooke, J.L. Simpson, and S. van der Poel. 2017. The International Glossary on Infertility and Fertility Care, 2017. *Fertil Steril*. 108:393-406.

Zhang, C., M. Hughes, and P.R. Clarke. 1999. Ran-GTP stabilises microtubule asters and inhibits nuclear assembly in Xenopus egg extracts. *J Cell Sci*. 112 (Pt 14):2453-2461.

Zhang, K., and G.W. Smith. 2015. Maternal control of early embryogenesis in mammals. *Reprod Fertil Dev*. 27:880-896.

Zhao, M., C.R. Shirley, S. Hayashi, L. Marcon, B. Mohapatra, R. Suganuma, R.R. Behringer, G. Boissonneault, R. Yanagimachi, and M.L. Meistrich. 2004. Transition nuclear proteins are required for normal chromatin condensation and functional sperm development. *Genesis*. 38:200-213.

Zhao, M., C.R. Shirley, Y.E. Yu, B. Mohapatra, Y. Zhang, E. Unni, J.M. Deng, N.A. Arango, N.H. Terry, M.M. Weil, L.D. Russell, R.R. Behringer, and M.L. Meistrich. 2001. Targeted disruption of the transition protein 2 gene affects sperm chromatin structure and reduces fertility in mice. *Mol Cell Biol*. 21:7243-7255.

Zheng, Y., M.L. Wong, B. Alberts, and T. Mitchison. 1995. Nucleation of microtubule assembly by a gamma-tubulin-containing ring complex. *Nature*. 378:578-583.

Zuccotti, M., V. Merico, S. Cecconi, C.A. Redi, and S. Garagna. 2011. What does it take to make a developmentally competent mammalian egg? *Hum Reprod Update*. 17:525-540.

ANNEXES

ANNEX 1:

The microtubules in the sperm flagella are composed of tubulin and are necessary for sperm movement. Tubulin can be modified post translationally by the addition or removal of different aminoacids, defining the flagellum functionality. Several tubulin PTMs have been described in *Drosophila* and sea urchin spermatozoa, where blocking tubulin polyglutamilation decreases sperm motility. Tubulin monoglycylation and acetylation are associated with axoneme stability, while preventing tubulin glycylation causes sperm defects and infertility in *Drosophila*. Despite the reported effect of PTMs on sperm fitness, very little is known about PTMs presence and role in human sperm functionality. On that line I started a side project which main objective was to characterize the presence and distribution of the human sperm tubulin PTMs along the sperm flagella and their relationship with sperm fitness.

Human spermatozoa axonemes are enriched in tubulin PTMs:

In order to known whether human sperm axonemes are also enriched in tubulin PTMs we performed WB of whole cell lysates and IF for most of the described C-terminal tail tubulin modifications as well as acetylation in normozoospermic samples (**Figure 1A and B**). We found that microtubules in the sperm flagella are highly modified overall; in fact we detected acetylation, polyglutamylation, ramification (branching glutamylation - GT335), lack of tyrosine, tyrosination and monoglycylation. The antibodies recognize specifically the tubulin modifications because no staining is observed apart from the sperm tail.

A

B
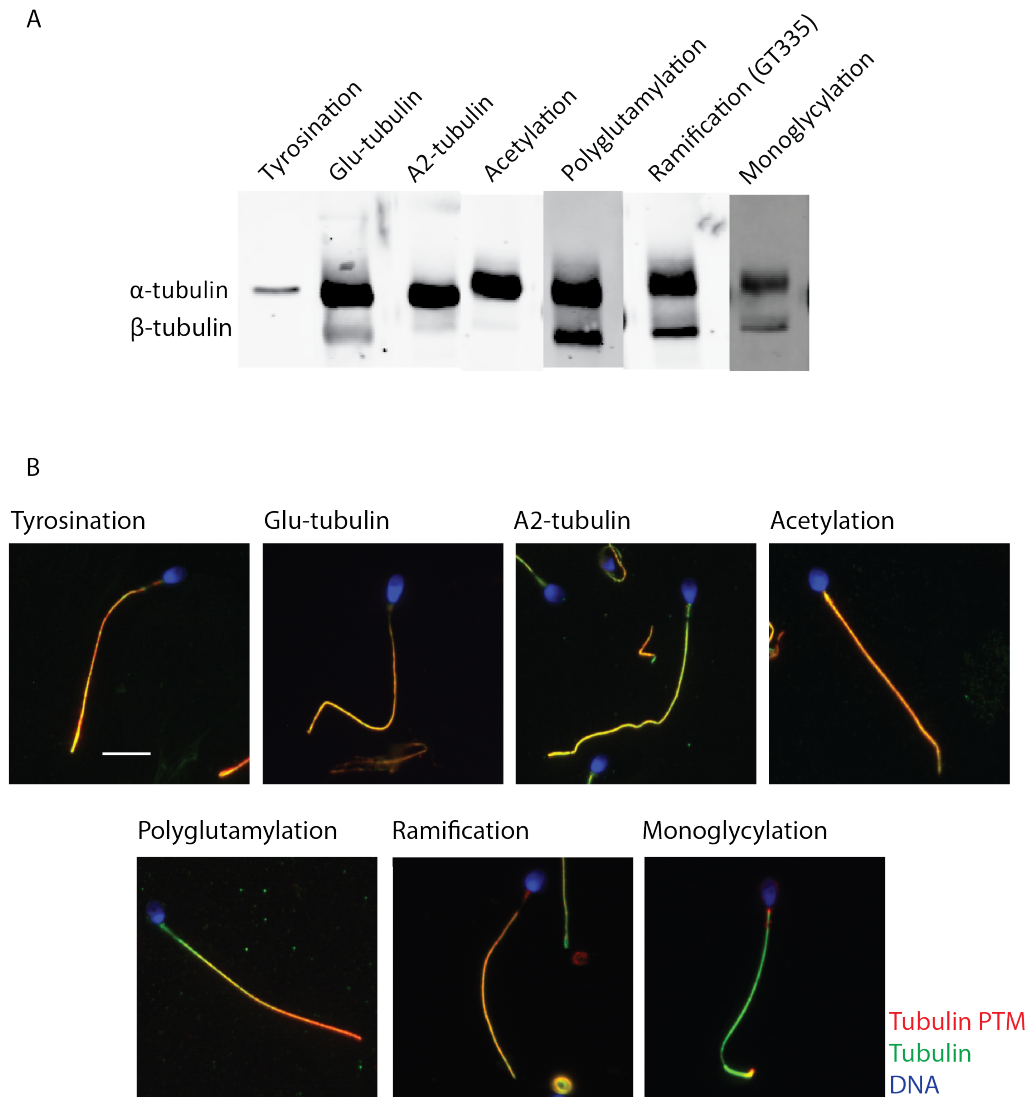
Figure 1: Identification of tubulin PTMs in human spermatozoa. A) WB against 7 selected tubulin PTMs. We tested these 7 modifications because, in exception of acetylation, all of them occur at the C-terminal tail of the tubulin. **B)** Co-staining of the 7 previous tested tubulin PTMs with tubulin (either α or β) to analyze the tail specific localization. Scale 10μm.

We observed that not all tubulin PTMs are equally distributed along the sperm tail. This suggests that each tubulin PTM could regulate different axoneme properties along the tail. We decided to focus on 4 specific tubulin PTMs that have been described to be involved in axoneme motility and stability in different animal models: acetylation, monoglycylation, polyglutamylation and ramification. In order to quantify their changes along the tail, we analyzed tubulin PTMs as well as tubulin intensity at every 0.1 μm. We divided each length value for the total length of the sperm tail in order to standardize each tail length to 1. To be more precise in the analysis we applied the mathematical equation of lineal regression to obtain an intensity value at each of the

0.001 units. The intensity of each tubulin PTM for each unit was then divided by the corresponding tubulin intensity **(Figure 2)**. As our observations suggested, not all tubulin PTMs are equally distributed along the sperm tail. Acetylation is the most stable modification, monoglycylation increases whereas polyglutamylation and ramification decreases along the tail.
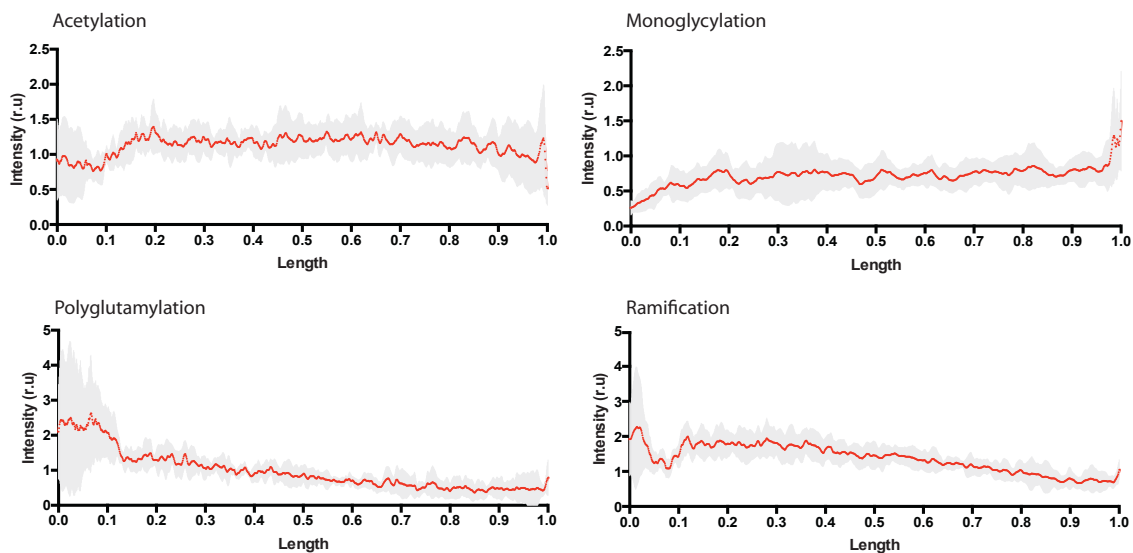
Figure 2: Quantitative analyses of tubulin PTMs distribution. A precise quantitative analysis of the ratio of tubulin PTM distribution versus tubulin was calculated at each 0.001 relative units of tail length. The distribution of tubulin PTM acetylation, monoglycylation, polyglutamylation and ramification is different in each case. n=10 spermatozoa per condition.

Human semen samples have different tubulin PTMs distribution:

The results I present in this section were performed once and are still ongoing, therefore they have to be taken with caution.

Because tubulin PTMs regulate axoneme stability and motility mediating the interaction of different proteins such as motor proteins and MAPs with the microtubule surface, we wondered whether samples with abnormal or immotile flagella could have an altered tubulin PTM distribution. We used a normozoospermic (progressive motility=37%, normal morphology=7%) and a teratozoospermic (progressive motility=34.8%, normal morphology=3% sample, both of them selected by swim-up, therefore we had 4 fractions:

- Normozoospermic sample motile (swim-up fraction).

- Normozoospermic sample mix (motile + immotile spermatozoa – pellet of the swim-up).

- Teratozoospermic sample motile (swim-up fraction).

- Teratozoospermic sample mix (motile + immotile spermatozoa – pellet of the swuim up).

We performed the same quantification analysis as described in the previous section but the fact that the sperm tails are highly enriched in tubulin PTMs made it difficult to detect any difference in intensity, therefore we decided to focus only on the last 10% of the sperm tail because this region is less enriched and, if any difference exist, we expect to detect them there. So far we only analyzed acetylated, monoglycylated and ramificated tubulin. We were not able to detect differences in intensities but we realized that the pattern of each tubulin PTM is not the same in each sample and fraction (**Figure 3)**. We found that reduction of tubulin acetylation starts closer to the sperm proximal part in teratozoospermic sample mix compared with normozoospermic motile fraction, which it is the one that starts to decrease more distally (Terato mix 0.90 > Normo mix 0.920 > Terato motle 0.931 > Normo motile 0.940). Regarding monoglycylation, mixes behave similar as motile samples do independently of their diagnoses (Terato mix 0.90 = Normo mix 0.90 > Terato motile 0.965 = Normo motile 0.963). Finally, in ramification we found that teratozoospermic motile fraction behaves similar to normozoospermic mix sample, suggesting that although motile spermatozoa are selected from teratozoospermic samples for assisted reproduction, molecularly they are not equivalent to normal motile spermatozoa in terms of tubulin glutamylation (Terato mix 0.90 > Terato motile 0.916 + Normo mix 0.917 > Normo motile 0.936).
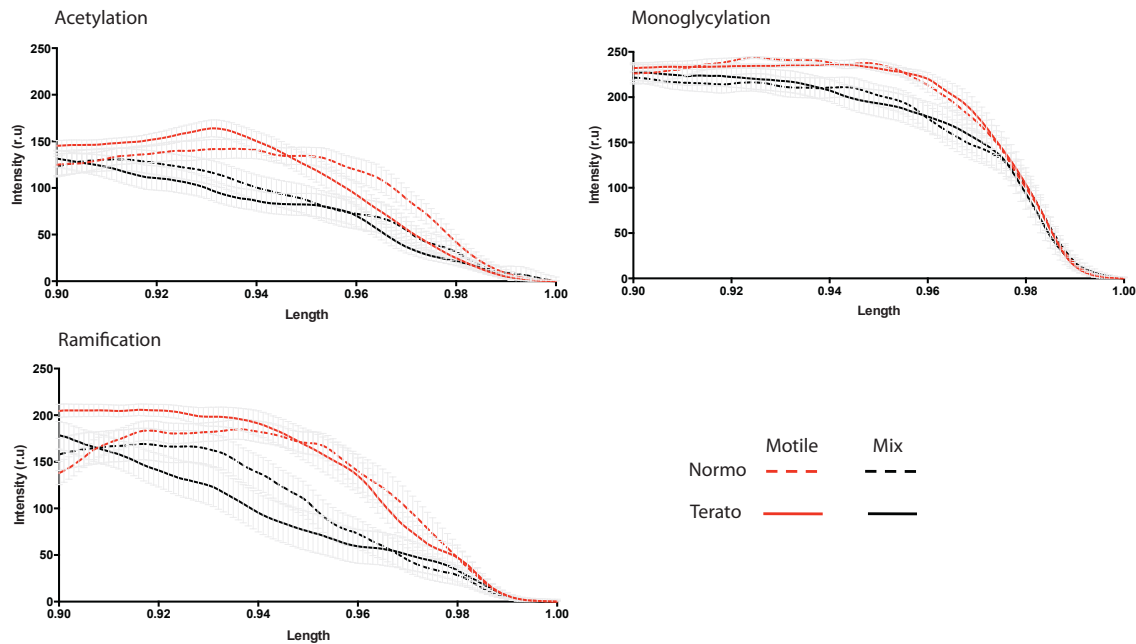
Figure 3: Quantitative analyses of the last 10% of the normozoospermic and teratozoospermic sperm samples. The decrease pattern for each tubulin PTM was analyzed in normozoospermic and teratozoospermic samples fractionated in motile and mix samples by the swim-up technique. n=20 spermatozoa per condition.

Data interpretation and conclusions:

Our results indicate that the human sperm tail is highly modified by tubulin PTMs as all C-terminal associated tubulin modifications are present along the sperm tail. To quantify precisely how tubulin PTMs distribute along the sperm tail, we established a method to analyze the intensity of each modification and found that each modification presents a specific pattern of distribution.

The analysis of the last 10% of the sperm tail are ongoing experiments and results should be taken with caution, however, we observed that in the mix fractions, acetylated and monoglycytaled tubulin ends in a more proximal region than motile fractions. When tubulin polyglycylation is inhibited in *Drosophila*, the sperm tails are less stable and some cannot form. Our results suggest that the mix sperm tails are less stable than the tails of the motile fraction. Regarding tubulin ramification, the mix fraction has fewer ramifications and the motile teratozoospermic fraction is similar to the mix fraction of a normozoospermic sample. We known that in sea urchin, when polyglutamylation is blocked, sperm motility is reduced, therefore motile fractions of teratozoospermic samples might have a less optimum motility in terms of beating dynamics and frequency than motile normozoospermic samples.

To conclude, these preliminary results suggest that tubulin PTMs fingerprinting could define the sperm fitness.

ANNEX 2:

Title: Tubulin post-translational modifications and their role in cytoskeletal function in gametes and embryos: from model systems to human reproduction.

Running title: tubulin in gametes and embryos.

Summary sentence: The tubulin code is emerging as an important regulator of microtubule function that impacts gamete and embryonic development.

Keywords:

Tubulin, tubulin isotypes, tubulin post-translational modifications (PTMs), spermatozoa, oocytes, early embryo development.

Authors: Amargant F [1,2,3], Barragan M[1], Vassena R[1,*], Vernos I.[2,4*]

Address:

1 Clínica EUGIN, Travessera de les Corts 322, Barcelona, 08029, Spain.

2 Cell and Developmental Biology Programme, Centre for Genomic Regulation (CRG), Barcelona Institute of Science and Technology, Doctor Aiguader 88, 08003 Barcelona, Spain.

3 Universitat Pompeu Fabra (UPF), Doctor Aiguader 88, 08003 Barcelona, Spain.

4 Institució Catalana de Recerca I Estudis Avançats (ICREA), Passeig de Lluis Companys 23, 08010 Barcelona, Spain.

*Authors for correspondence: rvassena@eugin.es, isabelle.vernos@crg.es

Table of contents:

Abstract:

Microtubules are intracellular filaments that define in time, but also in space, a large number of essential cellular functions such as intracellular transport, flagella and cilia assembly, and cell division. Their function is therefore essential for male and female gametes maturation and function, and for embryo development. The dynamic and functional properties of the microtubules are in large part defined by various classes of interacting proteins including MAPs (Microtubule Associated Proteins), microtubule dependent motors, and severing and modifying enzymes. Multiple mechanisms regulate these interactions. One of them is defined by the combinatorial diversity of the microtubules themselves through two mechanisms: various tubulin isotypes and a number of tubulin post-translational modifications (PTMs). This generates a so-called tubulin code that defines the specific set of proteins that associates with a given microtubule population thereby defining its properties and functions. The objective of this review is to provide an in depth description of tubulin isotypes and PTMs in spermatozoa, oocytes, and preimplantation embryos in various model systems and in the human species. We focus on functional implications of the tubulin code for cytoskeletal function, particularly on the field of human reproduction, with special emphasis on gamete quality and infertility. Finally, we discuss some of the knowledge gaps and propose future research directions.

Introduction:

Successful gamete and embryo development, including sperm flagellar beating, meiotic and mitotic spindle assembly, and polarization of blastomeres, rely on the fine regulation of the microtubule network in time and space **(Figure 1A)**.

Microtubules are intrinsically dynamic hollow polymers formed by the lateral interaction of protofilaments, each composed by the head to tail self-assembly association of alpha- and beta-tubulin dimers. Other members of the tubulin family have non-overlapping functions. Gamma tubulin is specifically required for microtubule nucleation (Kollman et al., 2011; Kollman et al., 2010). Epsilon and delta tubulins localize to the centrosome and play a role in centriole duplication and pericentriolar material organization (Chang and Stearns, 2000). Zeta tubulin is absent in humans and was found to be a component of the basal foot (Turk et al., 2015). In mammalian cells cytoplasmic microtubules have 13 protofilaments. Microtubules are polarized filaments with an exposed alpha-tubulin subunit at the so-called minus end and a beta-tubulin subunit exposed at the so-called plus end **(Figure 1A)**. In most cells, their minus-ends are focused at the centrosome (the main microtubule organizing center, MTOC) and their more dynamic plus-ends extend out toward the cell periphery. However, microtubules can organize different types of networks highly related to the specific function of different cell types. They can also form specialized cellular structures that can be either relatively stable like the axoneme of flagella and motile cilia, or highly dynamic like the bipolar meiotic or mitotic spindles, the molecular machines that segregate the chromosomes during cell division.

Microtubules alternate between phases of growth and shrinkage, an intrinsic property known as "dynamic instability". The length of dynamic microtubules therefore varies constantly. In the cell, the microtubule dynamic properties are regulated by several classes of interacting proteins that can promote their stabilization or, on the contrary, destabilize them. In addition, microtubule dependent motors define their intracellular organization and/or use them as tracks to drive the directed transport of different cellular components in a directional manner **(Figure 1A)**. Despite their homogeneous alpha-beta tubulin dimer core composition, two mechanisms generate diversity at the microtubule surface thereby defining different binding affinities for the associated proteins resulting in major functional implications. These mechanisms rely on the presence of small sequence differences at the exposed C-termini of the alpha and beta

tubulin isotypes, and on several tubulin PTMs that mostly occur on specific residues of these C-terminal sequences **(Figure 1B)** (Schatten and Sun, 2014)

Here we will review the mechanisms that generate microtubule diversity and our current understanding of their role during gamete maturation, fertilization, and early embryo development with a special emphasis on the putative implications for fertility in humans. In the light of these data, we will discuss the potential of designing novel tools that could be useful for ART.

Results:

Tubulin isotypes

The analysis of the human genome has shown that 12 genes encode alpha tubulins (9 genes, 2 pseudogenes and 1 putative gene) and 10 genes encode beta tubulins (9 genes and 1 pseudogene) **(Table 1)** (HGNC Database, HUGO Gene Nomenclature Committee (HGNC), EMBL Outstation - Hinxton, European Bioinformatics Institute, Welcome Trust Genome Campus, Hinxton, Cambridgeshire, CB10 1SD, UK www.genenames.org. Data retrieved on August 2016**)**. All alpha and beta tubulins have a highly conserved N-terminal globular domain and an unstructured C-terminal tail that extend outwards along the microtubule surface serving as docking site for a large number of associated proteins. These C-terminal tails show the highest sequence diversity amongst the different tubulin isotypes **(Table 1)**. For instance, TUBA4 A/B (tubulin alpha isotype 4 A/B), TUBA8 (tubulin alpha isotype 8) and TUBAL3 (tubulin alpha L3) do not contain the final tyrosine present in the other alpha tubulin isotypes (Gu et al., 1988) **(Table 1)**.

Interestingly, some tubulin isotypes are expressed in different cell types whereas others are restricted to certain cell types or specific developmental stages (Denoulet et al., 1986; Hurd et al., 2010; Lewis et al., 1987; Lewis et al., 1985). For example, TUBB8 (tubulin beta isotype 8) is specifically expressed in human oocytes and it is moreover the main beta tubulin present in these cells (Feng et al., 2016a). Another beta tubulin isotype, TUBB4 (tubulin beta isotype 4) is the main isotype expressed in ciliated tissues (Renthal et al., 1993). However, the functional consequences of these specific expression patterns are not as yet entirely clear, and no evidences exist at the moment

for the requirement of specific tubulin isotypes for the assembly of specific types of microtubules such as axonemal microtubules for instance (Lewis et al., 1987).

Tubulin PTMs: types and modifying enzymes

Several types of tubulin PTMs have been described including phosphorylation, polyamination, methylation, ubiquitination, palmitoylation, acetylation, (poly)glutamylation, (poly)glycylation and detyrosination. In this review, we will focus on the last four types of tubulin PTMs keeping a focus on their role in gamete maturation and early embryo development **(Figure 1B).**

Tubulin acetylation

Tubulin acetylation was identified for the first time in 1985 (L'Hernault and Rosenbaum, 1985a). It consists of the addition of an acetyl group to a lysine in a reversible reaction. Both alpha and beta tubulins can be acetylated on several sites including (Choudhary et al., 2009) lysine 40 (Lys40) of alpha-tubulin amongst several others (lysines 401, 394, 370, 311, 60, 112, 326…) and Lys58, Lys252, Lys324 of beta tubulin.

Although it was described that acetylation does not influence tubulin polymerization kinetics (Maruta et al., 1986), most reports indicate that acetylated microtubules are more stable than non-acetylated ones. However, the mechanism by which acetylation confers stability to the microtubule is not clear and some authors have even questioned this correlation (Brunke et al., 1982; Piperno et al., 1987; Schulze et al., 1987) (Matsuyama et al., 2002) (Asthana et al., 2013; Tran et al., 2007) (Zilberman et al., 2009) (Patel and Chu, 2014). In fact, the acetylation of beta tubulin Lys252 was found to negatively regulate the incorporation of tubulin heterodimers to the microtubule. However, acetylation of alpha tubulin Lys40 is a marker for stable microtubules. Unlike all the other tubulin PTMs, Lys40 acetylation occurs inside the lumen of the microtubule (Nogales et al., 1999). Recently it was proposed that acetylation of Lys40 induces the formation of a salt bridge promoting structural changes in the microtubule angle, stabilizing it (Cueva et al., 2012). However no significant changes in the microtubule lattice were observed in Lys40 acetylated microtubules versus non-acetylated ones by cryo-electron microscopy (Howes et al., 2014).

Overall, tubulin acetylation seems to modify the mechanical properties, structure and organization of the microtubules (Cueva et al., 2012; Topalidou et al., 2012) but it does not influence tubulin polymerization kinetics (Maruta et al., 1986).

Tubulin acetylation is catalyzed by several acetyltransferases including ARD1-NAT1 (Ohkawa et al., 2008), ELP3 (Creppe et al., 2009), San (Chu et al., 2011), GCN5 (Conacci-Sorrell et al., 2010) and αTAT1 (Shida et al., 2010) (Akella et al., 2010) (Topalidou et al., 2012).

The acetyltransferase San acetylates beta tubulin on Lys252 (Chu et al., 2011). αTAT1 is the major alpha-tubulin Lys40 acetyltransferase in mice. It is conserved in ciliated organisms and it was shown to be required for the acetylation of axonemal microtubules and for the normal kinetics of primary cilium assembly (Akella et al., 2010; Shida et al., 2010). Interestingly, although mice develop normally upon depletion of αTAT1, males have fertility problems and sperm motility defects (Kalebic et al., 2013). The mechanism by which αTAT1 acetylates alpha tubulin Lys40 inside the microtubule lumen was recently described. αTAT1 can enter the lumen from the microtubule ends (Coombes et al., 2016) and spread Lys40 acetylation along the microtubule (Ly et al., 2016).

Tubulin deacetylation is promoted by HDAC6 (Hubbert et al., 2002) (Zhang et al., 2003) and by the NAD-dependent class III deacetylase SIRT2 (North et al., 2003) that act specifically on alpha-tubulin Lys40. HDAC6 acts mainly on polymerized microtubules and is constitutively active whereas SIRT2 is a NAD dependent enzyme (Hubbert et al., 2002; North et al., 2003). Although HDAC6 and SIRT2 interact and may function together (North et al., 2003) (Nahhas et al., 2007), altering HDAC6 levels is sufficient to increase tubulin acetylation in fibroblasts (Zhang et al., 2008).

Tubulin tyrosination/detyrosination

Most alpha tubulin isotypes have a tyrosine residue at their C-terminus. The removal of this tyrosine generates detyrosinated tubulin also named Glu-tubulin (because the newly exposed C-terminal aminoacid is a glutamic acid). Glu-tubulin in turn can be re-tyrosinated (Arce et al., 1975; Hallak et al., 1977; Raybin and Flavin, 1977), generating a dynamic cycle of tubulin tyrosination /detyrosination (Gundersen et al., 1987; Valenzuela et al., 1981). Although tyrosinated and detyrosinated microtubules can co-exist in the same cell, different cell types and specific microtubule-based structures have

different ratio of tyrosinated/detyrosinated microtubules (Geuens et al., 1986; Gundersen et al., 1984; Raybin and Flavin, 1977). This ratio may in fact define the specific biochemical properties to the microtubule network. Indeed, dynamic microtubules have been found to be mostly tyrosinated, whereas stable ones like for example those forming centrioles, are mostly detyrosinated (Gundersen et al., 1987; Kreis, 1987).

The further removal of the glutamic acid exposed at the C-terminus of detyrosinated alpha tubulin generates the so-called Δ2 – tubulin. This modification is irreversible (Paturle-Lafanechere et al., 1991). Δ2 – tubulin is particularly enriched in very stable microtubules like those of cilia (primary or motile) and neurons. Strikingly, it constitutes 35% of all brain tubulin (Paturle-Lafanechere et al., 1994).

The enzyme that catalyzes the removal of the last tyrosine residue on alpha tubulin is the complex of vasohibin-1 with the small vasohibin binding protein (Aillaud et al., 2017), and the enzyme that catalyzes the addition of a tyrosine on Glu-tubulin was identified and characterized in bovine and porcine brain several years ago (Ersfeld et al., 1993; Raybin and Flavin, 1977). This enzyme named tubulin tyrosine ligase (TTL) enzyme requires ATP, magnesium ions and a terminal glutamic acid residue for its activity (Murofushi, 1980; Raybin and Flavin, 1977; Rudiger et al., 1994). TTL is the founding member of the large TTLL family (see below).

Tubulin glutamylation and glycylation

Chains of different lengths of identical amino acids, either glutamic acids or glycines, can be added on glutamic residues present in the C-terminal tail domains of alpha and beta tubulins. These modifications generate mono/poly-glutamylated or mono/poly-glycylated tubulin, respectively. These PTMs can occur on any tubulin independently of any other tubulin PTM (Edde et al., 1992). Interestingly, glutamylation and glycylation compete for the same sites at the C-terminal tail domains of tubulins (Wloga et al., 2009). However, they can also co-exist in a single molecule of tubulin (Mary et al., 1997). These tubulin PTMs are particularly versatile. Depending of the cell type and organism the branched aminoacid chains can range from as little as 1 to more than 20 residues (Edde et al., 1990).

Microtubule based structures, such as axonemes, are highly glycylated (indeed glycine lateral chain of up to 34 residues branching from alpha and/or beta tubulin subunits

were describen in *Paramecium* (Redeker et al., 1994) (Bre et al., 1998; Iftode et al., 2000), whereas dynamic microtubules, if they are modified, have shorter polyglycylated chains or no glycylation (in humans, see below) (Bre et al., 1998; Callen et al., 1994). This modification was detected in one of the oldest eukaryotes, *Giardia lamblia*, suggesting an important role through evolution (Weber et al., 1996). On the other hand, glutamylation is found both in stable and dynamic microtubules. It was characterized for the first time in 1990 in brain tubulin where it was found to represent about 40 to 50% of the total α – tubulin (Edde et al., 1990).

Several enzymes catalyze the addition of (poly)glutamates or (poly)glycines on the C-terminal tails of alpha and/or beta tubulin subunits. They were initially identified in mouse brain, *Tetrahymena thermophila* and zebrafish (Janke et al., 2005; Pathak et al., 2007; Regnard et al., 2003). These enzymes are highly related to TTL (see above) and constitute the tubulin tyrosine ligase-like family (TTLL) (Janke et al., 2005; van Dijk et al., 2007). Mammalian organisms have 13 different TTLL enzymes **(Table 2)** that catalyze tubulin mono and poly-glutamylation/glycylation through specific reactions. The initial branching reaction involves the formation of a γ-amide bond between a glutamic acid residue in the main chain of tubulin and a free glutamate/glycine. The addition of successive glutamic acid glycines residues on the first branched one occurs through the formation of α-amide bonds (peptide-like bond) (Redeker et al., 1991).

In the human species, microtubules can be mono or polyglutamylated. However microtubules can only be monoglycylated because the enzyme responsible for the elongation of a polyglycylated chain is not functional (Rogowski et al., 2009).

The enzymes responsible for the removal of the mono or polyglycylated chains have not been identified yet. Instead, the enzymes that remove the mono or polyglutamylated chains form a family of enzymes called Cytosolic carboxypeptidases (or CCPs), also known as Nna-like proteins or AGTBPs. These enzymes were first identified in studies of axonemal regeneration and Purkinje cell degeneration in animal models (Fernandez-Gonzalez et al., 2002; Harris et al., 2000). The CCP family consists of six members (CCP1 to CCP6) **(Table 2)**. They share a conserved Carboxypeptidase domain (300 residues approximately), which has catalytic activity and a shorter N-terminal domain (150 residues approximately) that has been proposed to act as a folding, regulatory or binding domain (Kalinina et al., 2007; Otero et al., 2012; Rodriguez de la Vega Otazo et al., 2013; Rogowski et al., 2010). The functional redundancy of the different TTLL and

CCP enzymes may provide a failsafe mechanism to support essential microtubule functions.

Functional implications of the tubulin code

The tubulin code has important functional implications either by directly changing the structural properties of the microtubules and/or by defining the specific binding affinities and properties of at least some interacting proteins. Altogether characterizing the tubulin code will provide novel insights into the mechanism that regulate microtubule dynamics and organization and thereby into cell physiology and function. Specific tubulin PTMs have been found to regulate the binding affinity of some MAPs and motors with the microtubule surface. Moreover tubulin PTMs can also change some functional properties of the associated proteins. For instance, some of them were shown to modify the processivity, velocity, and directionality of motors **(Table 3)**. (Peris et al., 2009)

The first evidence for the role of tubulin PTMs in the regulation of the binding of MAPs to microtubules was obtained in 1994 for Tau (Boucher et al., 1994). Tau has a higher affinity for microtubules with short polyglutamylated chains (up to 3 residues). Instead, MAP1A associates preferentially with microtubules having long polyglutamylated chains. It was therefore proposed that the potential binding competition of different MAPs for the microtubules is solved through the control of tubulin polyglutamylation chain length (Bonnet et al., 2001; Boucher et al., 1994). As a consequence, not only the combination of tubulin isotypes and different tubulin PTMs can regulate the binding of microtubule-associated proteins, but the extent of some modifications (chain length) has also different functional consequences.

In vitro experiments of chimaeric tubulin (composed of different human C-terminal tails and yeast core domains) with motor proteins demonstrated that Kinesin-1, Kinesin-2, MCAK or Kinesin-13 and dynein have different affinities for polyglutamylated, tyrosinated microtubules and for some tubulin isotypes (Sirajuddin et al., 2014) **(Table 3)**. For example, detyrosinated tubulin decreases the microtubule binding affinity of microtubule depolymerizing proteins such as Kinesin-13 family members. This could explain at least in part why this modification is enriched in stable microtubules (Peris et

al., 2009). Overall the tubulin code may provide a complex and fine mechanism for the regulation of microtubule function.

Tubulin isotypes and PTMs in the reproductive system and early embryos of model organisms and humans

The expression of specific tubulin isotypes and the presence of the enzymes that catalyze the tubulin PTMs in the human reproductive system (ovary, uterus, prostate, and testis) suggest that the tubulin code plays important functions in gamete and embryonic development.

Spermatozoa and flagellated organisms

The spermatozoon is a motile cell consisting of a head containing, among other structures, a set of chromosomes and a long tail, the flagellum. The central core of the flagellum is constituted by an axoneme, which is a structure also present in eukaryotic motile cilia and in some prokaryotes. The axoneme is a distinctive structure that consists of a central pair of microtubules surrounded by a circular sheaf of nine doublets of microtubules (called 9+2). Each doublet consists of a complete 13 protofilament microtubule (named A-tubule) associated with an incomplete 10 protofilament microtubule (named B-tubule). The axoneme is surrounded by the outer dense fibers (ODFs) and the fibrous sheaths (Fawcett, 1975) that provide elasticity and support to the beating flagellum and are therefore important for spermatozoa motility and stability (Lindemann and Lesich, 2016). Motile cilia that are present in the lung, respiratory tracks and middle ear also share a similar 9+2 axoneme organization. Primary cilia are present in many cells and function as sensory antennas. Although they also have an axoneme, it lacks the central microtubule pair. Primary cilia are immotile, underscoring the importance of the central pair in motility generation.

Sperm motility is essential for natural fertilization. Tail movements are powered by axonemal dynein, a large microtubule dependent motor complex and involves signaling pathways such as cAMP-dependent protein kinases pathway, mitochondria activity as the main spermatozoon ATP provider, ROS production and structural proteins such as septins (Pereira et al., 2017). Axonemal dynein was first identified in *Tetrahymena pyriformis* cilia (Gibbons and Rowe, 1965) and later found to be a central components of motile cilia and flagella in all species **(Figure 2)**. Cytoplasmic dynein, was identified later as a highly related microtubule minus-end directed motor complex with multiple

essential functions in all cells. Cytoplasmic and axonemal dyneins are multiprotein complexes that assemble around force generating subunits called the heavy chains. They all move towards the microtubule minus end in a ATP-dependent manner (Lindemann and Lesich, 2010).

Within the motile axoneme, dyneins power the reciprocal sliding of adjacent microtubule doublets generating the beating of the flagella. This mechanism involves stable and transient interactions of inner and outer arm dynein complexes with microtubules (Gibbons and Rowe, 1965; Ishikawa et al., 2007; Nicastro et al., 2006; Raff et al., 2008; Sui and Downing, 2006; Takada and Kamiya, 1994). Inner and outer arm dyneins have more stable interactions with the A-tubule within a microtubule doublet **(Figure 2)**. These dynein complexes then interact transiently in an ATP dependent manner with the B tubule of an adjacent microtubule doublet, producing a sliding movement of the microtubule doublets and the bending of the flagellum (Brokaw, 1972).

Mutations in any of the dynein arm subunits or their absence have been associated with male infertility (Ben Khelifa et al., 2014; Duquesnoy et al., 2009; Fliegauf et al., 2005; Kott et al., 2012), specifically asthenozoospermia. Moreover, a significantly lower expression of dynein was observed by transcription profiling in teratozoospermic human spermatozoa compared to the control normozoospermic samples. Some infertile patients with multiple morphological defects and reduced spermatozoa motility were indeed found to carry mutations in the gene DNAH1, which encodes an inner arm dynein heavy chain. Moreover, mutations in the DNAH1, DNAH5, DNAI1 and CCDC39 genes were found to correlate with ultrastructural axonemal abnormalities, such as the absence of inner dynein arms, displacement of the dense fiber and microtubule outer doublets or even the absence of the microtubule central pair (Ben Khelifa et al., 2014), all causing dysfunctional axonemes. Mice lacking a specific dynein heavy chain isoform (MDHC7) or impaired inner arm dynein function show multiple defects in spermatozoa movement that is associated with male infertility (Neesen et al., 2001), although females are fertile and the offsprings viable (Tanaka et al., 2004). The motility defects observed in these spermatozoa are often associated with morphological abnormalities at the level of the bending and/or curvature of the flagella. The impaired motility results from a reduction of straight-line velocity and progressive movement of the spermatozoa impairing the movement of the spermatozoa through the female genital tract to the oviduct (Neesen et al., 2001). In such cases, intracytoplasmatic sperm injection (ICSI), an advanced

assisted reproductive technique which consists in the injection of one isolated spermatozoon into the cytoplasm on a mature oocyte, is the only method that can ensure successful fertilization and the development of an offspring.

The assembly and function of the axoneme requires specific mechanisms of intraflagellar transport in particular to deliver axonemal components such as tubulin to its tip (Pazour et al., 2005) (Ostrowski et al., 2002). This transport mechanism, known as IFT (Intraflagellar transport), supports the bidirectional movement of molecules along the axoneme through the formation of IFT trains, which are supramolecular protein complexes. These IFTs trains can bind and transport different cargoes through the BBSome complex (Lechtreck et al., 2013; Lechtreck et al., 2009; Nachury et al., 2007). Two different motors mediate the movement of the IFT trains, the microtubule dependent motor plus end directed kinesin-2 for anterograde transport (Kozminski et al., 1995) (Scholey, 1996) and the minus end directed motor cytoplasmic dynein (or dynein 1b in invertebrates) (Pazour et al., 1999) (Porter et al., 1999) for retrograde transport. Each motor complex moves the IFT with a different velocity. Although there are still no evidences, it is tempting to speculate that the motor driven IFT movements can be regulated by tubulin PTMs.

IFTs are essential for the proper formation of the sperm flagella in the vast majority of organisms with a few exceptions like *Plasmodium* microgametes and *Drosophila* spermatids (Basiri et al., 2014; Han et al., 2003). Moreover, IFT are present in the mice testis but not in mature sperm. The absence of specific IFT proteins like IFT88 results in male sterility associated with two main phenotypes: first, a severe reduction of the number of spermatozoa (more than 350 times) and, second, the formation of spermatozoa with short flagella or no axoneme (San Agustin et al., 2015). In a similar way, the absence of Kif3A, a subunit of the kinesin-2 motor, in mice, results in sperm tail formation defects (Lehti et al., 2013). These data suggest that in mammals, the IFTs and their associated motor proteins are essential for sperm tail formation during spermatogenesis but not for axoneme maintenance. Therefore, it seems reasonable to hypothesize that those patients having spermatozoa with short and/or defective axonemes may carry mutations in genes encoding IFT complex proteins and/or their associated motor protein complexes, kinesin-2 and dynein. An interesting possibility is that defects at the level of tubulin PTMs in the axoneme alter the binding and motility of the IFTs. Future experiments should address whether tubulin PTMs can indeed regulate the transport of IFTs along the axoneme. Moreover, the genetic analysis of

patients with short or absent sperm flagella may reveal the presence of mutations in the genes encoding for IFT supramolecular components.

Different tubulin isotypes are expressed in human spermatozoa. Indeed, human spermatozoa contain mRNAs for 5 different alpha (TUBA1A, TUBA1C, TUBA3C, TUBA4A and TUBA4B) and beta (TUBB, TUBB2A, TUBB3, TUBB4B and TUBB6) tubulin genes. Interestingly, differences in the tubulin isotype transcription profiles were observed in human teratozoospermic sperm samples compared to control normozoospermic ones. For instance, the expression of TUBA3C, TUBA4A and TUBB4B is down-regulated in teratozoospermic samples, whereas that of TUBB2B is up-regulated. The functional implications of these differences is currently unclear but the truncation of the C-terminal tail domains of B2-tubulin in the model system *Drosophila melanogaster* resulted in the absence of sperm axoneme and infertility (Popodi et al., 2005; Popodi et al., 2008).

Axonemal microtubules are highly modified by polyglutamylation, polyglycylation and acetylation (Mary et al., 1996; Piperno and Fuller, 1985; Plessmann and Weber, 1997). Tubulin acetylation occurs uniformly along the microtubule doublets of the flagella in all the species analyzed. This modification is important for sperm motility. Interestingly, a reduction of the total level of tubulin acetylation was observed in asthenozoospermic human sperm samples compared with normozoospermic ones (Bhagwat et al., 2014). Since the destabilization of the axoneme during cilia resorption requires tubulin deacetylation (L'Hernault and Rosenbaum, 1983; L'Hernault and Rosenbaum, 1985b; Russell and Gull, 1984), it is possible that tubulin acetylation promotes axoneme formation and stability. Recently however, the presence of acetylated alpha-tubulin isoforms (TUBA3C and TUBA4A) has been correlated with sperm samples with poor motility. This suggests that additional work is required to fully understand the role of acetylation in flagella formation and motility.

The axonemal microtubules are also highly glutamylated (Bobinnec et al., 1999). The polyglutamylation of the axonemal B-tubule increases its negative charge. Since the inner dynein arms complexes are positively charged this may promote their transient interaction with the B-tubule providing a basic mechanism for driving sperm motility (Kubo et al., 2012; Kubo et al., 2010; Suryavanshi et al., 2010). On the other hand, the activity of the outer dynein arm is regulated by acetylation of α-tubulin Lys40 in the B-tubule that favors the unbound dissociation state (Alper et al., 2014) **(Figure 2)**.

The tubulin PTMs in spermatozoa occur either before or during their differentiation and maturation depending on species. In *Drosophila melanogaster*, most tubulin PTMs are already present in young and mature cysts, a germline stage that corresponds to spermatogonia and spermatocytes/spermatids, respectively. Tubulin (poly)glycylation however, is the only modification that occurs towards the end of spermatozoa maturation, specifically during *Drosophila melanogaster* sperm individualization, which is the physical separation of the 64 spermatids of the cyst into individual spermatozoa. (Bre et al., 1996; Bressac et al., 1995; Rogowski et al., 2009). Similar results were observed in *Paramecium* (Levilliers et al., 1995), suggesting that (poly)glycylation is the last modification occurring during the maturation of the male gamete. In mammals, there is also a differential expression of the tubulin family members (alpha, beta and gamma) and distribution of tubulin PTMs during the process of spermatozoa differentiation and maturation (Fouquet et al., 1998; Fouquet et al., 1997). In rats, the distribution of tyrosinated, detyrosinated and acetylated tubulins is specific for the different structures and cells of the seminiferous epithelium (spermatids, spermatocytes and Sertoli cells) (Hermo et al., 1991).

The distribution of tubulin PTMs along the sperm axoneme and in each of the microtubule doublets is not homogeneous (Mansir and Justine, 1998), generating a complex biochemical code that may promote transient and specific interactions with individual proteins. Polyglutamylation occurs on both the axoneme and the centrioles of mammalian spermatozoa at any stage of formation and maturation (Fouquet et al., 1994). However the length of the polyglutamate chains is not homogeneous along the sperm axoneme or in the outer and inner microtubule doublets in several organisms (Fouquet et al., 1996; Huitorel et al., 2002; Kann et al., 1995; Prigent et al., 1996). For instance, in mice and humans, the presence of branching glutamates decreases along the tail length but they are enriched at doublets 1, 5 and 6 as well as in the outer microtubule doublets versus the inner ones. The linear decrease of tubulin polyglutamylation along the sperm axoneme correlates with a decrease of dynein immunostaining (Fouquet et al., 1996; Kann et al., 1995; Prigent et al., 1996), in agreement with the proposed role of tubulin polyglutamylation in the regulation of the interaction of axonemal dynein with the microtubule doublets. However, data from other species suggest that this is not a general rule. Indeed, the distribution of this modification in the cilia of *Paramecium* (Pechart et al., 1999) is the opposite of the one

found in human sperm axonemes, reinforcing the observation that each tubulin PTMs pattern may be species specific.

The functional relevance of tubulin polyglutamylation in the flagella has been addressed in different model systems. In sea urchin sperm cells, blocking the glutamylation of tubulin with specific antibodies was found to induce a complete loss of sperm motility, by decreasing the amplitude of the flagellar beating, especially at its tip (Cosson et al., 1996; Mencarelli et al., 2004). Similar results were obtained after blocking dynein function, stressing the interdependency of dynein and tubulin mono/polyglutamylation for generating sperm motility. Interfering with the glutamylation-deglutamylation enzymes also has deleterious effects on sperm motility. In *Chlamydomonas,* the TTLL9-FAP234 protein complex is a tubulin polyglutamylase that determines the flagellar length (Kubo et al., 2014) by controlling tubulin turnover and thereby the axonemal stability (Kubo et al., 2015). In mice, mutations in one of the de-glutamylating enzymes, CCP1, result in male sterility associated with low concentration of spermatozoa that have an abnormal shape and motility (Fernandez-Gonzalez et al., 2002). On the other hand, mutations in mouse TTLL1 or TTLL5 (polyglutamylation), result in different levels of infertility, due to immotile spermatozoa or defects in progressive motility characterized by abnormal axonemal structures with shortened or absent flagella (Lee et al., 2013; Vogel et al., 2010). Therefore, it seems that the tight regulation of tubulin polyglutamylation is essential for spermatozoa functionality.

Mono/Polyglycylated tubulin is also strongly enriched in the axonemes of cilia and flagella (Mencarelli et al., 2000; Redeker et al., 1994). This tubulin PTM is preferentially found on the outer doublets 3 and 8 of the axonemes of mammalian spermatozoa, and like glutamylation it decreases towards the flagella tip (Pechart et al., 1999). In mammalian spermatozoa, monoglycylation is enriched in doublets 3 and 8 of the axoneme, whereas as described above, mono/polyglutamylation is enriched in doublets 1, 5 and 6. Since the two types of modifications compete for the same site on the tubulin sequence, they are mutually exclusive. Interestingly, in sea urchin sperm flagella, tyrosinated tubulin is mainly found at doublets 1, 5 and 6, that are polyglutamylated. Instead detyrosinated tubulin is enriched in doublets 3 and 8 (Kann et al., 1998; Multigner et al., 1996), that are those polyglycylated. Therefore, it seems that polyglutamylation and tyrosinated tubulin on one hand and detyrosination and polyglycylation on the other show some interdependence.

In sea urchin spermatozoa, blocking tubulin glycylation induces both motility and morphology defects, characterized by spermatozoa showing an erratic swimming movement with a reduction of the beating amplitude and frequency as well as an incorrect positioning of the sperm head during swimming (Bre et al., 1996).

The depletion of polyglycylases in different model organisms generates different defects. It was proposed that the polyglycyne chains help to reduce the negative charge of the C-terminal tails of alpha and beta tubulins, increasing microtubule stability (Bre et al., 1996). In *Drosophila melanogaster*, TTLL3 mutants show a male sterility phenotype characterized by only 2.4% of the males being able to generate some offsprings. Although the flagellum can assemble in these mutants, it is rapidly destabilized, either disassembling or becoming highly disorganized (Rogowski et al., 2009). In *Zebrafish,* the depletion of the same enzyme resulted in axonemes lacking the central microtubule doublets (Wloga et al., 2009) and thereby showing elongation and stability defects.

Interestingly, the transcription profiles of human teratozoospermic samples show alterations in the expression of various tubulin modifying enzymes. Most of these enzymes are down-regulated including TTLL5, TTLL6, TTLL7, TTLL9, TTLL13 pseudogene, CCP2 and CCP5 whereas another one SIRT2 is up-regulated. These data indicate that these teratozoospermic samples have lower levels of polyglutamylated and polyglycylated tubulin and higher levels of acetylated tubulin than normozoospermic ones. These changes most likely result in profound effects on the spermatozoa functionality, motility and/or axonemal stability, among others.

In summary, specific tubulin isotypes and PTMs are present in spermatozoa. Although there are differences in type and distribution in the axonemal microtubules in different species and cell types, all the data support the idea that they play an essential role in the differentiation, maturation and functionality of the spermatozoa in humans and other organisms.

Oocytes

In mammals, oocytes grow from a set of primordial germ cells (PGCs) during fetal life. Indeed, about seven million oocytes are formed within the first 7 months of fetal development, however, during the last two months of fetal development, this number

drops to less than 2 millions. Oocytes are arrested in the ovary at the Germinal Vesicle (GV) stage, i.e. the prophase of the first meiotic division, and remain in this stage until the woman reaches puberty. With the initiation of menstrual cycles, the monthly variations in follicle stimulating hormone (FSH) concentration, followed by a surge of luteinizing hormone (LH) recruit pools of follicles and the enclosed oocytes. As the follicles grow under FSH stimulation, the oocytes inside them prepare to sustain pre-implantation development. The LH surge triggers the exit from meiotic arrest and cytoplasmic maturation of the oocyte, and the ovulation of the follicle. In response to LH, the oocyte completes the first meiotic division, and extrudes half of the homologous chromosomes through the formation of the first polar body. The oocyte, arrested at the metaphase of meiosis II, leaves the follicles and awaits fertilization by a spermatozoon in the fallopian tubes. When fertilization occurs, the second meiotic division resumes.

One essential function of the microtubules in the oocyte is the assembly of the meiotic spindles. In most mammalian oocytes, including humans, the centrioles degenerate during maturation and the meiotic spindle assembly occurs in the absence of centrosomes. In this system the mechanism of spindle assembly relies therefore entirely on a microtubule assembly pathway triggered by RanGTP around the chromosomes (Cavazza and Vernos, 2015; Holubcova et al., 2015). Since spindle assembly and chromosome segregation involve numerous microtubule-associated proteins that regulate microtubule dynamics and organization, tubulin PTMs may provide a regulatory mechanism to determine the binding affinities of all these proteins. However, the identification and characterization of tubulin PTMs in the oocytes of model systems and in humans is still relatively poor due to the difficulties in sample collection in most cases, the limited availability of specific reagents and the transient state of tubulin PTMs. More information has been obtained for the tubulin PTMs present in mitotic spindles of somatic cells. All spindle microtubules are enriched in acetylated, polyglutamylated, tyrosinated and detyrosinated tubulin. Tubulin glycylation has not been detected. Interestingly, astral microtubules (which extend outward from the centrosome) and spindle microtubules (which form the bipolar spindle) are mostly tyrosinated whereas kinetochore microtubules (spindle microtubule attached to the chromosome kinetochores) are detyrosinated (Barisic et al., 2015; Bobinnec et al., 1998b; Geuens et al., 1986; Gundersen et al., 1984; Wilson and Forer, 1997). It is possible that similar patterns of tubulin PTMs exist in meiotic spindles but the only data

so far concern acetylated and tyrosinated tubulin. The pattern of tubulin acetylation varies with the different phases of cell division. It is high at the spindle poles in metaphase, distributed on the whole spindle in anaphase and restricted to the midbody in telophase (Matsubara et al., 2013; Schatten et al., 1988). During mouse oocyte activation, tubulin acetylation increases, due to a reduction of HDAC activity (Matsubara et al., 2013). Meiotic spindles are enriched in tyrosinated tubulin (de Pennart et al., 1988). Interestingly, CCP1 mutant female mice are subfertile and produce a reduced number of oocytes after ovarian stimulation. A reduction in ovary size at week 8 was also detected but no defects in oocyte meiotic spindle assembly and chromosome congression were found, probably because other CCPs could compensate the loss of CCP1 activity (Song et al., 2015). Overall, the data so far suggest that defects at the level of tubulin PTMs could account at least in part for the meiotic arrest of some oocytes. Further studies on the tubulin PTMs in oocytes will provide more insights into the mechanism of meiotic spindle assembly and chromosome segregation and reveal whether this may be the case.

The human oocyte contains mRNAs encoding several alpha tubulin isotypes (TUBAL3, TUBA1B, TUBA1C, TUBA3C, TUBA3D, TUBA3E and TUBA4B), but only one for beta tubulin: TUBB8. Recently, the genetic analysis of members of a family with female infertility problems along 4 generations revealed the existence of a mutation in their TUBB8 gene that is paternally transmitted. Further studies have identified other mutations in the same tubulin isotype gene in infertile women. These mutations are associated with oocyte maturation defects characterized by an abnormal or absent first meiotic spindle. Consistently, expression of the mutant forms of TUBB8 by microinjection of the mRNAs in mouse oocytes decreased significantly the extrusion of the polar body and this correlated with the presence of highly abnormal spindles (Feng et al., 2016a). Strikingly for two specific TUBB8 mutations, the oocytes extrude the first polar body but the 2nd meiotic spindle does not assemble. Once fertilized, the resulting embryos arrest at the cleavage stage (Feng et al., 2016b). Mechanistically, it was found that these mutations interfere with the folding and the assembly of the alpha-beta tubulin heterodimers. Moreover, the expression of these mutant forms of TUBB8 in somatic cells generate abnormal interphase microtubule networks. Future research should focus on the identification of mutations in tubulin isotypes with potential deleterious consequences on oocyte maturation and function.

Early embryos

Only a handful of articles have reported the tubulin isotypes and PTMs in embryos. In humans, several mRNAs encoding tubulin isotypes were identified in embryos: four encoding alpha tubulins (TUBA1A, TUBA1B, TUBA1C and TUBA3C) and six encoding beta tubulins (TUBB2A, TUBB2B, TUBB3, TUBB4A, TUBB4B and TUB6). Most of the information on tubulin PTMs in embryos has been obtained in model systems providing an experimental framework to address their function by interfering with specific enzymatic activities.

In mouse oocytes, microtubule acetylation has not been observed in interphase before fertilization but the first mitotic spindle of the zygote has acetylated microtubules particularly enriched at the spindle poles during metaphase (Matsubara et al., 2013; Schatten et al., 1988). Acetylated microtubules are also present at later stages of mouse early development. In humans, from the 8-cells to blastocyst stage, cells reorganize within the embryo and establish cell polarity by forming two differentiated cell layers, the extra-embryonic trophectoderm, which will give rise to the embryonic contribution to the placenta and extraembryonic tissues, and the inner cell mass (ICM), which will develop in the embryo proper. In mice (day E2.5 – E4.5), the mechanism driving cell internalization is mediated by differences in their surface contractility (Maitre et al., 2016) generated by the cortical tension (Samarage et al., 2015) and asymmetrical distribution of macromolecules such as PAR proteins between cell-contact domains (baso-lateral) versus non cell-contact domains (apical) (Vinot et al., 2005) (Korotkevich et al., 2017) by recruitment of the bipolar spindle by the apical domain. If the division plane is parallel to the apical domain, the daughter cell that receives the apical domain of the polarized mother cell will specialize as a trophectodermal cell, whereas the other daughter cell will be part of the inner cell mass (Johnson and Ziomek, 1981). The rapid and complex mechanism of cellular polarization also involves remodeling of the microtubule network that is very dynamic. At the 8-cell stage, the interphase cells on the outer layer are enriched in cytoplasmic and perinuclear microtubules. At the 16 and 32-cell stages, the cortex of the cells is enriched in acetylated microtubules, a pattern that is more pronounced in the inner cells (Houliston and Maro, 1989; Houliston et al., 1987).

3D cell cultures provide multiple advantages with respect to conventional 2D cell culture, as in living tissues exist in a 3D environment. This system is especially appropriate to address cell-cell and cell-extracellular matrix interaction and communication, cellular migration and polarization, and most of these processes are

essential during early embryo development. The pattern of tubulin PTMs has been characterized during the transition from 2D to 3D cell culture polarization of epithelial cells. It is characterized by a reduction of detyrosinated and polyglutamylated tubulin and an increase of acetylated tubulin (Quinones et al., 2011). Tubulin detyrosination has also been found to be essential for the differentiation of non-polarized cells into a polarized epithelial monolayer (Zink et al., 2012). Similar patterns and mechanisms may also exist in cells undergoing polarization during the early development of human embryos but it may be difficult to confirm this hypothesis due to experimental limitations.

Another essential function of the microtubules during development and in adult organisms is the formation of motile and primary cilia. Primary cilia have an axoneme without the central pair of microtubules which are present in motile cilia and flagella. Cilia play essential roles in development as transmitters of external osmotic and mechanical signals, and as key coordinators of signaling pathways, like Hedgehog, essential during development (Goetz and Anderson, 2010). Ciliary defects can promote alterations in organ laterality, hydrocephaly, cystic kidney disease and retinal degeneration, among others (Pazour et al., 2005). In mouse embryos, the primary cilia appear first at day 6 of development, in epiblast cells and subsequently in all the cells derived from them (Bangs et al., 2015). As mentioned above, the microtubules forming the axoneme of cilia are highly modified. In fact, the most common consequence of depleting tubulin modifying enzymes in any animal system is the formation of dysfunctional cilia with altered motility and/or structure. In *Zebrafish*, for instance, CCP5 depletion induces developmental errors such as body axis curvatures and hydrocephalus (Pathak et al., 2014) which are similar to the phenotypes observed upon depletion of TTLL3 and 6 (Pathak et al., 2011; Pathak et al., 2007). CCP1 protein mutation in mouse caused the *Purkinje cell degeneration* phenotype, which exhibits numerous adult defects such as degeneration of cerebellar Purkinje neurons and ataxia (Fernandez-Gonzalez et al., 2002). A tight balance of tubulin mono/polyglutamylation as well as mono/polyglycylacion appears therefore to be essential for embryo development, as well as for adult organisms. For example, only 50% of the *Drosophila melanogaster* mutants embryos for TTLL3 survive (Rogowski et al., 2009).

Altering the levels of tubulin acetylation also induces embryonic developmental defects associated with cilia dysfunctionalities. In *Zebrafish* embryos, for example, it produces

hydrocephaly, curved body shape, short body axis (Akella et al., 2010) and reduced rates of cilia assembly (Shida et al., 2010), among other phenotypes.

There are currently no available data on the other tubulin PTMs during early embryogenesis.

Future applications for ART:

For the past 4 decades, the parameters used to determine gametes and embryo quality have been chiefly morphological in nature, monitoring spermatozoa morphology, motility and concentration, polar body extrusion and dimorphisms in oocytes, and the timing and symmetry of the embryonic cell divisions. Relatively few molecular analyses to assess sperm and oocyte quality and early embryo development have been developed and validated so far. The pattern of the tubulin isotypes and their PTMs in the gametes and early embryos are emerging as putative useful markers for clinical applications. However, few experiments have still been performed in humans to establish a correlation between the tubulin isotypes and their PTMs with fertility. Here we summarize the most relevant data available.

Sperm cells:

Differences in the expression of tubulin isotypes have been observed in normozoospermic and teratozoospermic or asthenozoospermic sperm samples. Although there are no definitive evidences connecting these differences with defects in sperm morphology and motility, there is a strong correlation between the two phenomena. As previously discussed, multiple lines of evidence link tubulin PTMs to spermatozoa morphology, motility, and concentration as well as fertility in animal model systems. It would therefore be highly relevant to obtain a full description of the tubulin isotypes and their PTMs in infertile or subfertile patients by profiling the mRNAs encoding tubulins and the different modifying enzymes. These data will help to elucidate whether the deregulation of the tubulin PTMs and isotypes are a clinically significant cause of abnormal sperm morphology and/or motility.

Several data point to the importance of dynein and IFTs in gamete fitness. Dynein mutations were identified in sperm samples with low motility and dynein was found to be downregulated in teratozoospermic samples, causing axonemal ultrastructural defects

that cannot be detected by morphological analysis. Analyzing dynein sequence and expression levels could therefore be useful for diagnosis and prognosis, to evaluate the potential of successful embryo development and/or the transmission of a mutation to the offspring that may cause cilia defects that result in serious diseases such as primary ciliary dyskinesia (a motile cilia disorder). On the other hand, IFTs are essential for the sperm flagella formation but not for its maintenance. It would be extremely interesting to detect whether patients with samples that have these characteristics (typically categorized as teratozoospermic) carry any mutation in this supramolecular complex.

Oocytes:

The presence and importance of specific tubulin isotypes during oocyte maturation has also been observed in humans (Feng et al., 2016a). However, little research has been done in this direction. From the perspective of ART, it could be useful to sequence the TUBB8 gene of patients showing failures in oocyte maturation after controlled ovarian hyperstimulation and evaluate the potential of these data for diagnosis and prognosis. If TUBB8 mutation(s) are indeed indentified in these patients, oocyte donation could be considered.

Many human oocytes are aneuploid, but these defects cannot be detected with the conventional tools used in the clinic. Some of these aneuploidies may be due to cytoskeletal defects that could derive from mutations in the genes encoding tubulin isotypes and in PTMs modifying enzymes. It would therefore be useful to determine whether a correlation between these putative mutations and oocyte aneuploidy exists. This could easily be addressed by DNA sequencing from blood or saliva samples from patients. If a correlation is found this could be used to establish an oocyte likelihood score.

Preimplantation embryos:

Although knockouts for some of the tubulin PTMs enzymes in animal models can generate offsprings (albeit with different success rates and in some cases only after ART), these offsprings have multiple health problems, most of them due to cilia dysfunctions. Moreover, in most cases, these offsprings are infertile or subfertile. These data suggest that it would be essential to monitor the tubulin isotypes and PTMs of the progenitors, to avoid the transmission of deleterious mutations to the offsprings.

In addition, the identification of the causes for patient infertility could have an important and positive psychological implication, providing both an explanation for the infertile phenotype and closure to the patient.

Future perspectives:

So far, most research on tubulin isotypes and PTMs has been done in somatic cells and model organisms such as sea urchin, *Tetrahymena thermophila* and mice. The importance of tubulin isotypes and PTMs in human reproduction is far from being completely understood, but recent data in animal models and in humans, suggest that they have an important and direct functional role in reproduction. Therefore, the next immediate step is to obtain more data in human gametes and embryos through high-quality basic research, which could include single oocyte proteomics and single cell embryos qPCR, and then to translate the knowledge to the clinics.

A detailed analysis of tubulin PTMs in human spermatozoa is required in order to include molecular markers for sperm selection beyond those currently in use. First of all a panel for sperm tubulin isotypes and PTMs modifying enzymes expression, as well as tubulin PTMs presence along the sperm axoneme, should be performed in sperm cells with proven fertility. Once these data will be standardized, patient samples with different diagnosis can be analyzed and compared with the established standards. Furthermore it will be particularly relevant to compare normozoospermic samples with fertility problems, because although they are classified as "normal" in terms of morphology, motility and concentration, they could be aberrant at the molecular level.

Another point of analysis will be to compare motile versus non-motile sperm samples. Quantitative proteomics using iTRAQ labeling could be performed to detect different expression of the tubulin modifying enzymes. If their tubulin isotypes and PTMs expression and distribution patterns are different, the next step will be to compare capacitated and motile spermatozoa with different diagnosis to determine if their quality can be assessed molecularly.

In case mutations are found in the enzyme catalyzing tubulin PTMs, this could be addressed, in the future, by CRISPR/CAS9 technology (clustered regulatory interspaced short palindromic repeats/Cas9 genome editing technology) (Vassena et al., 2016). This

technology could be used in the spermatogonial sperm cells (SCC) to correct genetic defects in the proteins responsible of tubulin PTMs.

Data from the *Drosophila melanogaster* model suggest that polgyglycylation is the last modification occurring during the maturation of the male gamete. Sperm cells with lower levels of tubulin mono/polyglycylation could indicate that the sperm cell maturation was not fully completed. The level of maturation obtained by detecting mono/polyglycylation could also be correlated with other maturity defects, such as chromosome condensation. Monoglycylation could therefore be studied in patients and correlate this result with other processes occurring at the last steps of sperm maturation, with the final goal of using monoglycylation as a prognostic marker for sperm maturity.

In oocyte, beyond the analysis of the TUBB8 gene, the other alpha tubulin isotypes and their expression pattern could also be determined in patients with oocyte maturation problems. The tubulin isotype expression and the tubulin PTMs distribution of an *in vivo* matured MII oocyte could be compared to the oocytes matured *in vitro* to examine whether external factors, associated with the maturation media may induce changes. Another interesting question is whether the tubulin isotypes and PTMs may change in "old" oocytes respect to the younger ones. In aged oocytes, aneuploidy is a common alteration that can cause embryonic arrests at the pre- and post-implantation level, and spontaneous abortions. Many factors can contribute to the appearance of aneuploid oocytes, such as a higher concentration of reactive oxygen species (ROS), altered gene expression or a permissive SAC (spindle assembly checkpoint). It will be particularly relevant to address whether aging can also affect the expression and/or functionality of tubulin PTMs and isotypes. The abnormal expression of tubulin PTMs and isotypes would affect the binding and processivity of motor proteins necessary for the congression and/or separation of the chromosomes to the metaphase plate, as well as the correct assembly of the meiotic spindle. We posit that the analysis of tubulin isotypes and PTMs in human oocytes might provide answers to some of these questions.

The possibility to use CRISPR/CAS9 technology (Vassena et al., 2016) in oocytes and embryos (Tang et al., 2017) open the way to perform functional experiments in these systems and potentially to correct specific genomic defects. On the other hand, it was recently published the production of functional human oocytes generated by transferring

the genome of an MII oocyte polar body into a donor oocyte retrieved from its nucleus. These oocytes could be fertilized and developed up to blastocyst (Ma et al., 2017). This experimental approach opens the possibility to address not only the tubulin isotypes and PTMs expression and distribution from oocytes to blastocysts, but also the microtubule re-organization during cellular polarization. Moreover, a novel *in vitro* human embryo system (Deglincerti et al., 2016) (Shahbazi et al., 2016) was developed recently, which supports the development of embryos up to day 14 post-fertilization. This system opens multiple advantages as it can be used to study, for instance, how the cytoskeleton network (and therefore tubulin isotypes and PTMs) changes and drives implantation.

Concluding remarks:

The cytoskeleton is a key element for the proper organization of the cell, axoneme formation, intraflagellar transport, cell shape determination and cell division, among others. All these functions are in part regulated by the expression of various tubulin isotypes and by the combination of tubulin PTMs that altogether determine the interaction of MAPs and motor proteins with the microtubules. Defects in tubulin isotype expression and on their PTMs have profound consequences on many cytoskeletal dependent activities, such as sperm motility, flagella assembly and stabilization, oocyte maturation, pronuclear fusion and embryo early development **(Table 4)**. The characterization of these microtubule functionality regulators in human samples could provide novel molecular tools for assisted reproduction technologies.

Here we have reviewed the available information on tubulin isotypes and PTMs and their functional implications in the reproduction of animals and humans. These elements play essential roles for both gamete development and fitness and for the development of embryos. This emphasizes the importance to extend the tubulin isotypes and PTMs analysis to human samples, including sperm cells, oocytes and early embryos.

Authors' role

F.A. collected the information, designed the figures/tables and performed the analysis and writing of the manuscript. M.B. critically revised the manuscript and provided expert knowledge. R.V. and I.V. designed the concept and the figures/tables, provided expert knowledge and critically revised the manuscript. All authors have seen and approved the final version.

Acknowledgments

We want to thank all the members of Clínica Eugin and Vernos lab for critical discussion on the various aspects of the tubulin isotypes and PTMs in reproduction and their support in writing this review. We want to thank Désirée Garcia for their help in defining the research strategy as well as her advice during the manuscript preparation.

Conflict of interest

We declare no conflict of interest.

Bibliography:

Aillaud, C., C. Bosc, L. Peris, A. Bosson, P. Heemeryck, J. Van Dijk, J. Le Friec, B. Boulan, F. Vossier, L.E. Sanman, S. Syed, N. Amara, Y. Coute, L. Lafanechere, E. Denarier, C. Delphin, L. Pelletier, S. Humbert, M. Bogyo, A. Andrieux, K. Rogowski, and M.J. Moutin. 2017. Vasohibins/SVBP are tubulin carboxypeptidases (TCPs) that regulate neuron differentiation. *Science*. 358:1448-1453.

Akella, J.S., D. Wloga, J. Kim, N.G. Starostina, S. Lyons-Abbott, N.S. Morrissette, S.T. Dougan, E.T. Kipreos, and J. Gaertig. 2010. MEC-17 is an alpha-tubulin acetyltransferase. *Nature*. 467:218-222.

Alper, J.D., F. Decker, B. Agana, and J. Howard. 2014. The motility of axonemal dynein is regulated by the tubulin code. *Biophys J*. 107:2872-2880.

Arce, C.A., J.A. Rodriguez, H.S. Barra, and R. Caputo. 1975. Incorporation of L-tyrosine, L-phenylalanine and L-3,4-dihydroxyphenylalanine as single units into rat brain tubulin. *Eur J Biochem*. 59:145-149.

Asthana, J., S. Kapoor, R. Mohan, and D. Panda. 2013. Inhibition of HDAC6 deacetylase activity increases its binding with microtubules and suppresses microtubule dynamic instability in MCF-7 cells. *J Biol Chem*. 288:22516-22526.

Bangs, F.K., N. Schrode, A.K. Hadjantonakis, and K.V. Anderson. 2015. Lineage specificity of primary cilia in the mouse embryo. *Nat Cell Biol*. 17:113-122.

Barisic, M., R. Silva e Sousa, S.K. Tripathy, M.M. Magiera, A.V. Zaytsev, A.L. Pereira, C. Janke, E.L. Grishchuk, and H. Maiato. 2015. Mitosis. Microtubule detyrosination guides chromosomes during mitosis. *Science*. 348:799-803.

Basiri, M.L., A. Ha, A. Chadha, N.M. Clark, A. Polyanovsky, B. Cook, and T. Avidor-Reiss. 2014. A migrating ciliary gate compartmentalizes the site of axoneme assembly in Drosophila spermatids. *Curr Biol*. 24:2622-2631.

Ben Khelifa, M., C. Coutton, R. Zouari, T. Karaouzene, J. Rendu, M. Bidart, S. Yassine, V. Pierre, J. Delaroche, S. Hennebicq, D. Grunwald, D. Escalier, K. Pernet-Gallay, P.S. Jouk, N. Thierry-Mieg, A. Toure, C. Arnoult, and P.F. Ray. 2014. Mutations in DNAH1, which encodes an inner arm heavy chain dynein, lead to male infertility from multiple morphological abnormalities of the sperm flagella. *Am J Hum Genet*. 94:95-104.

Bhagwat, S., V. Dalvi, D. Chandrasekhar, T. Matthew, K. Acharya, R. Gajbhiye, V. Kulkarni, S. Sonawane, M. Ghosalkar, and P. Parte. 2014. Acetylated alpha-tubulin is reduced in individuals with poor sperm motility. *Fertil Steril*. 101:95-104 e103.

Bobinnec, Y., C. Marcaillou, and A. Debec. 1999. Microtubule polyglutamylation in Drosophila melanogaster brain and testis. *Eur J Cell Biol*. 78:671-674.

Bobinnec, Y., M. Moudjou, J.P. Fouquet, E. Desbruyeres, B. Edde, and M. Bornens. 1998. Glutamylation of centriole and cytoplasmic tubulin in proliferating non-neuronal cells. *Cell Motil Cytoskeleton*. 39:223-232.

Bonnet, C., D. Boucher, S. Lazereg, B. Pedrotti, K. Islam, P. Denoulet, and J.C. Larcher. 2001. Differential binding regulation of microtubule-associated proteins MAP1A, MAP1B, and MAP2 by tubulin polyglutamylation. *J Biol Chem*. 276:12839-12848.

Boucher, D., J.C. Larcher, F. Gros, and P. Denoulet. 1994. Polyglutamylation of tubulin as a progressive regulator of in vitro interactions between the microtubule-associated protein Tau and tubulin. *Biochemistry*. 33:12471-12477.

Bre, M.H., V. Redeker, M. Quibell, J. Darmanaden-Delorme, C. Bressac, J. Cosson, P. Huitorel, J.M. Schmitter, J. Rossler, T. Johnson, A. Adoutte, and N. Levilliers. 1996. Axonemal tubulin polyglycylation probed with two monoclonal antibodies: widespread evolutionary distribution, appearance during spermatozoan maturation and possible function in motility. *J Cell Sci*. 109 (Pt 4):727-738.

Bre, M.H., V. Redeker, J. Vinh, J. Rossier, and N. Levilliers. 1998. Tubulin polyglycylation: differential posttranslational modification of dynamic cytoplasmic and stable axonemal microtubules in paramecium. *Mol Biol Cell*. 9:2655-2665.

Bressac, C., M.H. Bre, J. Darmanaden-Delorme, M. Laurent, N. Levilliers, and A. Fleury. 1995. A massive new posttranslational modification occurs on axonemal tubulin at the final step of spermatogenesis in Drosophila. *Eur J Cell Biol*. 67:346-355.

Brokaw, C.J. 1972. Flagellar movement: a sliding filament model. *Science*. 178:455-462.

Brunke, K.J., P.S. Collis, and D.P. Weeks. 1982. Post-translational modification of tubulin dependent on organelle assembly. *Nature*. 297:516-518.

Callen, A.M., A. Adoutte, J.M. Andrew, A. Baroin-Tourancheau, M.H. Bre, P.C. Ruiz, J.C. Clerot, P. Delgado, A. Fleury, R. Jeanmaire-Wolf, and et al. 1994. Isolation and characterization of libraries of monoclonal antibodies directed against various forms of tubulin in Paramecium. *Biol Cell*. 81:95-119.

Cavazza, T., and I. Vernos. 2015. The RanGTP Pathway: From Nucleo-Cytoplasmic Transport to Spindle Assembly and Beyond. *Front Cell Dev Biol*. 3:82.

Chang, P., and T. Stearns. 2000. Delta-tubulin and epsilon-tubulin: two new human centrosomal tubulins reveal new aspects of centrosome structure and function. *Nat Cell Biol*. 2:30-35.

Choudhary, C., C. Kumar, F. Gnad, M.L. Nielsen, M. Rehman, T.C. Walther, J.V. Olsen, and M. Mann. 2009. Lysine acetylation targets protein complexes and co-regulates major cellular functions. *Science*. 325:834-840.

Chu, C.W., F. Hou, J. Zhang, L. Phu, A.V. Loktev, D.S. Kirkpatrick, P.K. Jackson, Y. Zhao, and H. Zou. 2011. A novel acetylation of beta-tubulin by San modulates microtubule polymerization via down-regulating tubulin incorporation. *Mol Biol Cell*. 22:448-456.

Conacci-Sorrell, M., C. Ngouenet, and R.N. Eisenman. 2010. Myc-nick: a cytoplasmic cleavage product of Myc that promotes alpha-tubulin acetylation and cell differentiation. *Cell*. 142:480-493.

Coombes, C., A. Yamamoto, M. McClellan, T.A. Reid, M. Plooster, G.W. Luxton, J. Alper, J. Howard, and M.K. Gardner. 2016. Mechanism of microtubule lumen entry for the alpha-tubulin acetyltransferase enzyme alphaTAT1. *Proc Natl Acad Sci U S A*. 113:E7176-E7184.

Cosson, J., D. White, P. Huitorel, B. Edde, C. Cibert, S. Audebert, and C. Gagnon. 1996. Inhibition of flagellar beat frequency by a new anti-beta-tubulin antibody. *Cell Motil Cytoskeleton*. 35:100-112.

Creppe, C., L. Malinouskaya, M.L. Volvert, M. Gillard, P. Close, O. Malaise, S. Laguesse, I. Cornez, S. Rahmouni, S. Ormenese, S. Belachew, B. Malgrange, J.P. Chapelle, U. Siebenlist, G. Moonen, A. Chariot, and L. Nguyen. 2009. Elongator controls the migration and differentiation of cortical neurons through acetylation of alpha-tubulin. *Cell*. 136:551-564.

Cueva, J.G., J. Hsin, K.C. Huang, and M.B. Goodman. 2012. Posttranslational acetylation of alpha-tubulin constrains protofilament number in native microtubules. *Curr Biol*. 22:1066-1074.

de Pennart, H., E. Houliston, and B. Maro. 1988. Post-translational modifications of tubulin and the dynamics of microtubules in mouse oocytes and zygotes. *Biol Cell*. 64:375-378.

Deglincerti, A., G.F. Croft, L.N. Pietila, M. Zernicka-Goetz, E.D. Siggia, and A.H. Brivanlou. 2016. Self-organization of the in vitro attached human embryo. *Nature*. 533:251-254.

Denoulet, P., B. Edde, and F. Gros. 1986. Differential expression of several neurospecific beta-tubulin mRNAs in the mouse brain during development. *Gene*. 50:289-297.

Duquesnoy, P., E. Escudier, L. Vincensini, J. Freshour, A.M. Bridoux, A. Coste, A. Deschildre, J. de Blic, M. Legendre, G. Montantin, H. Tenreiro, A.M. Vojtek, C. Loussert, A. Clement, D. Escalier, P. Bastin, D.R. Mitchell, and S. Amselem. 2009. Loss-of-function mutations in the human ortholog of Chlamydomonas reinhardtii ODA7 disrupt dynein arm assembly and cause primary ciliary dyskinesia. *Am J Hum Genet*. 85:890-896.

Edde, B., J. Rossier, J.P. Le Caer, E. Desbruyeres, F. Gros, and P. Denoulet. 1990. Posttranslational glutamylation of alpha-tubulin. *Science*. 247:83-85.

Edde, B., J. Rossier, J.P. Le Caer, J.C. Prome, E. Desbruyeres, F. Gros, and P. Denoulet. 1992. Polyglutamylated alpha-tubulin can enter the tyrosination/detyrosination cycle. *Biochemistry*. 31:403-410.

Ersfeld, K., J. Wehland, U. Plessmann, H. Dodemont, V. Gerke, and K. Weber. 1993. Characterization of the tubulin-tyrosine ligase. *J Cell Biol*. 120:725-732.

Fawcett, D.W. 1975. The mammalian spermatozoon. *Dev Biol*. 44:394-436.

Feng, R., Q. Sang, Y. Kuang, X. Sun, Z. Yan, S. Zhang, J. Shi, G. Tian, A. Luchniak, Y. Fukuda, B. Li, M. Yu, J. Chen, Y. Xu, L. Guo, R. Qu, X. Wang, Z. Sun, M. Liu, H. Shi, H. Wang, Y. Feng, R. Shao, R. Chai, Q. Li, Q. Xing, R. Zhang, E. Nogales, L. Jin, L. He, M.L. Gupta, Jr., N.J. Cowan, and L. Wang. 2016a. Mutations in TUBB8 and Human Oocyte Meiotic Arrest. *N Engl J Med*. 374:223-232.

Feng, R., Z. Yan, B. Li, M. Yu, Q. Sang, G. Tian, Y. Xu, B. Chen, R. Qu, Z. Sun, X. Sun, L. Jin, L. He, Y. Kuang, N.J. Cowan, and L. Wang. 2016b. Mutations in TUBB8 cause a multiplicity of phenotypes in human oocytes and early embryos. *J Med Genet*.

Fernandez-Gonzalez, A., A.R. La Spada, J. Treadaway, J.C. Higdon, B.S. Harris, R.L. Sidman, J.I. Morgan, and J. Zuo. 2002. Purkinje cell degeneration (pcd) phenotypes caused by mutations in the axotomy-induced gene, Nna1. *Science*. 295:1904-1906.

Fliegauf, M., H. Olbrich, J. Horvath, J.H. Wildhaber, M.A. Zariwala, M. Kennedy, M.R. Knowles, and H. Omran. 2005. Mislocalization of DNAH5 and DNAH9 in respiratory cells from patients with primary ciliary dyskinesia. *Am J Respir Crit Care Med*. 171:1343-1349.

Fouquet, J.P., B. Edde, M.L. Kann, A. Wolff, E. Desbruyeres, and P. Denoulet. 1994. Differential distribution of glutamylated tubulin during spermatogenesis in mammalian testis. *Cell Motil Cytoskeleton*. 27:49-58.

Fouquet, J.P., M.L. Kann, C. Combeau, and R. Melki. 1998. Gamma-tubulin during the differentiation of spermatozoa in various mammals and man. *Mol Hum Reprod*. 4:1122-1129.

Fouquet, J.P., M.L. Kann, I. Pechart, and Y. Prigent. 1997. Expression of tubulin isoforms during the differentiation of mammalian spermatozoa. *Tissue Cell*. 29:573-583.

Fouquet, J.P., Y. Prigent, and M.L. Kann. 1996. Comparative immunogold analysis of tubulin isoforms in the mouse sperm flagellum: unique distribution of glutamylated tubulin. *Mol Reprod Dev*. 43:358-365.

Geuens, G., G.G. Gundersen, R. Nuydens, F. Cornelissen, J.C. Bulinski, and M. DeBrabander. 1986. Ultrastructural colocalization of tyrosinated and detyrosinated alpha-tubulin in interphase and mitotic cells. *J Cell Biol*. 103:1883-1893.

Gibbons, I.R., and A.J. Rowe. 1965. Dynein: A Protein with Adenosine Triphosphatase Activity from Cilia. *Science*. 149:424-426.

Goetz, S.C., and K.V. Anderson. 2010. The primary cilium: a signalling centre during vertebrate development. *Nat Rev Genet*. 11:331-344.

Gu, W., S.A. Lewis, and N.J. Cowan. 1988. Generation of antisera that discriminate among mammalian alpha-tubulins: introduction of specialized isotypes into cultured cells results in their coassembly without disruption of normal microtubule function. *J Cell Biol*. 106:2011-2022.

Gundersen, G.G., M.H. Kalnoski, and J.C. Bulinski. 1984. Distinct populations of microtubules: tyrosinated and nontyrosinated alpha tubulin are distributed differently in vivo. *Cell*. 38:779-789.

Gundersen, G.G., S. Khawaja, and J.C. Bulinski. 1987. Postpolymerization detyrosination of alpha-tubulin: a mechanism for subcellular differentiation of microtubules. *J Cell Biol*. 105:251-264.

Hallak, M.E., J.A. Rodriguez, H.S. Barra, and R. Caputto. 1977. Release of tyrosine from tyrosinated tubulin. Some common factors that affect this process and the assembly of tubulin. *FEBS Lett*. 73:147-150.

Han, Y.G., B.H. Kwok, and M.J. Kernan. 2003. Intraflagellar transport is required in Drosophila to differentiate sensory cilia but not sperm. *Curr Biol*. 13:1679-1686.

Harris, A., J.I. Morgan, M. Pecot, A. Soumare, A. Osborne, and H.D. Soares. 2000. Regenerating motor neurons express Nna1, a novel ATP/GTP-binding protein related to zinc carboxypeptidases. *Mol Cell Neurosci*. 16:578-596.

Hermo, L., R. Oko, and N.B. Hecht. 1991. Differential post-translational modifications of microtubules in cells of the seminiferous epithelium of the rat: a light and electron microscope immunocytochemical study. *Anat Rec*. 229:31-50.

Holubcova, Z., M. Blayney, K. Elder, and M. Schuh. 2015. Human oocytes. Error-prone chromosome-mediated spindle assembly favors chromosome segregation defects in human oocytes. *Science*. 348:1143-1147.

Houliston, E., and B. Maro. 1989. Posttranslational modification of distinct microtubule subpopulations during cell polarization and differentiation in the mouse preimplantation embryo. *J Cell Biol*. 108:543-551.

Houliston, E., S.J. Pickering, and B. Maro. 1987. Redistribution of microtubules and pericentriolar material during the development of polarity in mouse blastomeres. *J Cell Biol*. 104:1299-1308.

Howes, S.C., G.M. Alushin, T. Shida, M.V. Nachury, and E. Nogales. 2014. Effects of tubulin acetylation and tubulin acetyltransferase binding on microtubule structure. *Mol Biol Cell*. 25:257-266.

Hubbert, C., A. Guardiola, R. Shao, Y. Kawaguchi, A. Ito, A. Nixon, M. Yoshida, X.F. Wang, and T.P. Yao. 2002. HDAC6 is a microtubule-associated deacetylase. *Nature*. 417:455-458.

Huitorel, P., D. White, J.P. Fouquet, M.L. Kann, J. Cosson, and C. Gagnon. 2002. Differential distribution of glutamylated tubulin isoforms along the sea urchin sperm axoneme. *Mol Reprod Dev*. 62:139-148.

Hurd, D.D., R.M. Miller, L. Nunez, and D.S. Portman. 2010. Specific alpha- and beta-tubulin isotypes optimize the functions of sensory Cilia in Caenorhabditis elegans. *Genetics*. 185:883-896.

Iftode, F., J.C. Clerot, N. Levilliers, and M.H. Bre. 2000. Tubulin polyglycylation: a morphogenetic marker in ciliates. *Biol Cell*. 92:615-628.

Ishikawa, T., H. Sakakibara, and K. Oiwa. 2007. The architecture of outer dynein arms in situ. *J Mol Biol*. 368:1249-1258.

Janke, C., K. Rogowski, D. Wloga, C. Regnard, A.V. Kajava, J.M. Strub, N. Temurak, J. van Dijk, D. Boucher, A. van Dorsselaer, S. Suryavanshi, J. Gaertig, and B. Edde. 2005. Tubulin polyglutamylase enzymes are members of the TTL domain protein family. *Science*. 308:1758-1762.

Johnson, M.H., and C.A. Ziomek. 1981. The foundation of two distinct cell lineages within the mouse morula. *Cell*. 24:71-80.

Kalebic, N., S. Sorrentino, E. Perlas, G. Bolasco, C. Martinez, and P.A. Heppenstall. 2013. alphaTAT1 is the major alpha-tubulin acetyltransferase in mice. *Nat Commun*. 4:1962.

Kalinina, E., R. Biswas, I. Berezniuk, A. Hermoso, F.X. Aviles, and L.D. Fricker. 2007. A novel subfamily of mouse cytosolic carboxypeptidases. *FASEB J*. 21:836-850.

Kann, M.L., Y. Prigent, and J.P. Fouquet. 1995. Differential distribution of glutamylated tubulin in the flagellum of mouse spermatozoa. *Tissue Cell*. 27:323-329.

Kann, M.L., Y. Prigent, N. Levilliers, M.H. Bre, and J.P. Fouquet. 1998. Expression of glycylated tubulin during the differentiation of spermatozoa in mammals. *Cell Motil Cytoskeleton*. 41:341-352.

Kollman, J.M., A. Merdes, L. Mourey, and D.A. Agard. 2011. Microtubule nucleation by gamma-tubulin complexes. *Nat Rev Mol Cell Biol*. 12:709-721.

Kollman, J.M., J.K. Polka, A. Zelter, T.N. Davis, and D.A. Agard. 2010. Microtubule nucleating gamma-TuSC assembles structures with 13-fold microtubule-like symmetry. *Nature*. 466:879-882.

Korotkevich, E., R. Niwayama, A. Courtois, S. Friese, N. Berger, F. Buchholz, and T. Hiiragi. 2017. The Apical Domain Is Required and Sufficient for the First Lineage Segregation in the Mouse Embryo. *Dev Cell*. 40:235-247 e237.

Kott, E., P. Duquesnoy, B. Copin, M. Legendre, F. Dastot-Le Moal, G. Montantin, L. Jeanson, A. Tamalet, J.F. Papon, J.P. Siffroi, N. Rives, V. Mitchell, J. de Blic, A. Coste, A. Clement, D. Escalier, A. Toure, E. Escudier, and S. Amselem. 2012. Loss-of-function mutations in LRRC6, a gene essential for proper axonemal assembly of inner and outer dynein arms, cause primary ciliary dyskinesia. *Am J Hum Genet*. 91:958-964.

Kozminski, K.G., P.L. Beech, and J.L. Rosenbaum. 1995. The Chlamydomonas kinesin-like protein FLA10 is involved in motility associated with the flagellar membrane. *J Cell Biol*. 131:1517-1527.

Kreis, T.E. 1987. Microtubules containing detyrosinated tubulin are less dynamic. *EMBO J*. 6:2597-2606.

Kubo, T., M. Hirono, T. Aikawa, R. Kamiya, and G.B. Witman. 2015. Reduced tubulin polyglutamylation suppresses flagellar shortness in Chlamydomonas. *Mol Biol Cell*. 26:2810-2822.

Kubo, T., T. Yagi, and R. Kamiya. 2012. Tubulin polyglutamylation regulates flagellar motility by controlling a specific inner-arm dynein that interacts with the dynein regulatory complex. *Cytoskeleton (Hoboken)*. 69:1059-1068.

Kubo, T., H.A. Yanagisawa, Z. Liu, R. Shibuya, M. Hirono, and R. Kamiya. 2014. A conserved flagella-associated protein in Chlamydomonas, FAP234, is essential for axonemal localization of tubulin polyglutamylase TTLL9. *Mol Biol Cell*. 25:107-117.

Kubo, T., H.A. Yanagisawa, T. Yagi, M. Hirono, and R. Kamiya. 2010. Tubulin polyglutamylation regulates axonemal motility by modulating activities of inner-arm dyneins. *Curr Biol*. 20:441-445.

L'Hernault, S.W., and J.L. Rosenbaum. 1983. Chlamydomonas alpha-tubulin is posttranslationally modified in the flagella during flagellar assembly. *J Cell Biol*. 97:258-263.

L'Hernault, S.W., and J.L. Rosenbaum. 1985a. Chlamydomonas alpha-tubulin is posttranslationally modified by acetylation on the epsilon-amino group of a lysine. *Biochemistry*. 24:473-478.

L'Hernault, S.W., and J.L. Rosenbaum. 1985b. Reversal of the posttranslational modification on Chlamydomonas flagellar alpha-tubulin occurs during flagellar resorption. *J Cell Biol*. 100:457-462.

Lechtreck, K.F., J.M. Brown, J.L. Sampaio, J.M. Craft, A. Shevchenko, J.E. Evans, and G.B. Witman. 2013. Cycling of the signaling protein phospholipase D through cilia requires the BBSome only for the export phase. *J Cell Biol*. 201:249-261.

Lechtreck, K.F., E.C. Johnson, T. Sakai, D. Cochran, B.A. Ballif, J. Rush, G.J. Pazour, M. Ikebe, and G.B. Witman. 2009. The Chlamydomonas reinhardtii BBSome is

an IFT cargo required for export of specific signaling proteins from flagella. *J Cell Biol*. 187:1117-1132.

Lee, G.S., Y. He, E.J. Dougherty, M. Jimenez-Movilla, M. Avella, S. Grullon, D.S. Sharlin, C. Guo, J.A. Blackford, Jr., S. Awasthi, Z. Zhang, S.P. Armstrong, E.C. London, W. Chen, J. Dean, and S.S. Simons, Jr. 2013. Disruption of Ttll5/stamp gene (tubulin tyrosine ligase-like protein 5/SRC-1 and TIF2-associated modulatory protein gene) in male mice causes sperm malformation and infertility. *J Biol Chem*. 288:15167-15180.

Lehti, M.S., N. Kotaja, and A. Sironen. 2013. KIF3A is essential for sperm tail formation and manchette function. *Mol Cell Endocrinol*. 377:44-55.

Levilliers, N., A. Fleury, and A.M. Hill. 1995. Monoclonal and polyclonal antibodies detect a new type of post-translational modification of axonemal tubulin. *J Cell Sci*. 108 (Pt 9):3013-3028.

Lewis, S.A., W. Gu, and N.J. Cowan. 1987. Free intermingling of mammalian beta-tubulin isotypes among functionally distinct microtubules. *Cell*. 49:539-548.

Lewis, S.A., M.G. Lee, and N.J. Cowan. 1985. Five mouse tubulin isotypes and their regulated expression during development. *J Cell Biol*. 101:852-861.

Lindemann, C.B., and K.A. Lesich. 2010. Flagellar and ciliary beating: the proven and the possible. *J Cell Sci*. 123:519-528.

Lindemann, C.B., and K.A. Lesich. 2016. Functional anatomy of the mammalian sperm flagellum. *Cytoskeleton (Hoboken)*. 73:652-669.

Ly, N., N. Elkhatib, E. Bresteau, O. Pietrement, M. Khaled, M.M. Magiera, C. Janke, E. Le Cam, A.D. Rutenberg, and G. Montagnac. 2016. alphaTAT1 controls longitudinal spreading of acetylation marks from open microtubules extremities. *Sci Rep*. 6:35624.

Ma, H., R.C. O'Neil, N. Marti Gutierrez, M. Hariharan, Z.Z. Zhang, Y. He, C. Cinnioglu, R. Kayali, E. Kang, Y. Lee, T. Hayama, A. Koski, J. Nery, R. Castanon, R. Tippner-Hedges, R. Ahmed, C. Van Dyken, Y. Li, S. Olson, D. Battaglia, D.M. Lee, D.H. Wu, P. Amato, D.P. Wolf, J.R. Ecker, and S. Mitalipov. 2017. Functional Human Oocytes Generated by Transfer of Polar Body Genomes. *Cell Stem Cell*. 20:112-119.

Maitre, J.L., H. Turlier, R. Illukkumbura, B. Eismann, R. Niwayama, F. Nedelec, and T. Hiiragi. 2016. Asymmetric division of contractile domains couples cell positioning and fate specification. *Nature*. 536:344-348.

Mansir, A., and J.L. Justine. 1998. The microtubular system and posttranslationally modified tubulin during spermatogenesis in a parasitic nematode with amoeboid and aflagellate spermatozoa. *Mol Reprod Dev*. 49:150-167.

Maruta, H., K. Greer, and J.L. Rosenbaum. 1986. The acetylation of alpha-tubulin and its relationship to the assembly and disassembly of microtubules. *J Cell Biol*. 103:571-579.

Mary, J., V. Redeker, J.P. Le Caer, J. Rossier, and J.M. Schmitter. 1996. Posttranslational modifications in the C-terminal tail of axonemal tubulin from sea urchin sperm. *J Biol Chem*. 271:9928-9933.

Mary, J., V. Redeker, J.P. Le Caer, J. Rossier, and J.M. Schmitter. 1997. Posttranslational modifications of axonemal tubulin. *J Protein Chem*. 16:403-407.

Matsubara, K., A.R. Lee, S. Kishigami, A. Ito, K. Matsumoto, H. Chi, N. Nishino, M. Yoshida, and Y. Hosoi. 2013. Dynamics and regulation of lysine-acetylation during one-cell stage mouse embryos. *Biochem Biophys Res Commun*. 434:1-7.

Matsuyama, A., T. Shimazu, Y. Sumida, A. Saito, Y. Yoshimatsu, D. Seigneurin-Berny, H. Osada, Y. Komatsu, N. Nishino, S. Khochbin, S. Horinouchi, and M. Yoshida. 2002. In vivo destabilization of dynamic microtubules by HDAC6-mediated deacetylation. *EMBO J*. 21:6820-6831.

Mencarelli, C., M.H. Bre, N. Levilliers, and R. Dallai. 2000. Accessory tubules and axonemal microtubules of Apis mellifera sperm flagellum differ in their tubulin isoform content. *Cell Motil Cytoskeleton*. 47:1-12.

Mencarelli, C., D. Caroti, M.H. Bre, N. Levilliers, D. Mercati, L.G. Robbins, and R. Dallai. 2004. Glutamylated and glycylated tubulin isoforms in the aberrant sperm axoneme of the gall-midge fly, Asphondylia ruebsaameni. *Cell Motil Cytoskeleton*. 58:160-174.

Multigner, L., I. Pignot-Paintrand, Y. Saoudi, D. Job, U. Plessmann, M. Rudiger, and K. Weber. 1996. The A and B tubules of the outer doublets of sea urchin sperm axonemes are composed of different tubulin variants. *Biochemistry*. 35:10862-10871.

Murofushi, H. 1980. Purification and characterization of tubulin-tyrosine ligase from porcine brain. *J Biochem*. 87:979-984.

Nachury, M.V., A.V. Loktev, Q. Zhang, C.J. Westlake, J. Peranen, A. Merdes, D.C. Slusarski, R.H. Scheller, J.F. Bazan, V.C. Sheffield, and P.K. Jackson. 2007. A core complex of BBS proteins cooperates with the GTPase Rab8 to promote ciliary membrane biogenesis. *Cell*. 129:1201-1213.

Nahhas, F., S.C. Dryden, J. Abrams, and M.A. Tainsky. 2007. Mutations in SIRT2 deacetylase which regulate enzymatic activity but not its interaction with HDAC6 and tubulin. *Mol Cell Biochem*. 303:221-230.

Neesen, J., R. Kirschner, M. Ochs, A. Schmiedl, B. Habermann, C. Mueller, A.F. Holstein, T. Nuesslein, I. Adham, and W. Engel. 2001. Disruption of an inner arm dynein heavy chain gene results in asthenozoospermia and reduced ciliary beat frequency. *Hum Mol Genet*. 10:1117-1128.

Nicastro, D., C. Schwartz, J. Pierson, R. Gaudette, M.E. Porter, and J.R. McIntosh. 2006. The molecular architecture of axonemes revealed by cryoelectron tomography. *Science*. 313:944-948.

Nogales, E., M. Whittaker, R.A. Milligan, and K.H. Downing. 1999. High-resolution model of the microtubule. *Cell*. 96:79-88.

North, B.J., B.L. Marshall, M.T. Borra, J.M. Denu, and E. Verdin. 2003. The human Sir2 ortholog, SIRT2, is an NAD+-dependent tubulin deacetylase. *Mol Cell*. 11:437-444.

Ohkawa, N., S. Sugisaki, E. Tokunaga, K. Fujitani, T. Hayasaka, M. Setou, and K. Inokuchi. 2008. N-acetyltransferase ARD1-NAT1 regulates neuronal dendritic development. *Genes Cells*. 13:1171-1183.

Ostrowski, L.E., K. Blackburn, K.M. Radde, M.B. Moyer, D.M. Schlatzer, A. Moseley, and R.C. Boucher. 2002. A proteomic analysis of human cilia: identification of novel components. *Mol Cell Proteomics*. 1:451-465.

Otero, A., M. Rodriguez de la Vega, S. Tanco, J. Lorenzo, F.X. Aviles, and D. Reverter. 2012. The novel structure of a cytosolic M14 metallocarboxypeptidase (CCP) from Pseudomonas aeruginosa: a model for mammalian CCPs. *FASEB J*. 26:3754-3764.

Patel, V.P., and C.T. Chu. 2014. Decreased SIRT2 activity leads to altered microtubule dynamics in oxidatively-stressed neuronal cells: implications for Parkinson's disease. *Exp Neurol*. 257:170-181.

Pathak, N., C.A. Austin, and I.A. Drummond. 2011. Tubulin tyrosine ligase-like genes ttll3 and ttll6 maintain zebrafish cilia structure and motility. *J Biol Chem*. 286:11685-11695.

Pathak, N., C.A. Austin-Tse, Y. Liu, A. Vasilyev, and I.A. Drummond. 2014. Cytoplasmic carboxypeptidase 5 regulates tubulin glutamylation and zebrafish cilia formation and function. *Mol Biol Cell*. 25:1836-1844.

Pathak, N., T. Obara, S. Mangos, Y. Liu, and I.A. Drummond. 2007. The zebrafish fleer gene encodes an essential regulator of cilia tubulin polyglutamylation. *Mol Biol Cell*. 18:4353-4364.

Paturle-Lafanechere, L., B. Edde, P. Denoulet, A. Van Dorsselaer, H. Mazarguil, J.P. Le Caer, J. Wehland, and D. Job. 1991. Characterization of a major brain tubulin variant which cannot be tyrosinated. *Biochemistry*. 30:10523-10528.

Paturle-Lafanechere, L., M. Manier, N. Trigault, F. Pirollet, H. Mazarguil, and D. Job. 1994. Accumulation of delta 2-tubulin, a major tubulin variant that cannot be tyrosinated, in neuronal tissues and in stable microtubule assemblies. *J Cell Sci*. 107 (Pt 6):1529-1543.

Pazour, G.J., N. Agrin, J. Leszyk, and G.B. Witman. 2005. Proteomic analysis of a eukaryotic cilium. *J Cell Biol*. 170:103-113.

Pazour, G.J., B.L. Dickert, and G.B. Witman. 1999. The DHC1b (DHC2) isoform of cytoplasmic dynein is required for flagellar assembly. *J Cell Biol*. 144:473-481.

Pechart, I., M.L. Kann, N. Levilliers, M.H. Bre, and J.P. Fouquet. 1999. Composition and organization of tubulin isoforms reveals a variety of axonemal models. *Biol Cell*. 91:685-697.

Pereira, R., R. Sa, A. Barros, and M. Sousa. 2017. Major regulatory mechanisms involved in sperm motility. *Asian J Androl*. 19:5-14.

Peris, L., M. Wagenbach, L. Lafanechere, J. Brocard, A.T. Moore, F. Kozielski, D. Job, L. Wordeman, and A. Andrieux. 2009. Motor-dependent microtubule disassembly driven by tubulin tyrosination. *J Cell Biol*. 185:1159-1166.

Piperno, G., and M.T. Fuller. 1985. Monoclonal antibodies specific for an acetylated form of alpha-tubulin recognize the antigen in cilia and flagella from a variety of organisms. *J Cell Biol*. 101:2085-2094.

Piperno, G., M. LeDizet, and X.J. Chang. 1987. Microtubules containing acetylated alpha-tubulin in mammalian cells in culture. *J Cell Biol*. 104:289-302.

Plessmann, U., and K. Weber. 1997. Mammalian sperm tubulin: an exceptionally large number of variants based on several posttranslational modifications. *J Protein Chem*. 16:385-390.

Popodi, E.M., H.D. Hoyle, F.R. Turner, and E.C. Raff. 2005. The proximal region of the beta-tubulin C-terminal tail is sufficient for axoneme assembly. *Cell Motil Cytoskeleton*. 62:48-64.

Popodi, E.M., H.D. Hoyle, F.R. Turner, K. Xu, S. Kruse, and E.C. Raff. 2008. Axoneme specialization embedded in a "generalist" beta-tubulin. *Cell Motil Cytoskeleton*. 65:216-237.

Porter, M.E., R. Bower, J.A. Knott, P. Byrd, and W. Dentler. 1999. Cytoplasmic dynein heavy chain 1b is required for flagellar assembly in Chlamydomonas. *Mol Biol Cell*. 10:693-712.

Prigent, Y., M.L. Kann, H. Lach-Gar, I. Pechart, and J.P. Fouquet. 1996. Glutamylated tubulin as a marker of microtubule heterogeneity in the human sperm flagellum. *Mol Hum Reprod*. 2:573-581.

Quinones, G.B., B.A. Danowski, A. Devaraj, V. Singh, and L.A. Ligon. 2011. The posttranslational modification of tubulin undergoes a switch from detyrosination to acetylation as epithelial cells become polarized. *Mol Biol Cell*. 22:1045-1057.

Raff, E.C., H.D. Hoyle, E.M. Popodi, and F.R. Turner. 2008. Axoneme beta-tubulin sequence determines attachment of outer dynein arms. *Curr Biol*. 18:911-914.

Raybin, D., and M. Flavin. 1977. Modification of tubulin by tyrosylation in cells and extracts and its effect on assembly in vitro. *J Cell Biol*. 73:492-504.

Redeker, V., J.P. Le Caer, J. Rossier, and J.C. Prome. 1991. Structure of the polyglutamyl side chain posttranslationally added to alpha-tubulin. *J Biol Chem*. 266:23461-23466.

Redeker, V., N. Levilliers, J.M. Schmitter, J.P. Le Caer, J. Rossier, A. Adoutte, and M.H. Bre. 1994. Polyglycylation of tubulin: a posttranslational modification in axonemal microtubules. *Science*. 266:1688-1691.

Regnard, C., D. Fesquet, C. Janke, D. Boucher, E. Desbruyeres, A. Koulakoff, C. Insina, P. Travo, and B. Edde. 2003. Characterisation of PGs1, a subunit of a protein complex co-purifying with tubulin polyglutamylase. *J Cell Sci*. 116:4181-4190.

Renthal, R., B.G. Schneider, M.M. Miller, and R.F. Luduena. 1993. Beta IV is the major beta-tubulin isotype in bovine cilia. *Cell Motil Cytoskeleton*. 25:19-29.

Rodriguez de la Vega Otazo, M., J. Lorenzo, O. Tort, F.X. Aviles, and J.M. Bautista. 2013. Functional segregation and emerging role of cilia-related cytosolic carboxypeptidases (CCPs). *FASEB J*. 27:424-431.

Rogowski, K., F. Juge, J. van Dijk, D. Wloga, J.M. Strub, N. Levilliers, D. Thomas, M.H. Bre, A. Van Dorsselaer, J. Gaertig, and C. Janke. 2009. Evolutionary divergence of enzymatic mechanisms for posttranslational polyglycylation. *Cell*. 137:1076-1087.

Rogowski, K., J. van Dijk, M.M. Magiera, C. Bosc, J.C. Deloulme, A. Bosson, L. Peris, N.D. Gold, B. Lacroix, M. Bosch Grau, N. Bec, C. Larroque, S. Desagher, M. Holzer, A. Andrieux, M.J. Moutin, and C. Janke. 2010. A family of protein-deglutamylating enzymes associated with neurodegeneration. *Cell*. 143:564-578.

Rudiger, M., J. Wehland, and K. Weber. 1994. The carboxy-terminal peptide of detyrosinated alpha tubulin provides a minimal system to study the substrate specificity of tubulin-tyrosine ligase. *Eur J Biochem*. 220:309-320.

Russell, D.G., and K. Gull. 1984. Flagellar regeneration of the trypanosome Crithidia fasciculata involves post-translational modification of cytoplasmic alpha tubulin. *Mol Cell Biol*. 4:1182-1185.

Samarage, C.R., M.D. White, Y.D. Alvarez, J.C. Fierro-Gonzalez, Y. Henon, E.C. Jesudason, S. Bissiere, A. Fouras, and N. Plachta. 2015. Cortical Tension Allocates the First Inner Cells of the Mammalian Embryo. *Dev Cell*. 34:435-447.

San Agustin, J.T., G.J. Pazour, and G.B. Witman. 2015. Intraflagellar transport is essential for mammalian spermiogenesis but is absent in mature sperm. *Mol Biol Cell*. 26:4358-4372.

Schatten, G., C. Simerly, D.J. Asai, E. Szoke, P. Cooke, and H. Schatten. 1988. Acetylated alpha-tubulin in microtubules during mouse fertilization and early development. *Dev Biol*. 130:74-86.

Schatten, H., and Q.Y. Sun. 2014. Posttranslationally modified tubulins and other cytoskeletal proteins: their role in gametogenesis, oocyte maturation, fertilization and Pre-implantation embryo development. *Adv Exp Med Biol*. 759:57-87.

Scholey, J.M. 1996. Kinesin-II, a membrane traffic motor in axons, axonemes, and spindles. *J Cell Biol*. 133:1-4.

Schulze, E., D.J. Asai, J.C. Bulinski, and M. Kirschner. 1987. Posttranslational modification and microtubule stability. *J Cell Biol*. 105:2167-2177.

Shahbazi, M.N., A. Jedrusik, S. Vuoristo, G. Recher, A. Hupalowska, V. Bolton, N.M. Fogarty, A. Campbell, L.G. Devito, D. Ilic, Y. Khalaf, K.K. Niakan, S. Fishel, and M. Zernicka-Goetz. 2016. Self-organization of the human embryo in the absence of maternal tissues. *Nat Cell Biol*. 18:700-708.

Shida, T., J.G. Cueva, Z. Xu, M.B. Goodman, and M.V. Nachury. 2010. The major alpha-tubulin K40 acetyltransferase alphaTAT1 promotes rapid ciliogenesis and efficient mechanosensation. *Proc Natl Acad Sci U S A*. 107:21517-21522.

Sirajuddin, M., L.M. Rice, and R.D. Vale. 2014. Regulation of microtubule motors by tubulin isotypes and post-translational modifications. *Nat Cell Biol*. 16:335-344.

Song, N., N. Kim, R. Xiao, H. Choi, H.I. Chun, M.H. Kang, J.H. Kim, K. Seo, N. Soundrarajan, J.T. Do, H. Song, Z.J. Ge, and C. Park. 2015. Lack of Cytosolic Carboxypeptidase 1 Leads to Subfertility due to the Reduced Number of Antral Follicles in pcd3J-/- Females. *PLoS One*. 10:e0139557.

Sui, H., and K.H. Downing. 2006. Molecular architecture of axonemal microtubule doublets revealed by cryo-electron tomography. *Nature*. 442:475-478.

Suryavanshi, S., B. Edde, L.A. Fox, S. Guerrero, R. Hard, T. Hennessey, A. Kabi, D. Malison, D. Pennock, W.S. Sale, D. Wloga, and J. Gaertig. 2010. Tubulin glutamylation regulates ciliary motility by altering inner dynein arm activity. *Curr Biol*. 20:435-440.

Takada, S., and R. Kamiya. 1994. Functional reconstitution of Chlamydomonas outer dynein arms from alpha-beta and gamma subunits: requirement of a third factor. *J Cell Biol*. 126:737-745.

Tanaka, H., N. Iguchi, Y. Toyama, K. Kitamura, T. Takahashi, K. Kaseda, M. Maekawa, and Y. Nishimune. 2004. Mice deficient in the axonemal protein Tektin-t exhibit male infertility and immotile-cilium syndrome due to impaired inner arm dynein function. *Mol Cell Biol*. 24:7958-7964.

Tang, L., Y. Zeng, H. Du, M. Gong, J. Peng, B. Zhang, M. Lei, F. Zhao, W. Wang, X. Li, and J. Liu. 2017. CRISPR/Cas9-mediated gene editing in human zygotes using Cas9 protein. *Mol Genet Genomics*. 292:525-533.

Topalidou, I., C. Keller, N. Kalebic, K.C. Nguyen, H. Somhegyi, K.A. Politi, P. Heppenstall, D.H. Hall, and M. Chalfie. 2012. Genetically separable functions of the MEC-17 tubulin acetyltransferase affect microtubule organization. *Curr Biol*. 22:1057-1065.

Tran, A.D., T.P. Marmo, A.A. Salam, S. Che, E. Finkelstein, R. Kabarriti, H.S. Xenias, R. Mazitschek, C. Hubbert, Y. Kawaguchi, M.P. Sheetz, T.P. Yao, and J.C. Bulinski. 2007. HDAC6 deacetylation of tubulin modulates dynamics of cellular adhesions. *J Cell Sci*. 120:1469-1479.

Turk, E., A.A. Wills, T. Kwon, J. Sedzinski, J.B. Wallingford, and T. Stearns. 2015. Zeta-Tubulin Is a Member of a Conserved Tubulin Module and Is a Component of the Centriolar Basal Foot in Multiciliated Cells. *Curr Biol*. 25:2177-2183.

Valenzuela, P., M. Quiroga, J. Zaldivar, W.J. Rutter, M.W. Kirschner, and D.W. Cleveland. 1981. Nucleotide and corresponding amino acid sequences encoded by alpha and beta tubulin mRNAs. *Nature*. 289:650-655.

van Dijk, J., K. Rogowski, J. Miro, B. Lacroix, B. Edde, and C. Janke. 2007. A targeted multienzyme mechanism for selective microtubule polyglutamylation. *Mol Cell*. 26:437-448.

Vassena, R., B. Heindryckx, R. Peco, G. Pennings, A. Raya, K. Sermon, and A. Veiga. 2016. Genome engineering through CRISPR/Cas9 technology in the human germline and pluripotent stem cells. *Hum Reprod Update*. 22:411-419.

Vinot, S., T. Le, S. Ohno, T. Pawson, B. Maro, and S. Louvet-Vallee. 2005. Asymmetric distribution of PAR proteins in the mouse embryo begins at the 8-cell stage during compaction. *Dev Biol*. 282:307-319.

Vogel, P., G. Hansen, G. Fontenot, and R. Read. 2010. Tubulin tyrosine ligase-like 1 deficiency results in chronic rhinosinusitis and abnormal development of spermatid flagella in mice. *Vet Pathol*. 47:703-712.

Weber, K., A. Schneider, N. Muller, and U. Plessmann. 1996. Polyglycylation of tubulin in the diplomonad Giardia lamblia, one of the oldest eukaryotes. *FEBS Lett*. 393:27-30.

Wilson, P.J., and A. Forer. 1997. Effects of nanomolar taxol on crane-fly spermatocyte spindles indicate that acetylation of kinetochore microtubules can be used as a marker of poleward tubulin flux. *Cell Motil Cytoskeleton*. 37:20-32.

Wloga, D., D.M. Webster, K. Rogowski, M.H. Bre, N. Levilliers, M. Jerka-Dziadosz, C. Janke, S.T. Dougan, and J. Gaertig. 2009. TTLL3 Is a tubulin glycine ligase that regulates the assembly of cilia. *Dev Cell*. 16:867-876.

Zhang, Y., S. Kwon, T. Yamaguchi, F. Cubizolles, S. Rousseaux, M. Kneissel, C. Cao, N. Li, H.L. Cheng, K. Chua, D. Lombard, A. Mizeracki, G. Matthias, F.W. Alt, S. Khochbin, and P. Matthias. 2008. Mice lacking histone deacetylase 6 have hyperacetylated tubulin but are viable and develop normally. *Mol Cell Biol*. 28:1688-1701.

Zhang, Y., N. Li, C. Caron, G. Matthias, D. Hess, S. Khochbin, and P. Matthias. 2003. HDAC-6 interacts with and deacetylates tubulin and microtubules in vivo. *EMBO J*. 22:1168-1179.

Zilberman, Y., C. Ballestrem, L. Carramusa, R. Mazitschek, S. Khochbin, and A. Bershadsky. 2009. Regulation of microtubule dynamics by inhibition of the tubulin deacetylase HDAC6. *J Cell Sci*. 122:3531-3541.

Zink, S., L. Grosse, A. Freikamp, S. Banfer, F. Muksch, and R. Jacob. 2012. Tubulin detyrosination promotes monolayer formation and apical trafficking in epithelial cells. *J Cell Sci*. 125:5998-6008.
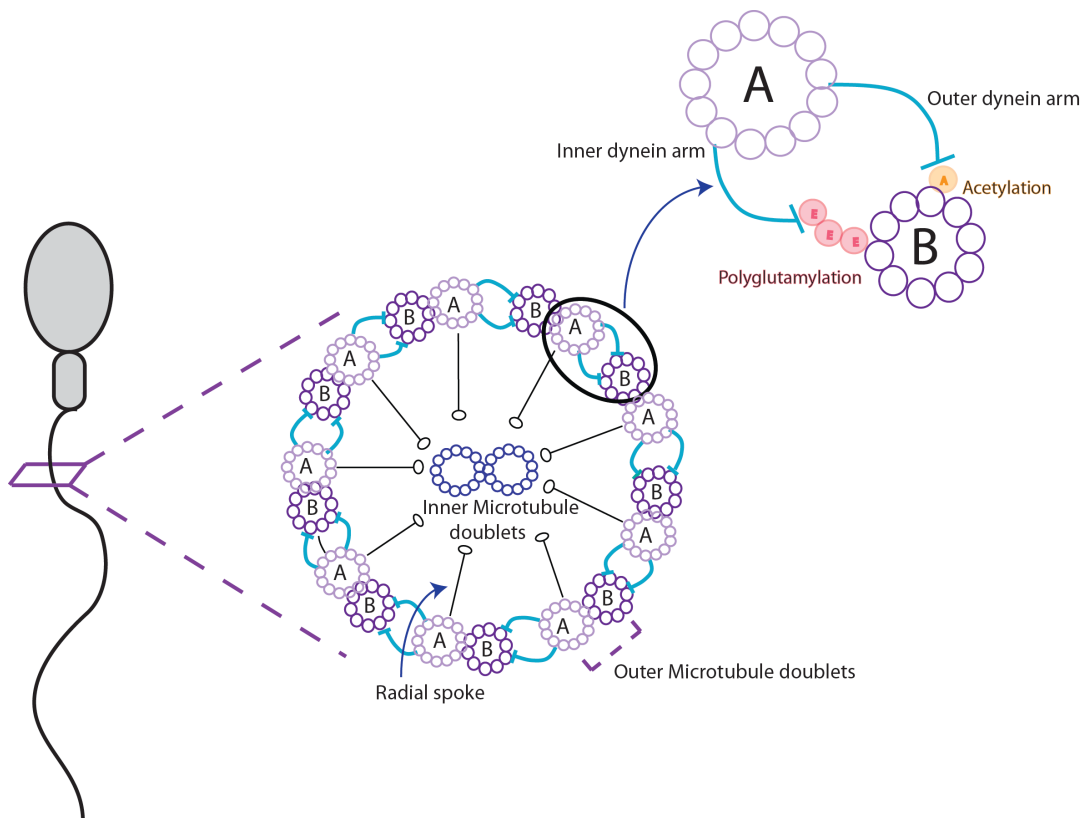
Figures:

A
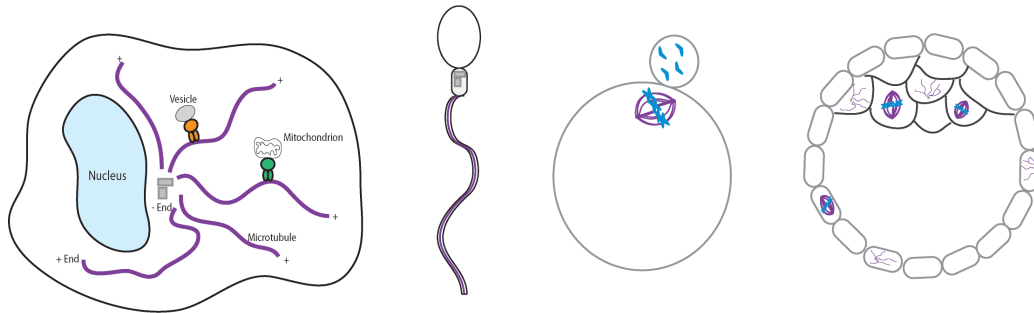
B
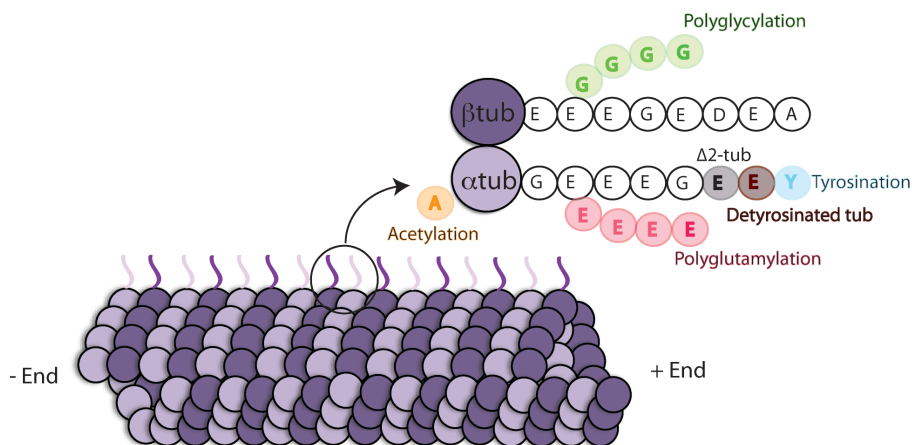
Figure 1: Microtubules and tubulin PTMs. A) Microtubules are polarized polymers with a negative and positive end. They form part of the cytoskeletal network of the cell, and are involved in many cellular processes such as vesicles and organelles' transport. In the reproductive system, they are essential in both gametes as well as during early embryo development. In the spermatozoa, microtubules are the main components of the axoneme. In oocytes and early development embryos, microtubules, for example, build up the bipolar spindle, the molecular machine responsible of the genetic material segregation to the two daughter cells. **B)** All the described tubulin PTMs, with the exception of acetylation, occur at the C-terminus of alpha and beta-tubulins exposed at the microtubule surface. Detyrosination and Δ2 tubulin are specific modifications of

tyrosinated isotypes of alpha-tubulin. Glutamylation and glycylation occur on the C-terminal tail of both alpha and beta-tubulin. The best characterized acetylation occurs on Lys40 of alpha-tubulin inside the lumen of the microtubule.

Figure 2: Molecular mechanism of flagellar beating. The axoneme of the sperm cell is formed by 9 outer doublets of microtubules (A and B) and an inner microtubule doublet. The movement of the flagella is powered through the interaction of the inner and outer dynein arms extending from the A tube of the outer doublets with the B tube of the adjacent doublet. These interactions are regulated by tubulin PTMs: polyglutamylation for the inner dynein arm and acetylation for the outer dynein arm.

Table 1: Alpha and beta tubulin isotypes in humans. TUBB: Beta-tubulin, TUBA: Alpha-tubulin.

Genes	C-terminus	Tissue expression
ALPHA-TUBULIN ISOTYPES		
TUBAL3	RDYEEVAQSF	Intestine, colon, oocyte, mucosa
TUBA1A	GEGEEEGEEY	Fetal brain, embryo, bone narrow
TUBA1B	GEGEEEGEEY	Brain, respiratory system, embryo
TUB1C	ADGEDEGEEY	Respiratory system, oocyte, embryo, spinal cord
TUBA3C	EAEAEEGEEY	Testis, sperm, oocyte, brain, respiratory system
TUBA3D	EAEAEEGEEY	Testis, platelet, oocyte, brain, liver, uterus
TUBA3E	EAEAEEGEAY	Testis, heart, placenta, oocyte
TUBA4A	SYEDEDEGEE	Brain, skeletal muscle, platelets
TUBA4B	MPALSLPTRW	Oocyte, respiratory system, oviduct
TUBA8	FEEENEGEEF	Platelet, heart, bone narrow
BETA-TUBULIN ISOTYPES		
TUBB	DFGEEAEEEA	Respiratory system, brain, embryo, placenta
TUBB1	AEMEPEDKGH	Blood, leukocytes, muscle, liver
TUBB2A	FEEEEGEDEA	Brain, liver, hair follicle
TUBB2B	FEEEEGEDEA	Brain, embryo, testis
TUBB3	EEESEAQGPK	Respiratory system, nervous system
TUBB4a	FEEEAEEEVA	Brain, testis, female gonad, heart, colon
TUBB4B	FEEEAEEEVA	Respiratory system, testis, brain, oocyte
TUBB6	FEDEEEEIDG	Breast, respiratory system, muscle, placenta
TUBB8	DEEYAEEEVA	Oocyte, blood system

Table 2: The CCP family in mammals. CCPs classified according to their activity and substrate specificity (alpha and/or beta-tubulin, or other proteins).

Protein	Activity	Substrate	Reaction	Bibliography
CCP1	Deglutamylase	Alpha- and Beta-tubulin Myosin light chain kinase 1	Removal of glutamates from lateral chains and the branching one (TTLL6 dependent)	(Berezniuk et al., 2012; Rogowski et al., 2010; Wu et al., 2015)
CCP2	Deglutamylase	Alpha and Beta tubulin	Removal of glutamates from lateral chains	(Tort et al., 2014)
CCP3	Deglutamylase Deaspartylase	Alpha and Beta tubulin	Removal of glutamates from lateral chains Removal od aspartic acid	(Tort et al. 2014)
CCP4	Deglutamylase	Alpha and Beta tubulin. Myosin light chain kinase 1	Removal of glutamates from lateral chains	(Rogowski et al., 2010; Wu et al., 2015)
CCP5	Deglutamylase	Alpha and Beta tubulin.	Removal of the branching glutamates	(Berezniuk et al., 2013; Kimura et al., 2010)
CCP6	Deglutamylase	Alpha and Beta tubulin. Myosin light chain kinase 1	Removal of glutamates from lateral chains and the branching one	(Rogowski et al., 2010; Wu et al., 2015)

Berezniuk I, Lyons PJ, Sironi JJ, Xiao H, Setou M, Angeletti RH, Ikegami K, and Fricker LD. Cytosolic carboxypeptidase 5 removes alpha- and gamma-linked glutamates from tubulin. *J Biol Chem* 2013: **288**; 30445-30453.

Berezniuk I, Vu HT, Lyons PJ, Sironi JJ, Xiao H, Burd B, Setou M, Angeletti RH, Ikegami K, and Fricker LD. Cytosolic carboxypeptidase 1 is involved in processing alpha- and beta-tubulin. *J Biol Chem* 2012: **287**; 6503-6517.

Kimura Y, Kurabe N, Ikegami K, Tsutsumi K, Konishi Y, Kaplan OI, Kunitomo H, Iino Y, Blacque OE, and Setou M. Identification of tubulin deglutamylase among Caenorhabditis elegans and mammalian cytosolic carboxypeptidases (CCPs). *J Biol Chem* 2010: **285**; 22936-22941.

Rogowski K, van Dijk J, Magiera MM, Bosc C, Deloulme JC, Bosson A, Peris L, Gold ND, Lacroix B, Bosch Grau M, *et al*. A family of protein-deglutamylating enzymes associated with neurodegeneration. *Cell* 2010: **143**; 564-578.

Tort O, Tanco S, Rocha C, Bieche I, Seixas C, Bosc C, Andrieux A, Moutin MJ, Aviles FX, Lorenzo J, *et al*. The cytosolic carboxypeptidases CCP2 and CCP3 catalyze posttranslational removal of acidic amino acids. *Mol Biol Cell* 2014: **25**; 3017-3027.

Wu HY, Rong Y, Correia K, Min J, and Morgan JI. Comparison of the enzymatic and functional properties of three cytosolic carboxypeptidase family members. *J Biol Chem* 2015: **290**; 1222-1232.

Table 3: Microtubule associated proteins regulated by the tubulin code Tubulin PTMs and isotypes that alter the binding affinities and/or the activity of the indicated MAPs and motor proteins.

Tubulin PTM	Proteins and the type of regulation	Bibliography
Acetylation	Kinesin-1- increased microtubule binding affinity and behavior. Axonemal dynein- increased microtubule binding affinity.	(Alper et al., 2014; Cai et al. 2009; Kaul et al., 2014; Reed et al., 2006)
Polyglutamylation	Increased Kinesin-2 velocity and processivity, independently of the polyglutamylation chain length. Both alpha and beta-tubulin. Increased Kinesin-1 processivity. Only with long polyglutamylation chains. Both alpha and beta-tubulin. Axonemal dynein - increased microtubule binding affinity . Tau - increased microtubule binding affinity. MAP2 - increased microtubule binding affinity. MAP1A/B - increased microtubule binding affinity . Spastin – stimulates Spastin activity.	(Boucher et al., 1994; Kubo et al., 2012; Kubo et al., 2010; Lacroix et al., 2010; Sirajuddin et al., 2014; Suryavanshi et al., 2010)
Polyglycylation	Uncharacteried.	
Tyrosination	kinesin-2- Inhibitory effects on processivity and velocity. Kinesin-13 (MCAK)- Increased microtubule	(Konishi and Setou, 2009; McKenney et al., 2016; Sirajuddin et al., 2014)

	depolymerization rate. Dynein-dynactin complex - Initiation. Kinesin-1 – axon movement.	
Detyrosinated tubulin	Kinesin-2 (anterograde intraflagellar transport)- increased processivity and velocity. MCAK and KIF2A- inhibition of microtubule depolymerization activity. CENP-E/Kinesin-7- enhancement of chromosome dependent microtubule transport Kinesin-1- Increased landing rate.	(Barisic et al., 2015; Cai et al., 2009; Dunn et al., 2008; Kaul et al., 2014)
Δ2-tubulin	Not characterized.	
Alpha-tubulin isotypes	Not characterized.	
Beta-tubulin isotypes	Kinesin-1- motor processivity reduced by TUBB1 and TUBB3.	(Sirajuddin et al., 2014)

Alper JD, Decker F, Agana B, and Howard J. The motility of axonemal dynein is regulated by the tubulin code. *Biophys J* 2014: **107**; 2872-2880.

Barisic M, Silva e Sousa R, Tripathy SK, Magiera MM, Zaytsev AV, Pereira AL, Janke C, Grishchuk EL, and Maiato H. Mitosis. Microtubule detyrosination guides chromosomes during mitosis. *Science* 2015: **348**; 799-803.

Boucher D, Larcher JC, Gros F, and Denoulet P. Polyglutamylation of tubulin as a progressive regulator of in vitro interactions between the microtubule-associated protein Tau and tubulin. *Biochemistry* 1994: **33**; 12471-12477.

Cai D, McEwen DP, Martens JR, Meyhofer E, and Verhey KJ. Single molecule imaging reveals differences in microtubule track selection between Kinesin motors. *PLoS Biol* 2009: **7**; e1000216.

Dunn S, Morrison EE, Liverpool TB, Molina-Paris C, Cross RA, Alonso MC, and Peckham M. Differential trafficking of Kif5c on tyrosinated and detyrosinated microtubules in live cells. *J Cell Sci* 2008: **121**; 1085-1095.

Kaul N, Soppina V, and Verhey KJ. Effects of alpha-tubulin K40 acetylation and detyrosination on kinesin-1 motility in a purified system. *Biophys J* 2014: **106**; 2636-2643.

Konishi Y and Setou M. Tubulin tyrosination navigates the kinesin-1 motor domain to axons. *Nat Neurosci* 2009: **12**; 559-567.

Kubo T, Yagi T, and Kamiya R. Tubulin polyglutamylation regulates flagellar motility by controlling a specific inner-arm dynein that interacts with the dynein regulatory complex. *Cytoskeleton (Hoboken)* 2012: **69**; 1059-1068.

Kubo T, Yanagisawa HA, Yagi T, Hirono M, and Kamiya R. Tubulin polyglutamylation regulates axonemal motility by modulating activities of inner-arm dyneins. *Curr Biol* 2010: **20**; 441-445.

Lacroix B, van Dijk J, Gold ND, Guizetti J, Aldrian-Herrada G, Rogowski K, Gerlich DW, and Janke C. Tubulin polyglutamylation stimulates spastin-mediated microtubule severing. *J Cell Biol* 2010: **189**; 945-954.

McKenney RJ, Huynh W, Vale RD, and Sirajuddin M. Tyrosination of alpha-tubulin controls the initiation of processive dynein-dynactin motility. *EMBO J* 2016: **35**; 1175-1185.

Reed NA, Cai D, Blasius TL, Jih GT, Meyhofer E, Gaertig J, and Verhey KJ. Microtubule acetylation promotes kinesin-1 binding and transport. *Curr Biol* 2006: **16**; 2166-2172.

Sirajuddin M, Rice LM, and Vale RD. Regulation of microtubule motors by tubulin isotypes and post-translational modifications. *Nat Cell Biol* 2014: **16**; 335-344.

Suryavanshi S, Edde B, Fox LA, Guerrero S, Hard R, Hennessey T, Kabi A, Malison D, Pennock D, Sale WS, *et al*. Tubulin glutamylation regulates ciliary motility by altering inner dynein arm activity. *Curr Biol* 2010: **20**; 435-440.

Table 4: Take-home messages. Summary of the most important concepts of this review.

Take-home messages	
1	Tubulin isotypes and PTMs generate the tubulin code, which in turn regulates microtubule functionality.
2	Both tubulin isotypes and PTMs induce changes mainly at the C-terminal tail of α and/or β tubulin subunits.
3	Tubulin in gametes is highly modified by tubulin PTMs, and some of them have a specific isotype expression.
4	In sperm cells, deregulation of tubulin PTMs induces reduction of motility, morphological defects, low sperm concentration and sterility.
5	In oocytes, tubulin β isotype mutations are related with maturation failures.
6	In embryos, tubulin PTMs defects are related to cilia dysfunction, inducing serious diseases such as primary ciliary dyskinesia.
7	Most of the knock down animal models for tubulin PTMs enzymes are infertile or subfertile.
8	Tubulin isotypes and PTMs are emerging as new molecular markers for gamete and embryo selection and quality.